Investigating the role of ZEB1 in adult hippocampal neurogenesis

A thesis submitted for the Doctor of Philosophy

By

Bhavana Gupta

School of Biosciences
Cardiff University

January 2020

Acknowledgements

The past four years have been some of the most challenging years yet, and I know that I could not have gotten through them without the unwavering support of a number of people.

First and foremost, I owe all my gratitude to Dr. Florian Siebzehnrubl for being the most supportive and talented supervisor (with an infinite amount of patience for my endless questions) that I could have hoped to work with during my PhD. He has guided me at every step of this journey and has shaped me into a better scientist. I cannot thank him enough for having given me the opportunity to pursue such an interesting project with excellent guidance. I would also like to thank my second supervisor, Dr. Catherine Hogan, and review panel convenor, Dr. Isabel-Martinez-Garay for their helpful advice and guidance.

This project would not have been possible without the funding that Cancer Research UK provided for my studentship, and I would like to express my deep gratitude to them.

I am very grateful to Professor Magdalena Götz, Professor Thomas Brabletz, and Professor Owen Sansom for providing the mice utilised in this project. In addition I would like to thank the entire staff at the Heath JBIOS facility, especially Kerry, Deborah, Pat, Katie, Oliver, and Charlotte, for their technical guidance and assistance, which was momentous for the completion of this project.

Thank you to Dr. Mark Young and Thomas Freeman for discussing the behavioural task protocols and for helping me shape the study. A big thank you is also owed to to Dr. Trevor Humby for all his guidance and assistance with the behavioural task analysis, he helped me tackle a mountain of data which I could not have done without his help.

Thank you to Ana JP for being the kindest and most supportive person to work beside. Her hard work has been an inspiration for me, and I cannot thank her enough for having always been there when I needed to talk to someone. I would also like to thank all the current members of the FS group, especially Dorit for her help with some of the histology, and Vasili and Ben, for all their encouragement and enthusiasm along the way. A big thank you is owed to past members Holly, Alex L.,

Laura, and Alex J., for giving me the opportunity to develop my teaching skills, as well as for all their help and input in the project.

Thank you to everyone in ECSCRI, past and present, for their enthusiasm, encouragement, and advice throughout the project, I have really enjoyed working alongside all of them!

I owe everything I am today to my family who are my biggest source of strength, this thesis is dedicated to all of them. Thank you Mummy and Papa for being my inspiration and for your unwavering belief in me. Your lifelong love and support have always given me the strength to challenge myself and achieve things I could never have imagined. Thank you to my siblings Swati and Arpit, and my brother-in-law Shehan, for being my best friends (and cheerleaders!), and for always being there to pick me up when things were difficult. I would also like to thank the Cuffs for being the most loving and caring in-laws. I do not think I can put in words just how grateful I am for my family every day of my life.

Lastly, I would like to thank my fiancé, Jordan, for everything that he has done and continues to do for us. I know that years down the line, when this is all but a memory, you will still be by my side.

Abstract

Neural stem cells (NSCs) persist within neurogenic niches in the adult mammalian central nervous system (CNS) and generate neurons throughout the lifespan of an animal. This neurogenesis constitutes a step-wise process that is governed by cell intrinsic transcriptional regulators that function in synchrony in NSCs as well as successive progenies at each step. Several transcriptional regulators of adult neurogenesis have been identified, most of which are tissue-specific. Whether broader-functioning 'master regulators' that govern stem cell function across multiple tissues also impact on adult NSCs is incompletely understood. The transcription factor *zinc finger E-box binding homeobox 1* (ZEB1) is a known regulator of stem cell self-renewal in many epithelial tissues, but also functions to maintain NSCs in an undifferentiated state during embryonic CNS development. Whether ZEB1 also functions in adult neurogenesis remains unclear and is addressed here.

A novel transgenic mouse model to target ZEB1 expression in astrocytes and NSCs was used to investigate self-renewal and differentiation of adult NSCs in the hippocampus. Inducible and conditional deletion of Zeb1 in mice resulted in the precocious differentiation of hippocampal NSCs into neurons and a gradual depletion of the stem cell pool. Newborn neurons showed a greater survival during the process of maturation, and behavioural studies suggested that this amplification in granule neurons did not alter the cognitive function of Zeb1-deficient mice. Contrastingly, astrocyte numbers in the dentate gyrus were reduced following the ablation of Zeb1. This indicates that ZEB1 regulates both stem cell self-renewal and cell fate in the adult brain.

Dissecting how ZEB1 regulates adult neurogenesis will increase our understanding of the basic mechanisms underlying stem cell maintenance in the adult brain. This will set the foundation for future work to identify mechanistic targets of ZEB1 in adult neurogenesis.

Table of content

List of Tables

List of Figures

Abbreviations

Symbols/units

°C= Degrees Celsius
% = Percent
+ = Positive
− = Negative
+/- = Heterozygous loss-of-function
-/- = Homozygous loss-of-function
β = Beta
δ = Delta
g = Gram
fl/fl = Homozygously floxed allele
µL = Microlitre
µm = Micrometre
µM = Micromolar
mg = Milligram
mL = Millilitre
mm = Millimetre

A

Ach = Acetylcholine
AMPA = α-amino-3-hydroxy-5-methyl-4-isoxazolepropionic acid
ANOVA = Analysis of variance
AraC = Cytosine-β-D-arabinofuranoside
Ascl1 = Achaete-scute homolog 1

B

BDNF = Brain-derived neurotrophic factor
BLBP = Brain-lipid binding protein
bp = Base pairs
BrdU = 5'-bromo-2-deoxyuridine
BSA = Bovine serum albumin

C

CAG = Cytomegalovirus enhancer/chicken β–actin promoter
CBD = p3000/p-CAF binding domain
CHD = Central homeodomain
CID = C-terminal binding protein (CtBP)-interacting domain
CFP = Cyan fluorescent protein
CNPase = 2',3'-cyclic nucleotide 3'-phosphodiesterase
CNS = Central nervous system
Cre = Cre recombinase
$CreER^{T2}$ = Cre recombinase-estrogen receptor fusion transgene
CtBP = C-terminal-binding protein
CZF = C-terminal zinc finger

D

DCX = Doublecortin
ddH_2O = Double distilled H_2O
DG = Dentate gyrus
DI = Discrimination index
DNA = Deoxyribonucleic acid

E

E# = Embryonic day
EAAT1 = Excitatory amino acid transporter 1
EDTA = Ethylenediaminetetra-acetic acid
EdU = 5-ethynyl-2'-deoxyuridine
EE =Environmental enrichment
EGF = Epidermal growth factor
EGFP = Enhanced green fluorescent protein
EGFR = Epidermal growth factor receptor
EMT = Epithelial-mesenchymal transition
EMT-TF = Epithelial-mesenchymal transition transcription factors
ER = Estrogen receptor

F

FGF2 = Fibroblast growth factor-2
Flox = Flanked by loxP sites
FOXO3 = Forkhead box O3
FSB-T = Fish-skin gelatin buffer with 0.1% Triton X-100
F-statistic = Ratio of two mean squares (variation between two groups)

G

GABA = Gamma-aminobutyric acid
GBM = Glioblastoma
gDNA = Genomic deoxyribonucleic acid
GDNF = Glial-derived neurotrophic factor
GFAP = Glial fibrillary acidic protein
GFP = Green fluorescent protein
GL = Granule layer
GLAST = Glutamate-aspartate transporter
GLT1 = Glutamate transporter 1
GR = Glucocorticoid receptor

H

HDAC = Histone deacetylase
HES = Hairy and enhancer of split
HMG = High mobility group
HPA = Hypothalamic-pituitary axis
Hsp90 = Heat-shock protein 90

I

IF = Immunofluorescence
IP = Intraperitoneal
IPC = Intermediate progenitor cell
ITF-1 = Immunoglobulin transcription factor-1

K

KA = Kainic acid

L

LoxP = Locus of crossover in P1
Lsl = LoxP-stop-loxP

M

Mash1 (ASCL1) = Mammalian achaete scute homolog-1
MAPK = Mitogen-activated protein kinase
MCM2 - Minichromosome maintenance protein 2
MEGF10 = Multiple EGF-like domains 10
MERTK = MER tyrosine kinase
MET = Mesenchymal-epithelial transition
Min = Minute
miR = MicroRNA
ML = Molecular layer
mRNA = Messenger ribonucleic acid

N

n = Number of biological replicates
NE = North-east
NeuN = Neuronal nuclei protein
NeuroD1 = Neurogenic differentiation factor 1
NFIA = Nuclear factor IA
NMDA = N-methyl-D-aspartate
NOL = Novel object location
NOR = Novel object recognition
NSC = Neural stem cell
NT-3 = Neurotrophin-3
NW = North-west
NZF = N-terminal-binding protein

O

OB = Olfactory bulb
OCT = Optimal cutting temperature
OLIG2 = Oligodendrocyte transcription factor 2

P

P# = Postnatal day
PAX6 = Paired box protein-6
PI3K = Phosphoinositide 3-kinase
PBS = Phosphate buffered saline
PBS-T = Phosphate buffered saline with 0.1% Triton X-100
PCR – Polymerase chain reaction
PSA-NCAM = Polysialylated-neural cell adhesion molecule
PROX1 = Prospero homeobox protein 1
P-value = Probability value

R

RBPJ = Recombination signal binding protein for immunoglobulin kappa J region
REST = Repressor element 1-silencing transcription factor
RG = Radial glia
RGL = Radial glia-like
RISC = RNA-induced silencing complex
RMS = Rostral migratory stream
RNA = Ribonucleic acid
RT = Room temperature

S

SE = South-east
SEM = Standard error of mean
SID = Smad interacting domain
SOX = Sex determining region Y-box
SGZ = Subgranular zone
SSRI = Selective serotonin reuptake inhibitor
SVZ = Subventricular zone
SW = South-west

T

TAE = Tris-acetate EDTA
TBR2 = T-box brain protein 2
td(Tomato) = Tandem dimer
TGFβ - Transforming growth factor β
TLX = Tailless
Trk = Tropomyosin receptor kinase
TuJ1 = βIII tubulin

U

UK = United Kingdom
USA = United States of America
UTR = Untranslated region
UV = Ultraviolet

V

V = Volt
VEGF = Vascular endothelial growth factor
Vs = versus
v/v = Volume per volume

W

WT = Wild-type
w/v = Weight per volume

Z

ZEB = Zinc finger E-box binding homeobox
ZF = Zinc finger

Chapter 1 - General introduction

> *Once the development was ended, the founts of growth and regeneration of the axons and dendrites dried up irrevocably. In the adult centers, the nerve paths are something fixed, ended, and immutable. Everything may die, nothing may be regenerated. It is for the science of the future to change, if possible, this harsh decree. (Santiago Ramón y Cajal, 1928)*

The traditional view of the adult brain being a post-mitotic organ was famously postulated in the early 20th century by the Nobel-prize winning histologist Santiago Ramón y Cajal, also coined the father of neuroscience owing to his great contribution in the recognition of neurons as independent units composing the nervous system. Contradicting this dogma, several decades of research have now provided evidence for the actuality of adult neurogenesis. The term neurogenesis describes a complex process that encompasses the birth, survival, and integration of new neurons in the central nervous system (CNS). A multicellular niche, coupled with the interplay between various intrinsic and extrinsic cues, provides guidance and support for this highly controlled process that lends plasticity to the brain. The focus of this thesis will be the regulation of adult mouse neurogenesis by the transcription factor ZEB1 in the hippocampus, one of the two main regions in the brain where the formation of new neurons occurs throughout adulthood.

In this chapter I will present some of the current body of knowledge that elucidates the complexity of adult neurogenesis and the precise spatiotemporal regulation required for successful granule neuron formation and integration. I will start by describing the sequential process by which neurons are formed in the hippocampus, following which I will discuss some of the research that has been carried out by other groups to characterise the roles of various transcriptional regulators of neurogenesis. Subsequently, I will address ZEB1, the focus of this thesis, and its relevance to adult neurogenesis.

1.1 Defining stem cells

To date, the definition that Potten and Loeffler assigned to describe a stem cell remains widely accepted; a true stem cell has the ability to proliferate to either self-renew, or to produce differentiated tissue-constituting daughter cells, and through the latter, also regenerate tissue post-injury (Potten and Loeffler 1990). The former is the process by which stem cells divide to form new stem cells, thus

maintaining their population during the lifespan of an organism. Stem cells can undergo either asymmetrical division, whereby they give rise to a lineage-committed cell and a stem cell, or symmetrical division, through which they divide into either two lineage-restricted or two stem cells (Lin 2008).

Embryonic pluripotent stem cells can give rise to all lineages of cells to fuel embryonic development, whilst postnatal resident multipotent stem cells give rise to a restricted lineage of cells within a tissue to support natural cell turnover as well as tissue repair under pathologic conditions (Zakrzewski *et al.* 2019). By contrast, cells with stemness potential have the capacity to exhibit a number, if not all, of the aforementioned stemness features, when prompted, but do not do so under normal circumstances; this is becoming an increasingly recognised concept termed cellular plasticity in which cells have the ability to "de-differentiate" into a more precursor-like state (Mills *et al.* 2019).

In this thesis, the term "neural stem cell" will be used to identify the putatively multipotent CNS cells which give rise to neural cells that become incorporated in either the developing embryonic CNS or pre-existing adult CNS circuits. In the context of the CNS, the major neural cell lineages generated through embryonic development and adulthood are divided into neuronal and glial. The glial lineage can be subdivided into macroglia that consist of astroglia and oligodendrocytes, and microglia, of which the latter has haematopoietic origins, and so does not descend directly from neural precursor cells residing within the brain. During neurogenesis, neural stem cells (NSCs) give rise to unipotent "progenitor cells" that are lineage restricted and act as a proliferative intermediary in the generation of mature neurons. The term "precursor" cell will instead be used to identify a population of cells that is not fully differentiated, which can include both stem and progenitor cells. Adult NSCs are considered to be remnants from embryonic neurodevelopment, and thus I will next briefly introduce embryonic NSCs to elucidate the origin of their adult counterparts.

1.2 Embryonal neural stem cells

Embryonic neurogenesis has been extensively studied (Urbán and Guillemot 2014), and as the focus of this thesis is adult neurogenesis, in this section I will *briefly*

discuss the putative cell of origin, the radial glia, that gives rise to the adult NSC population.

During embryogenesis, the occurrence of two processes, termed neurogenesis and gliogenesis, is crucial for the formation of the nervous system. The former precedes and is the process by which new neurons are born, whilst the latter begins during late embryogenesis and occurs predominantly postnatally, and denotes the development of new glial cells. Macroglia have distinctive non-excitatory roles in the CNS as crucial supportive cells in the maintenance of CNS homeostasis and correct neuronal function; a third glial subtype are the microglia, which are mesodermal-derived and form the main CNS immune defence (reviewed in Barres 2008).

The very first neural precursor cells to appear preceding embryonic cortical development are the neuroepithelial cells, that form the pseudostratified epithelial wall of the ectodermal neural tube, which subsequently proceeds to develop into the ventricular system. Neuroepithelial cells are classified as multipotent stem cells as they can generate lineage-restricted neural cells; initially they divide symmetrically to generate more neuroepithelial cells to form the neural tube, following which at approximately E9-E10 (E; embryonic day) they begin to divide asymmetrically to give rise to radial glial (RG) cells (Misson *et al.* 1988; Merkle *et al.* 2004). Similar to their cell of origin, the soma of RG cells is located in the ventricular zone, with radial processes projected through to the pial surface. The defining difference between neuroepithelial and RG cells is the glial features of the latter cells; as cortical development progresses, RG cells begin to express astroglial-specific markers such as GLAST (an astrocyte-specific glutamate transporter also known as EAAT1; Slc1a3 gene), brain lipid-binding protein (BLBP; Fabp7 gene), calcium-binding protein S100β (S100β gene), and glial fibrillary acidic protein (GFAP; Gfap gene), as well as other intermediate filament proteins such as nestin and vimentin. The RG cells subsequently generate the majority of neurons formed during embryonal CNS development. A study highlighted a cerebral cortical-radial glial-specific marker Pax6, that was shown to be crucial for mediating their function as a scaffold for the migration of newborn neurons away from the neurogenic layer into the developing brain (Götz *et al.* 1998; reviewed in Malatesta and Gotz 2013). It has been shown that

the majority of RG cells differentiate into parenchymal astrocytes perinatally, although a subset of SVZ RG cells survive and originate adult NSCs (reviewed in Kriegstein and Alvarez-Buylla 2009; Fuentealba *et al.* 2015), which will be further discussed in the subsequent section.

1.3 Adult neurogenesis

The discovery of brain plasticity through the ability to generate new neurons challenged the dogma of the post-mitotic state of the brain. The development of ^{3}H-thymidine and 5-bromo-2'-deoxyuridine (BrdU; a measurable thymidine analogue, alongside other analogues such as EdU, that becomes incorporated into dividing cells), cell labelling techniques drove this revolutionary breakthrough by allowing the study of neurogenesis in the brain of various adult animals, including rat (Altman and Das 1965; Kuhn *et al.* 1996), songbird (Goldman and Nottebohm 1983), mouse (Reynolds and Weiss 1992), and eventually human (Eriksson *et al*. 1998; Sanai *et al*. 2004). This led to the discovery of two major neurogenic regions in the adult mammalian brain, the subventricular zone (SVZ) and the hippocampus. The first step in the process of adult neurogenesis is the division of multipotent NSCs to generate a transit-amplifying cell population, that develop into neuronal-committed migratory progenitor cells, termed neuroblasts, which eventually differentiate into fully functional neurons and become integrated in established synaptic circuits. In the subsequent sections, I will further describe this process and the regulatory mechanisms involved in its maintenance.

1.3.1 (Glial) origin of adult NSCs

In the developing brain, the neural precursor cells take the form of RG (discussed in section 1.2). The majority of RG cells give rise to parenchymal astrocytes post-cortical development (Misson *et al.* 1988; Voigt 1989), but a subset persist and become the resident adult NSC population, as evidenced in the SVZ (Fuentealba *et al.* 2015). A seminal study was published in 1999 that provided evidence for the RG origin of adult SVZ NSCs; the authors used [^{3}H]-thymidine and SVZ retroviral-GFP labelling to demonstrate that SVZ-residing astrocytes are label-retaining cells that give rise to labelled neurons in the olfactory bulb; moreover, it was also reported

that these cells survive anti-mitotic treatment and can subsequently repopulate the SVZ compartment (Doetsch *et al.* 1999). A follow-up study was subsequently carried out which was led also by Alvarez-Buylla, and it was demonstrated that tagged SVZ-residing RG cells in P0 mice give rise to all four types of brain cells: neurons, astrocytes, oligodendrocytes, and ependymal cells (Merkle *et al.* 2004).

The SVZ and hippocampal NSCs share various features with differentiated astrocytes. Both NSCs and astrocytes not only display similar marker expression profiles including proteins such as GLAST, GFAP, and BLBP, they also show morphological similarities including intracellular glycogen granules and endfeet on blood vessels. Thus, the identity of NSCs in the adult brain is of glial origin; this observation has led to the questioning of the classical view of astrocytes as terminally differentiated glial cells that are separate from the neuronal lineage. Moreover, this has suggested a more important role for glial cells that have traditionally been viewed as the support cells in the CNS. A key element that is needed for NSCs to maintain their stem cell identity is a supporting niche.

1.3.2 Neurogenic niches in the adult mammalian brain

A neurogenic niche is defined as a region where neural precursor cells are present within a microenvironment that encourages the birth of new neurons through a combination of intercellular interactions and signalling factors. This permissive milieu supports the survival of the neural precursor cells, as well as playing a role in their fate determination, from establishing quiescence or activation, to providing guiding signals for differentiation once activated. Evidence for the importance of the microenvironment in establishing a neurogenic zone has been provided through various transplantation studies, involving the grafting of neural precursor cells in both neurogenic and non-neurogenic niches. Gage *et al.* demonstrated that upon transplantation into the adult rat hippocampus, cultured adult hippocampal precursor cells generated neurons that became successfully incorporated in the dentate gyrus (Gage *et al.* 1995). Furthermore, the same precursor cells differentiated into olfactory interneurons when implanted in the RMS of adult rats, but failed to establish a neuronal population in the cerebellum (Suhonen *et al.* 1996), suggesting that adult hippocampal neural precursor cells have

the capacity to generate neurons when provided with the correct neurogenic cues, regardless of their site of origin. Precursor cells isolated from the adult rat spinal cord, a gliogenic but not neurogenic permissive region, differentiated into granule neurons when implanted into the adult hippocampus, which was not seen in the neocortex (Shihabuddin *et al.* 2000). This raises the question of the extent to which neurogenic potential is intrinsic to precursor cells and how much of it is governed by the microenvironment.

The best characterised neurogenic niches in the adult mammalian brain are the SVZ that lines the lateral walls of the lateral ventricles, and the subgranular zone (SGZ), which lies at the interface between the hilus and granular layer (GL) of the dentate gyrus in the hippocampus (further discussed in Section 1.4).

Adult neurogenesis follows a continuous cascade of events that are exemplified in the SVZ (Tramontin *et al.* 2003). In this region, resident NSCs (termed Type B cells) give rise to transit-amplifying cells (Type C cells), that proliferate rapidly to divide into immature neurons (neuroblasts, also termed Type A cells); these subsequently migrate through the rostral migratory stream (RMS) towards the olfactory bulb (OB), where they eventually differentiate into mature interneurons and become incorporated in the olfaction-supporting synaptic circuits (Gonzalez-Perez 2012; Ponti *et al.* 2013). The terms Type B, C, and A cells evolved from the early works that topographically analysed the SVZ niche using electron microscopy, through which these three cell types were identified (Doetsch *et al.* 1997). It is important to note that although there is evidence for a canonical neurogenic region residing in the SVZ of the adult rodent brain, its relevance for the adult human brain is still debated; this will be further discussed in Section 1.6.

Various studies have been published to date regarding the neurogenic capacities of other regions in the adult mammalian brain, including the neocortex, hypothalamus, and striatum (reviewed in Feliciano *et al*. 2015). Neural precursor cells from these regions can be isolated and propagated *in vitro* (albeit with lower cell viability when compared to adult SVZ and hippocampal precursor cell cultures) using paradigms that have been established for adult hippocampal precursor cell propagation (Palmer *et al.* 1999); however, their neurogenic capacity *in vivo,* excluding the hypothalamus (Cheng 2013), is still debated. Pathological conditions

that occur in both neurogenic and non-neurogenic regions are known to induce the production of new neurons. Enhanced neurogenesis, which was detected by increased BrdU incorporation and the expression of the immature neuronal cell marker doublecortin (DCX; Brown *et al.* 2003), was seen in the SGZ and SVZ of rats following focal cerebral ischemia (Mao *et al.* 2002). This has also been reported in other conditions including hippocampal lesions (Gould and Tanapat 1997), epileptic seizures (Geschwind *et al.* 2018), and neurodegenerative diseases such as Alzheimer's and Huntington's (reviewed in Winner *et al*. 2011). Studies have demonstrated that brain injury can lend neurogenic capacity to non-neurogenic regions; Kim *et al.* reported that activated NSCs from the subcallosal zone, a gliogenic region, gained the ability to generate neurons in the cortex following brain injury, although they needed the support of exogenous anti-apoptotic factor and brain-derived neurotrophic factor (BDNF) supplementation (Kim *et al.* 2016). This finding corroborated a previous study by Magavi and colleagues, who demonstrated that a lesion in the adult mouse neocortex prompted the resident precursor cells to switch from a gliogenic to a neurogenic fate, although the authors proposed that migrating neuroblasts from the SVZ, in response to injury, could be the source of these new neurons (Magavi *et al.* 2000). Thus, it can be argued that the SGZ and SVZ are *bona fide* adult mammalian neurogenic regions, and other areas of the brain that harbour neural precursor cells can transition from a pro-gliogenesis to a pro-neurogenesis identity following a stimulus. For the purposes of this thesis, I will concentrate on the adult neurogenic niche in the hippocampus.

1.4 Anatomy of the hippocampus

In the adult mammalian hippocampus, the SGZ is formed of a thin layer of cells that lie between the hilus and the GL of the dentate gyrus, and is responsible for the formation of new glutamatergic granule neurons; these cells relay information from the entorhinal cortex through to the CA3 region through mossy fibres (**Figure 1.1**). This forms the first step of the trisynaptic hippocampal circuit, that is involved in memory processing and long term consolidation (Basu and Siegelbaum 2015).

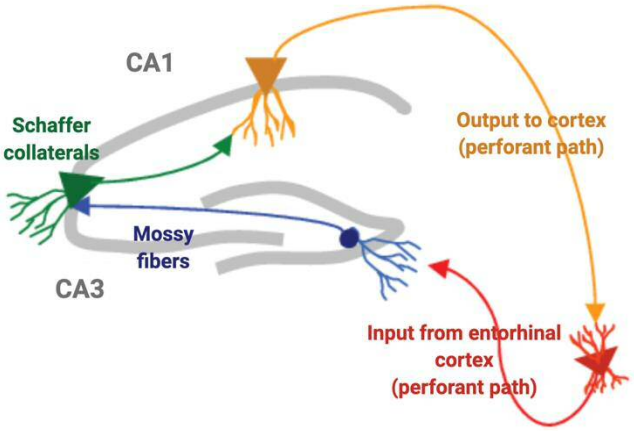

Figure 1.1. Hippocampal trisynaptic circuit - The hippocampal trisynaptic circuit is composed of three synapses, 1) from the entorhinal cortex to the DG through the perforant path, 2) from the DG to the CA3 region via the mossy fibers, and 3) from the CA3 to the CA1 region via the Schaffer collaterals. Image adapted from Castilla-Ortega *et al.* (2011), in Biorender.

The dentate gyrus can be structurally divided into the septal and temporal poles (**Figure 1.2**); studies have shown that both regions display similar neurogenic capacity, although it has been observed that the density of granule cells in the septal dentate gyrus is greater than the temporal area (Snyder *et al.* 2012). Furthermore, the septal dentate gyrus NSCs have been reported to divide more asymmetrically, and this region features a more rapid maturation of neurons compared to the temporal dentate gyrus; this likely holds functional relevance as the septal dentate gyrus is implicated in memory and the spatial learning process, which requires a continuous supply of new granule neurons, whilst the temporal dentate gyrus is involved in emotional processes (reviewed in Bekiari *et al*. 2015). The septal dentate gyrus can be further subdivided into the suprapyramidal and infrapyramidal blades; neurogenesis rates have been shown to be similar in both blades, but there is a greater BrdU+ proliferative cell population stability, and thus higher neuronal survival in the former (Snyder *et al.* 2012; Chryssa Bekiari *et al.* 2015). In this study, I will focus on neurogenesis in the suprapyramidal blade of the septal dentate gyrus, as it has previously been suggested that the suprapyramidal blade contains a greater

proportion of active granule neurons, and thus modulation of NSCs in this blade may have a greater effect on hippocampal functionality (Schmidt *et al.* 2012).

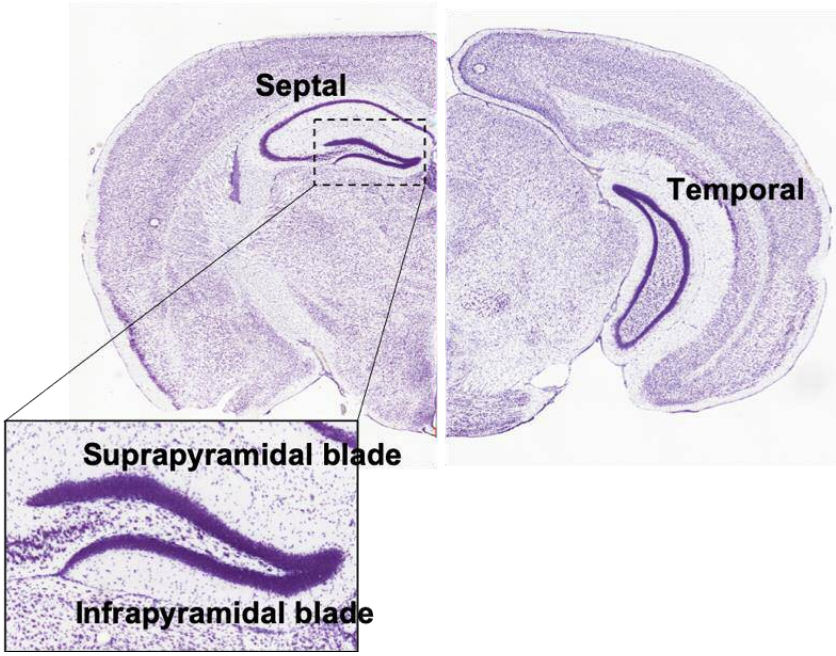

Figure 1.2. Anatomy of the rodent dentate gyrus - The septo-temporal axis of the hippocampus is established during development, and there are differences in the neurogenic capacities and contributions of the dentate gyrus along this axis. The dentate gyrus can be further divided into the suprapyramidal and infrapyramidal blades. Image adapted from the Paxino's Mouse Brain Atlas (2001).

1.5 Neurogenesis in the adult hippocampus

The process of adult hippocampal neurogenesis begins with the division of hippocampal NSCs (termed Type 1 cells, Section 1.5.1) in the SGZ to produce highly proliferative intermediate progenitor cells (Type 2 cells, Section 1.5.2) that give rise to neuronal lineage-committed neuroblasts (Type 3 cells, Section 1.5.3), which in turn fully differentiate into immature neurons (Kempermann *et al.* 2004). Immature neurons subsequently undergo maturation and become incorporated in the granule cell layer. This complex chain of events spans approximately three to four weeks, with full neuronal maturation requiring a further two to three weeks (Kee *et al.* 2007; Gu *et al.* 2012; Vivar and van Praag 2013). Contrary to the long distance that SVZ-originated neuroblasts travel to reach their maturation destination in the OB bulb, hippocampal neuroblasts migrate a short distance into the granule layer (GL) to mature into granule neurons (**Figure 1.3**).

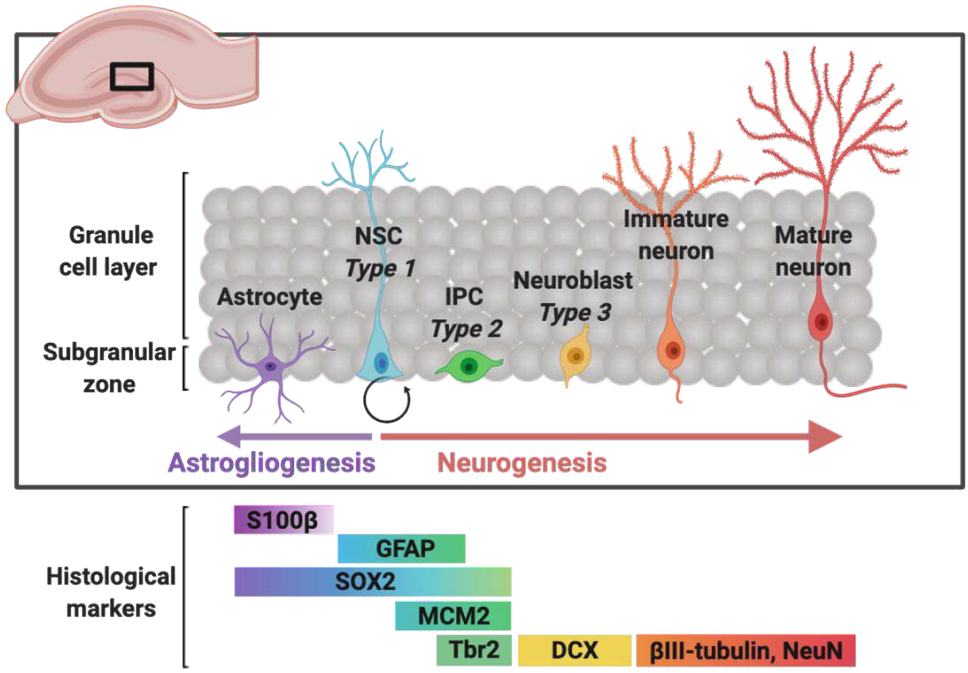

Figure 1.3. Adult hippocampal neurogenesis and gliogenesis - Both neurogenesis and gliogenesis occur in the adult hippocampus, stemming from the Type 1 cell population located in the SGZ. The process of neurogenesis encompasses a sequential series of steps through which various intermediary cell populations are derived, which eventually become neuronally-committed and mature into functional neurons that can become integrated in the established hippocampal networks. At each stage of the process, cell identity can be distinguished by the histological markers that these cells express. Image created in Biorender.

1.5.1 Hippocampal type 1 cells

Hippocampal type 1 cells, that are also termed radial glial-like (RGL) cells due to their shared morphological features and marker expression similarities with embryonic RG cells (described in section 1.2), are the fount for adult-born granule neurons. The characteristic triangular soma of Type 1 cells is situated in the SGZ, and a radial process projects from the soma spanning the GL and ending in the molecular layer (ML), making contact with synapses and vasculature.

Type 1 cells share characteristics of astrocytes in the hippocampus: Seri and colleagues demonstrated that subsequent to the ablation of actively diving cells with cytostatic drugs, the first cells to reappear are proliferative GFAP-expressing cells with a radial morphology (Seri *et al.* 2001). This also elucidates the existence of a subpopulation of "quiescent" NSCs, which evade the anti-mitotic treatment due to their low proliferation rates and can subsequently repopulate the hippocampal neurogenic niche. Furthermore, the authors also reported that when either GFAP or nestin-expressing Type 1 cells were infected with an avian virus carrying the alkaline phosphatase reporter gene, labelled-immature neurons were detected by 15 days post-infection. In addition to their radial morphology and GFAP expression, hippocampal Type 1 cells also exhibit electrophysiological characteristics inherent to astrocytes, such as passive conductance (Filippov *et al.* 2003).

Over the years, extensive research has been carried out to elucidate the heterogeneity of Type 1 cells, and in a unifying manner, the evidence generated thus far indicates the existence of a quiescent and an active hippocampal stem cell population. Lugert and colleagues characterised two distinct Notch signalling-responsive Type 1 cell populations that could be morphologically distinguished as radial quiescent cells, or horizontally-placed activated cells (Lugert *et al.* 2010). Moreover, they also reported that these two cell populations demonstrated selective responses to stimuli, with physical exercise inducing the activation of the former, and epileptic seizures promoting the amplification of the latter. A few years later, a study led by Amelia Eisch reported antigenic heterogeneity of Type 1 cells, with distinctive functions of GLAST- and nestin-expressing Type 1 cells (Decarolis *et al.* 2013); whilst GLAST+ Type 1 cells were able to contribute to hippocampal neurogenesis in both

stimulation (wheel running) and ablation (AraC-induced anti-mitotic) of neural progenitor experiments, nestin+ Type 1 cells lacked this ability. Furthering the previous research on Type 1 cell heterogeneity, Gebara *et al*. reported the existence of an α and a β Type 1 cell population; Type 1α cells represented approximately 75% of RGL cells and featured a long radial process that extended into the molecular layer, with expression of NSCs markers such as GFAP, SOX2, SOX1, Prominin1, and nestin; meanwhile, Type 1β cells constituted 25% of RGL cells, had shorter processes that were limited to the GL layer, and expressed GFAP, SOX2, GLT1 and S100β, with a subset further expressing NSCs markers SOX1, Prominin1, and nestin (Gebara *et al.* 2016). Akin to the previously discussed study, Type 1α cells were able to generate neurons, astrocytes, and Type 1β cells, whilst the latter population did not display proliferative abilities. The authors suggested that Type 1α cells may represent the NSCs of the hippocampus, whilst Type 1β cells are possibly a transformative intermediate in the generation of hippocampal astrocytes.

Thus, efforts to characterise the hippocampal Type 1 cell have revealed a level complexity that is indicative of cell subpopulations, which differ in their state of quiescence and activation.

1.5.2 Type 2 cells

The immediate progeny of Type 1 cells are transit-amplifying (or intermediate progenitor cells; IPCs) cells known as Type 2 cells, which undergo extensive proliferation and rapid turnover. The purpose of this intermediary cell population is to provide a rapidly expanding pool of yet undifferentiated cells lacking self-renewal capacity. Importantly, their expansion is limited, with a live imaging study of hippocampal precursors *in vitro* suggesting up to five division cycles (Costa *et al.* 2011). More recently, a separate study utilised *in vivo* live imaging of the adult hippocampus to demonstrate that non-radial progenitors divide asymmetrically up to six times, which amplifies the pool of non-radial progenitors whilst giving rise to a neuronal lineage-specified cell (Pilz *et al.* 2018); this novel finding evidences the clonal expansion that takes place at the Type 2 cell stage.

Type 2 cells can be subdivided into Type 2a and Type 2b cells, which both continue to express nestin and high levels of proliferative markers (e.g. Ki67). Type

2a cells display more glial characteristics and stain positive for BLBP and SOX2, whereas Type 2b cells show a more neuronal phenotype and express both doublecortin (DCX) and polysialylated-neural cell adhesion molecule (PSA-NCAM), markers of immature neurons (Kronenberg *et al.* 2003; Steiner *et al.* 2006). Type 2 cells also express the transcription factor TBR2, which binds to and inhibits SOX2 expression, thus rendering it essential for the successful transition from stem cells to committed neuronal progenitor cells (Hodge *et al.* 2012).

1.5.3 Type 3 cells and neuronal maturation/integration

Type 2 cells proliferate and give rise to migratory Type 3 cells, also termed neuroblasts. These cells lack nestin, but express early neuronal markers including DCX, the granule cell and hilar interneuron marker PROX1 (Prospero Homeobox protein 1), and NeuroD1 (Neurogenic Differentiation factor 1; reviewed in Zhang and Jiao 2015). Neuroblasts migrate tangentially along blood vessels (Sun *et al.* 2015), moving short distances within the inner GL where they further differentiate into granule cells, that express markers of mature neurons such as NeuN (Rbfox3) and Ca^{2+}-binding calretinin. Programmed cell death at this stage is critical to control the overall neuronal numbers as well as to ensure correct formation of circuits; remarkably, a BrdU-label retention study, and other supporting studies, have demonstrated that 30-70% of immature neurons undergo apoptosis during the first four weeks after their birth in the rodent dentate gyrus, following which the surviving neurons were found to persist for a minimum of five months (Dayer *et al.* 2003; Sierra *et al.* 2010; Encinas *et al.* 2011). The surviving granule neurons feature a maturation switch from calretinin to calbindin expression, and establish neuronal polarity through the extension of dendritic branches towards the ML and axonal projections into the hippocampal CA3 region. They initially demonstrate excitatory responses to inhibitory GABAergic signalling, with a subsequent ionic composition change with maturation, following which these inhibitory stimuli induce neuronal hyperpolarisation. The main function of granule cells is to become integrated into the established hippocampal trisynaptic circuit, where they transmit entorhinal afferents to the CA3 region via hilar mossy fibres (Toni and Schinder 2016).

1.6 Evidence for neurogenesis in the adult human hippocampus

A key question that emerged since the discovery of adult hippocampal NSCs and neurogenesis in mammals was how much of the evidence derived from animal models applies to the adult *human* brain (reviewed in Petrik and Encinas 2019). The invasive nature of current technologies employed in neurogenesis studies renders such endeavours highly challenging and most studies involving human tissue are consequently reliant on indirect evidence. The initial study that put adult human neurogenesis in the spotlight was led by Fred H. Gage and Peter Eriksson, who reported the post-mortem hippocampal detection of labelled neurons in the brains of cancer patients treated with BrdU (Eriksson *et al.* 1998). Nearly 12 years later, Knoth and colleagues demonstrated that DCX-immunoreactive immature neurons are found within the dentate gyrus from 0-100 years old human brains, that co-express markers of proliferation and mature neurons, albeit with a decreasing marker immunoreactivity with age (Knoth *et al.* 2010). In the same vein, a separate study recently investigated hippocampal tissue from healthy human brains aged 14-79 years, and found that despite a decreasing pool of quiescent stem cells, the numbers of intermediate progenitor cells, immature neurons, and granule neurons were sustained across the increasing ages (Boldrini *et al.* 2018). These findings provide evidence in favour of human hippocampal neurogenesis that persists to an indeterminate extent throughout adulthood.

These studies have been further supported with research of adult human neurogenesis in the SVZ. A study published in 2004 demonstrated the colocalisation of DCX and cell proliferation markers such as Ki67, as well as other early neuronal-lineage commitment markers such as calretinin, in the post-mortem adult OB (Bédard and Parent 2004). Corroborating these findings, Curtis and colleagues described the existence of a human RMS that encased an extension from the lateral ventricles to the OB, and harboured a stream of migrating neuroblasts (Curtis *et al.* 2007). These important studies established the actuality, whether that was context-dependent or globally applicable, of neurogenesis in the adult human SVZ. Importantly, the use of immunohistochemical post-mortem tissue labelling techniques in aged brains must be evaluated with the caveat that cells in

neurodegenerative conditions may express a differential panel of markers to healthy cells in response to stress, thus potentially reporting false positive immunoreactivity.

With the development of a new technique for birthdating neurons using carbon-14 dating, Frisen *et al.* reported that a substantial amount of neurogenesis takes place in the adult human hippocampus, with the addition of about 700 new neurons on a daily basis, and an annual turnover of 1.75% (Spalding *et al.* 2013), although high interindividual variability was seen which was alluded to potential psychiatric conditions.

Alvarez-Buylla and colleagues challenged the pro-adult human neurogenesis belief and published a study in 2004, in which they identified a population of SVZ-residing astrocytes that show proliferative capacity *in vivo* and could generate multiple cell lineages *in vitro*. Furthermore, although they found evidence of a structure akin to the RMS leading to the OB, they did not observe migrating immature neurons in this structure (Sanai *et al.* 2004). A follow-up study investigated SVZ neurogenesis during the human lifespan ranging from infancy to adulthood, and reported a migrating immature neuroblast population in the RMS that originated in the SVZ, in infants up to the age of 18 months, following which there was a decline in this migrating neuroblast population, to rarely identified in the adult brain (Sanai *et al.* 2011). This was validated by Sorrells and colleagues who reported a steep decline in the number of new neurons incorporated into the granule layer during the first few years after birth in humans and other non-human primates, and subsequently this number became negligible in adults (Sorrells *et al.* 2018).

This library of conflicting evidence casts uncertainty over the homology of adult mouse and human physiology. Nevertheless, based on the increasing number of studies that have provided some form of evidence implying neurogenesis in the adult human brain, as well as the increasing demands and consequential complexity of brain function with age, it is likely that the human brain is not a completely post-mitotic structure and displays a certain level of plasticity throughout adulthood to support the functional demands.

1.7 Determinants of neurogenesis

Adult neurogenesis is a highly dynamic process susceptible to modulation by a variety of cell extrinsic and local intrinsic factors. These determinants influence three key stages of the process: the proliferation of the precursor cells, the cell fate specification decision, and the survival of newly generated neurons. It must be appreciated that the regulation of adult neurogenesis is multifaceted and the separate cell extrinsic and intrinsic mechanisms that govern stem cell activity are deeply interlaced, as the latter function to intracellularly relay signals from the former. Here I will first introduce some environmental/cell extrinsic factors and then discuss the underlying paracrine and intracellular molecular mechanisms that regulate the behaviour of NSCs and their immediate progeny; these are summarised in **Figure 1.4.**

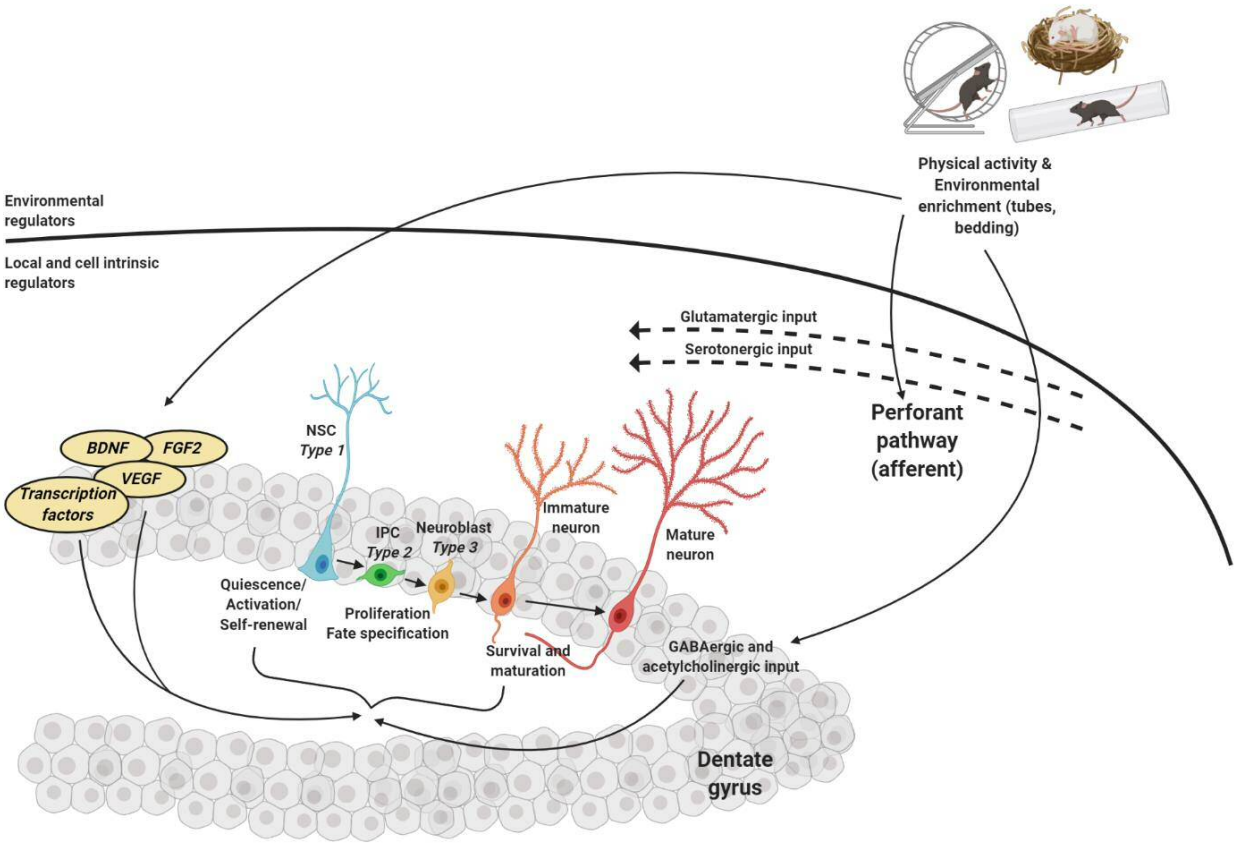

Figure 1.4. Environmental and local/intracellular regulators of adult hippocampal neurogenesis. Image created in Biorender.

1.7.1 Cell extrinsic

The broadly termed "cell extrinsic" factors that alter an animal's acquired experiences and can dynamically regulate adult hippocampal neurogenesis include both negative regulators such as age and extreme stress levels, as well as positive influencers such as exercise and environmental enrichment, both of which present themselves as moderate stressors.

1.7.1.1 Age

One of the first seminal studies to provide evidence for the age-related decrease in adult rodent hippocampal neurogenesis was published by Kuhn and colleagues, who suggested that both a decrease in the proliferative activity of progenitor cells, as well as a decrement in the correct development of newborn neurons underlies this phenomenon (Kuhn *et al.* 1996). Since then, significant research has been carried out to address the effectors in the age-related reduction in neurogenesis, and various hypotheses have been proposed.

Two such seminal studies were published simultaneously in 2011 and contested different views regarding the long-term self-renewal of hippocampal Type 1 cells in ageing. Encinas and colleagues used predominantly a fluorescent nestin-GFP transgenic mouse line to track neural stem and progenitor cell populations, coupled with BrdU labelling to analyse proliferation and long-term lineage commitment of these cells (Encinas *et al.* 2011). Based on their observations, the authors proposed that the NSC pool is exhausted with time through a limited number of cell divisions upon activation, with their terminal transformation into astrocytes; this was evidenced by the reduced detection of the former labelled population, and a simultaneous increase in the label-retaining latter cell population (Encinas *et al.* 2011). In contrast, Bonaguidi and colleagues used a fluorescent nestin-Cre based approach to label a sparse population of quiescent Type 1 cells with application of low dose tamoxifen, to allow for long-term lineage tracing of individual clonal clusters (Bonaguidi *et al.* 2011); this study suggested that the NSC population has the ability to self-renew as well as to generate neurons and astroglia throughout adulthood, with a sustained NSC pool for continued neurogenesis throughout the lifetime of an animal (Bonaguidi *et al.* 2011). Although these two studies arrive at

seemingly conflicting conclusions, it may be that they are two sides of the same coin, and the self-renewal capacity of Type 1 cells is subpopulation, as well as context-dependent. The study by Bonaguidi *et al.* identified some subclones that were either unipotent, or completely lacking Type 1 cells, which suggests terminal division of Type 1 cells, whilst the majority contained at least one Type 1 cell. This indicates a level of heterogeneity within the self-renewal capacity of individual Type 1 cells; as Encinas and colleagues assessed the population of labelled Type 1 cells on the whole, alongside their subsequent progeny, this would have rendered the detection of heterogeneity irresolvable. It is also conceivable that the adult NSC population is generally "disposable" and will become exhausted over time, but individual NSCs can be challenged to realise their neurogenic potential by pro-neurogenic stimuli; this also contributes to the heterogeneity of adult NSCs. Furthermore, Bonaguidi and colleagues carried out their study in 8-10 week old mice (with a follow-up at 12 months post-induction), whilst Encinas and his group performed birthdating at various ages that ranged from 3 weeks to 24 months; it is possible that the discrepancy between the two studies may be explained by age, by which the continuous self-renewal model applies at a younger age, but as animals become aged, the stem cell pool becomes increasingly depleted, reflecting the disposable-stem cell model.

Thus, although no consensus has been reached regarding the maintenance of a self-renewing subpopulation of adult rodent NSCs, it is possible that with increasing age, the majority of NSCs become depleted due to division-coupled lineage commitment, but a small subset (that varies between individuals) of NSCs may persist.

1.7.1.2 Stress

Stress constitutes one of the most significant external factors influencing neurogenesis and affects progenitor cell proliferation as well as the survival of newborn neurons. However, rather than inhibiting neurogenesis linearly, the graphical relationship between stress and neurogenesis has an inverted U-shape (reviewed in Saaltink and Vreugdenhil 2014): low stress levels, defined by a sedentary lifestyle or a poorly-enriched environment, stimulate low levels of cell proliferation,

whilst mild levels of controlled stress, such as environmental enrichment, physical activity, and animal handling (Parihar *et al.* 2011), stimulate cell proliferation and the integration of neurons in the hippocampal circuit. By contrast, high levels of stress, e.g. by introducing animals to situations with predator stress, physical restraint, or foot shocks, cause a downregulation in neurogenesis (Lagace *et al.* 2010).

1.7.1.2.1 Environmental enrichment (EE)

The housing environment of laboratory rodents can be enriched through the provision of a larger cage, or toys and tunnels to encourage exploratory behaviour and spatial awareness. This enhances the motor, sensory, and cognitive abilities of the animals (Sampedro-Piquero and Begega 2016). The first report that identified environmental enrichment as a key regulator of adult neurogenesis was published in 1997 (Kempermann, H. G. Kuhn, *et al.* 1997); the authors reported that although there was no difference in the number of proliferating cells that incorporated BrdU at 1 day post-treatment between two groups of mice of which one was housed with enrichment provisions and the other in standard housing conditions, by 4 weeks the experimental group displayed an increased number of BrdU-labelled cells in comparison to their control counterparts, which suggested that EE enhances the survival of newborn hippocampal cells rather than the proliferation of progenitor cells. A study published a decade later utilised a short 24-hour EE exposure paradigm and reported a specific increase in the number of BrdU+Prox1+ Type 3 cells, evidencing the effects of EE on the postmitotic cells in the neurogenic niche (Steiner *et al.* 2008). Several other studies have further highlighted the effects of EE on the enhancement of neurogenesis as well as subsequent hippocampus-dependent functional benefits, with a markedly improved performance in memory tasks involving spatial navigation and pattern separation (Nilsson *et al.* 1999; Speisman *et al.* 2013; Garthe *et al.* 2016; further reviewed in Eisinger and Zhao 2018).

The molecular mechanisms involved in the EE-driven enhancement of cell survival in the hippocampus include the upregulation of brain-derived neurotrophic factor (BDNF; this will be discussed further in the context of neurogenesis in Section 1.7.2.2), and other neurotrophic factors including glial-derived neurotrophic factor (GDNF), and neurotrophin-3 (NT-3; Ickes *et al.* 2000; Gualtieri *et al.* 2017). GDNF has

been shown to promote cell proliferation and neuronal differentiation (Chen *et al.* 2005), whilst NT-3 contributes to increasing neurite outgrowth and branching, as well as neuronal survival (Morfini *et al.* 1994; Bertollini *et al.* 1997).

1.7.1.2.2 Physical activity

The effects of physical activity in rodents are studied through the provision of a running wheel, and this has been shown to benefit neurogenesis in the adult brain (Van Praag *et al.* 1999; Huang *et al.* 2018). However, unlike EE, physical activity enhances the proliferation of progenitor cells; Kronenberg and colleagues demonstrated that voluntary wheel running induced progenitor cell proliferation (predominantly in Type 1 and Type 2 cells) which peaked as early as at 3 days of running (Kronenberg *et al.* 2006). Physical activity promotes the concentration of trophic factors including BDNF, fibroblast growth factor 2 (FGF2), and vascular endothelial growth factor (VEGF), and these will be discussed later in more depth regarding their role in enhancing neurogenesis (Gómez-Pinilla *et al.* 1997; Adlard *et al.* 2004). Importantly, further evidence supports the additive benefits of EE and physical activity in comparison to the presence of a single stimulus (Fabel *et al.* 2009).

1.7.2 Molecular mechanisms for executing extrinsic signals

The hippocampal neurogenic niche is highly complex and home to a myriad of intricately linked signaling cues that influence important decisions underlying long-term self-renewal and lineage specification of NSCs. Morphogens, trophic factors, and neurotransmitters modulate the behaviour of NSCs and their progeny via the triggering of intracellular signaling pathways, and are themselves mediators of extrinsic factor-induced regulation, such as the above-discussed exercise and environmental enrichment.

Although several cell types, including astrocytes, microglia, and endothelial cells, reside within the neurogenic milieu and contribute to the activity-dependent regulation of neurogenesis, neuronal activity is one of the predominant mediators of intracellular regulation of neurogenesis, upon receiving environmental cues. Thus, I will focus on neurotransmitters and neuronally-derived factors as two of the major molecular mechanisms that act as an interface for the regulation of adult neurogenesis through environmental influences.

1.7.2.1 Neurotransmitters

The contribution of neuronal activity in the regulation of hippocampal neurogenesis has become increasingly accepted with studies demonstrating the effects of blocking specific neuronal signaling pathways.

Glutamatergic signaling links the entorhinal cortex to the dentate gyrus through fibres spanning the perforant pathway. As the main excitatory neurotransmitter, glutamate provides balanced regulation of hippocampal neurogenesis through its various receptors: the N-methyl-D-aspartate (NMDA), kainic acid (KA), and a-amino-3-hydroxy-5-methyl-4-isoxazole propionic acid (AMPA) receptors. The expression of NMDA receptor subunits NR1 and NR2B is found in Type 1 cells as well as a number of newly born granule cells 2 weeks following their generation (Nácher *et al.* 2007); this indicates function of NMDA-dependent glutamatergic neurotransmission at the level of precursor cell proliferation and early neuronal survival/maturation stages. Specific inhibition of the NMDA receptor with the antagonist MK-801 led to increased hippocampal neurogenesis under physiological conditions (Gould *et al.* 1994; Mark Redmond *et al.* 1995; Okuyama *et al.* 2004). By contrast, it has been reported that the stimulation of KA receptor-mediated glutamatergic signaling, that produces seizures, results in enhanced hippocampal neurogenesis rates (Jessberger *et al.* 2007); in the same vein, increased hippocampal cell proliferation was also observed with AMPA receptor stimulation (Bai *et al.* 2003). Taken together, this indicates that glutamatergic signaling plays a dual-faceted role in the regulation of hippocampal neurogenesis, through which it maintains a fine balance.

Acetylcholinergic (Ach) input regulates hippocampal cognitive functions involving adult neurogenesis, and loss of this in Alzheimer's disease plays a role in the reduced hippocampal-based memory function that presents as a pathological symptom of the disease (reviewed in Haam and Yakel 2017). Both nicotinic and muscarinic Ach receptors are found on PSA-NCAM+ neuronal precursor cells in the DG, and it is proposed that Ach signaling promotes cell survival in the DG, as the administration of a muscarinic Ach receptor agonist reduced precursor cell survival (Cooper-Kuhn *et al.* 2004; Kotani *et al.* 2006).

Serotonin is synthesized primarily by the raphe nuclei of the medulla oblongata and is subsequently projected to the hippocampus through the afferent pathway. It has been shown that that the use of selective serotonin reuptake inhibitors (SSRIs), which are common antidepressant drugs, results in the enhancement of adult neurogenesis (Malberg *et al.* 2000; Wang *et al.* 2008). In particular, fluoxetine was demonstrated to target early intermediate progenitor cells (Type 2a) by increasing the number of symmetric divisions, with the expansion of these cells later manifesting in increased neuronal numbers (Encinas *et al.* 2006). Interestingly, a link between serotonergic signaling and BDNF has been drawn in the induction of neurogenesis, as it has been demonstrated that serotonin upregulates BNDF levels, which subsequently increases neurogenesis (reviewed in Foltran and Diaz 2016).

GABA (γ-aminobutyric acid) acts as the main inhibitory neurotransmitter in the adult CNS and its levels are controlled by multiple classes of interneurons in the dentate gyrus. GABAergic inputs have been shown to affect several key stages in the process of adult neurogenesis, including Type 1 cells quiescence, neuroblast migration, and neuronal differentiation. Parvalbumin-expressing interneurons within the adult DG have been shown to release GABA that subsequently inhibits quiescent Type 1 cell activation through the γ2-subunit of the GABA-A receptor, and conditional deletion of this specific subunit allows Type 1 cells to become activated and undergo symmetric self-renewing divisions (Song *et al.* 2012). Meanwhile, the effects of GABAergic signaling on neuroblast migration are subunit-dependent, as mice lacking the α4 subunit display reduced migration, whilst α2-subunit deficiency results in a greater distance migrated into the GL. GABA also plays a significant role in the differentiation of Type 2 cells, through the induction of NeuroD expression; the $GABA_A$ receptor has been implicated in this process, and a receptor-specific agonist was found to strongly increase the number of new BrdU-labelled neurons (Tozuka *et al.* 2005).

1.7.2.2 Growth/neurotrophic factors

Neurotrophic and growth factors have a recognized role in promoting the proliferation and differentiation of NSCs, both in the developing and adult CNS. These

include, to name a few, brain-derived neurotrophic factor (BDNF), fibroblast growth factor 2 (FGF2), and vascular endothelial growth factor (VEGF).

The pro-neurogenic function of BDNF has been widely studied in the adult DG and has been shown to activate intracellular pathways, such as the mitogen-activated protein kinase (MAPK) and phosphoinositide 3-kinase (PI3K) pathways, via the tropomyosin receptor kinase (Trk) receptors type A and B, which allow it to upregulate both neurogenesis and the survival of adult-born neurons (Duman and Monteggia 2006). Previous studies have reported that separate models of BDNF and TrkB depletion demonstrated decreased levels of hippocampal NSC proliferation and neurogenesis (Lee *et al.* 2002; Li *et al.* 2008), whilst exogenous administration of BDNF induced the development of new neurons (Waterhouse *et al.* 2012; Quesseveur *et al.* 2013).

The importance of FGF2 in the maintenance of the neurogenic niche was initially raised in experiments that investigated the establishment and propagation of neurospheres *in vitro* (Ray *et al.* 1993; Deleyrolle and Reynolds 2009). Since then, studies have reported that the knockout of FGF2 and its receptors leads to a decrement in NSCs, and their subsequent progeny (Werner *et al.* 2011; Kang and Hébert 2015). FGF2 maintains NSC proliferation rates by modulating key cell cycle proteins, including the upregulation of cyclin D2 and the downregulation of the cyclin-dependent kinase inhibitor $p27^{kip1}$ (Lukaszewicz *et al.* 2002; Maric *et al.* 2007). In addition, FGF2 has also been identified as an important factor for the differentiation and maturation of neurons, evidenced by the promotion of neurogenesis and enhanced neuronal dendritic growth in response to FGF2 (Jin *et al.* 2003; Rai *et al.* 2007).

Vascular endothelial growth factor (VEGF) is an angiogenic factor with important proliferative functions in the DG. It has been demonstrated that the intracerebroventricular administration of VEGF promotes proliferation and neuronal differentiation in the hippocampus (Jin *et al.* 2002). Importantly, Kirby and colleagues have shown that SGZ-residing neural stem and progenitor cells express and secrete VEGF both *in vivo* and *in* vitro and the targeted ablation of stem and progenitor cell-derived VEGF resulted in the disruption of stem cell maintenance in the hippocampal neurogenic compartment (Kirby *et al.* 2015). Furthermore, in a separate study, the

deleterious effects on neurogenesis *in* vivo following the knockout of VEGFB, a member of the VEGF family, were restored with the intraventricular administration of VEGFB, indicating the importance of signaling through this angiogenic factor for sustained neurogenesis (Sun *et al.* 2006).

1.7.2.3 Transcription factors

Transcription factors (TFs) tightly regulate the progression of events in adult neurogenesis, spanning the proliferation of NSCs through to their differentiation into mature neurons, by inducing changes in gene expression. It can be argued that they are the main regulators of this complex process, and other regulatory influences, such as environmental factors, act through transcriptional changes to modulate neurogenesis. Loss-of- and gain-of-function studies are popular tools to dissect how transcription factors regulate neurogenesis.

Here, I will briefly discuss some of the transcription factors that are known to regulate NSCs and their immediate progeny in the adult hippocampus (summarised in **Figure 1.5**).

1.7.2.3.1 Type 1 cell self-renewal and proliferation maintenance

The self-renewal and proliferation of Type 1 cells is tightly regulated by an interlinked signalling cascade formed by several transcriptional regulators; notable factors that have been focused on greatly in research include SOX2, TLX, REST, Notch, Pax6, and FoxO3.

The family of SRY-related high mobility group (HMG) box transcription factors (SOX) is highly conserved in vertebrates and regulates cell fate specification and differentiation during development. The HMG box allows the SOX transcription factors to bind specific DNA motifs, resulting in either activation or repression of gene expression. There are 20 known SOX proteins, and based on a sequence identity greater than 80% in the HMG domain, they are divided into 8 families, with some functional redundancy between proteins of the same families (Wegner 2010); SOXB1 family members are involved in the maintenance of NSCs, whilst SOXC proteins have been linked to the induction of neuronal differentiation, which will be further discussed in Section 1.7.2.3.2.

SOX1-3 are members of the SOXB1 family and these proteins play roles in neurogenesis and stem cell maintenance; they are expressed in both radial and horizontal GFAP+/nestin+ hippocampal Type 1 cells as well as early proliferating Type 2a cells in the hippocampus (Steiner *et al.* 2006), and in the corresponding cell types in the SVZ (Steiner *et al.* 2006). A conditional nestin-dependent ablation of SOX2 resulted in the complete loss of all hippocampal cell types, indicating its crucial role in the maintenance of the hippocampal neurogenic niche, through its expression in nestin+ progenitor cells (Favaro *et al.* 2009).

SOX2 is widely regulated by other signalling cues within Type 1 cells, such as Notch/RBPJk signalling; Ehm and colleagues showed that the inactivation of RBPJk, a major effector of Notch signalling, resulted in the downregulation of SOX2 in progenitor cells, leading in turn to their premature neuronal differentiation (Ehm *et al.* 2010). On the contrary, akin to a master regulator, SOX2 can also regulate the downstream expression of various factors that are essential for the self-renewal of stem cells. These include the positive regulation of the orphan receptor tailless (TLX) (Islam *et al.* 2015) and Sonic hedgehog (Shh) (Favaro *et al.* 2009). SOX2 also prevents the expression of the pro-neuronal factor NeuroD, through the inhibition of Wnt signalling (Gao *et al.* 2009).

The nuclear orphan receptor TLX is expressed in Type 1 cells, and functions to maintain the proliferation competence of these cells through the canonical Wnt signalling pathway, whilst also possibly repressing pathways that enhance NSC quiescence, including the p53 and PTEN-PI3K signalling pathways (Qu *et al.* 2010; Niu *et al.* 2011). There is evidence that TLX silences the expression of its target genes through the recruitment of histone deacetylases HDAC3 and HDAC5 as well as histone demethylase lysine-specific demethylase 1 (Sun *et al.* 2007; Qu *et al.* 2010).

Repressor element 1-silencing transcription factor (REST) suppresses the expression of neuronal genes in Type 1 and early Type 2 cells, and is also expressed in low levels in mature granule neurons. A study has demonstrated the biphasic effects of conditional REST deletion in Type 1 cells: initially, REST ablation resulted in an increased proliferation of Type 1 cells, whilst at a later timepoint there was a decrease in Type 1 cell proliferation accompanied by the induction of genes involved in neuronal differentiation, including NeuroD1 (Gao *et al.* 2011; Kim *et al.* 2015).

Thus, REST may play a key role in the prevention of precocious neuronal differentiation of NSCs.

Notch is both a signalling pathway as well as a transcriptional regulator, and it is one of the prominent and best understood pathways in the regulation of stem cells and lineage specification. The binding of Notch ligands expressed on adjacent cells to the cell surface-bound Notch receptor causes the proteolytic cleavage and release of its active intracellular domain; this subsequently translocates into the nucleus where it forms a transcriptional complex that upregulates the expression of pro-stemness genes. Importantly it has been shown that Notch signalling is a key promoter of NSC self-renewal. Ablation of Notch signalling depletes the Type 1 cell population through their terminal neuronal differentiation (Imayoshi *et al.* 2010). The main functions of Notch signalling can be divided across two phases of the neurogenic process; the maintenance of the NSC pool (Ables *et al.* 2010), and cell lineage determination; studies have demonstrated that Notch signalling suppresses neurogenesis and promotes gliogenesis through downstream activation of GFAP and HES genes, the latter of which downregulate pro-neuronal genes (reviewed in Zhou *et al*. 2010).

The paired box 6 (Pax6) transcription factor is expressed in GFAP and nestin-expressing NSCs and early progenitor cells as well as a subset of early Type 3 cells. The levels of Pax6 in NSCs have been correlated with a fine balance between self-renewal and induction of neurogenesis; it has been shown that the ablation of Pax6 resulted in decreased NSC self-renewal, with an increase in the number of cells undergoing neuronal differentiation in the dentate gyrus (Maekawa *et al.* 2005).

The forkhead box protein O3 (FOXO3) is a member of the FoxO family of transcription factors that are named after their distinct forkhead DNA-binding domain. FoxO3 is expressed in adult NSCs and early progenitor cells, and its deficiency in the SGZ has been reported to prevent the return of NSCs to quiescence, which leads to the depletion of the stem cell pool as well as long-term decrease in neurogenesis (Paik *et al.* 2009; Renault *et al.* 2009).

1.7.2.3.2 Cell lineage specification and differentiation

Akin to the regulation of Type 1 cell self-renewal and proliferation, there are various transcription factors that mediate the processes of cell fate specification and neuronal differentiation in the neurogenic programme.

Intermediate progenitor cells (IPCs) form a transient neuronal-lineage committed cell pool in the differentiation transition between NSCs and immature neurons (see section 1.5.2); the T-box brain protein 2 (TBR2; also known as eomesodermin) transcription factor is expressed primarily during this transition period in Type 2 cells. In a Tbr2-driven fluorescence transgenic line, it was shown that IPCs were exclusively labelled, and further lineage tracing revealed their unipotent capacity to generate immature neurons (Berg *et al.* 2015). Supporting this, a separate study reported that following the deletion of Tbr2, there was a decrement in neuronal differentiation, suggesting TBR2 is necessary for the correct development of neurons from IPCs in the adult brain (Hodge *et al.* 2012). Interestingly, the same study also reported an increased proliferation of quiescent radial Type 1 cells, as well as activated Type 2a cells, resulting in an accumulation of these two cell populations due to the downstream blockaded neuronal differentiation. The authors proposed that TBR2 stimulates the neuronal fate commitment of Type 1 cells through the inhibition of SOX2 expression.

Mammalian achaete-scute homolog (Mash1, or also ASCL1), is a basic helix-loop-helix transcription factor that also promotes proliferation and neuronal specification in dividing Type 2 cells (Uda *et al.* 2007). ASCL1 expression levels have been demonstrated to affect its function in the adult hippocampus; oscillating expression of ASCL1 induced the proliferation of progenitor cells, whilst stable levels promote neuronal differentiation (Imayoshi *et al.* 2013). This may be due to the inhibition of Ascl1 by Notch, which has previously been evidenced by increased ASCL1 expression following loss of RPBJk/Notch signalling in NSCs, as well as the predominant absence of ASCL1 in quiescent NSCs (Andersen *et al.* 2014). The initial decrease in Notch signalling when quiescent NSCs become activated may trigger the oscillation of ASCL1 2015 levels, which eventually stabilise with complete loss of Notch-driven quiescence cues as cells progress in the neurogenic programme.

Contrary to the pro-stemness function of SOXB family members, SOXC family proteins SOX4 and SOX11 have been implicated in the induction of neuronal differentiation, with their localisation predominantly in the adult neurogenic zones. The two SOXC proteins are expressed in Type 2b cells, with the co-expression of DCX (Haslinger *et al.* 2009; Mu *et al.* 2012). The SOXC proteins were found to also be co-expressed in cells with NeuroD1, but not the mature granule cell marker Calbindin (Haslinger *et al.* 2009), which suggests that the expression of these two SOX proteins is associated with a neuronal cell fate specification step. Further functional evidence was provided through loss-of and gain-of-function studies; ablation of either SOX4 or SOX11 resulted in the loss of neurogenesis both *in vitro* and *in vivo*, whereas overexpression of the proteins greatly promoted *in vitro* neurogenesis (Mu *et al.* 2012). Thus, SOX4 and SOX11 activate the expression of pro-neuronal proteins with some functional redundancy, although it is also known that SOX4 activates TBR2 to maintain the Type 2 cell population, whilst SOX11 interacts with Neurogenin1 to activate the pro-neuronal gene NeuroD1 (Chen *et al.* 2015).

One of the main transcription factors that regulates the differentiation and maturation of granule neurons is NeuroD1. The expression of NeuroD1 is highest in late Type 2b (>90%) and DCX-expressing Type 3 cells (approximately 100%). Gao and colleagues have demonstrated that NeuroD1 regulates the survival and maturation of neurons in the adult brain, and the depletion of this transcription factor results in irregular granule neuron morphology, indicating the functional importance of this factor in the correct formation of adult-born neurons (Gao *et al.* 2009). Mechanistically, NeuroD1 binds directly to regulatory elements of pro-neuronal genes to activate their transcription, that are otherwise epigenetically silenced (Pataskar *et al.* 2016).

The prospero-related homeobox gene 1 (PROX1) is another pro-neuronal transcription factor that is required for the maintenance of Type 2 progenitor cells as well as their neuronal fate specification; this has been demonstrated in a conditional Prox1 ablation model in which Type 2 cells failed to develop into Type 3 cells, and subsequently, a lack of adult granule neuron generation resulted in a reduced DG size (Lavado *et al.* 2010). Furthermore, a separate study targeted the deletion of Prox1 to post-mitotic granule neuron and reported their subsequent transformation

into CA3 pyramidal neurons (Iwano *et al.* 2012), which suggests that PROX1 plays an important role in the maintenance of granule neuron identity.

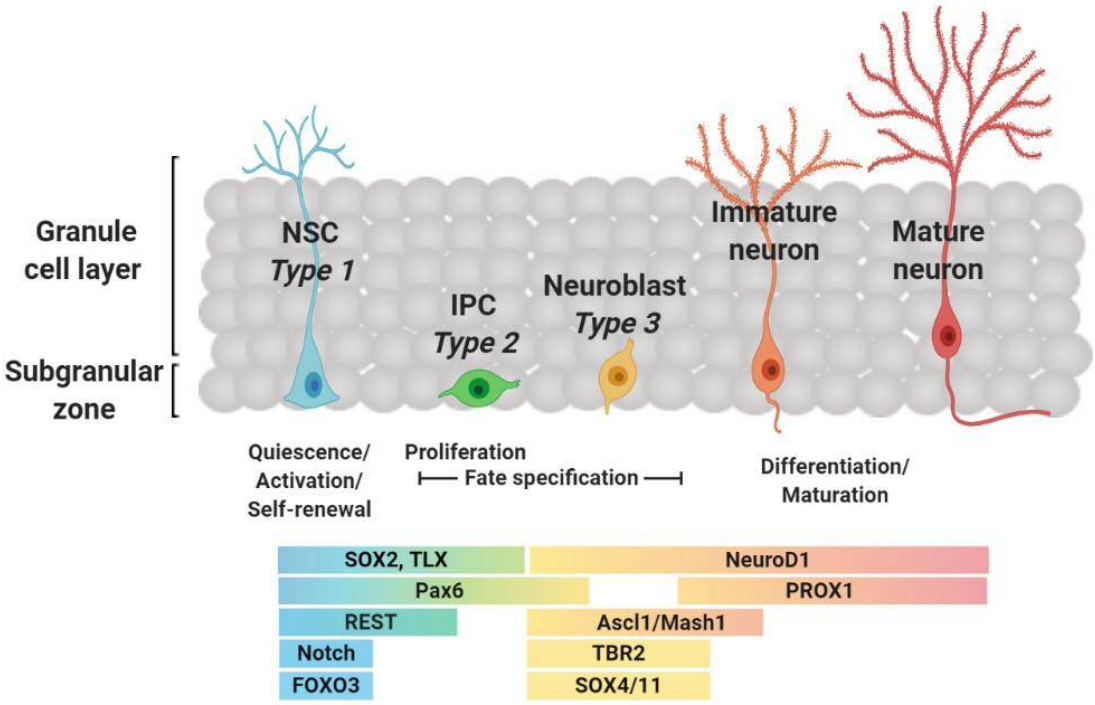

Figure 1.5. Transcriptional regulation of the major milestones in the process of neurogenesis. Image created in Biorender.

1.8 ZEB transcription factors

Having introduced some of the transcription factors that have been identified and studied extensively in adult hippocampal neurogenesis, I will now discuss the ZEB transcription factors, and in particular ZEB1, whose functions in adult neurogenesis are not yet fully understood, but previous studies have implicated this family of transcription regulators in embryonic neurogenesis.

The zinc finger E-box binding homeobox (ZEB) family of transcription factors consists of two multidomain members, ZEB1 (TCF-8, NIL2A, AREB6, δEF1, Zfhep, ZFHX1A) and ZEB2 (also known as SMAD-interacting protein 1; SIP1), encoded by the ZFHX1a gene on human chromosome 10 and mouse chromosome 18, and ZFHX1b gene on human/mouse chromosome 2.

1.8.1 ZEB family and structure

The structural namesake features of these transcription factors are two unique clusters of zinc finger (ZF) domains found at either terminal of the proteins; zinc finger domains are protein structures that are maintained by zinc ions binding different combinations of cysteine (C) and histidine (H) residues for protein structural formation (Cassandri *et al.* 2017). The N-terminal cluster (NZF) of ZEB1 has four ZF domains that (three CCHH and one CCHC), whilst the C-terminal cluster (CZF) has three CCHH ZF domains. There is considerable sequence homology between the NZF (88%) and CZF (93%) of ZEB1 and ZEB2, which indicates that the two factors may have similar DNA-binding affinities; however, the other domains of the proteins share homology to a much lower degree (reviewed in Fardi *et al.* 2019). Functionally, the two zinc finger clusters bind a DNA response element, termed the enhancer box (E-box) with the canonical sequence 5'-CANNTG-3' in the promoters of their target genes (Llorens *et al.* 2016).

The two ZF regions flank a central homeodomain (CHD), which does not bind DNA and instead likely mediates protein-protein interactions (Smith and Darling 2003). Further domains found on both transcription factors are a SMAD-interacting domain (SID), a C-terminal binding protein (CtBP)-interacting domain (CID), and a p300/p-CAF binding domain (CBD) (Fortini *et al.* 1991; Liu *et al.* 2008).

Structural analysis of the chicken homologue for ZEB1, δEF1, has revealed that the gene consists of 9 exons **(Figure 1.6**). Exons 5-7 encode the NZF, 8 and 9 the CZF, and exon 7, which is the largest in size at approximately 7 kb long, constitutes the majority of the residues between the ZF clusters, including the CHD. A high sequence homology exists between the chicken and mouse genes, although it was reported that exon 3 of the chicken δEF1 gene is not present in the mouse homologue (Sekido *et al.* 1996).

Initial reports suggested that ZEB family members exclusively activate gene expression, but it is now known that transcriptional regulation by ZEB factors is more complex and governed by interaction partners. Both ZEB1 and ZEB2 mediate transcriptional activation or repression through the recruitment of coactivators and corepressors via the SBD, CID, and CBD. One of the main functions of the ZEB family

is the self-renewal and subsequent maintenance of the stem cell population in an undifferentiated state in a number of tissues (Brabletz *et al.* 2011; Denecker *et al.* 2014; Singh *et al.* 2016; Wang *et al.* 2019). They execute this primarily through the transcriptional repression of microRNAs, in a negative feedback loop manner (as discussed further in section 1.8.2.1). However, there are distinctions in the expression and binding activity of ZEB1 and ZEB2. For instance, Postigo and Dean noted that ZEB1 and ZEB2 expression levels are largely similar across foetal and adult tissue, with the exception of the thymus where ZEB1 was expressed and ZEB2 was absent, and the expression of ZEB2 in B-lymphocyte cells and the spleen, where ZEB1 was not detected. Moreover, they found that ZEB2 represses some transcription factors that are not repressed by ZEB1, such as ITF-1 and myoD, suggesting that ZEB2 may have the ability to regulate a wider range of transcription factors (Postigo and Dean 2000).

I will focus here on ZEB1, as I detected only ZEB1 expression in the adult hippocampal NSCs in the model used in the current study (Section 3.3.2.3).

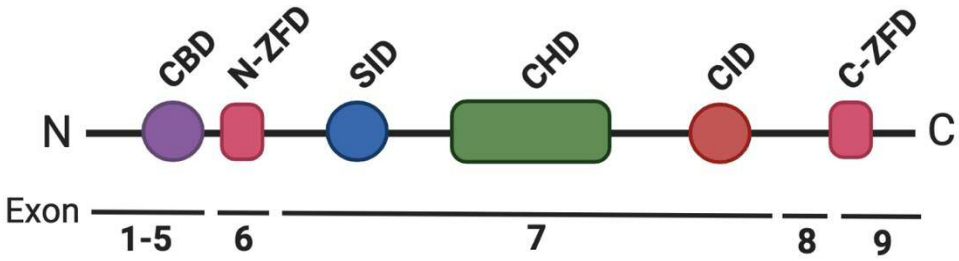

Figure 1.6 Structure of ZEB1 - ZEB1 hosts a number of binding domains through which it carries out either its transcriptional activation (CBD, SID) or repression (CID) functions. Image adapted from Chung *et al*. (2014), in Biorender.

1.8.2 Regulatory functions of ZEB1

1.8.2.1 MicroRNAs and stemness

As previously stated, one of the predominant functions of ZEB1 is the inhibition of differentiation of the stem cell population in a number of tissues, which it carries out by repressing the function of microRNAs, and specifically the microRNA-200 (miR-200) family.

MicroRNAs are a subgroup of non-coding RNAs that regulate gene expression. They become incorporated into the RNA-induced silencing complex (RISC) through coupling with Argonaute proteins, and base-pair with their target mRNA to subsequently lead to either its degradation through RNase activity or the inhibition of its translation (reviewed in Pratt and MacRae 2009).

The miR-200 family consists of five members (miR-200a, -200b, -200c, -141, and -429) that have been associated with the epithelial-mesenchymal transition (EMT; further discussed in Section 1.8.2.2). Decreased expression levels of all five microRNAs were detected in cells following TFGβ-mediated EMT *in vitro*, and all five members were found to regulate the expression of ZEB1 (Gregory *et al.* 2008); this has also been demonstrated in various cancers, including pancreatic, colorectal (Wellner *et al.* 2009), and brain (Siebzehnrubl *et al.* 2013).

ZEB1 and miR-200 regulate each other in a double-negative feedback loop which controls EMT, stemness, senescence, and cell survival, processes that are commonly seen in both normal embryonic development and in pathological states such as tumour progression. Mechanistically, ZEB1 binds to a conserved E-box motif in a promoter region upstream of the transcription start site of miR-200, which represses the expression of the microRNA (Bracken *et al.* 2008); conversely, miR-200 family members bind to target sites in the 3' UTR region of ZEB1, preventing its transcription (Korpal *et al.* 2008). Moreover, ZEB1 has also been shown to suppress the expression of miR-183 and miR-203 which regulate factors associated with stem cell maintenance such as BMI1, SOX2, and KLF4 (Wellner *et al.* 2009). Importantly, both miR-200 and miR-203 have been implicated in the promotion of cell differentiation in both healthy embryonic neural precursors (Beclin *et al.* 2016; Liu *et al.* 2017) as well as tumour cells (Siebzehnrubl *et al.* 2013; Deng *et al.* 2016). This raises the question of a) the implication of ZEB1 in the miR-200/203 regulation of neurogenesis, and b) whether this potential relationship holds relevance in adult neurogenesis.

A study by Brabletz and colleagues reported increased Notch signalling following the repression of miR-200 family members by ZEB1. The Notch ligand Jagged1, as well as transcriptional coactivators Maml2 and Maml3 were identified as miR-200 targets, and an upregulation of ZEB1 and Jagged1 was seen alongside a

simultaneous reduction in miR-200 levels in a basal breast cancer subtype as well as pancreatic adenocarcinoma (Brabletz *et al.* 2011). Notch signalling is a crucial pathway in several cellular functions, including the maintenance of NSCs in the developing brain. Thus, one mechanism for the promotion of a stemness phenotype by ZEB1 is through the inhibition of miR-200, which allows the function of Notch signalling.

1.8.2.2 Cell polarity regulation through EMT

Although the brain is composed of nerve tissue and lacks epithelial/mesenchymal tissue, I will briefly describe the epithelial-mesenchymal transition (EMT) and the induction of this process by ZEB1, as it occurs in both embryonic development and cancer, two processes that have been greatly correlated with ZEB1 expression. Moreover, as it is postulated that adult neurogenesis is a continuation of the processes that occur during embryonic neurodevelopment (Berg *et al.* 2019), an understanding of the function of ZEB1 in development will allow for a clearer speculation of the function of this transcription factor in adult neurogenesis. Importantly, the role of the EMT has been broadened over the years and is now not only recognised as a process that mediates tumour metastasis and invasion, but as a determinant of cell fate specification in stem cells (reviewed in Goossens *et al.* 2017), which is one of the fundamental concepts that this thesis addresses. Cell polarity, that is regulated by EMT, has been shown to be crucial not only for the correct establishment of the symmetric-asymmetric cleavage plane of NSCs that governs their fate (Gómez-López *et al.* 2014), but also in the correct migration of differentiating progenitor cells to their position within the developing CNS (further discussed in Section 1.8.3.2).

EMT is a process that delineates the transformation of epithelial to mesenchymal cells, through a suppression of genes that promote the former phenotype with a simultaneous upregulation of genes that induce the latter phenotype. It is a crucial step in various biological processes that occur in both healthy and disease states, such as embryonic development, tissue repair, and cancer progression.

The most evident target through which ZEB1 promotes EMT is the repression of CDH1, a gene that encodes epithelial cadherin (E-cadherin). E-cadherin is a protein involved in the formation of epithelial sheets through the maintenance of cell adhesion (through the formation of intercellular adherens junctions) and polarity (Gloushankova *et al.* 2017). Aberrant E-cadherin expression results in the disruption of these adhesive junctions, which is a key trigger of increased cell motility during EMT; this renders E-cadherin a hallmark suppression target in EMT to allow for cell migration in both healthy and disease states, such as embryonic development and tumour metastasis, respectively. CDH1 contains an E-box motif that ZEB1 recognises and binds to, subsequently recruiting the co-repressor CtBP1, and supressing the transcription of E-cadherin (Shi *et al.* 2003).

Based on the aforementioned negative feedback regulation loop formed by ZEB1 and the miR-200 family (Section 1.8.2.1) it is worth mentioning that these microRNAs have been shown to favour mesenchymal-epithelial transition (MET) whilst inhibiting EMT through ZEB1 repression, thus forming a second important ZEB1 target for EMT induction (Perdigão-Henriques *et al.* 2016). Gene expression changes associated with EMT induction by ZEB1 influence the migratory abilities of neural precursors that underpin correct neurodevelopment, as discussed later in Section 1.8.3.2.

1.8.3 Functions of ZEB1 during embryonic neurodevelopment

During embryogenesis, several cycles of EMT and its reverse process mesenchymal-epithelial transition (MET), are required for correct tissue morphogenesis and organ development. Due to its key role in EMT induction, ZEB1 expression is crucial for correct embryonic development.

The developmental importance of ZEB1 was initially identified through a study that demonstrated the deleterious effects of constitutive loss of Zeb1 on the development of mouse embryos. Heterozygous expression of ZEB1 generated viable mice, but complete loss of the gene resulted in perinatal death, with T cell deficiency, failure of the respiratory system, and abnormal skeletal formation with severe defects; exencephaly and neural tube closure defects (rare) were also observed (Takagi *et al.* 1998). This coincided with the loss of vimentin in mesenchymal cells,

and increased E-cadherin expression indicating the occurrence of MET in the absence of ZEB1 (Liu *et al.* 2008). Following this, in an elaborate study to shed further light on the importance of ZEB proteins in correct embryonic development, Brabletz and colleagues developed a conditional knockout mouse model for Zeb1, in which the deletion of Zeb1 can be induced in a spatio-temporal manner (Brabletz *et al.* 2017). The authors confirmed that although Zeb1-heterozygous mice developed normally, Zeb1-null mice died perinatally with skeletal defects including malformed ribs, craniofacial abnormalities, and limb defects, as well as respiratory failure and T cell deficiency; these observations are in accordance with the previously reported roles of ZEB1 in chondrogenesis and T cell formation (Higashi *et al.* 1997; Takagi *et al.* 1998).

The findings of a recently published study challenged the established role of ZEB1 in the maintenance of stem cells (Jiang *et al.* 2018). The authors assessed both the deletion and overexpression of Zeb1 in human embryonic stem cells and reported that ZEB1 is required for neuronal differentiation, with the finding of ZEB1 overexpression accelerating both neuronal differentiation and maturation. Whilst this study contradicts the currently recognised role of ZEB1 in the maintenance of stem cells in an undifferentiated state, it should be noted that the majority of the previously reported findings were derived in mouse models *in vivo*, whilst the study in question utilised human-derived cells. Due to the embryonic nature of the human-derived cells, the results will reflect early stages of neural development. It is possible that embryonic stem cells respond differently to expression level variations of ZEB1, in comparison to more tissue-specific stem cells, due to the presence of a diverse range of coregulators. Moreover, as the study by Jiang and colleagues was carried out *in vitro*, this does not account for the highly complex microenvironment of the neurogenic niches in the adult brain, that modulates the process of neurogenesis through a variety of intrinsic and extrinsic cues. As discussed later in Section 5.4.1, the role of astrocytes and microglia is critical for the differentiation and development of neurons within the hippocampal neurogenic niche. Thus, whilst it is difficult to reconcile the findings of Jiang and colleagues with previously published studies assigning a pro-stemness role to ZEB1, differences in methodology may account for this.

1.8.3.1 Early neurogenesis/neurulation

Although the main focus of this thesis is ZEB1 and its role in adult hippocampal neurogenesis, it is important to note that during embryonic development, ZEB2 is predominantly expressed during neurulation and early migration of neural crest cells (Duband 2010). The expression of ZEB1 only becomes detectable following the initiation of neural crest cell migration, as seen in the Xenopus, chick, and mouse embryos, whilst in zebrafish it regulates cell rearrangements through modulation of cell-cell adhesion via E-cadherin suppression during gastrulation (Vannier *et al.* 2013); following this, the function of ZEB1 becomes crucial for the correct formation of the embryonic CNS, as is discussed next.

1.8.3.2 ZEB1 in cerebellar and cortical neurodevelopment

Studies have implicated ZEB1 in the formation of various brain regions (Singh *et al.* 2016; Wang *et al.* 2019). Following their birth and development, new neurons undergo cellular changes that allow them to become polarised and emigrate from their germinal zone to their correct position within the brain where they form connections with other neurons to develop synaptic circuits. Correct cell polarisation is critical for neuronal function as the direction of axonal and dendritic projections dictates the correct flow of information. A recent study by Singh and colleagues found that the expression of ZEB1 is high in unpolarised cerebellar granule neuron progenitors, which decreases as they become polarised. ZEB1 gain-of-function confers a mesenchymal state to granule neuronal progenitors (GNPs) with shorter neurite extensions, as well suppressing cell differentiation and sustaining cell proliferation *in vitro*; in *ex vivo* slices, GNPs remained in the external granule layer and displayed steady EdU (a BrdU analogue; Section 1.3) incorporation. Conversely, silencing of Zeb1 in *ex vivo* slices resulted in the migration of cells into the inner granule layer as well as in decreased incorporation of EdU. The authors demonstrated that ZEB1 represses the expression of polarity-associated genes including Pard6a, Pard3a, Dlg2, and Lin7a, as well as the cell adhesion molecule gene Cdh1 (Singh *et al.* 2016).

This is supported by a study exploring neuronal differentiation and migration in embryonic cortical formation, which demonstrated that overexpression of ZEB1

prevented the neuronal commitment of basal RG cells and IPCs during cell differentiation through the repression of the pro-neuronal gene NeuroD1, with a significant decrease in mature TBR2-expressing IPCs as well as neurons at the cortical plate level (Wang *et al.* 2019). Moreover, this work also demonstrated that the interaction between ZEB1 and CtBP2 is crucial for the multipolar to bipolar morphological transition that newborn neurons undergo during their migration to the cortical plate.

An important study by Liu and colleagues revealed the importance of high ZEB1 expression from E9.5 throughout active mouse neocortical neurogenesis; using a Zeb1 knockout *in vivo* model, they reported that the depletion of Zeb1 resulted in a decreased progenitor pool size, which was a result of premature neuronal differentiation, whilst cell survival remained unaffected. Furthermore, Zeb1 ablation led to an increase in an oblique and horizontal cleavage plane orientation which is the driving force in the promotion of neurogenic cell division in RGCs. Mechanistically, ZEB1 functions with protein arginine methyltransferase 5 (PRMT5) to repress Pak3, a factor shown to be involved in the promotion of neuronal differentiation and migration in Xenopus (Liu *et al.* 2019).

Thus, ample evidence demonstrates that ZEB1 regulates neocortical neurogenesis, and although whether this function persists in the healthy adult brain is currently unknown, this transcription factor has been identified as a key inducer of cancer progression.

1.8.4 ZEB1 and cell plasticity in cancer

Given the importance of ZEB1 as an inducer of EMT as well as in the maintenance of stem cells in healthy tissue, it is likely that this transcription factor conveys similar functions in diseases where increased cell plasticity is germane to disease progression, such as cancer. A large body of literature attests to the relevance of ZEB1 for the malignant progression of many cancers, including breast, lung, pancreatic, and brain (reviewed in Caramel *et al*. 2018).

ZEB1 expression is absent in cancer cells in well-differentiated areas of tumours, but contrastingly high in invasive cells at the edge in several cancers, including colorectal (Spaderna *et al.* 2006), lung (Dohadwala *et al.* 2006), and brain

(Siebzehnrubl *et al.* 2013). This indicates that ZEB1 promotes the metastatic capacity of tumour cells. Siebzehnrubl *et al*. demonstrated that the expression of ZEB1 correlated with both the invasiveness of primary GBM cell lines *in vivo*, as well as with overall patient survival (Siebzehnrubl *et al.* 2013). High ZEB1 expression, as well as its correlation with greater tumour invasiveness, have been reported in gliomas in other studies as well (Euskirchen *et al.* 2017; Suzuki *et al.* 2018).

1.9 Mouse models for studying neurogenesis

Genetically engineered animal models have become the gold standard in the study of gene function, a field of research that has accelerated several ground-breaking biomedical discoveries owing to the works of many esteemed scientists, including two prominent Cardiff University-based pioneers, Sir Martin Evans and the late Professor Alan Clarke. The generation of transgenic animal models involves the deletion or insertion of a transgene into the genome of these animals, following which the resulting phenotype can be studied *in vitro* and *in vivo*. These transgenic animal models have been a commonly used tool to understand the contribution of various genes to the process of adult neurogenesis; one of the key differences in these models is the mouse strains utilised. The effect of the genetic background of mice on the levels of neurogenesis was initially considered in an elaborate study carried out by Kempermann and colleagues, in which they compared the proliferation of neural precursors, survival of newborn cells, and cell lineage specification in four commonly used mouse strains. The baseline levels of neurogenesis varied considerably across the strains, with certain strains demonstrating greater cell proliferation and others boasting a higher number of surviving cells (Kempermann, G. Kuhn, *et al.* 1997). Since then, several other studies have followed suit and reported similar findings (Clark *et al.* 2011; Freund *et al.* 2013; Kim *et al.* 2017). Fundamentally, these studies show that although neurogenesis can be modulated by environmental factors, genetics play a major role in this process that contributes to brain plasticity.

1.9.1 Cre-lox system

Detrimental effects can sometimes arise as a consequence of transgene presence in animal disease models, such as the perinatal lethality of constitutive loss-of-function Zeb1 mutations (Takagi *et al.* 1998), which renders these studies challenging. The Cre-lox transgene induction system was developed as a means to gain spatial and temporal control over DNA recombination in these models, particularly where constitutive deletion/transgene expression is undesirable, or where effects in a defined cell population are studied.

The *Cre* (cyclisation recombination) gene encodes a recombinase enzyme that was first discovered in the bacteriophage P1. Cre recombination relies on site-specific recombination; the enzyme recognises the 34bp loxP (locus of crossover in P1) gene sequence, a short DNA sequence that has a pair of palindromic sequences flanking an 8bp spacer sequence (Sauer and Henderson 1988; Orban *et al.* 1992). For loss-of-function studies, the gene of interest is flanked by loxP sites (floxed) with the loxP insert sequences in the same direction, and as the Cre recombinase binds to the loxP sites, it creates a loop that leads to the excision of the gene of interest (**Figure 1.7**). Similarly, gain-of-function studies can also be conducted using the Cre lox system; a cassette harbouring a floxed *STOP* domain placed upstream of the gene of interest is inserted into the universal ROSA26 locus; the *STOP* domain suppresses gene expression in the absence of active Cre recombinase, but the activation of the enzyme leads to the excision of the *STOP* cassette, resulting in the expression of the gene of interest (Sauer 1998).

Cre recombinase expression can be restricted to tissues of interest by placing the *Cre* gene downstream of a tissue-specific gene promoter; this prevents off-target deleterious effects of transgene induction by limiting Cre recombinase expression to the cells that express the aforementioned gene. Furthermore, temporal control can be gained over the induction of DNA recombination through the fusion of the estrogen receptor (ER) ligand-binding domain to the Cre recombinase. Control can be asserted over transgene induction by administration of tamoxifen, an estrogen analogue, which binds to cytoplasmically localised CreER, leading to nuclear

translocation of this complex, where the Cre recombinase can interact with the DNA (Gierut *et al.* 2014).

The advent of genetically engineered animal models has particularly benefited the study of adult neurogenesis as a depth of knowledge has been garnered regarding proteins that are essential for successful neuron formation and integration.

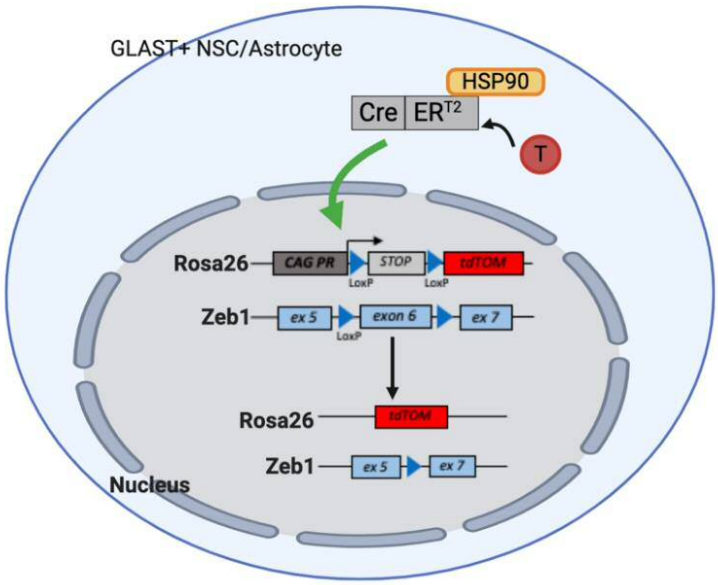

Figure 1.7. Cre recombinase-driven induction of transgenes in this project - Tamoxifen (T) binding to CreER^{T2} results in its displacement of heat-shock protein 90 (HSP90) and allows the translocation of the Cre-recombinase to the nucleus. This results in recombination of the loxP sites surrounding the STOP codon in the tdTomato expression cassette (located in the ROSA26 locus), as well as the loxP sites flanking the Zeb1 exon 6, to allow the expression of tdTomato in the GLAST-CreER^{T2}:R26-tdTOM line, with a simultaneous deletion of Zeb1 in the GLAST-CreER^{T2}:R26-tdTOM-Zeb1$^{f/f}$ strain, as further discussed in Section 2.1.1. Image created in Biorender.

1.9.2 Current models to study neurogenesis

Over the past few decades several transgenic mouse models have been created that allow the study of neurogenesis in the embryonic and adult brains, and individual models target the different cell populations that appear during the neurogenic development process to identify its regulators. To fully understand what governs successful neurogenesis, it is imperative to dissect the role and contribution of each cell population towards successful adult-born neuron production. This is particularly challenging in the study of adult neural precursor cells as there is great

overlap in the gene expression profiles of the quiescent and activated NSCs, as well as early IPCs.

1.9.2.1 Nestin

One of the most widely used transgenic mouse models in the study of adult neurogenesis is driven by the promoter of the intermediate filament nestin (Section 1.5.1). A study generated a system for visualising neurogenesis *in vivo* using a nestin-GFP mouse model; Yamaguchi and colleagues demonstrated GFP+ nestin-expressing cells are found in the adult dentate gyrus, SVZ, and RMS (Yamaguchi *et al*. 2000), and subsequently evidence was provided for the expression of nestin in NSCs and activated progenitor cells in the adult SVZ (Yamaguchi *et al.* 2000), as well as corresponding cells, and non-progenitor populations such as endothelial cells, in the hippocampus (Mignone *et al.* 2004). To combat the cytoplasmic expression of the nestin-driven GFP, which was ideal for studying cell morphology but rendered cell counting more difficult, a new mouse model was developed with the fluorescent protein CFP fused to a nuclear localisation signal, thus, allowing the fluorescent visualisation of the nuclei of nestin-expressing cells in the neurogenic zones (Encinas *et al.* 2011).

Despite the breadth of knowledge that nestin-dependent transgenic lines have contributed to our understanding of the adult neurogenic niche, they have their limitations. Of the nine transgenic mouse lines that have been generated to date that rely on the nestin promoter, only a few target both neurogenic niches in the brain, with further varying degrees of efficiency and specificity (Encinas *et al.* 2006), which can be attributed to different construct designs (reviewed in Sun *et al.* 2014). In particular, as nestin is expressed in both NSCs and transit amplifying progenitor cells, this can interfere with initial NSC-labelling studies that aim to carry out lineage tracing; these studies generally employ the use of anti-mitotic treatment for the elimination of proliferating progenitor cells, prior to NSC labelling.

1.9.2.2 GFAP

Mouse models that employ GFAP-driven expression of fluorescent proteins have been invaluable for the study of the NSC population in the adult neurogenic niches in the brain, due to their characteristic radial morphology. A GFAP-GFP mouse

model has been used to label both activated and quiescent NSCs in the SVZ (Sun *et al.* 2014). Moreover, the study of this model provided evidence of "astrocytes" giving rise to adult-born neurons (Pastrana *et al.* 2009; Codega *et al.* 2014). Subsequently, a separate model with inducible ablation of proliferating GFAP+ precursor cells was created to show that GFAP+ cells originate adult neurons in both neurogenic niches (Seri *et al.* 2001).

In the same vein as the previously discussed model, GFAP expression is not only restricted to quiescent and activated NSC populations, but also to a subset of parenchymal astrocytes; this shortcoming is commonly accounted for with the co-investigation of other NSC markers such as EGFR and CD133 in the SVZ (Garcia *et al.* 2004).

1.9.2.3 SOX2

The first Sox2-GFP transgenic mouse line was created by D'Amour and Gage in 2003 and was used to establish the expression of SOX2 in the NSCs, IPCs, and astrocytes in the dentate gyrus (Suh *et al.* 2007; Codega *et al.* 2014). Further evidence for the SOX2-expressing identity of embryonic and adult NSCs was provided by Favaro and colleagues who showed that the ablation of Sox2 in a Sox2-CreER^{T2} transgenic line resulted in abnormal dentate gyrus formation in the embryo, and a decrement in hippocampal Type 1 cells in the adult brain (Favaro *et al.* 2009).

Like the GFAP-dependent transgenic line, the main limitation of transgenic strains based on the Sox2 promoter is the detection of this protein in cell populations other than NSCs, including astrocytes.

1.9.2.4 GLAST

The first piece of evidence that established the expression of GLAST in neural precursor cells in the adult brain was provided by Namba and colleagues who demonstrated that the majority of proliferating BrdU-incorporating and Ki67-expressing cells in the dentate gyrus were GLAST+ (Namba *et al.* 2005). Since then, a GLAST-CreER^{T2} transgenic line has been created that targets NSCs as well as astrocytes with high efficiency in the adult dentate gyrus and SVZ (Mori *et al.* 2006; Ninkovic *et al.* 2007). This model revealed the extent of the multipotency potential of GLAST and nestin-expressing precursor cell populations; it was shown that GLAST-

expressing precursor cell populations could give rise to granule cells indefinitely, and could also reinstate neurogenesis following the ablation of actively proliferating progenitors, whilst nestin-expressing cells demonstrated a limited multipotent capacity, and did not contribute to neurogenesis after AraC-mediated ablation (Decarolis *et al.* 2013). A separate transgenic model that utilises the GLAST-promoter for driving Cre recombinase expression was also developed (GLAST-CreER^{T}; Nathans 2010), and although to my knowledge there have not been any studies that have directly compared the two GLAST-driven transgenic lines, due to the fewer mutations in the CreER^{T} ligand binding domain in comparison to the CreER^{T2} fusion protein (Sandlesh *et al.* 2018), it is plausible that the latter demonstrates a greater sensitivity to tamoxifen, limiting activation by the endogenous ligand.

1.10 Hypotheses

Adult hippocampal neurogenesis is a complex process modulated by various factors in the multicellular niche in the SGZ. The expression of the transcription factor ZEB1 is crucial for the maintenance of the progenitor population in an undifferentiated state as well as temporally regulating the migration of differentiating progenitors in the cortex and cerebellum through the downregulation of its expression; moreover, it is also a mediator of plasticity-driven tumour progression. Based on the known functions of this transcription factor in these systems, it is hypothesised, and will be tested here, that ZEB1 regulates stem cell maintenance in the healthy adult brain as well.

Specifically, I hypothesise that ZEB1 is expressed in undifferentiated cells within the adult neurogenic niches, including the NSC and early IPC populations. I further hypothesise that ZEB1 functions as a pro-stemness regulator in the adult hippocampus, where it maintains the NSCs in a quiescent state. Lastly, based on the necessity of ZEB1 expression downregulation for the migration of neuronal progenitors to their maturation location during embryonic cerebellum and cortical development, I speculate that ZEB1 expression impedes successful neuronal differentiation.

1.11 Aims/objectives

The main aim of this study is to elucidate the specific functions of ZEB1 during adult mouse hippocampal neurogenesis, which will be investigated using a GLAST:CreER^{T2}-driven Zeb1 knockout model. The specific objectives of this study are:

1) To determine the overlap of ZEB1 expression with markers of corresponding neural cell populations in areas of neurogenesis as well as largely non-neurogenic regions of the adult brain.

   Based on reports from embryonic neurogenesis and in line with the hypothesised function as pro-stemness regulator, I expect an overlap between ZEB1 expression and NSCs, but not with lineage-committed progeny.

2) To assess whether ZEB1 regulates adult hippocampal NSC self-renewal and fate-specification *in vivo*, using a conditional Zeb1 loss-of-function model.

As ZEB1 confers stem-cell like properties to cancer cells, I hypothesise that it is a stem cell maintenance factor and expect a depletion of NSCs following Zeb1 ablation.

3) To investigate functional consequences of loss of Zeb1 on the maturation and integration of adult-born hippocampal granule neurons.

   This objective will resolve any potential downstream effects of Zeb1 deletion on the survival of newborn neurons and their integration into the hippocampal circuitry, as well as consequences for animal behaviour.

Chapter 2 - Materials and Methods

2.1 Mouse models

All animal procedures and experiments were carried out under the Animals (Scientific Procedures) Act 1986, in accordance with UK Home Office regulations.

2.1.1 Strains

The transgenic mouse strains used in this project are shown in **Figure 2.1**. All mice were maintained on a mixed genetic background.

The GLAST:CreER^{T2}-transgenic mice were a kind gift from Professor Magdalena Götz (Ludwig-Maximilians University, Munich, Germany). The Cre gene was fused with a variant of the estrogen receptor (ER) carrying three mutations in its ligand-binding domain that renders the receptor insensitive to its natural ligand, reducing background activity in the absence of the synthetic receptor ligand, tamoxifen. The expression of the construct was targeted to the GLAST (glutamate aspartate transporter protein) locus, resulting in the specification of the expression of the Cre recombinase to cells expressing GLAST protein (Mori *et al.* 2006).

The Rosa26-tdTomato reporter (Ai9) mice were a kind gift from Professor Owen Sansom, Beatson Institute, Glasgow. A construct carrying a CAG promoter-driven tdTomato reporter gene, with an upstream stop cassette flanked by loxP sites was inserted in the ubiquitously expressed Rosa26 locus; administration of tamoxifen would lead to the recombination of the loxP sites, resulting in the excision of the stop cassette, and subsequently allowing endogenous pan-cellular expression of the fluorescent tdTomato reporter (Madisen *et al.* 2010).

The conditional Zeb1 knockout mice were a generous gift from Professor Thomas Brabletz (Nikolaus-Fiebiger Center for Molecular Medicine, University of Erlangen-Nuremberg, Germany). This strain featured two loxP sequences flanking exon 6 of the ZEB1 gene; this exon encodes one of the two major DNA-binding zinc finger domains, and induction of transgenic recombination resulted in a truncated transcript with premature stop of translation (Brabletz *et al.* 2017).

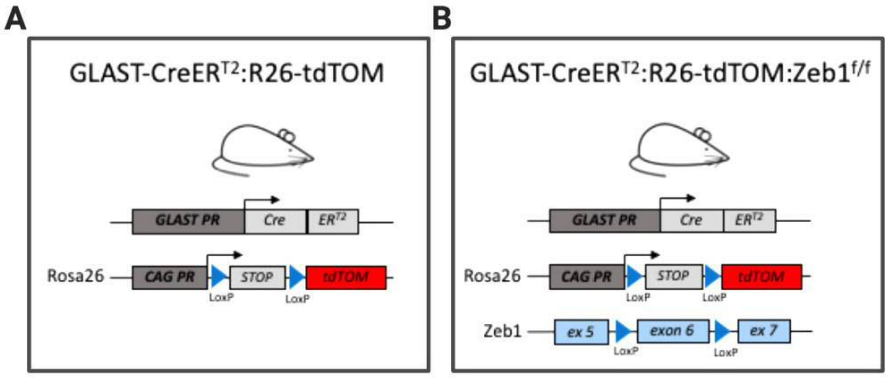

Figure 2.1. Inducible Cre-driven tdTomato expression and Zeb1 deletion models – (A) Glast:CreER^{T2}-Rosa$^{lsl\text{-}tdTomato}$ mice exhibit Cre recombinase-based inducible expression of CAG promoter-driven fluorescent tdTomato protein in GLAST-expressing cells. (B) Glast:CreER^{T2}-Rosa26$^{lsl\text{-}tdTomato}$ -ZEB1$^{fl/fl}$ feature the inducible deletion of ZEB1 expression in GLAST-expressing cells (endogenous Zeb1 gene bearing loxP sites flanking exon 6).

2.1.2 Husbandry

All mice were kept in 12-hour light/dark cycles in filter top cages (Tecniplast) and given access to food (Teklad 2919 irradiated 19% protein extruded diet, Envigo) and water ad libitum. Cages were cleaned weekly, and nesting material (Bed-r'Nest; Datesand Group) as well as cardboard tunnels were provided for environmental enrichment.

2.1.3 Breeding

Breeding was set up either as a pair or in a trio consisting of two females and a male. Mice were weaned at approximately 21 days of age when able to feed independently, and were housed in separate cages according to sex. At weaning, ear biopsies were taken for individual identification purposes as well as for genotyping to determine transgene status (Section 2.1.4).

2.1.4 Genotyping

2.1.4.1 Ear biopsies and DNA extraction

Ear biopsies were taken at the time of weaning using an ear punch (VetTech). Genomic DNA (gDNA) was extracted from the ear biopsy samples for genotyping using the MyTaq Extract-PCR kit (Bioline) according to the manufacturer's protocol. Briefly, ear clippings were placed in clean 1.5 mL reaction tubes (Greiner Bio-One)

and were incubated with appropriate amounts of Buffer A (20 μL/sample), Buffer B (10 μL/sample; Buffers A and B constitute the proprietary lysis solution), and nuclease-free H_2O (70 μL/sample; Thermo Fisher Scientific) in a pre-heated block at 75°C for 5 minutes; samples were vortexed briefly at halfway and at the end of this incubation period. Samples were then immediately transferred to another pre-heated block and incubated at 95°C for 10 minutes for enzyme deactivation. Subsequently, samples were either used immediately, or stored at 4°C for long-term storage.

2.1.4.2 Polymerase chain reaction (PCR)

PCR reactions were carried out in nuclease-free 12-well PCR strips (Thermo Fisher Scientific) using the MyTaq HS Red Mix 2X (Bioline) according to the manufacturer's protocol. The PCR reaction was set up in a volume of 25 μL per sample, according to **Table 2.1,** and added to the wells of the PCR strips. The strips were then covered with domed PCR cap strips (Thermo Fisher Scientific), and tapped firmly on a bench surface to remove trapped air bubbles. The strips were subsequently placed on PCR machines set with appropriate cycling conditions (**Table 2.2**).

Table 2.1. Volumes of reagents used in PCR for genotyping purposes

Reagent	Amount
gDNA (as extracted in section 2.1.4.1)	0.1 μL
MyTaq HS Red Mix 2X	12.5 μL
Primers (20 μM)	0.5 μL each
H_2O	up to 25 μL

Table 2.2. PCR cycling conditions for transgene detection

PCR step	Glast		ZEB1 flox	
1) Initial denaturation	95°C, 5 mins		95°C, 5 mins	
2) Denaturation	95°C, 30 secs	Steps 2-4 x34 cycles	95°C, 30 secs	Steps 2-4 x34 cycles
3) Annealing	55°C, 30 secs		64°C, 30 secs	
4) Extension	72°C, 1 min		72°C, 1 min	
5) Final extension	72°C, 10 mins		72°C, 10 mins	
6) Hold	4°C		4°C	

PCR step	tdTomato	
1) Initial denaturation	94°C, 2 mins	
2) Denaturation	94°C, 20 secs	Steps 2-4 x10 cycles
3) Annealing	65°C, 15 secs (-0.5°C per cycle decrease)	
4) Extension	68°C, 10 secs	
5) Denaturation	94°C, 15 secs	Steps 5-7 x28 cycles
6) Annealing	60°C, 15 secs	
7) Extension	72°C, 10 secs	
8) Final extension	72°C, 2 mins	
9) Hold	4°C	

2.1.4.3 Gel electrophoresis for PCR product visualisation

Visualisation of PCR products was done using gel electrophoresis. 1.6% [w/v] gels were made up by combining 1.6 g agarose (Bioline) with 100 mL 1X tris-acetate-EDTA (TAE) buffer (diluted 1:10 from 10X TAE; **Table 2.5)** in a 250 mL conical flask, and heating in a microwave for 2.5 mins until the agarose was fully dissolved. The agarose solution was then cooled under running cold water with constant flask agitation, following which 4 μL SYBR Safe DNA gel stain (Thermo Fisher Scientific) was added to allow for DNA visualisation. The gel was poured into a gel casting tray

(Biorad) with an appropriately sized well-comb, chosen based on number of samples being electrophoresed, and was left to set for approximately 20 mins. The gel was then placed into a horizontal electrophoresis cell (Biorad) with a sufficient volume of 1X TAE buffer to submerge gel, and the comb was gently removed, leaving wells for DNA addition. A 100bp molecular weight DNA ladder (Bioline) was loaded into the first well, followed by the loading of 10 μL of samples into each individual well; the samples were electrophoresed for 30 mins at 120V using a PowerPac basic power supply (Biorad). Subsequently, the DNA bands on the gel were imaged using Image Lab software (Bio-Rad) on a Molecular Imager GelDoc XR+ System with a UV transilluminator (Bio-Rad). The resulting images were analysed according to expected band sizes (**Table 2.3**).

Table 2.3. Primer sequences and expected band sizes for transgenes

Gene	Forward primer sequence (5'-3')	Reverse primer sequence (3'-5')	3rd primer	Band size (bp)
GLAST:Cre	GAGGCACTTGGCTAGGCTCTGAG	GAGGAGATCCTGACCGATCAGTT	GGTGTACGGTCAGTAAATTGGAC (Cre)	WT - 700 Mutant - 400
ZEB1 flox	CGTGATGGAGCCAGAATCTGACCCC	GCCCTGTCTTTCTCAGCAGTGTGG	GCCATCTCACCAGCCCTTACTGTGC (Exon 6)	WT – 230 Flox – 295 Exon 6 deletion - 367
tdTomato	WT-AAGGGAGCTGCAGTGGAGTA	WT-GGCATTAAAGCAGCGTATCC		WT – 297 Mutant – 196
	Mutant-CCGAAAATCTGTGGGAAGTC	Mutant-CTGTTCCTGTACGGCATGG		

2.1.5 Tamoxifen treatment

A stock solution (20 mg/mL) of tamoxifen (Sigma-Aldrich) was prepared by dissolving the compound in corn oil (Sigma-Aldrich) at 70°C in a ThermoMixer (Eppendorf) for one hour, which was subsequently aliquoted to be stored at -20°C to avoid freeze-thaw cycles. Mice were treated *in vivo* with tamoxifen to activate transgenic recombination at 4 weeks of age with daily 2 mg tamoxifen intraperitoneal (IP) injections, using 26G 3/8" needles (BD Microlance) with 1 mL syringes (Terumo), for five consecutive days (between 8 and 10am; (Slezak *et al.* 2007)). Following the

appropriate chase period, tissue was harvested from the mice following the method described in Section 2.2.1.

2.1.6 5-ethynyl-2'-deoxyuridine (EdU) cell labelling

To detect proliferating cells and to trace their lineage *in vivo*, mice were administered 50 mg/kg EdU (Sigma) by IP injection, using 26G 3/8" needles (BD Microlance) with 1 mL syringes (Terumo), for five consecutive days (between 8 and 10am). Following either the short-labelling chase period of 24 hours, or the long-labelling period of 4 week, mice were sacrificed and the tissue was harvested according to the method described in Section 2.2.1 (**Figure 2.2).**

To detect incorporated EdU, the *In viv*o EdU-488 Click-it kit (Sigma) was utilised, according to the manufacturer's protocol. Click chemistry is a relatively novel approach for the cell-labelling both *in vivo* and *in vitro*. It constitutes a two-step process that involves the initial incorporation of 5-ethynyl-2'-deoxyuridine into DNA during synthesis; the methyl group at the position 5 of the pyrimidine ring of EdU has a terminal alkyne group replacement. The EdU can subsequently be detected by a reaction of the alkyne group with fluorescent azides in a copper catalyst-dependent reaction, through which the alkyne and azide "click" and form a stable bond (Salic and Mitchison 2008)

Briefly, chosen tissue sections were placed in a clean 24-well plate (Greiner Bio-One) and incubated with the permeabilisation solution PBS-T (**Table 2.5**) for 1 hour on a RotaMax 120 (Heidolph Instruments; all incubation and wash steps were carried out on the rotating platform) following which the sections were washed twice (10 mins each) with 500 μL of 3% BSA (Thermo Fisher Scientific) in 1X PBS. Meanwhile, the reaction cocktail was prepared as described in **Table 2.4** in a 1.5ml reaction tube (250 μL final volume/well), and the second wash buffer was replaced with 500 μL of the reaction cocktail, and incubated for 30 mins at RT (hereafter, the sections were maintained in the dark to prevent fluorophore photo-bleaching). Subsequently, the reaction cocktail was removed, and the tissues were washed three times (10 mins each) with 500 μL of 3% BSA in 1X PBS, and then further immunofluorescence staining was carried out (described in Section 2.2.4).

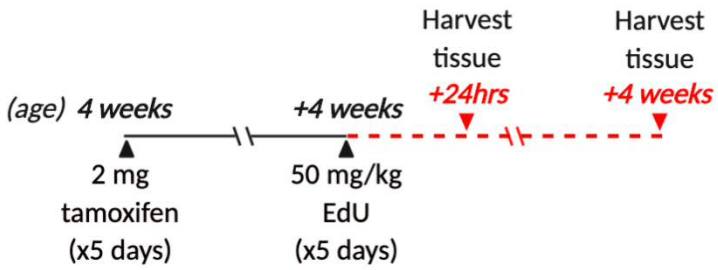

Figure 2.2. EdU administration and tissue harvesting protocol used for assessing cell proliferation and lineage tracing.

Table 2.4. Reagents and volumes for EdU-488 Click-it assay sufficient for one well of tissue sections

Reagent	Volume per assay
Deionised water	189.5 µL
Reaction buffer (10X)	25 µL
Catalyst solution	10 µL
Dye azide	0.5 µL
Buffer additive (10X)	25 µL
Total volume	250 µL

2.2 Tissue processing and immunofluorescence

2.2.1 Tissue harvesting

Transcardial perfusion fixation was carried out prior to tissue harvesting (Siebzehnrubl *et al.* 2013); this technique makes use of the vascular system of the animal for the delivery of the fixative to the tissues of interest in a time-efficient manner. This allows for better tissue architecture preservation as well as the inactivation of proteolytic enzymes to prevent sample degradation.

At the end of experiments, mice were sacrificed by CO_2 overdose. Following this, mice were immediately secured to a Styrofoam platform and their limbs fixated with needles in a dorsal recumbent position for maximal thoracic exposure. Holding the skin above the xiphoid process taut with a pair of Adson forceps, a shallow incision was made immediately below this area with a pair of iris scissors, followed by small shallow lateral incisions on either side of the xiphoid process towards the collarbone to allow the removal of the upper skin layer covering the rib cage. Holding the now more visible xiphoid process, a small vertical incision was made through the dermis, revealing the xiphoid process. This was then gently pulled upwards and held

with the forceps so that two lateral incisions could be made on either side through the abdominal walls to reveal the diaphragm. Subsequent cuts were made through the diaphragm, followed by the careful cutting and removal of the ribs, to leave the chest cavity exposed. Gentle incisions were made to remove the pericardium, whilst avoiding damage to the heart and lungs, so that the lower left ventricle was visible. A small incision was next made into the right atrium using Westcott Spring Scissors Slightly Curved (Interfocus) to allow perfused solutions to drain from the vascular system. Holding the heart steady with the forceps, a 21G butterfly needle (Greiner Bio-One) attached via the tubing adaptor to a 20 mL Luer lock IV syringe (Medicina) with 20 mL ice-cold 1X PBS, was inserted into the left ventricle, and immediately the buffer was slowly and steadily injected through the vascular system to exsanguinate the mouse. The 1X PBS exsanguination was repeated until the solution draining from the right atrium was clear, and visual liver clearance was used as a further assessment of complete exsanguination. The needle was removed from the heart and a second syringe containing 20 mL ice-cold 2% [v/v] formaldehyde (Santa Cruz Biotechnology) in 1X PBS was attached to the needle, which was promptly re-inserted into the heart in the same location, and using controlled pressure the formaldehyde was perfused through the vascular system to fix and preserve tissue architecture .

Following perfusion fixation, the mouse was decapitated to allow brain harvesting. A midline scalp incision was performed using iris scissors to expose the underlying skull, followed by a second midline incision from the posterior of the cerebellum to the anterior of the olfactory bulb, to allow the removal of the skull plates on either side of the midline incision using Adson forceps, with care being taken whilst removing the meninges to prevent them from tearing into the brain tissue. Further small lateral incisions were made from the midline incision to ease the removal of the skull plates. Using a spatula, the brain was released from the skull and placed immediately in a clean 20 mL scintillation vial (Thermo Fisher Scientific) with 4 mL ice-cold 2% formaldehyde for overnight postfixation.

2.2.2 Tissue cryopreservation

Following the overnight postfixation, the 2% formaldehyde was removed using a Pasteur pipette and replaced with 4 mL 1X PBS for an overnight wash at 4°C

to allow for the clearance of excess fixative. After the overnight wash, the 1X PBS was replaced with 4 mL of a 30% [w/v] sucrose solution (Sigma-Aldrich; in 1X PBS) for tissue dehydration, and following the complete saturation of the tissue with the sucrose solution (indicated by the sinking of the tissue to the bottom of the vial which usually occurred after 48 hours of incubation at 4°C), the 30% sucrose solution was replaced with 4 mL of a solution of 60% [w/v] sucrose (in 1X PBS) diluted at a ratio of 1:1 in Optimal Cutting Temperature compound (OCT; Thermo Fisher Scientific) for a further overnight incubation at 4°C. The brain tissue was subsequently embedded and frozen for cryosectioning (Section 2.2.3).

2.2.3 Tissue processing (embedding/cryosectioning)

Cryosectioning of brain tissue was carried out to obtain thin tissue sections for immunofluorescence staining. The brain tissue was transferred from the scintillation vial to a petri dish using curved dissecting forceps, and the cerebellum was cut off using a #11 sterile scalpel (Swann-Morton). The tissue was subsequently transferred to a clear peelable plastic embedding mould (Polysciences, Inc), and the brain was orientated with the cerebellum facing the bottom and the olfactory bulb facing the top to allow for coronal sectioning. The plastic mould was then filled with OCT to submerge the tissue, and using long forceps, the mould was held in the vapor phase of liquid nitrogen in a benchtop container until the tissue-OCT block was frozen, indicated by the OCT becoming solid and white in colour. The frozen block was subsequently stored at -80°C for long term storage and transferred to -20°C for approximately 1 hour prior to sectioning. Tissue cryosectioning was carried out on a Leica CM1860UV cryostat (Leica Biosystems) at -20°C, and the tissue sections were cut in the coronal plane at a thickness of 30 μm. The cut sections were placed in a 96-well plate (one section/well) with 180 μL cryoprotectant (**Table 2.5**), and plates were stored at 4°C for long term storage.

2.2.4 Immunofluorescence microscopy

Immunofluorescence is a technique used to assess protein distribution and localisation in tissue using visualisation of fluorescently labelled antibodies against the protein of interest.

Indirect immunofluorescence, that involves the binding of a primary antibody to the protein of interest, and a secondary fluorochrome-tagged antibody targeted to the primary antibody, has the ability to amplify the detected fluorescent signal as multiple secondary antibodies can bind to primary antibodies, thus allowing the visualisation of proteins with low expression. Moreover, the use of multiple fluorescent dyes permits protein colocalisation studies.

2.2.4.1 Blocking and antibody incubation

For immunofluorescence staining, chosen sections were transferred using a fine-angled paintbrush to a 24-well plate containing 500 μL of PBS-T (**Table 2.5**) per well, with a maximum of 4 sections/well. The sections were incubated in the wash buffer for 10 mins on a Rotamax 120 (Heidolph Instruments; all incubation and wash steps were carried out on the rotating platform) with 20 rotations/min at RT to remove cryoprotectant as well as to permeabilise the sections for better antibody penetration. Subsequently, the PBS-T was removed using a fine Pasteur pipette (Greiner Bio-One), and 500 μL of Fish-skin gelatin buffer with 0.1% Triton X-100 [v/v] (hereafter referred to as FSB-T; **Table 2.5**) was added for incubation at RT for 1 hour; FSB-T is a blocking buffer that reduces non-specific antibody binding. Subsequently, primary antibodies were prepared by appropriate dilution (**Table 2.6**) in 250 μL FSB-T in 1.5 mL reaction tubes; the FBS-T was removed and the diluted antibodies were pipetted into the well with the tissue and incubated overnight at 4°C. The following morning, 5X 5-minute washes were carried out with PBS-T, after which appropriately diluted secondary antibodies (**Table 2.6)** in FSB-T were added to the sections, and the plates were then incubated for 3 hrs at RT in the dark (hereafter, tissue section exposure to light was kept at a minimum to prevent photobleaching). After this incubation period, the secondary antibody solution was removed, and the nuclear counterstain Hoechst-33342 (Thermo Fisher Scientific) was diluted in PBS-T at 1:500 and added to the sections for 10 mins at RT. Subsequently, 4X 5-min washes with PBS-T were carried out.

2.2.4.2 Mounting

Following the staining protocol, tissue sections were mounted onto microscope slides for visualisation. A glass petri dish lid was filled with PBS-T and clear frosted microscope slides (VWR) were submerged up to the label. The tissue sections were transferred to the petri dish and using a fine angled paintbrush, the sections were gently mounted onto the slide. The slides were carefully removed from the petri dish and placed in a slide rack to air-dry for 10 mins; meanwhile, ProLong Diamond Antifade mountant (Thermo Fisher Scientific) was thawed at RT and once the slides were dry, 100 μL of the mountant was pipetted horizontally across the centre of the slide, following which a 24x60mm coverslip (Thermo Fisher Scientific) was carefully lowered onto the slide at an angle using fine forceps, to avoid introducing air bubbles. Slides were then propped vertically onto tissue for 10 mins to drain excess mountant, following which they were dried at RT overnight, and then stored at 4°C in slide books (2BScientific) for long term storage. Tissue sections were imaged on a Zeiss LSM710 confocal microscope with Zeiss ZEN software.

2.2.5 Imaging and counting

For each immunofluorescence sample, one image was taken using a 10X objective for an overview to ascertain that comparable locations along the hippocampus were being assessed for counting purposes for the control and Zeb1$^{-/-}$ models. Specifically, the dorsal hippocampus at a median bregma -1.8, according to the Mouse Brain Atlas (Paxinos and Franklin 2001), was used for inter-genotype comparison. For cell quantification, four z-stack images (with a z-step of 1-2 μm) were captured spanning the length of the suprapyramidal blade of the dentate gyrus, starting at the inner region of the dentate gyrus and ending at the end of the blade, as shown in **Figure 2.3**. Images were obtained on a Zeiss LSM710 confocal microscope with Zeiss ZEN software using a 40X (1.3 NA) oil-immersion lens. Subsequently, different cell populations were counted using the Point Tool in ImageJ 1.52K. Cell-specific marker expression and morphology were used to determine the inclusion of cells within the counts (**Table 2.7**). Only tdTomato-expressing cells of interest were quantified as the expression of the reporter indicated recombination with the tamoxifen administration. The primary researcher was not blinded during

quantification, although a minimum of one set of technical replicate counts per cell marker per genotype were quantified and confirmed by a secondary blinded researcher.

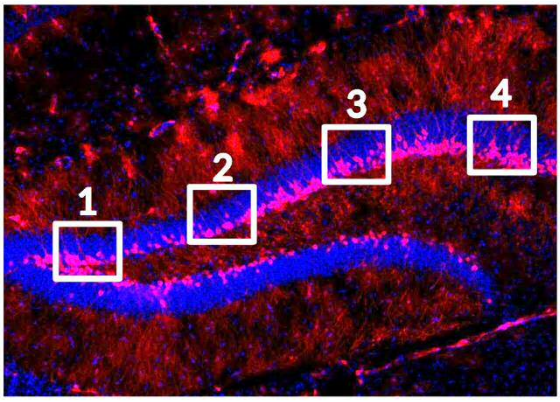

Figure 2.3. Visual fields imaged for representative cell quantification of hippocampal cell populations during adult neurogenesis

Table 2.5. Reagents and components used in the current study

Reagent	Component	Amount	Supplier
1X PBS	10X PBS	100 mL	Thermo Fisher Scientific
	Deionised water	900 mL	
10X TAE	Tris base	48.5 g	Sigma
	Glacial acetic acid	11.4 mL	
	EDTA	3.7 g	
	Deionised water	1 L	
Cryoprotectant	0.1M phosphate buffer	250 mL	Sigma
	Ethylene glycol	125 mL	
	Glycerin	150 mL	
PBS-T	10X PBS	100 mL	Thermo Fisher Scientific
	Triton X-100	1 mL	Merck
	Deionised water	900 mL	
FSB-T	1X PBS	500 mL	
	BSA	5 g	Thermo Fisher Scientific
	Sodium azide	0.1 g	Merck
	Teleostean gelatin	2 mL	
	Triton X-100	500 µL	

Table 2.6. Primary and secondary antibodies used in this project

Primary antibodies			
Antigen	**Host**	**Dilution**	**Supplier**
CD31	Goat	1:100	R&D Systems
Cleaved caspase 3	Rabbit	1:250	Cell Signalling
Doublecortin (DCX)	Chicken	1:250	Aves Labs
GFAP	Chicken	1:1000	Aves Labs
GFAP	Mouse	1:250	Sigma
Ki67	Chicken	1:500	Encor
MCM2	Rabbit	1:500	Abcam
Nestin	Chicken	1:500	Encor
NeuN	Mouse	1:500	Merck
S100β	Rabbit	1:250	NeoMarkers
SOX2	Mouse	1:250	Abcam
TBR2	Rabbit	1:500	Abcam
TuJ1	Mouse	1:500	Promega
ZEB1	Rabbit	1:500	Atlas Antibodies
ZEB2 (SIP1)	Mouse	1:250	Active Motif

Secondary antibodies				
Antigen	**Fluorochrome**	**Host**	**Dilution**	**Supplier**
Anti-chicken	Alexa-405 Alexa-488 Alexa-594 Alexa-647	Donkey	1:500	Thermo Fisher Scientific
Anti-goat				
Anti-mouse				
Anti-rabbit				

Table 2.7. Cell population-specific marker expression and morphological features used as a criterion for cell quantification

Marker	Cell population	Localisation	Morphological features
GFAP	Type 1	Cytoplasmic (cytoskeletal)	GFAP expression throughout soma (in the SGZ), spanning the radial projection through the GL to the ML
Nestin	Type 1, Type 2a	Cytoplasmic (cytoskeletal)	Nestin expression throughout soma and radial projections (Type 1), or shorter projections (Type 2a)
SOX2	Type 1, Type 2a, astrocytes	Nuclear	Nuclear signal in cells located in the SGZ (both with and without a radial projection)
MCM2	Late Type 1, Type 2a	Nuclear	Nuclear signal in cells located in the SGZ
Ki67	Type 2a	Nuclear	Nuclear signal in cells located in the SGZ
Tbr2	Type 2b	Nuclear	Nuclear signal in cells located in the SGZ
DCX	Type 3	Cytoplasmic	DCX expression throughout the soma (surrounding the nucleus), and in the short processes, of cells both in the SGZ and in the GL
TuJ1	Pan-neurons	Cytoplasmic (cytoskeletal)	TuJ1 expression throughout neuronal structure, in cells located in the entire dentate gyrus
NeuN	Mature neurons	Cytoplasmic	NeuN expression throughout neuronal structure, in cells located in the entire dentate gyrus
S100β	Astrocytes	Cytoplasmic/nuclear	Pan-cellular expression in astrocytes in the SGZ, GL, and ML
EdU	Proliferating cells	Nuclear	Nuclear signal in cells located throughout the dentate gyrus
Cleaved-caspase 3	Apoptotic cells	Nuclear/cytoplasmic	Pan-cellular signal in cells located throughout the dentate gyrus

2.3 Behavioural analysis

2.3.1 Novel object recognition/location task

The novel object recognition task is employed to test the visual recognition memory of animals. In mice, the basis of this task is the approach behaviour that rodents show towards novel objects due to their innately exploratory nature. NOR testing assesses non-spatial recognition of objects, which is known to involve several brain regions; the involvement of the hippocampus in NOR tasks has previously been shown through studies in which hippocampal lesions significantly impaired the performance of mice in this task (reviewed in Squire *et al.* 2007; Broadbent *et al.* 2010). Meanwhile, the novel object location (NOL) task evaluates the discrimination of objects based on spatial encoding and consolidation, which is processed within the hippocampus (Mumby *et al.* 2002; Vogel-Ciernia and Wood 2014). It has been shown that the rate of neurogenesis in the hippocampus is linked with spatial memory consolidation (Sarkisyan and Hedlund 2009). These tasks were performed following a 10-week rest after tamoxifen-induced transgene recombination, to assess the functionality of the mature adult-born neurons (**Figure 2.4**).

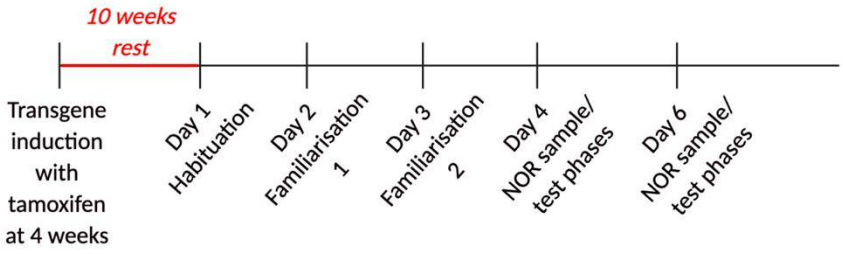

Figure 2.4. Timeline of NOR and NOL tasks.

2.3.1.1 Object selection considerations and experimental set up for each day prior to task start

1) Objects were chosen that were visually interesting, but also a height that could not be climbed by the mice to discourage them from sitting on top of the objects during the task which would minimise their exploratory activity (**Figure 2.5A**). Moreover, the objects used as the novel object

(from Object sets C and D) as well as their left/right position in the arena was counterbalanced within the control and Zeb1$^{-/-}$ groups to limit object bias (for object set choice and duration of each session, see **Table 2.8**).

2) The arena and objects were thoroughly cleaned with isopropanol before and in between each task and mouse to remove distinguishing odour cues.

3) All mice to be tested were introduced into the testing room 30 mins prior to the start of the task, for acclimatisation to the new room conditions.

4) To limit handling-triggered stress, the mice were transferred from their holding cage into the arena using either a tube or a tilted cage, and once the task was completed, tested mice were placed into new holding cages that did not contain mice waiting to be tested.

2.3.1.2 Day 1 – NOR Habituation

Following the acclimatisation period, the first mouse was placed inside the arena, and allowed to explore freely for 10 minutes to become habituated with the arena (

Figure 2.6). The mouse was then removed and placed into a new holding cage. Subsequently, the arena was cleaned thoroughly with isopropanol and the task was repeated with the remaining mice.

2.3.1.3 Day 2 and 3 – NOR Familiarisation 1 and 2

At the start of days 2 and 3, the arena was prepared for testing before the mice were brought into the testing room; the duplicate objects from Set A or B were evenly spaced in the arena (NW and NE corners) and attached to the arena floor with removable mounting putty. The camera was positioned directly overhead of the arena (**Figure 2.5B**).

After the acclimatisation period, the first mouse was placed inside the arena (facing S wall; **Figure 2.5C**), and allowed to explore freely for 5 minutes. The mouse was then removed from the arena and placed inside a clean holding cage, where it was allowed to rest for five minutes, whilst the arena and objects were cleaned with isopropanol. Subsequently, the mouse was returned to the arena, and the

familiarisation protocol was repeated twice with the same object set. The mouse was then placed into a clean holding cage at the end of the task, and the protocol was repeated with the remaining mice.

The protocol from day 2 was repeated for day 3, which was the second familiarisation day. However, for this stage of the task, the object set from A and B that was not used the previous day was used on day 3, so that novel identical objects were used.

2.3.1.4 Day 4 – NOR sample and test phases

As for the previous two days, the arena and objects were set up before the mice were introduced into the testing room. The identical objects from set C were spaced evenly and attached to the arena floor with removable mounting putty (NW and NE corners). All mice to be tested were acclimatised to the testing room for 30 minutes. Following this, the first mouse was placed inside the arena (facing S wall) and allowed to explore freely for 10 minutes. After this, the mouse was taken out and placed in a new holding cage for 5 minutes during which the arena and objects were cleaned thoroughly. The sample phase protocol was then repeated twice, to amount to 30 minutes of exploratory time in the arena during the sample phase with the same object set.

The mouse was then placed in its holding cage for five minutes, which marked the delay time between the sample and test phases. During the delay period, the arena was cleaned with isopropanol and one of the objects from set C was replaced with an object from set D, which were subsequently placed in the arena (NW and NE corners; placement varied based on counterbalancing). For the test phase, the mouse was introduced into the arena facing away from the objects (S wall), and allowed to explore for 10 minutes, following which it was placed in a new holding cage, and all objects and arena were cleaned thoroughly with isopropanol. The sample and test phases were then repeated with the remaining mice.

2.3.1.5 Day 6 – NOL sample and test phases

As with day 4 of the NOR task, the NOL started with the arena set-up; the arena and two identical objects from set E were thoroughly cleaned and placed within the arena (NW and NE corners). The mice were then brought into the testing

room for acclimatisation for 30 minutes. Following this period, the sample phase was carried out as described for the NOR task (Section 2.3.1.4) and repeated twice to allow for a total of 30 minutes of exploration time of the same object locations. Subsequently, the mouse was taken out of the cage and placed into a new holding cage for a delay period of five minutes, during which the arena and objects were thoroughly cleaned and one of the objects from the same set was fixed inside the arena at the SE corner (location varied between SW and SE corners depending on counterbalancing within groups). The mouse was then reintroduced into the arena (facing either SW or SE corner, away from the corner the novel object), and allowed to explore freely for 10 minutes. The mouse was then removed, placed into a new holding cage, and the sample and test phases were repeated with the remaining mice.

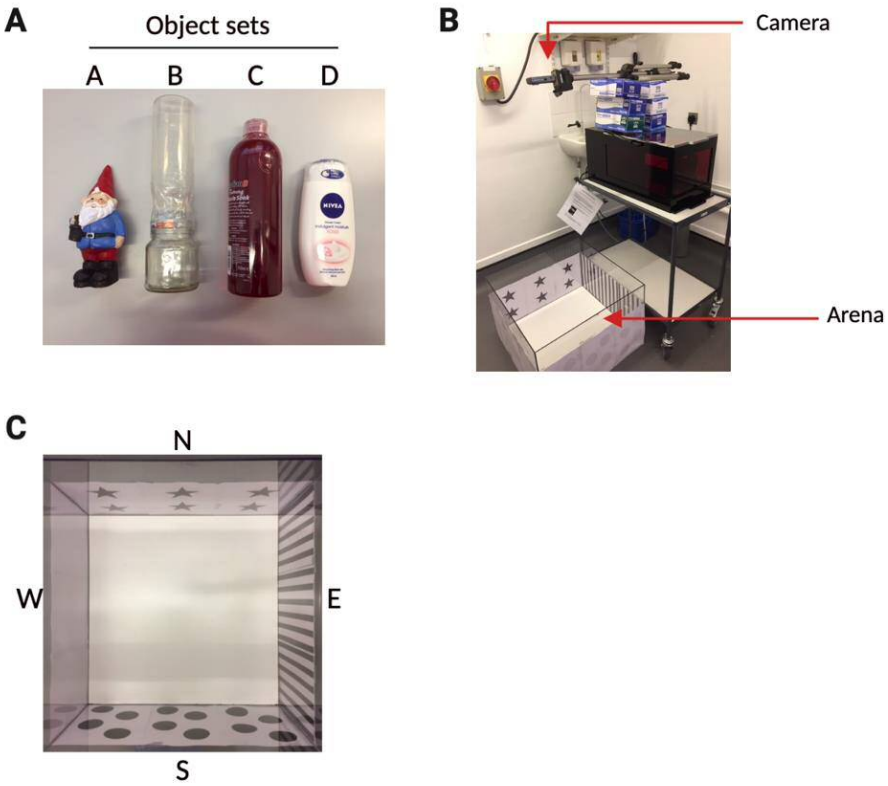

Figure 2.5. Set up for NOR and NOL tasks - (A) Objects sets used in the NOR task; object set used in NOL task was identical to Object C, with the exception of being dark blue in colour. (B) The camera was positioned directly over the centre of the arena to capture the movement of the mice. (C) The arena walls were covered with patterned paper for spatial cues, and spatial coordinates (N, S, E, W) were used to distinguish between familiar and novel object placements.

Table 2.8. Duration of each session of the NOR and NOL tasks

Day	Task step	Duration		Objects
1	Habituation	10 mins		None
2	Familiarisation 1	5 mins	X3	AA
3	Familiarisation 2	5 mins	X3	BB
4	NOR Sample phase 1	10 mins		CC
4	NOR Sample phase 2	10 mins		CC
4	NOR Sample phase 3	10 mins		CC
4	NOR Test phase	10 mins		CD
6	NOL Sample phase 1	10 mins		EE
6	NOL Sample phase 2	10 mins		EE
6	NOL Sample phase 3	10 mins		EE
6	NOL Test phase	10 mins		EE

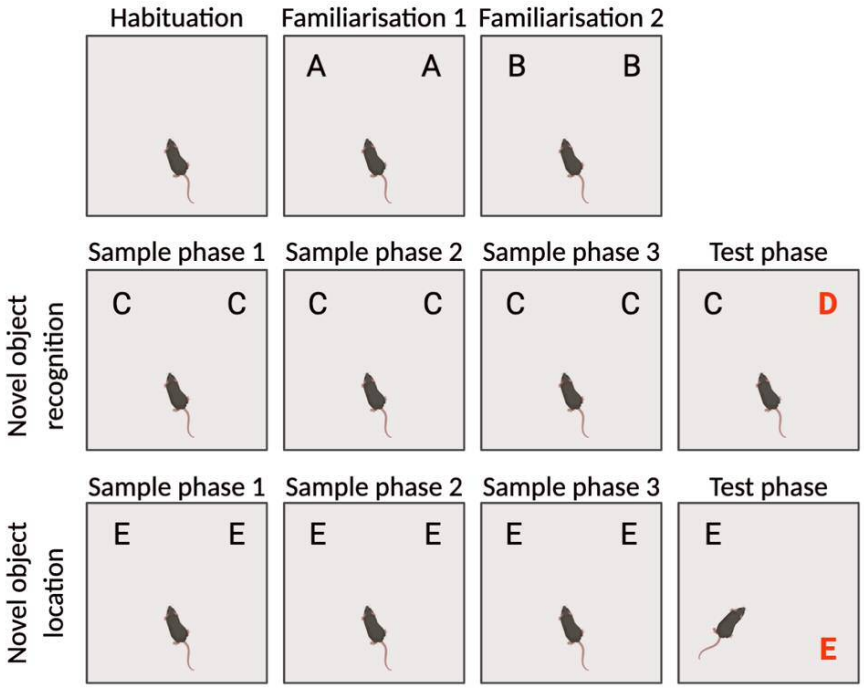

Figure 2.6. Layout of the arena with the object sets of choice for each session of the NOR and NOL tasks.

2.3.1.6 Scoring

I analysed all videos post-hoc using EthoVision XT Version 11.5 (Noldus). Interaction with objects was defined by time spent sniffing, tactile exploring, or with the head orientated towards the object within a distance of <1-2cm. Sitting on the

object and rearing/standing within 1-2cm with body orientation away from the object was not counted as exploratory behaviour (Antunes and Biala 2012).

To assess differences in the object exploration of the control and Zeb1$^{-/-}$ mice during the test phases of the NOR and NOL tasks, a discrimination index (DI) was calculated based on the exploration of the novel object, divided by the total exploration of the two objects; this measure takes into account differences in the exploratory activity of the control and experimental groups, and reports object interactions as a relative measure (Akkerman *et al.* 2012).

2.4 Statistical analyses

All data sets were graphically represented and statistically analysed in GraphPad Prism 8.3.0. Only biological replicates were used to calculate the mean and standard error of mean of data sets. Prior to analysing significant differences between sample groups, all data were tested for normality using the Shapiro Wilk test. P-values were considered significant if less than 0.05; further p-value significance scoring is included in each figure legend (*p<0.05, **p<0.01, ***p<0.001, ****p<0.0001).

2.4.1 T-test

Unless otherwise specified, an unpaired two-tailed t-test was used to analyse significant differences between two normally distributed data sets, and an unpaired Mann-Whitney U test for data sets that did not follow Gaussian distribution. All data are reported as mean of cohort ± standard error of mean (SEM) when normally distributed, and as median of cohort with IQR, otherwise. Biological (number of individual animals tested) and technical replicates (number of tissue sections assessed from an individual animal) are reported within figure legends.

One-sample Wilcoxon tests were performed when assessing significant differences between a single data set and a set value, as seen in Sections 5.3.5.2 and 5.3.5.3.

2.4.2 Two-way ANOVA

Two-way ANOVA tests were used to compare the effects of two individual variables on a dependent variable in data sets that followed the Gaussian

distribution. In instances of non-normal distribution, data were transformed logarithmically, and then once normality was confirmed through the Shapiro Wilk test, two-way ANOVA modelling was performed. Sidak's multiple comparisons test was used to assess inter- and intra-genotype significant differences; and further interactions between different experimental factors (genotype, task session, object identity as defined by familiar vs. novel for the NOR task, and object placement defined as familiar vs. displaced in the NOL task), were investigated to assess differences between groups (Section 5.3.5).

Table 2.9. Suppliers for all reagents and materials used in this study

Supplier	Supplier location
2BScientific	Heyford Park Innovation Centre 77 OX25 5HD, UK
Abcam	Discovery Drive, Cambridge Biomedical Campus, Cambridge, CB2 0AX, UK
Active Motif	Office Park Nysdam, Avenue Reine Astrid, 92, B-1310 La Hulpe, Belgium
Atlas Antibodies	Voltavägen 13A, 168 69 Bromma, Sweden
Aves Labs	12571 SW Main St, Tigard, OR 97223, US
BD Biosciences	Edmund Halley Road - Oxford Science Park, OX4 4DQ Oxford, UK
BioLine Reagents Ltd.	Edge Business Centre, Humber Rd, London NW2 6EW, UK
Bio-Rad Laboratories	The Junction, Station Rd, Watford WD17 1ET, UK
BioRender	BioRender, 639 Queen Street West, Toronto, Canada
Datesand Group	Datesand Ltd. P.O. Box 45, Manchester. M11 3ER, UK
Envigo	Huntingdon, Cambridgeshire, UK
Eppendorf Ltd.	Eppendorf House, Arlington Business Park, Gateway 1000, Whittle Way, Stevenage SG1 2FP
GraphPad Software, Inc.	7825 Fay Avenue, Suite 230, La Jolla, CA 92037, USA
Greiner Bio-One GmbH	Unit 5/Brunel Way, Stonehouse GL10 3SX, UK
Heidolph Instruments	Shire hill, Saffron Walden Essex CB11 3AZ, UK
Image J	NIH and the Laboratory for Optical and Computational Instrumentation, USA
Interfocus	Cambridge Rd, Linton, Cambridge CB21 4NN, UK
Leica Biosystems	Larch House, Woodlands Business Park, Milton Keynes, MK14 6FG, UK
Leica Microsystems	Davy Avenue Knowlhill, Milton Keynes, MK5 8LB, UK
Medicina Ltd.	Station Rd, Blackrod, Bolton BL6 5BN, UK
Merck Chemicals Ltd.	University Pkwy, Chilworth, Southampton SO16 7QD, UK
NeoMarkers	47790 Westinghouse Dr., Fremont, California 94539, USA
Polysciences, Inc.	400 Valley Road, Warrington, PA, USA
Promega	Science Park, 2 Benham Rd, Chilworth, Southampton SO16 7QJ, UK
R&D Systems	614 McKinley Pl NE, Minneapolis, MN 55413, USA
Sigma-Aldrich	The Old Brickyard, New Rd, Gillingham, Dorset, SP8 4XT, UK
Santa Cruz Biotechnology	Inc. Bergheimer Str. 89-2 69115 Heidelberg, Germany
Swann-Morton	Owlerton Green, Sheffield S6 2BJ, UK
Tecniplast	Via I Maggio, 6, 21020, Buguggiate, VA, Italy
Terumo	Otium House, 2 Freemantle Road, Bagshot, Surrey, GU19 5LL, UK
Thermo Fisher Scientific	Bishop Meadow Road, Loughborough, Leicestershire, LE1 5RG, UK
VetTech	Congleton, Cheshire, UK
VWR International Ltd.	Hunter Blvd, Lutterworth LE17 4XN, UK
ZEISS	Coldhams Lane CB1 3JS Cambridge, UK

Chapter 3 - Characterising the expression of ZEB1 in the adult mouse brain

3.1 Introduction

Correct embryonic development requires a great degree of cell plasticity as well as the capacity for differentiating cells to migrate to their correct location of maturation. These fundamental characteristics are stimulated by the epithelial to mesenchymal transition (EMT), which is mediated in part by the transcription factor ZEB1. Due to the well-characterised function of ZEB1 in the process of EMT, past studies have focused on identifying the function of this transcription factor in EMT-driven processes such as neurodevelopment and disease progression in cancer. In particular, ZEB1 plays an inhibitory role in the neuronal commitment of radial glia and neural progenitors in the developing cerebellum and cortex (Singh *et al.* 2016; Wang *et al.* 2019); this is supported by evidence demonstrating a decreased neural progenitor pool size following embryonic Zeb1 ablation (Liu *et al.* 2019), as previously discussed in Section 1.8.3.2. In the same vein, previously it has been shown that ZEB2 has important functions in correct neural crest development as well as subsequent neural crest cell migration and further development of the various CNS regions, which is also mediated by ZEB1 (Section 1.8.3.1). Thus, there is some overlap between the functions of ZEB1 and ZEB2 in the developing CNS, but it remains unclear whether the two ZEB transcription factors share functions in the adult CNS as well.

Furthermore, although hypotheses can be formulated based on current knowledge of the transcriptional regulatory functions of ZEB1, little has been evidenced regarding its expression and role in the healthy adult brain due to the perinatal lethality of constitutive knockout models, and a lack of conditional loss-of-function models. Importantly, it is yet unclear whether ZEB1 is expressed in the adult stem cell niches where it may contribute to the generation of new neurons, mirroring its role in development. Understanding the expression pattern of ZEB1 is key to unravelling its location-dependent functions in the adult brain.

This chapter aimed to first assess similarities in the expression patterns of the two transcription factors in the adult mouse brain. This was followed by the characterisation of the expression of ZEB1 in the adult brain, using IF staining of wild-type mouse brain sections to investigate co-expression of ZEB1 with cell markers

commonly used to identify distinct neural cell populations. Through this, I sought to understand the possible stem-cell related role that ZEB1 may play postnatally. The resultant finding of ZEB1 expression in the hippocampus in this chapter raised the question of its function in a canonical neurogenic niche in the adult brain, which was subsequently investigated through the generation of a loss-of-function mouse model in this project.

3.2 Aims and objectives

1) To elucidate the differential expression patterns of the two ZEB transcription factor family members ZEB1 and ZEB2 in the cortical, SVZ, and hippocampal adult brain compartments.
2) To assess the expression of ZEB1 in neural cell types in the cortex, representative of a largely post-mitotic region, and in the SVZ and hippocampus, the two major neurogenic regions in the adult brain.
3) To validate the transgenic mouse model by demonstrating cell-specific efficiency of Zeb1 deletion post-induction with the established tamoxifen administration regime.

3.3 Results

3.3.1 Characterisation of the expression patterns of ZEB1 and ZEB2

The ZEB family of transcription factors is made up of two members, ZEB1 and ZEB2 (Sip1). Both factors are known to be crucial for correct neurodevelopment (Section 1.8.3). A constitutive knockout study demonstrated that the deletion of ZEB2 results in severe CNS deformities and embryonic lethality at E9.5 (De Putte *et al.* 2003), whilst a compound model featuring heterozygous ZEB2 deletion and homozygous ZEB1 deletion resulted in death at E13.5, with neural tube deformities that are not seen in a Zeb1 loss-of-function model alone (Miyoshi *et al.* 2006). This suggests that the two ZEB factors have additive functions with some gene interaction in the developing CNS. Thus, as previous studies have reported some expression and functional redundancy between the two proteins in embryos (Postigo and Dean 2000), it was of interest to investigate whether their expression overlapped in the adult brain. I assessed the co-expression of ZEB1 and ZEB2 in wild-type adult mouse brain sections using IF staining.

I observed that overlap in the expression of the two ZEB proteins was region dependent. In the cortex, there was little to no overlap between ZEB1+ and ZEB2+ cells (**Figure 3.1A,** yellow arrowhead and arrow, respectively), with distinct cell populations expressing either one transcription factor or the other. This observation was mirrored in the hippocampus, where ZEB1 and ZEB2 were expressed in different cell populations. ZEB1 was located in the nucleus of GFAP-expressing Type 1 cells (**Figure 3.1B**, yellow arrowhead), whereas ZEB2 was detected in the cytoplasm and was notably absent in Type 1 cells (**Figure 3.1B**, yellow arrow). A different staining pattern could be discerned in the SVZ, where ZEB1 and ZEB2 colocalised in the nuclei of a subset of cells, although the expression of ZEB2 was not consistent and appeared to be fainter in some cells than others (**Figure 3.1C**).

Thus, ZEB2 expression was not identified in the nucleus of hippocampal Type 1 cells. In support of this observation, mining of published, single-cell RNA-Seq data of the juvenile and adult mouse dentate gyrus demonstrated that ZEB1 is predominantly expressed in the precursor cell and astroglial populations. Contrastingly, ZEB2 expression was primarily observed in the differentiated neuronal

and oligodendrocyte populations (Hochgerner *et al.* 2018; Appendix A). Together, this indicates that ZEB2 may function in lineage-committed cells, in comparison to ZEB1, which is associated with undifferentiated cells. With this in mind, as well as the availability of an inducible Zeb1 loss-of-function mouse line, I decided to pursue ZEB1 as a potential transcriptional regulator of neurogenesis in the adult hippocampus.

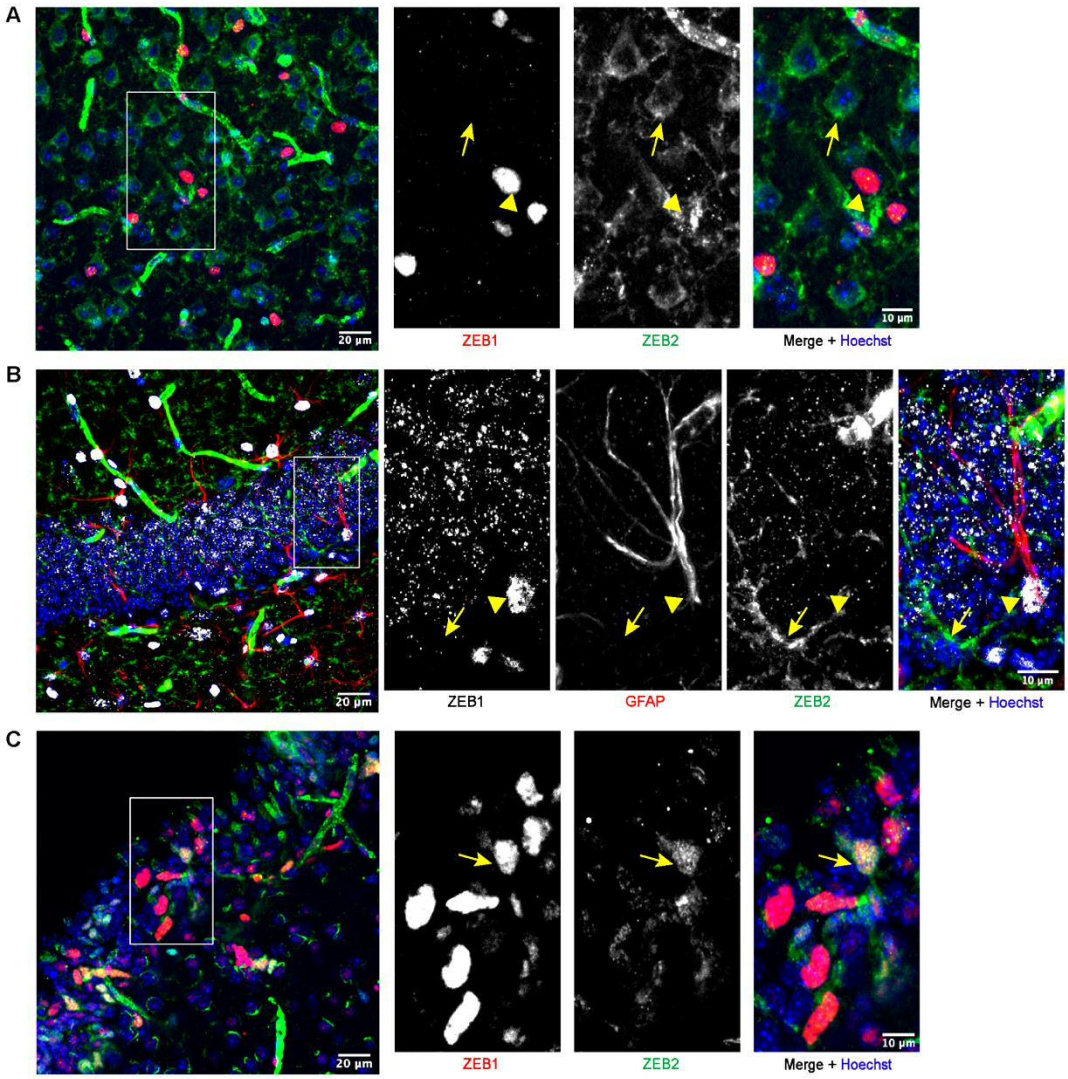

Figure 3.1. ZEB1 and ZEB2 show limited overlap in the adult mouse brain - IF co-staining for ZEB1 and ZEB2 was performed to investigate potential overlap in their expression in 12 week old mouse brain tissue. (A) In the cortex, there were distinct populations of cells either expressing ZEB1 (yellow arrowhead) or ZEB2 (yellow arrow), with no overlap. (B) Similarly, ZEB1 and ZEB2 expression did not exhibit co-expression in Type 1 cells in the hippocampus (yellow arrow and arrowhead show a ZEB2-expressing cell and GFAP+ NSC with ZEB1 expression, respectively). (B) Contrarily, there was some co-expression of the two transcription factors in the SVZ (yellow arrow). Nuclei were counterstained with Hoechst (blue). Scale represents 20 µm, and for inset images 10 µm, n=1.

3.3.2 Expression of ZEB1 in non-germinal regions and canonical stem cell niches in the adult mouse brain

To further characterise the cell-type specificity of ZEB1 in the adult mouse brain, sections from a 12-week old GLAST:CreER^{T2}-Rosa26$^{lsl\text{-}tdTomato}$ mouse in which the GLAST:CreERT2 locus was of a wild-type nature, were stained for ZEB1 and other established cell markers for major cell types in the brain. These included glial fibrillary acidic protein (GFAP) to identify neural stem cells (Section1.5.1), doublecortin (DCX) to label neuroblasts, βIII tubulin (TuJ1) as a pan-neuronal marker, 2',3'-cyclic nucleotide 3'phosphodiesterase (CNPase) to identify mature oligodendrocytes, and cluster of differentiation 31 (CD31) to label endothelial cells. Expression of ZEB1 in mature astrocytes was omitted (except for in the cortex which was assessed using a fluorescent reporter coupled with astrocytic morphology; Section 3.3.2.1) due to the cross-reactivity of the primary astrocyte-specific S100β antibody with the primary ZEB1 antibody due to the same host species. I assessed ZEB1 expression in the cortex, which is a largely post-mitotic region, as well as in the SVZ and hippocampus, which constitute the primary germinal niches in the adult brain.

3.3.2.1 ZEB1 expression in the cerebral cortex

The adult neocortex consists of mature postmitotic glial and neuronal cells, and is generally classified as a non-neurogenic brain compartment, although there is evidence suggesting that brain injury can induce neurogenesis through potential local latent neural progenitor cells (Magavi *et al.* 2000; reviewed in Lei *et al.* 2019). Thus, it was of interest to investigate the cell types in which ZEB1, a transcription factor that is linked to a pro-stemness cellular phenotype, was expressed in a primarily non-neurogenic region under homeostatic conditions.

I studied the expression of ZEB1 in the major cell populations in the cortex, including mature astrocytes and oligodendrocytes, neurons, and endothelial cells. Due to antibodies being raised in the same primary species as the ZEB1 antibody and thus secondary antibody cross-reactivity, with unsuccessful attempts at sequential immunostaining, I was unable to carry out IF staining using a mature astrocyte-specific marker such as S100β or GLAST. As an alternative, a mouse model was

utilised with inducible Cre recombinase-mediated tdTomato fluorescent protein expression driven by the ROSA26 promoter, in cells with the GLAST:CreER^{T2} construct (further details in Section 3.3.3). GLAST (also known as excitatory amino acid transporter 1, EAAT1), is an astrocyte-specific glutamate and aspartate transporter that is expressed by the majority of astrocytes, in contrast to other astrocyte markers such as GFAP, that are not expressed in cortical astrocytes. Thus, the use of a GLAST-specific tdTomato fluorescent reporter allowed the identification of astroglia in the cortex (Jungblut *et al.* 2012). ZEB1 expression was detected in the majority of tdTomato+GLAST+ astrocytes in the cortex (**Figure 3.2A**, yellow arrow). Conversely, no ZEB1 expression was found in TuJ1+ neurons and CNPase+ mature oligodendrocytes in this region (**Figure 3.2B**, and **Figure 3.2C**, respectively, yellow arrows). I observed that the majority of endothelial cells, identified by CD31 staining, were not immunoreactive for ZEB1, but there were a few cells in which ZEB1 protein was expressed (**Figure 3.2D,** yellow arrow).

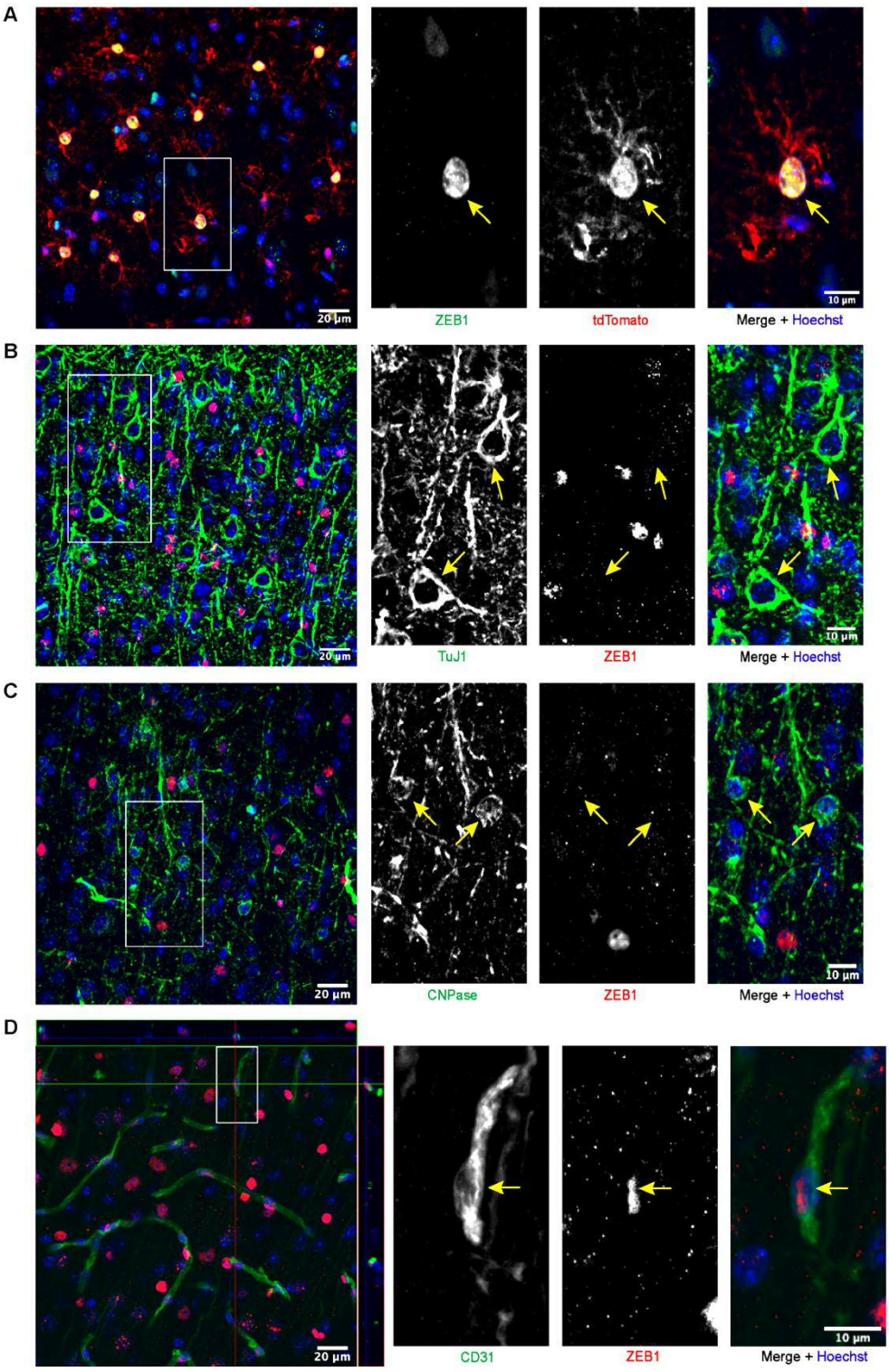

Figure 3.2. Characterisation of ZEB1 expression in the adult mouse cortex - Dual immunofluorescence characterisation of ZEB1 expression in the major neural cell populations in the cortex demonstrated that (A) ZEB1 colocalises with tdTomato expression in astrocytes (yellow arrow) in a GLAST-specific tdTomato reporter mouse model. (B) However, no ZEB1 protein was detected in TuJ1-expressing neurons, and (C) CNPase-expressing mature oligodendrocytes. (D) A minority of CD31+ endothelial cells were immunoreactive for ZEB1 expression, although the majority lacked ZEB1 protein. Nuclei were counterstained with Hoechst (blue). Scale represents 20 µm, and for inset images 10 µm; n=1.

3.3.2.2 ZEB1 expression in the SVZ

After establishing that ZEB1 is expressed in cortical astrocytes and a subset of endothelial cells, but not in cortical neurons and mature oligodendrocytes, I questioned what cells express this transcription factor in the germinal zones of the adult brain. For this, I first investigated ZEB1 expression in the SVZ, and found that ZEB1 is expressed in Type B cells (SVZ-residing NSCs; Section 1.3.2), which were identified by their GFAP expression as well as a ventricle-contacting radial process (**Figure 3.3A**, yellow arrow). Meanwhile, neuroblasts which were identified by DCX immunoreactivity and their chain-like migratory morphology, did not show positivity for ZEB1 (**Figure 3.3B**, yellow arrows). Similarly, TuJ1+ neurons also lacked ZEB1 expression (**Figure 3.3C**, yellow arrow). A subpopulation of mature oligodendrocytes that were immunoreactive for CNPase, also expressed ZEB1 (**Figure 3.3D**; yellow arrow), although another CNPase+ oligodendrocyte in the vicinity appeared to lack ZEB1 protein (**Figure 3.3D;** yellow arrowhead). Lastly, in line with the observations from the cortex, the majority of endothelial cells lacked ZEB1 expression in the SVZ, although there was a subpopulation of cells in which ZEB1 protein was detected (**Figure 3.3E**, yellow arrow).

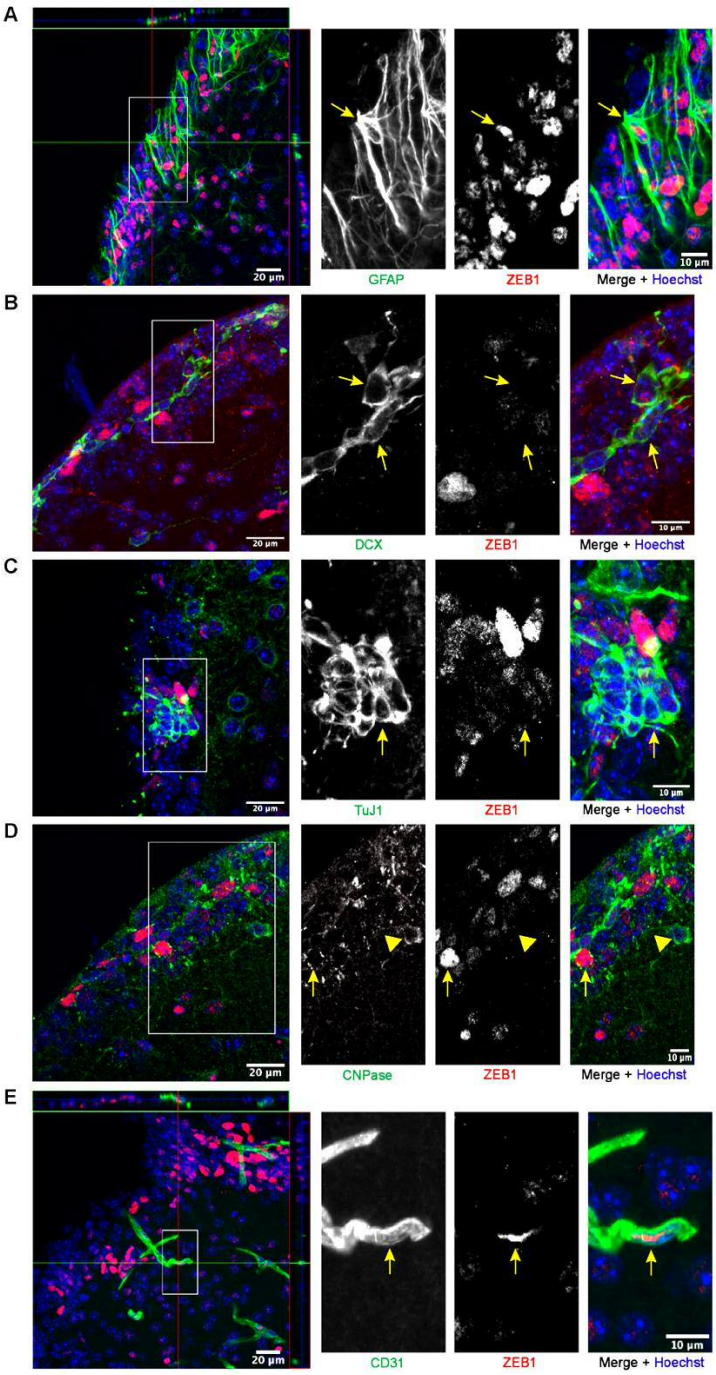

Figure 3.3. Expression of ZEB1 protein in the adult mouse SVZ – (A) ZEB1 protein was detected in GFAP+ Type B cells in the SVZ (yellow arrow), which can be seen distinctly in the orthogonal projection as ZEB1 protein is contained in the nucleus of Type B cells with GFAP+ projections. (B) Migrating DCX+ neuroblasts were observed to be ZEB1 deficient (yellow arrows), which was also the case for TuJ1+ neurons (C; yellow arrow). (D) A subset of CNPase-expressing oligodendrocytes located within in the SVZ region appeared to express ZEB1 (yellow arrow), whilst another subpopulation lacked ZEB1 protein expression (yellow arrowhead). (E) ZEB1 expression in CD31+ endothelial cells varied as some cells expressed the transcription factor (yellow arrow), whilst a large proportion demonstrated a lack of protein expression (in the orthogonal projections, an endothelial cell can be seen with CD31-localisation in the cytoplasm that visibly envelopes the ZEB1+ nucleus). Nuclei were counterstained with Hoechst (blue). Scale represents 20 µm, and for inset images 10 µm; n=1.

3.3.2.3 ZEB1 expression in the hippocampus

The hippocampus was the next brain region in which I sought to assess the protein expression of ZEB1. In line with the observations from the SVZ, I found that ZEB1 was expressed in the Type 1 NSC population, distinguished by the immunoreactivity of GFAP in morphologically radial cells with their soma located within the SGZ of the dentate gyrus (**Figure 3.4A**, yellow arrows). I also detected ZEB1 in GFAP+ astrocytes in the ML (**Figure 3.4A**, yellow arrowhead). However, ZEB1 protein expression could not be detected in DCX+ neuroblasts (**Figure 3.4B,** yellow arrows), or TuJ1+ neurons (**Figure 3.4C**, yellow arrows), which further corroborated the observations in the SVZ and the neocortex. Moreover, akin to the observations made in the cortex and SVZ, I did not detect ZEB1 in the majority of endothelial cells, although there were a limited number of ZEB1-immunoreactive cells (**Figure 3.4D**, yellow arrowhead and arrow, respectively).

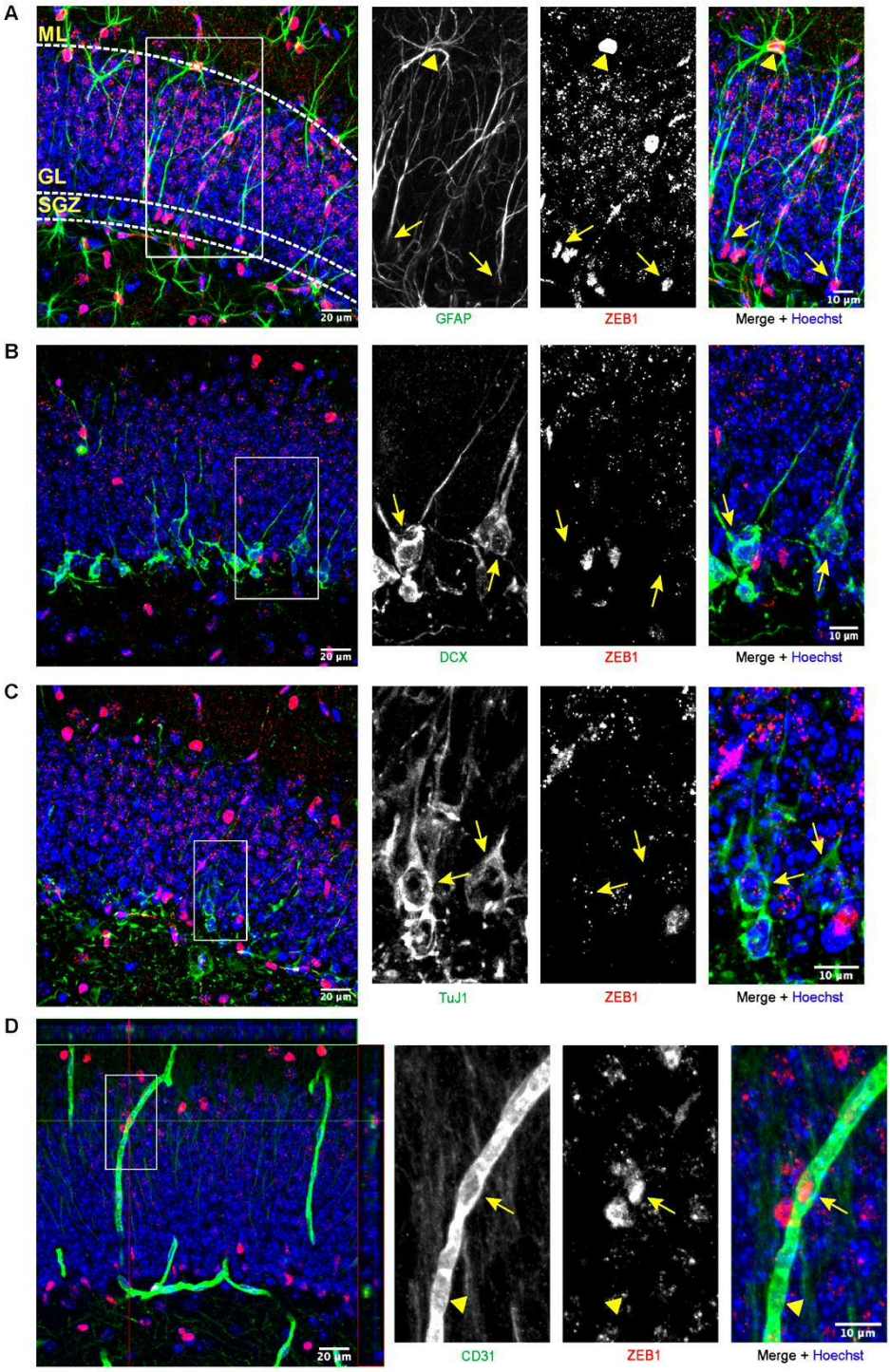

Figure 3.4. ZEB1 expression in the adult mouse hippocampus – (A) Dual IF staining was performed on 12-week old mouse brain sections, which revealed that ZEB1 protein is expressed in GFAP-expressing Type 1 NSCs as well as astrocytes in the ML (yellow arrows and arrowhead, respectively). The distinct subcompartments of the dentate gyrus (SGZ, GL, and ML) are demarcated in the first panel. (B) ZEB1 was not detected in DCX+ neuroblasts (yellow arrows), and (C) TuJ1-expressing neurons (yellow arrows). (D) Meanwhile, the majority of CD31+ endothelial cells lacked ZEB1 expression (yellow arrowhead), although a few cells that were ZEB1+ were present in the granule layer (yellow arrow). Nuclei were counterstained with Hoechst (blue). Scale represents 20 µm, and for inset images 10 µm; n=1.

3.3.3 Generation of a mouse model for conditional and inducible deletion of Zeb1

Because ZEB1 is expressed in NSCs in the hippocampus and SVZ, I decided to further investigate its potential functions in regulating adult NSC maintenance and neurogenesis. New neurons born in the SVZ emigrate from the lateral ventricle through the rostral migratory stream (RMS) several hundreds of microns to reach the olfactory bulb (OB), the site of their maturation and integration. Contrastingly, in the hippocampus new neurons are born in the SGZ and migrate only a short distance upwards into the granule layers where they become incorporated into pre-existing trisynaptic hippocampal circuits. Because of this intimate spatial relationship between NSCs and their mature neuronal progenies, neurogenesis in the hippocampus can be monitored within a single visual field. Moreover, functional assessment of Zeb1 deletion in the hippocampus (as covered later in Section 5.4.3) can be carried out using established memory function and behavioural tests, whilst olfaction learning is more difficult to study and assess. Therefore, I opted to focus on the functions of ZEB1 in the hippocampal region of the adult brain.

Gene knockout experiments are widely used to elucidate the functions of genes by studying the resulting phenotype following gene deletion. Similar studies were used to initially evaluate the function of ZEB1 following its discovery over two decades ago. Using a constitutive Zeb1 knockout mouse model, Takagi and colleagues showed that mouse embryos with heterozygous expression of ZEB1 are viable, but complete ZEB1 ablation results in perinatal death with a variety of symptoms such as T cell deficiency, respiratory system failure, and severe anomalies in skeletal formation, alongside infrequent neural tube closure defects (Takagi *et al.* 1998). Thus, the generation of a conditional, inducible knockout model for Zeb1 is needed to study ZEB1 functions in adult tissues as it allows for temporal control of gene deletion in specific cell types/tissues, limiting adverse side-effects.

In this project, the resultant phenotype of Zeb1 ablation in the adult mouse hippocampus was investigated through the breeding of a Zeb1 loss-of-function mouse model that utilises Cre-lox technology (Section 1.9.1). I crossed a transgenic mouse line with loxP sites flanking exon 6 of the Zeb1 gene (Brabletz *et al.* 2017), that encodes one of the main DNA-binding zinc finger domains (Section 1.8.1), with

a mouse line where the Cre recombinase gene fused with a modified estrogen receptor was expressed under control of the GLAST gene promoter (Mori *et al.* 2006). I further crossbred the resulting mouse line with the Ai9 mouse strain bearing a lox-stop-lox:tdTomato fluorescent reporter cassette in the ROSA26 locus, that would result in tdTomato protein expression with tamoxifen administration in all Cre recombinase-bearing mice (Madisen *et al.* 2010). The resultant mice of the genotype GLAST:CreER^{T2}-Rosa26$^{lox\text{-}stop\text{-}lox\text{-}tdTomato}$-Zeb1$^{flox/flox}$ are hereafter referred to as the Zeb1$^{fl/fl}$ strain (or Zeb1$^{-/-}$ following homozygous Zeb1 deletion). Administration of tamoxifen permits both temporal and cell-specific Zeb1 deletion, allowing the investigation of the resulting phenotype in GLAST-expressing mature astrocytes and NSCs in the adult brain (**Figure 1.7**; Section 1.9.1). I first investigated heterozygous Zeb1 loss-of-function to assess whether a single copy of the Zeb1 gene was sufficient to maintain wild-type functions, but I observed a dose-dependent phenotypic effect in Zeb1$^{+/-}$ mice (Appendix B). Hence, the control mouse model that I utilised in this project with wild-type ZEB1 expression was generated by crossing the GLAST:CreER^{T2} strain with the Rosa26$^{lox\text{-}stop\text{-}lox\text{-}tdTomato}$ cassette-carrying mice, which resulted in the genotype GLAST:CreER^{T2}-Rosa26$^{lox\text{-}stop\text{-}lox\text{-}tdTomato}$ (hereafter referred to as the control strain), thus controlling for any off-target effects of the fluorescent protein or Tamoxifen administration. Previous studies have reported a low-level leakiness of the GLAST:CreER^{T2}- dependent transgene recombination; assessment of this in the current study was found to be minor (Appendix C). Thus, potential leakiness effects in NSCs could be disregarded.

3.3.3.1 GLAST locus-specific Cre recombinase-driven Zeb1 knockout results in decreased ZEB1 expression in adult hippocampal neural stem cells

Due to the mixed genetic backgrounds of the mice used in the control and Zeb1$^{fl/fl}$ models, it was imperative to ascertain that the efficiency of Cre recombinase-mediated tdTomato recombination in the Type 1 cell population by tamoxifen administration was not significantly different between the two models. I investigated the percentage of GFAP+/tdTomato+ Type 1 cells as part of the total number of GFAP+ Type 1 cells one day after the last tamoxifen injection (six days after the first injection). In the control model, the efficiency of labelling Type 1 cells with the

tdTomato reporter was 85.5% ± 1.4%, compared to 86.7% ± 2.7% in the $Zeb1^{-/-}$ model ($p=0.8032$; **Figure 3.5A**). This demonstrates that the recombination efficiency is comparable between the two models and that their respective genetic backgrounds did not interfere with the recombination of transgenes.

Next, I sought to determine the efficiency of hippocampal NSC-specific Zeb1 deletion in the GLAST-$CreER^{T2}$-$Rosa26^{lsl\text{-}tdTomato}$-$Zeb1^{fl/fl}$ model. For this, I assessed the numbers of Type 1 cells (identified by radial morphology and GFAP immunoreactivity) expressing tdTomato and ZEB1, and Type 1 cells expressing tdTomato but lacking ZEB1 expression, using IF staining in hippocampal sections harvested one day after the completion of the tamoxifen administration protocol (six days after the first injection; Section 2.1.5). There was a strong decrease in the number of tdTomato+ Type 1 cells that expressed ZEB1 protein following tamoxifen administration in the $Zeb1^{-/-}$ mice (1,050 ± 503 cells/mm^3; **Figure 3.5B**, left black bar), compared to the control group (16,422 ± 579 cells/mm^3; $p<0.0001$; **Figure 3.5B**, left white bar). Conversely, a large number of tdTomato+ Type 1 cells lacked ZEB1 expression in the $Zeb1^{-/-}$ mice (18,118 ± 1,025 cells/mm^3; **Figure 3.5B**, right black bar), which in the control group was a relatively small population (1,488 ± 320 cells/mm^3; $p<0.0001$; **Figure 3.5B**, right white bar). Importantly, this demonstrates that at 1 day post-tamoxifen administration, the baseline pool size of Type 1 cells is equivalent in both models, which indicates that no NSCs are dying immediately after tamoxifen administration or Zeb1 deletion.

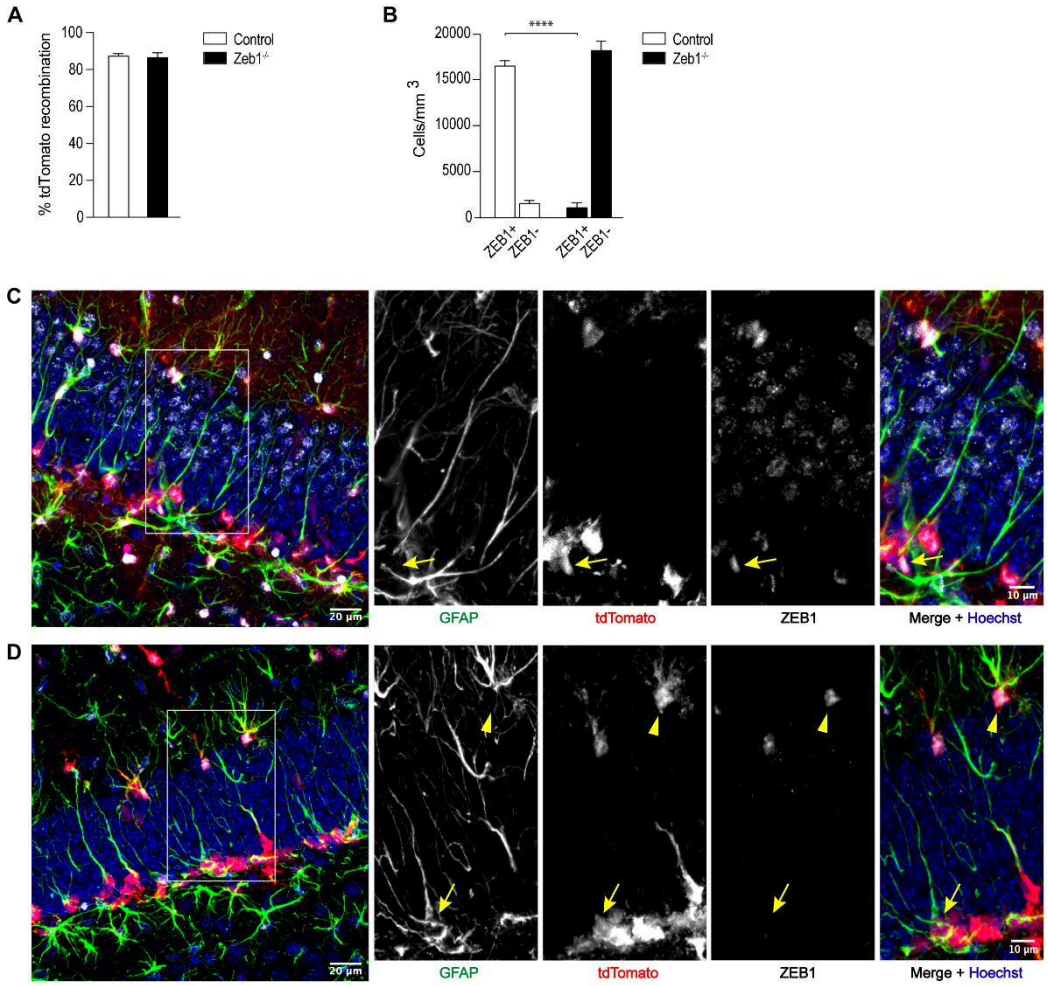

Figure 3.5. Quantification of Cre-mediated induction of tdTomato and deletion of Zeb1 in hippocampal Type 1 cells 1 day post-tamoxifen administration - (A) Using IF staining of tissue from control and Zeb1-/- mice 1 day after the last tamoxifen injection, the percentage of GFAP+ Type 1 cells with tdTomato to total GFAP+ Type 1 cells in the SGZ demonstrated that the induction efficiency was high in this cell population and comparable between the two genotypes. (B) Quantification of the number of Type 1 cells expressing ZEB1 and tdTomato after recombination in both genotypes validated the knockout of Zeb1 as this was significantly lower in the $Zeb1^{-/-}$ animals. Numerical data shown as mean ± SEM and are representative of three independent animals per genotype, with two sections analysed per animal, one-tailed t-test, **** $p<0.001$.
(C-D) Representative IF images of dentate gyri of the control and $Zeb1^{-/-}$ strains shown in which presence of ZEB1 in former model can be seen in GFAP+ Type 1 cells (C, yellow arrow), which is ablated with tamoxifen-mediated transgene recombination in Type 1 cells in $Zeb1^{-/-}$ mice (D, yellow arrow). Of note, GFAP+ astrocytes at the granule-molecular layer interface continued to express ZEB1 (D, yellow arrowhead). Nuclei were counterstained with Hoechst (blue). Scale represents 20 μm, and for inset images 10 μm.

3.4 Discussion

3.4.1 ZEB1 is expressed in cortical astrocytes and adult NSCs in the mouse hippocampus and SVZ

One of the main objectives of this chapter was to determine the cell-type specificity of ZEB1 in the cerebral cortex, that houses a large population of postmitotic cells, as well as in the two main neurogenic niches, the hippocampus and SVZ. This would allow the further investigation of any potential transcriptional regulatory roles of ZEB1 in the adult brain.

Based on previously published research, I hypothesised that ZEB1 protein would be detected in the germinal regions of the adult brain, and would show limited expression in the cortex, due to the absence of stem cells in this region. Unexpectedly, I observed that an overwhelming majority of cortical astrocytes expressed ZEB1, as well as some endothelial cells. Moreover, ZEB1 protein was also detected in astrocytes situated in the ML of the dentate gyrus. This supports data mined from the publicly available dentate gyrus single-cell RNA-Seq study published by the Linnarsson group (Hochgerner *et al.* 2018) in which I found that ZEB1 was expressed in a variety of non-NSC populations including immature and mature astrocytes, and endothelial cells. Taken together, this suggests that the transcriptional regulatory functions of ZEB1 may not be solely restricted to stem cells. Whilst the functions that ZEB1 may have in non-SC regions is undetermined, two possible scenarios can be speculated: 1) ZEB1 may be an astroglial lineage-specifying factor (this will be further discussed in light of other findings in Section 5.4.2), and 2) this factor may be involved in injury and inflammation-related responses in the brain, as both astrocytes and endothelial cells are known to undergo proliferation in pathological conditions (Gotts and Chesselet 2005; Buffo *et al.* 2008). In particular, Buffo and colleagues demonstrated in their study that mature quiescent astroglia can gain multipotent stem cell-like properties as a repair mechanism in brain injury (Buffo *et al.* 2008); as EMT transcription factors are becoming increasingly recognised for their function in conferring cell plasticity, it is possible that ZEB1 may be present

in astrocytes to mediate pathological responses. However, this will not be further explored as it is outside the remit of this thesis.

I observed that NSCs in both the hippocampus and SVZ expressed ZEB1 protein. This is consistent with data extracted from the aforementioned DG-based single-cell RNA Seq study; amongst a variety of hippocampal cells isolated from the dentate gyri of juvenile and adult mice, quiescent radial glia-like cells, which form the adult NSC population, express Zeb1 mRNA. Furthermore, the expression of ZEB1 in the NSC population in the SVZ is in accordance with data published by Sabourin and colleagues in which they identified ZEB1 protein in GFAP+ Type B cells in the adult mouse SVZ (Sabourin *et al.* 2009).

3.4.2 ZEB1 expression declines with neuronal differentiation

Following the observation of ZEB1 expression in NSCs in the hippocampus and SVZ, I carried out subsequent IF staining to study whether the transcription factor was also detectable in neuroblasts, cells that are committed to the neuronal lineage, as well as fully differentiated young neurons.

I observed that neuroblasts in the aforementioned brain regions generally lacked ZEB1 expression, although in this study it was later found that a small number of neuroblasts continued to express ZEB1 at 7 weeks old (further discussed below) Similarly, young postmitotic TuJ1+ neurons in both regions did not exhibit ZEB1 protein expression, which further suggests that ZEB1 expression ceases once cells undergo differentiation.

In the abovementioned report published by Sabourin *et al.*, the researchers demonstrated using IF staining that the majority of young neurons with expression of polysialylated neuronal cell adhesion molecule (PSA-NCAM) lacked ZEB1 protein expression (Sabourin *et al.* 2009); neuroblasts are identified with both DCX and PSA-NCAM as cell markers (Nacher *et al.* 2002), and so observations made in PSA-NCAM+ neuroblasts can be translated to DCX+ neuroblast population findings in the current study. Further accordance between the two studies lies in the observation of a small population of neuroblasts that are ZEB1+; in the current study, I observed 429 ± 171 cells/mm^3 DCX+ZEB1+ neuroblasts in the hippocampus labelled with the tdTomato reporter at two weeks post-induction in 6 week old mice, which was significantly

fewer cells than the 20,522 ± 1,592 cells/mm^3 DCX+ZEB1- neuroblasts observed in the same tissue ($p<0.0001$, two-tailed t-test; quantification of DCX+ZEB1+ neuroblasts in the SVZ was not carried out).

The results are further in line with previous studies that have investigated the expression of ZEB1 in embryonic tissue systems. In the brain, Singh *et al*. reported that ZEB1 is expressed in cerebellar granule neuron progenitors but is subsequently switched off as the progenitor cells differentiate into cerebellar granule neurons (Singh *et al.* 2016). Furthermore, a similar study investigating the embryonic neocortex found that ZEB1 protein is detected in embryonic cortical neural progenitors, but is extinguished with the differentiation of the progenitors and their migration into the developing cortex (Wang *et al.* 2019).

In summary, I found that ZEB1 is expressed in astrocytes in the cortex and hippocampus, as well as in the NSC population in the two major neurogenic niches, the hippocampus and the SVZ. However, ZEB1 protein was not detected in the majority of neuroblasts and all young mature neurons in both regions. This suggests that ZEB1 is involved in the transcriptional regulation of precursor cells in the neurogenic niches, but is predominantly downregulated once neuronal lineage-specification occurs. This will be further investigated in Chapters 4 and 5. The function of ZEB1 in astrocytes in the adult brain is unclear, but as discussed in Section 3.4.1, it can be speculated that this may be associated either with lineage specification or with the protective function of astrocytes in response to injury.

3.4.3 ZEB1, but not ZEB2, is expressed in adult hippocampal NSCs

The ZEB family of transcription factors consists of ZEB1 and ZEB2. The zinc finger domains on the two proteins show considerable homology (95% and 80% similarity between the proteins in the N-terminal and C-terminal ZF domains, respectively), while the other binding domains are structurally largely distinct between the two factors. There is some overlap in the expression patterns of ZEB1 and ZEB2; Postigo and Dean characterised their protein expression using fetal and adult tissue from various tissue systems and reported an incomplete overlap between the two factors, with ZEB2 being expressed at a higher level in certain tissues such as the heart (Postigo and Dean 2000).

In the current study, one of the objectives was to characterise potential overlap between the two ZEB transcription factors in the adult brain, and in particular in the hippocampus. I found that whilst ZEB1 was expressed in GFAP+ Type 1 cells in the hippocampus, these cells lacked ZEB2 expression.

Postigo and Dean demonstrated using Northern blotting of adult human tissue that the expression of Zeb1 mRNA was higher than Zeb2 in the temporal lobe, which houses the hippocampus (Postigo and Dean 2000). In addition, single-cell RNA-Seq data mined from the Hochgerner *et al.* study revealed lower Zeb2 transcript levels in radial glia-like cells, compared to Zeb1 in the juvenile and adult mouse dentate gyrus (Hochgerner *et al.* 2018; Appendix A); this corroborates with the observations of low ZEB2 protein expression in the hippocampus in the present study. However, it has previously been reported that the ablation of Zeb2 in mouse embryos resulted in a deficiency in hippocampal formation, with decreased proliferation, and differentiating cells undergoing apoptosis (Miquelajauregui *et al.* 2007). These results suggest that ZEB2 is crucial for the correct formation of the embryonic hippocampus, although it is possible that this programming changes in the adult brain, with a switch occurring between the roles of ZEB1 and ZEB2.

Therefore, I focused on investigating ZEB1 and its function in adult hippocampal neurogenesis, as ZEB2 was not detected in the NSC population in this germinal niche.

3.4.4 GLAST-Cre model efficiency

The inducible expression of Cre recombinase driven by promoters that are specific for Type 1 and Type 2 hippocampal cells is a key method for studying neurogenesis, and several models that employ this method have already been created for the purposes of lineage tracing *in vivo*. Mori and colleagues developed a GLAST-specific Cre recombinase model that can be used to investigate hippocampal Type 1 cell and astrocyte populations in the brain (Mori *et al.* 2006). Moreover, this model can be used to trace hippocampal Type 1 cells from embryonic development through to adulthood, allowing the comparison of this cell population at various stages of mammalian life (Mori *et al.* 2006).

The GLAST:CreER^{T2} mouse model has been widely used to perform lineage tracing, delineating adult-born neurons that arise from labelled GLAST-expressing cells, and in turn providing evidence of the stem cell identity of the latter cell population (Section 1.9.2.4). A study characterised the expression of β-galactosidase in adult GLAST:CreER^{T2} mice and reported that following tamoxifen administration, hippocampal neural stem cells were labelled and 19 days post-induction, labelled DCX+ cells were also detected, verifying the identity of the putative adult neural stem cells (Slezak *et al.* 2007). Similarly, Yang and colleagues demonstrated that conditional expression of tdTomato in GLAST:CreER^{T2} mice resulted in the labelling of newborn neurons which matured functionally and became incorporated in the hippocampal synaptic network (Yang *et al.* 2015). Importantly, a comparison between neurogenic recovery after ablation of proliferating progenitors in nestin-Cre and GLAST-Cre mice demonstrated that only Type 1 cells in the latter model contributed to cell proliferation (Decarolis *et al.* 2013). The findings from these studies confirm that the GLAST:CreER^{T2} model successfully targets Type 1 NSCs in the hippocampus; this was the basis of the model of choice for the current study.

In this study, I calculated that tdTomato expression in the GLAST:CreER^{T2}-Rosa26$^{lsl\text{-}tdTomato}$ model overlapped with approximately 87.5% of all GFAP-expressing hippocampal Type 1 cells, whilst the overlap was 86.7% in the GLAST:CreER^{T2}-Rosa26$^{lsl\text{-}tdTomato}$-Zeb1$^{fl/fl}$. In the first published study that characterised the model, the authors demonstrated that Cre recombinase expression stemming from the GLAST locus overlapped with approximately 60-80% of S100β and glutamine synthetase-expressing astrocytes (Mori *et al.* 2006). Moreover, they examined the recombination efficiency in adult Type B cells in the SVZ using a Connexin43:LacZ mouse, and found that 65.9% ± 15.6% GFAP+ cells expressed β-galactosidase; however, adult hippocampal Type 1 cells were not investigated. The results demonstrate that the efficiency of NSC-labelling in the models in the present study was either on par or higher than in previously published literature (Ninkovic *et al.* 2007; Jahn *et al.* 2018).

Interestingly, I observed that although ZEB1 expression was ablated from the Type 1 cell population in the SGZ, it was still detected in the ML-residing astrocytes

in the hippocampus, and these astrocytes also expressed tdTomato protein (**Figure 3.4A**, inset, yellow arrowhead). There is evidence suggesting that chromatin structure within a cell can alter gene expression through varied DNA accessibility; chromatin structure in turn is influenced by numerous post-translational modifications such as DNA methylation and acetylation. Therefore, it can be hypothesised that the ROSA26 locus is more accessible than the Zeb1 locus, rendering the Cre-induced expression of tdTomato more comprehensive than the deletion of Zeb1. This is likely the case as the ROSA26 locus has ubiquitous transcriptional activity and so may be more accessible to transcriptional machinery when compared to the Zeb1 locus. The administration of a higher tamoxifen dose may be more efficient in targeting the aforementioned cells that still express ZEB1 despite also demonstrating induction of tdTomato expression (Mori *et al.* 2006).

In summary, thus far it was found that the two ZEB transcription factor family members, ZEB1 and ZEB2, were expressed somewhat differentially in the adult mouse brain. ZEB1 expression was detected predominantly in the neural precursor cell populations in the hippocampus and SVZ, following which its expression decreased with neuronal cell lineage specification in both neurogenic zones. Subsequently, I aimed to evaluate the functions of ZEB1 in the adult hippocampal neurogenic niche, for which I generated an inducible Zeb1 loss-of-function mouse model, featuring GLAST-expressing Type 1 cell and astrocyte-specific Zeb1 deletion, alongside the expression of tdTomato fluorescent protein in cells targeted with tamoxifen. The efficiency of tdTomato expression induction was equivalent in the Zeb1 deletion model and the control mouse line for this model, bearing the inducible tdTomato fluorescent reporter cassette whilst exhibiting wild-type ZEB1 expression. The Zeb1 deletion efficiency was also observed to be very high with the chosen tamoxifen treatment regime. This model will be used in subsequent chapters to further explore the resulting phenotype of Zeb1 deficiency in the hippocampal neurogenic niche.

Chapter 4 - ZEB1 promotes the self-renewal of Type 1 cells in the adult hippocampus

4.1 Introduction

The pro-stemness function of ZEB1 in the developing CNS has been established through a series of important studies. It has been reported that this transcription factor inhibits the differentiation of neural precursors in the embryonic brain, namely in the development of the cerebellum and cortex (Singh *et al.* 2016; Liu *et al.* 2019; Wang *et al.* 2019). Moreover, ZEB1 has been extensively shown to impart a stemness phenotype to cancer cells in a number of tumours, including breast, lung, pancreatic, and brain (reviewed in Caramel *et al.* 2018).

Drawing upon this line of evidence, I aimed to assess the function of ZEB1 in adult hippocampal neurogenesis. In the previous chapter, I detected ZEB1 expression in the Type 1 cells in the hippocampal neurogenic niche, but not in the neuroblasts and neurons (Section 3.3.2.3). Consequently, I queried the role of this transcription factor in the stem cell compartment housed in the SGZ of the dentate gyrus. In particular, I hypothesised that ZEB1 would have pro-stemness functions in the healthy adult brain, analogous to its functions in the developing embryonic brain, as well as in cancer progression in which it mediates cell plasticity to propagate cancer stem cells. To evaluate the functions of Zeb1, I utilised the two mouse models (described in Section 2.1.1) that I generated through breeding of pre-existing mouse strains; the first model had the experimental genotype GLAST:CreER^{T2}-Rosa26$^{lsl\text{-}tdTomato}$-Zeb1$^{fl/fl}$ and featured tamoxifen-inducible Zeb1 deletion in GLAST-expressing cells. The second mouse model, with the genotype GLAST:CreER^{T2}-Rosa26$^{lsl\text{-}tdTomato}$ and wild-type ZEB1 expression, was developed as a control for the Zeb1 deletion phenotype.

In this chapter, my main aim was to determine the functions of ZEB1 in the maintenance of hippocampal neurogenesis, at the level of hippocampal Type 1 cells and Type 2 proliferating progenitor cells. Understanding whether the loss of Zeb1 affects the stem and early progenitor cell populations is the first step in identifying the larger phenotype, as in the previous chapter, it was found that ZEB1 is expressed in the NSCs in the adult brain. This bears consequences for neural cell populations derived from these precursor cells.

4.2 Aims and objectives

1) To evaluate whether ZEB1 regulates the self-renewal of hippocampal Type 1 cells through the assessment of cell population size and stem cell activation.

2) To determine the effects of Zeb1 deletion on the proliferation of Type 2 cells, which was assessed through cell proliferation and Type 2-specific cell marker expression.

4.3 Results

4.3.1 Effects of Zeb1 ablation in the hippocampal Type 1 cell population

The study of the diverse intermediate cell types that arise during the complex multistep process of neurogenesis exploits different cell type-specific markers expressed at distinct stages of the process. These markers are widely used in the field, and, coupled with cell morphology as well as localisation within the dentate gyrus, can be used as a panel to demarcate cell identities along the continuum from NSC to progenitor cell to neuroblast to mature neuron.

One of the main objectives of this study was to elucidate the pro-stemness role of ZEB1 in the self-renewal and proliferation of stem cells. Adult mouse hippocampal Type 1 cells exhibit radial morphology with the soma located in the SGZ and a GL-traversing process that branches out in the inner ML. They exist in two states, quiescent and activated, that can be distinguished by their cell marker profile. I drew a panel of markers consisting of GFAP and minichromosome maintenance protein 2 (MCM2) to demarcate the Type 1 cells; quiescent Type 1 cells were identified by the expression of GFAP and a lack of MCM2 expression, whilst the activated cells were distinguished by their co-expression of GFAP and MCM2 (Niu *et al.* 2011).

I quantified the number of GFAP+MCM2- cells (with expression of tdTomato) in the control and $Zeb1^{-/-}$ mice at 1 day post-recombination (6 days after the first injection), to evaluate changes in the quiescent Type 1 cell population; at this timepoint there was no significant difference in this cell population between the two genotypes (12,684 ± 1,528 cells/mm^3, and 10,204 ± 894 cells/mm^3, respectively; p=0.1169; **Figure 4.1A**). At 4 weeks post-recombination, there was a statistically significant difference in the number of quiescent Type 1 cells between the control (16,423 ± 1,314 cells/mm^3) and $Zeb1^{-/-}$ mice, (9,071 ± 2,625 cells/mm^3; p=0.0332; **Figure 4.1B**). Based on the suggestive quiescent Type 1 cell population decrement seen in the $Zeb1^{-/-}$ mice, I queried whether a similar effect would be seen in the activated Type 1 cells with Zeb1 deficiency. As early as 1 day post-recombination, there was a significant decrease in the number of activated Type 1 cells in the $Zeb1^{-/-}$ mice in comparison to the control group (2,884 ± 618 cell/mm^3 and 5,441 ± 641

cells/mm^3, respectively; p=0.0227; **Figure 4.1C**). This decrease was equally pronounced at 4 weeks (control: 1,993 ± 376 cells/mm^3; Zeb1$^{-/-}$: 673 ± 347 cells/mm^3; p=0.0307; **Figure 4.1D**). Representative IF images are shown in **Figure 4.1E-H** that demonstrate the quiescent (yellow arrowheads) and activated (yellow arrows) Type 1 cell populations in the control and Zeb1$^{-/-}$ mice at 1 day (E and F, respectively) and 4 weeks (G and H, respectively).

As I observed an overall decrease in both quiescent and activated Type 1 cells at 4 weeks post-Zeb1 deletion, I resolved to investigate whether this was maintained at later timepoints, namely 8, 12, and 26 weeks; for this I considered the quiescent and activated Type 1 cells together. By 8 weeks post-induction, the total number of Type 1 cells in the Zeb1$^{-/-}$ mice was 3,978 ± 67 cells/mm^3, which was significantly fewer than observed in control mice (9,171 ± 1,038 cells/mm^3; p=0.0038; **Figure 4.2A**). This difference was further amplified by 12 weeks following loss of Zeb1, with only 2,073 ± 386 cells/mm^3 in the Zeb1$^{-/-}$ mice, whereas the total number of Type 1 cells remained stable in the control group (9,154 ± 1,139 cells/mm^3; p=0.0021; **Figure 4.2B**). By 26 weeks post-recombination, the number of Type 1 cells in the Zeb1$^{-/-}$ mice remained lower than in the control group (2,315 ± 97, and 10,948 ± 347 cells/mm^3, respectively; p<0.0001; **Figure 4.2C**). Representative images that illustrate the cell numbers are provided in **Figure 4.2D-I**; in comparison to the control mice a gradual depletion of Type 1 cells can be observed between 8 and 26 weeks post-Zeb1 deletion in the Zeb1$^{-/-}$ mice.

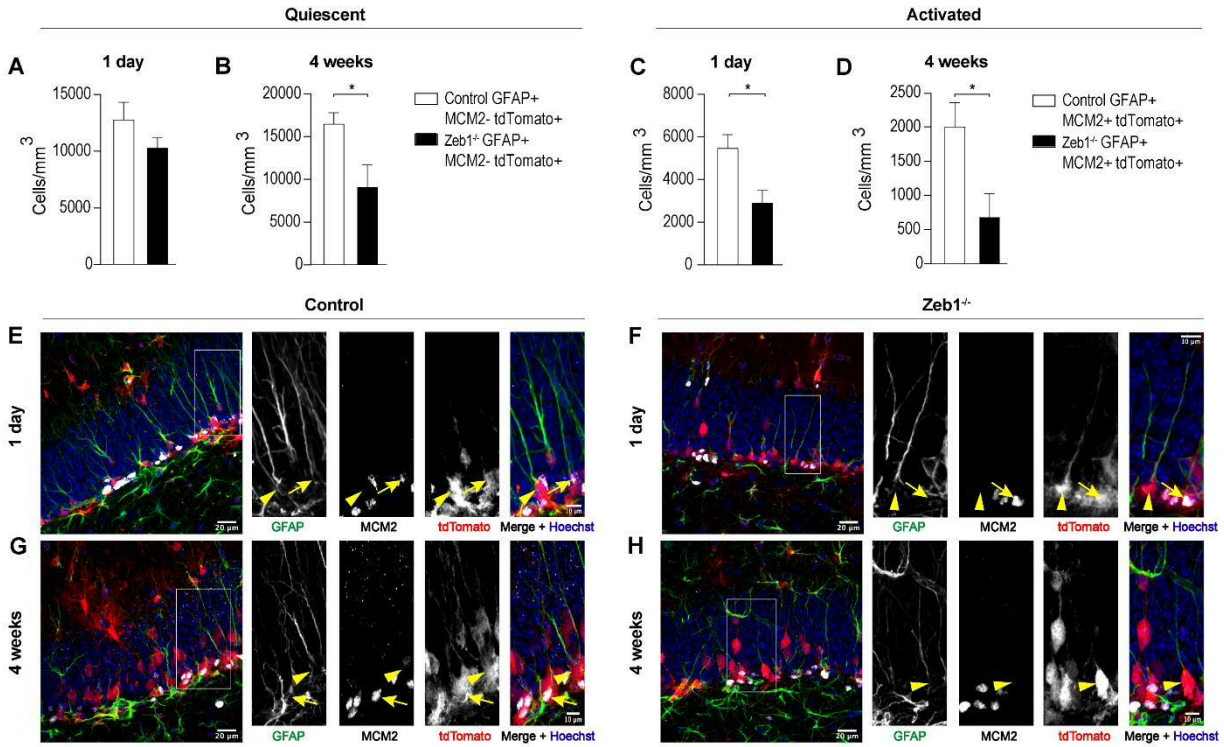

Figure 4.1. Reduction of both quiescent and activated Type 1 cells following loss of Zeb1 - (A-B) Quantification of quiescent GFAP/tdTomato-expressing Type 1 cells that lacked MCM2 at 1 day and 4 weeks, respectively, showed no significant difference at the former timepoint in the Zeb1$^{-/-}$ group (black bars) in comparison the control mice (white bars), but a significant decrease was detected by 4 weeks. (C-D) Similar quantification of activated GFAP/tdTomato/MCM2-expressing Type 1 cells revealed a gradual decline starting already at 1 day post-tamoxifen administration. Numerical data shown as mean ± SEM and are representative of three independent animals per genotype, with a minimum of two sections analysed per animal, one-tailed t-test, * $p<0.05$.
Representative IF images of the quiescent (yellow arrowheads) and activated (yellow arrows) Type 1 cells in the control and Zeb1$^{-/-}$ mice at 1 day (E and F, respectively), and 4 days (G and H, respectively). Scale represents 20 μm, and for inset images 10 μm.

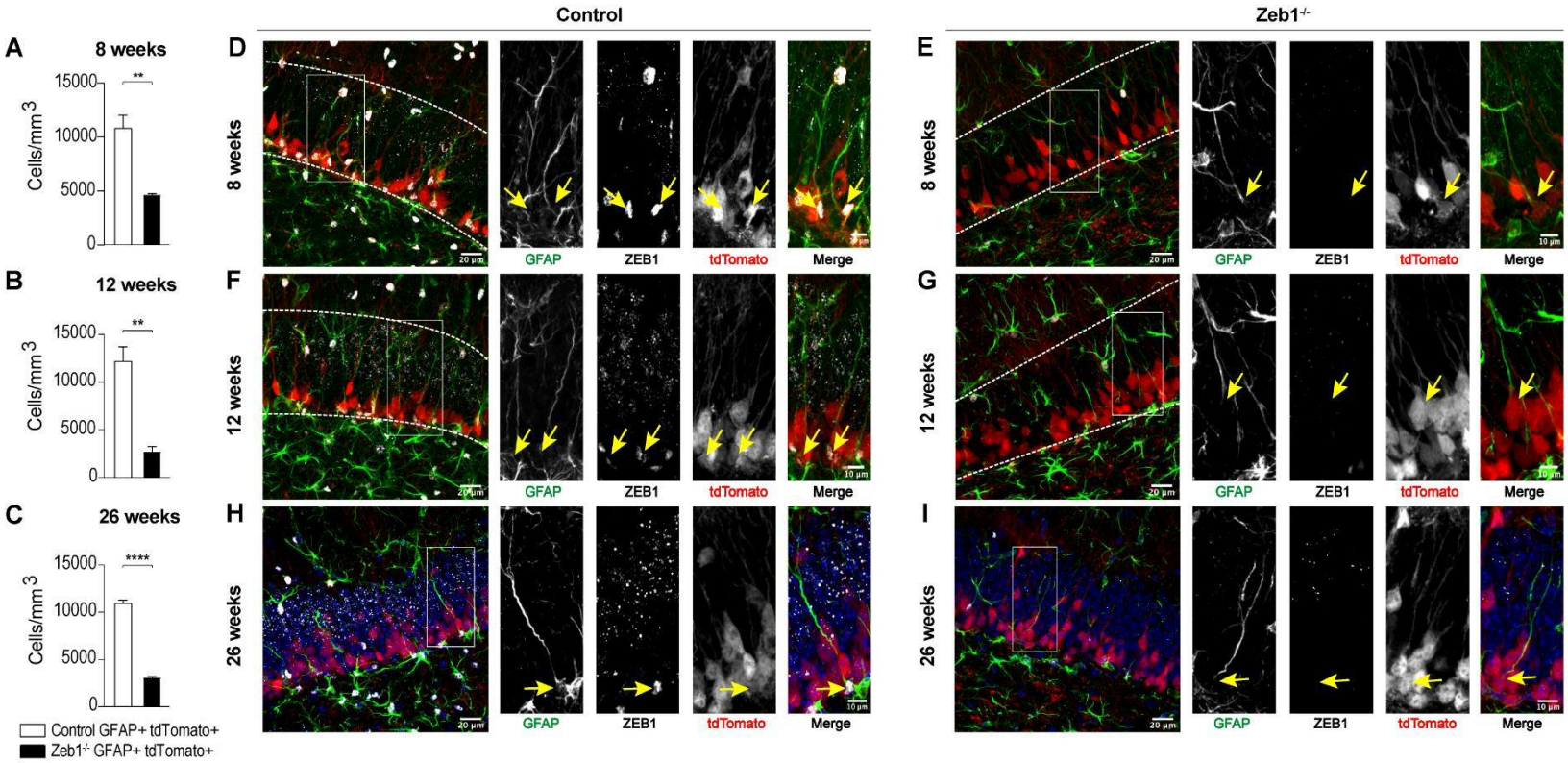

Figure 4.2. Zeb1 deficiency results in the gradual depletion of hippocampal Type 1 cells – (A-C) Counts of Type 1 cells (quiescent and activated together) steadily declined in the Zeb1$^{-/-}$ mice (black bars) compared to the control mice (white bars) over 26 weeks (with 8, 12, and 26 weeks investigated). Numerical data shown as mean ± SEM and are representative of three independent animals per genotype, with a minimum of two sections analysed per animal, one-tailed t-test, ** $p<0.01$, **** $p<0.0001$.
Representative images of IF staining for control (D, F, and H), and Zeb1$^{-/-}$ (E, G, and I) mice at 8, 12, and 26 weeks (respectively), demonstrating the gradual decrement in the GFAP-expressing Type 1 cell population (yellow arrows). Nuclei were counterstained with Hoechst in the images at 26 weeks. Dashed lines delineate the boundaries of the DG. Scale represents 20 µm, and for inset images 10 µm.

I decided to further investigate changes in the Type 1 cell population driven by the deletion of Zeb1, using SOX2 as a recognised Type 1 and Type 2a cell marker that has been identified as a critical transcription factor for the proliferative and multipotent characteristics of Type 1 cells (Steiner *et al.* 2006; Favaro *et al.* 2009; Nicola *et al.* 2015). Interestingly, I did not observe a significant decrease in the number of SOX2-expressing cells in the SGZ up to 8 weeks following Zeb1 deletion, compared to the control group. At 2 weeks post-deletion (**Figure 4.3A)**, I quantified 22,268 ± 1,553 cells/mm^3 in the control mice which was not significantly different to the 18,616 ± 1,795 cells/mm^3 present in the Zeb1$^{-/-}$ group (p=0.0994). Similarly, at 4 (**Figure 4.3B**) and 8 weeks (**Figure 4.3C**), the control mice had 13,968 ± 2,453 and 15,750 ± 711 cells/mm^3, respectively, which once again did not differ remarkably from the number of cells quantified in the Zeb1$^{-/-}$ group (12,126 ± 2,175 at 4 weeks and 14,930 ± 2,392 cells/mm^3 at 8 weeks; p=0.3021 and 0.3796, respectively). However, at 12 weeks there was a significant decrease in the number of SOX2+ cells with the Zeb1$^{-/-}$ group presenting 3,173 ± 344 cells/mm^3, compared to 9,972 ± 1,124 cells/mm^3 quantified in the control group (p=0.0022; **Figure 4.3D**).

Representative images, provided in **Figure 4.3E-L**, demonstrate the comparable numbers of SOX2+ cells (yellow arrows) that also express tdTomato, at 2, 4, and 8 weeks in the SGZ of control mice (**Figure 4.3E, G,** and **I**, respectively) and Zeb1$^{-/-}$ mice (**Figure 4.3F, H,** and **J**, respectively). At 12 weeks post-induction, the SOX2+ cell population in the Zeb1$^{-/-}$ mice in panel L of **Figure 4.3** which exhibits a representative field of view of the dentate gyrus of the Zeb1$^{-/-}$ mice, are reduced in number in the SGZ when compared to the control group (**Figure 4.3K**).

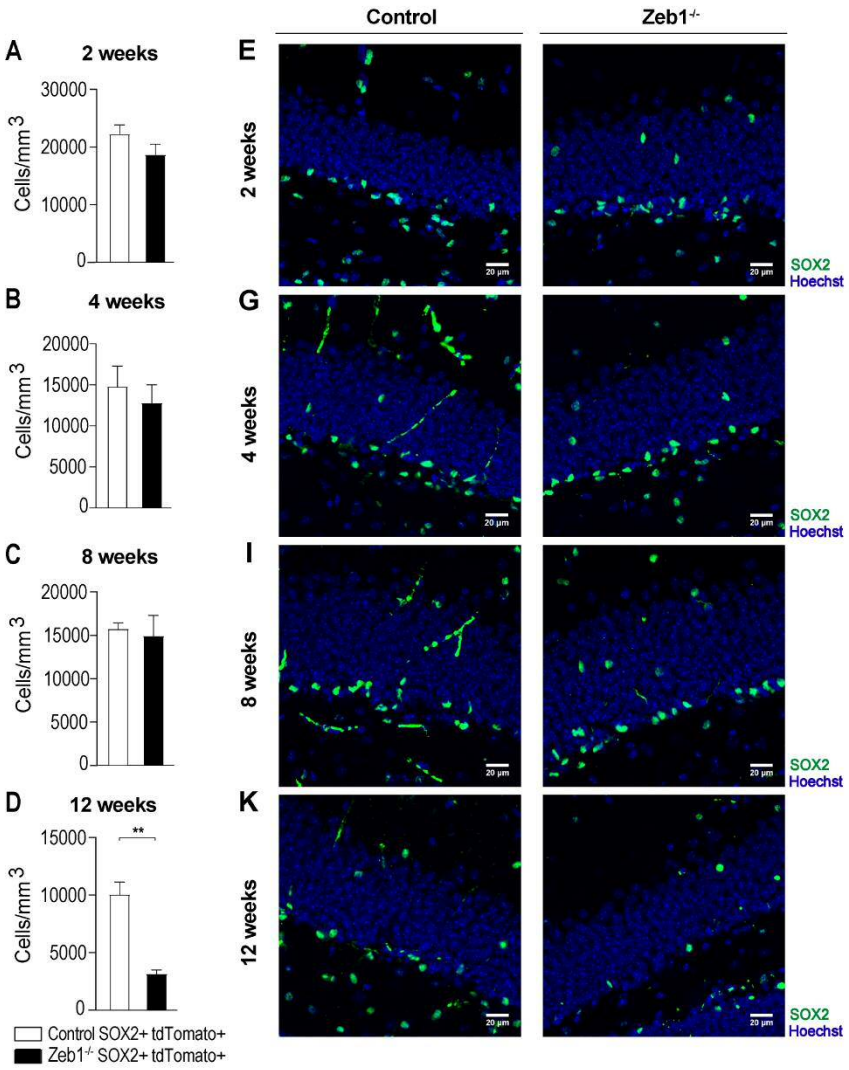

Figure 4.3. Zeb1 ablation results in a slow reduction in SOX2-expressing cells in the SGZ – (A-D) SOX2-expressing cells in the SGZ were quantified at 2, 4, 8, and 12 weeks, respectively, in the control (white bars) and Zeb1$^{-/-}$ mice (black bars), and no difference was seen up to 8 weeks post-Zeb1 deletion. By 12 weeks there was a significant decline in the SOX2-expressing cell population in the SGZ of Zeb1$^{-/-}$ mice (D). Numerical data shown as mean ± SEM and are representative of three independent animals per genotype, with a minimum of two sections analysed per animal, two-tailed t-test, ** $p<0.01$. Representative IF images demonstrate no differences in the SOX2+ cells (yellow arrows) between the control (E, G, I) and Zeb1$^{-/-}$ mice (F, H, J) at 2, 4, and 8 weeks, respectively, post-transgene recombination, whilst in comparison to the control group at 12 weeks (K) a significant decrease was observed in the Zeb1$^{-/-}$ mice (L). Nuclei were counterstained with Hoechst (blue). Scale represents 20 μm, and for inset images 10 μm.

4.3.2 Zeb1 deletion effects on cell proliferation in the SGZ

Thus far in this chapter, Zeb1 deficiency resulted in a gradual depletion of Type 1 cells. This prompted me to query whether the proliferation of Type 2 IPCs was also affected as a result of the deletion of Zeb1. Consequently, I evaluated the proliferation rates of the progenitor cell pool as an indicator of the fate of the Type 1 cell population, as increased lineage-commitment divisions of Type 1 cells would increase the pool of Type 2 cells undergoing proliferation and differentiation into neurons. I used IF staining for MCM2 and Ki67, as well as the incorporation of the thymidine analogue EdU (which will be discussed in Section 5.3.4) to investigate possible changes in cell mitotic activity in the Zeb1$^{-/-}$ mice compared to the control group. I chose to assess both MCM2 and Ki67 as their expression is not wholly overlapping; MCM2 is a cell cycle marker that identifies both cycling cells as well as cells with proliferative potential, and its expression is maintained throughout the cell cycle, bar the quiescence G0 phase, whilst Ki67 is expressed predominantly in the G2 and S phases of the cell cycle, thus demonstrating a shorter detection window (Wharton *et al.* 2001).

4.3.2.1 MCM2

Late Type 2 cells, also termed Type 2b cells, are IPCs that lack resemblance to their precursors through the downregulation of GFAP expression; I identified these cells by quantifying the number of MCM2+GFAP- non-radial cells in the SGZ of both mouse lines. At 1 day post-recombination, there was a significant reduction in the number of Type 2b cells following Zeb1 deletion (28,648 ± 4,757 cells/mm^3), in comparison to the control group (16,023 ± 1,628 Type 2 cells/mm^3; p=0.0330; **Figure 4.4A**). However, by 4 weeks the Type 2b cell population size was more comparable between both groups (control: 8,747 ± 739 cells/mm^3, Zeb1$^{-/-}$ mice: 4,574 ± 2,616 cells/mm^3; p=0.0998; **Figure 4.4B**). **Figure 4.4C-D** exhibits representative IF images which show the Type 2 cell population (yellow arrowheads) in the control and Zeb1$^{-/-}$ mice (panels C and D, respectively).

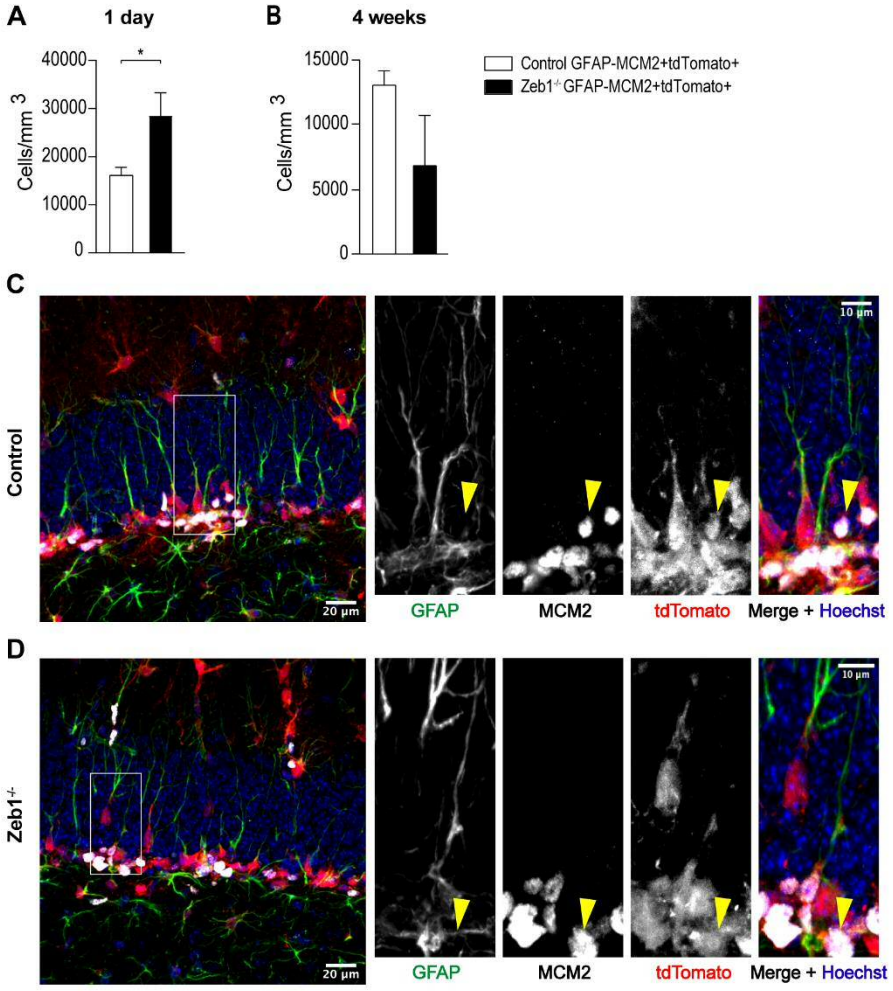

Figure 4.4. Zeb1 ablation results in a transient amplification of Type 2 IPCs – (A) The numbers of proliferation competent Type 2 IPCs in the dentate gyrus was significantly higher in the Zeb1$^{-/-}$ mice (black bars) than the control group (white bars) at 1 day post-tamoxifen, which was subsequently remarkably reduced by 4 weeks (B). Numerical data shown as mean ± SEM and are representative of three independent animals per genotype, with a minimum of two sections analysed per animal, one-tailed t-test, * $p<0.05$.
Representative IF images demonstrate the populations of GFAP- MCM2+ Type 2 cells (yellow arrowheads) in the control (C) and Zeb1$^{-/-}$ (D) mice, at 1 day following transgene recombination. Nuclei were counterstained with Hoechst (blue). Scale represents 20 μm, and for inset images 10 μm.

4.3.2.2 Ki67

To validate my observations of the initial increased Type 2b cell pool followed by a dramatic reduction in the Zeb1$^{-/-}$ mice, I quantified Ki67, another proliferation marker whose expression is limited to the proliferative cells undergoing G2 and S phases of the cell cycle. I counted Ki67-expressing proliferative progenitor cells at 1 day, as well as 4, 8, and 12 weeks post-recombination resulting in loss of Zeb1. One day post-deletion, the number of Ki67+ cells was comparable between the control and Zeb1$^{-/-}$ mice (10,399 ± 1,255, and 12,176 ± 1,148 cells/mm^3, respectively; p=0.3552, **Figure 4.5A**). This was sustained at 4 weeks, when the numbers were once again similar between the control and Zeb1$^{-/-}$ mice, with the former featuring 2,811 ± 495 cells/mm^3 and the latter 2,937 ± 1,235 cells/mm^3 (p=0.9294; **Figure 4.5B**). However, by 8 weeks succeeding Zeb1 deletion, the proliferation rates in the Zeb1$^{-/-}$ group decreased, with 780 ± 170 cells/mm^3 counted, which was significantly fewer than in the control group (1,767 ± 289; p=0.0421; **Figure 4.5C**). This difference was somewhat maintained up to 12 weeks post-deletion as the control group presented with 1,665 ± 504 cells/mm^3, in comparison to 538 ± 347 Ki67+ cells/mm^3 in the Zeb1$^{-/-}$ mice, although this was not statistically significant (p=0.1395; **Figure 4.5D**). **Figure 4.5E-L** show representative IF staining images evidencing the gradual loss of Ki67+ proliferating cells in the Zeb1$^{-/-}$ mice compared to the control group at the different timepoints (panels F, H, J, L, and panels E, G, I, K respectively).

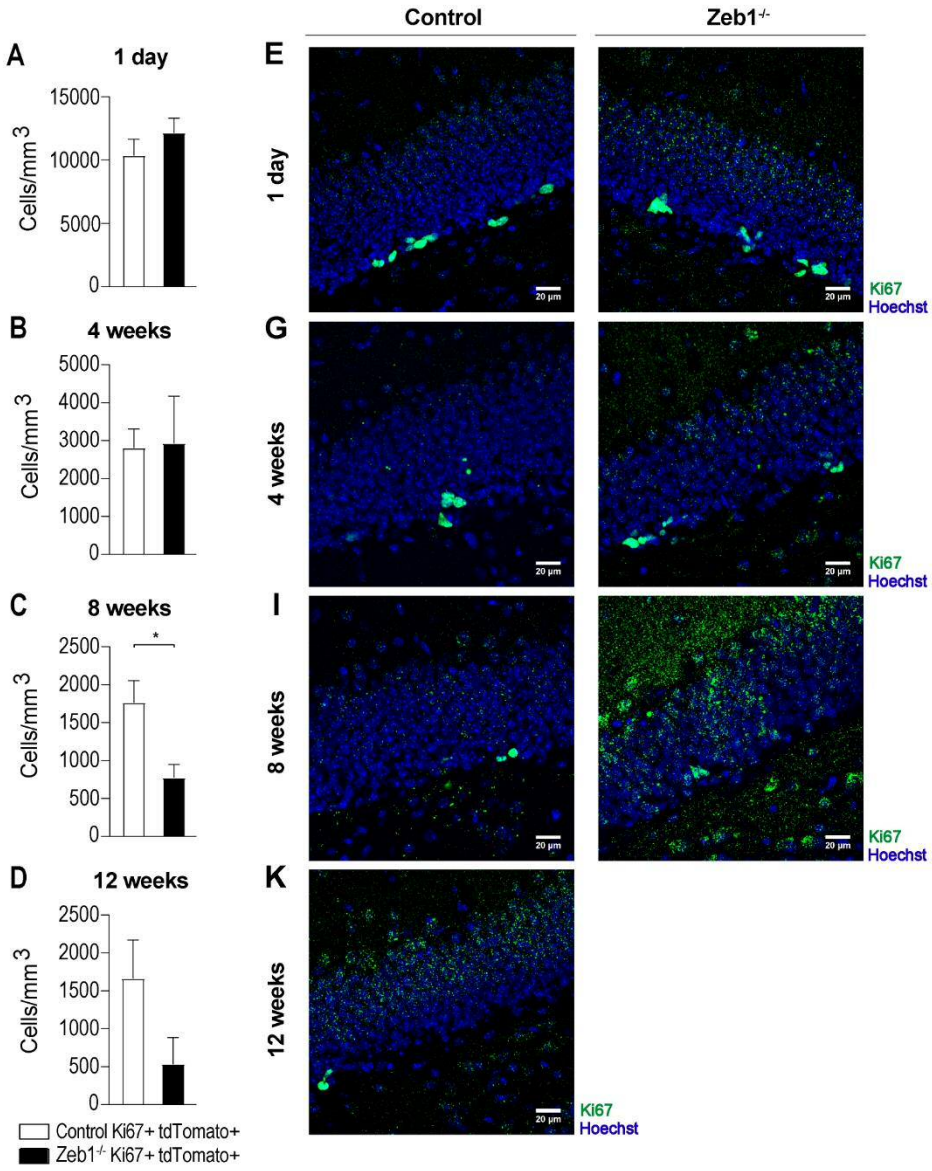

Figure 4.5. Loss of Zeb1 leads to a reduction in the number of proliferating cells in the SGZ – (A-D) Quantification of the number of Ki67-expressing proliferating cells in the G2/S phase of the cell cycle at 1 day, as well as 4, 8, and 12 weeks post-transgene recombination revealed a gradual decline in this cell population in the Zeb1$^{-/-}$ mice (black bars) in comparison to the control group (white bars), which was especially notable after 8 weeks. Numerical data shown as mean ± SEM and are representative of three independent animals per genotype, with a minimum of two sections analysed per animal, two-tailed t-test, * $p<0.05$. Representative images taken at 1 day, as well as 4, 8, and 12 weeks of control (E, G, I, and K, respectively) and Zeb1$^{-/-}$ mice (F, H, J, and L, respectively) following Zeb1 deletion in the latter, exhibit the steady loss in the detection of Ki67-expressing cells in the Zeb1$^{-/-}$ mice with time. Nuclei were counterstained with Hoechst (blue). Scale represents 20 µm, and for inset images 10 µm.

4.3.3 Effects of deletion of Zeb1 in the hippocampal IPC cell population numbers

To further confirm the pro-differentiation divisions of the gradually depleting Type 1 cell population in the Zeb1$^{-/-}$ mice, I decided to assess changes in the Type 2 cell population in the control and Zeb1$^{-/-}$ mice post-transgene recombination. Type 2 IPCs can be identified by their expression of the cell-specific transcription factor T-box brain gene 2 (TBR2; Eomes gene) (Hodge *et al.* 2012). I carried out IF staining to quantify the number of TBR2-expressing IPCs in the control and Zeb1$^{-/-}$ mice over a period of 12 weeks following Zeb1 deletion.

At 2 weeks post-induction, I observed a significant increase in the number of Type 2 cells in the Zeb1$^{-/-}$ mice (5,687 ± 881 cells/mm^3) compared to the control group (2,413 ± 372 cells/mm^3; p=0.0267; **Figure 4.6A**). However, at 4 weeks post-Zeb1 deletion, Type 2 cells showed a tendency towards a decrease in numbers, although not statistically significantly, in the Zeb1$^{-/-}$ mouse hippocampi (1,129 ± 500 cells/mm^3), whilst the number of IPCs remained stable in the control group (2,506 ± 181 cells/mm^3; p=0.0608; **Figure 4.6B**). At 8 weeks, the number of Type 2 cells indicated a further decrease in the Zeb1$^{-/-}$ mice in comparison to the control mice (58 ± 58 cells/mm^3 and 1,060 ± 514 IPCs/mm^3, respectively), although this was not significant (p=0.1247; **Figure 4.6C**). By 12 weeks, the Zeb1$^{-/-}$ mice presented significantly fewer Type 2 cells (168 ± 99 cells/mm^3) in comparison to the control group (1,448 ± 405 cells/mm^3; p=0.0373; **Figure 4.6D**). **Figure 4.6E-L** exhibit representative IF images that demonstrate this gradual loss of TBR2-expressing Type 2 cells over the period of 12 weeks post-Zeb1 deletion in the Zeb1$^{-/-}$ mice (panels F, H, J, and L), in comparison to the control group (panels E, G, I , and K).

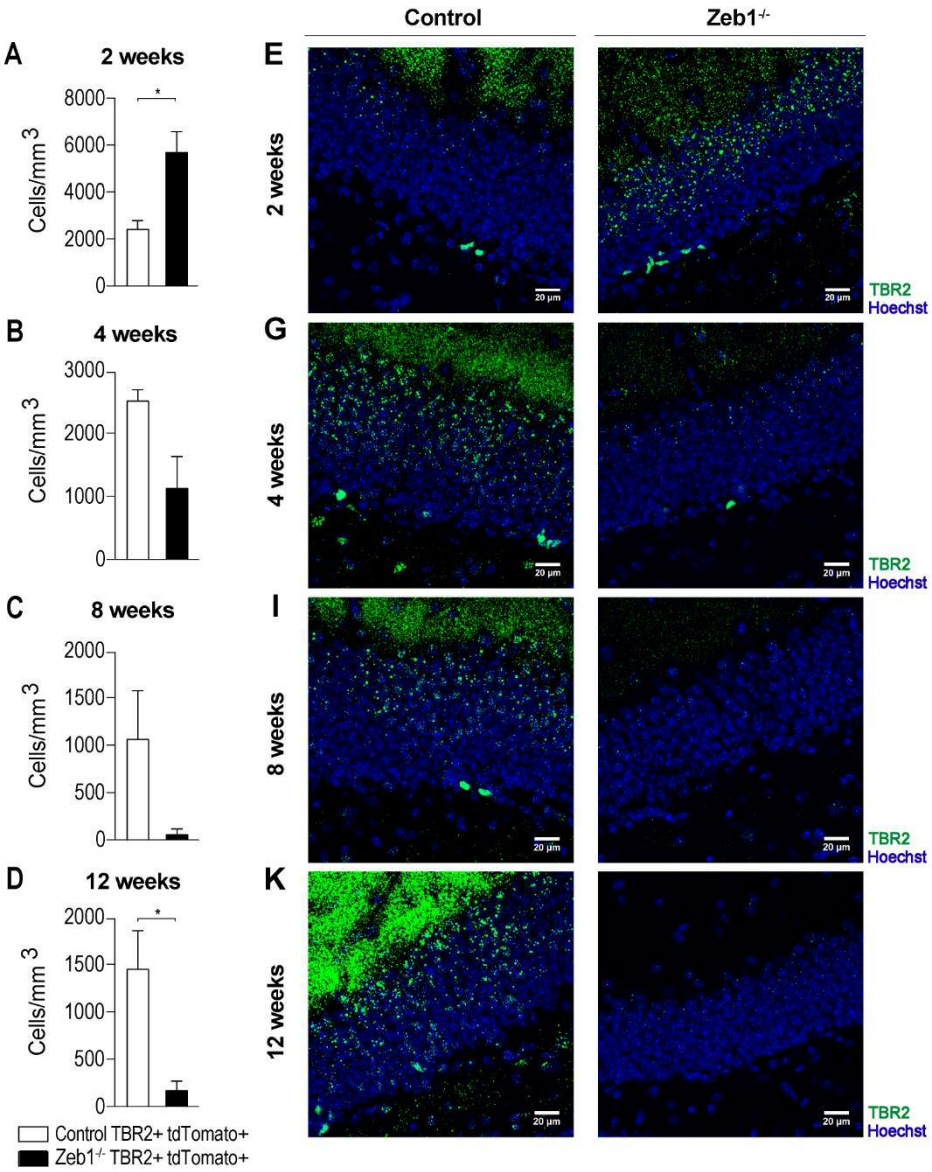

Figure 4.6. Zeb1 deletion results in an initial increase in the TBR2+ Type 2 cell population which subsequently becomes depleted – (A) The Type 2 cell population was transiently increased at 2 weeks post-Zeb1 deletion in the Zeb1$^{-/-}$ mice (black bar), in comparison to the control group (white bar). (B-D) Subsequently, at 4, 8, and 12 weeks, the Type 2 cells became depleted with very few detected by the last timepoint investigated in the Zeb1$^{-/-}$ group. Numerical data shown as mean ± SEM and are representative of three independent animals per genotype, with a minimum of two sections analysed per animal, two-tailed t-test, * $p<0.05$.

Representative IF images between 2 and 12 weeks show the fairly consistent expression of TBR2 in Type 2 cells (yellow arrows) in the control mice (E, G, I, and K), in comparison to an initial surge at 2 weeks in the Zeb1$^{-/-}$ group (F), followed by a steady decline at 4, 8, and 12 weeks (H, J, and L, respectively). Nuclei were counterstained with Hoechst (blue). Scale represents 20 µm, and for inset images 10 µm.

4.4 Discussion

ZEB1 has been recognised as a transcription factor that promotes epithelial-mesenchymal cell transition. Whilst the traditional view of EMT emphasises its importance for changes in cell adhesion and polarity that are prerequisites for tumour metastasis, and which recapitulate the increased motility of cells seen in embryonic development, more recently EMT transcription factors (EMT-TFs) are being considered as regulators of cell plasticity, stemness, and fate specification (reviewed in Goossens *et al.* 2017). During embryonic development, the majority of EMT-TFs are expressed in the neural crest, and EMT is essential for the migration of neural crest cells into the periphery. Recent work has found that ZEB1 and ZEB2 also function during later stages of embryonic CNS development, including cerebellar granule neuron progenitors (Singh *et al.* 2016) and cortical progenitors (Wang *et al.* 2019). In line with the view of EMT-TFs as regulators of stemness, the ZEB family of transcription factors appears of particular importance among EMT-TFs in regulating embryonic neurogenesis. Whether EMT-TFs regulate adult neurogenesis remains unclear.

In the current study, my main objective was to elucidate the function of ZEB1 in the stem cell niche in the healthy adult brain. Research over the past few decades has evidenced the existence of two major neurogenic niches in the adult brain – the SGZ of the hippocampus and the SVZ in the lateral ventricles. Focusing on the hippocampal stem cell niche, I hypothesised that ZEB1 regulates the maintenance of the Type 1 cell population in this region. To evaluate this, I employed a loss-of-function of Zeb1 approach using the experimental mouse strain GLAST:CreER^{T2}-Rosa26$^{lsl\text{-}tdTomato}$-Zeb1$^{fl/fl}$, and corresponding control strain GLAST:CreER^{T2}-Rosa26$^{lsl\text{-}tdTomato}$, as discussed previously in Section 3.3.3.

4.4.1 Zeb1 deletion results in the loss of Type 1 cell self-renewal

In this chapter, I first investigated the effects of loss of Zeb1 within the Type 1 cell population. The cell marker GFAP labels both quiescent and activated Type 1 cells in the hippocampus, which are subsequently distinguishable by the additional expression of cell proliferation proteins such as Ki67 and MCM2. The number of proliferation-competent (also referred to as activated) GFAP+MCM2+ Type 1 cells

was reduced as early as one day after the last tamoxifen injection, whilst the GFAP+MCM2- cell population (demarcating the quiescent Type 1 cells) decreased in size by 4 weeks post-Zeb1 deletion. Both pools of Type 1 cells gradually became depleted over 26 weeks following Zeb1 deletion. The exhaustion of the Type 1 cell population suggests that there is a loss-of-function phenotype in the $Zeb1^{-/-}$ mice; importantly, ZEB1 is known to repress the function of factors (such as microRNAs; Section 1.8.1) that promote the differentiation of NSCs, and the deletion of Zeb1 will inevitably result in the loss of this repression. Although the specific mechanism through which Type 1 cells become depleted following Zeb1 ablation has not been determined in this study, it is evident that there is a loss of the function of Zeb1 that maintains the hippocampal NSC pool, and this will be further discussed in the context of the effects of Zeb1 deletion in the neuronal population in Section 5.4.1.1.

4.4.1.1 Implications of ZEB1 in the mode of stem cell division

Although both the quiescent and activated Type 1 cell populations reduced within the first four weeks post-Zeb1 deletion, the decrement in the quiescent pool was slower than the activated cell population. Adult NSCs are required to self-renew (if their population is to be sustained over time), as well as to give rise to progeny; this cell fate choice is dependent on a finely balanced play between asymmetric and symmetric divisions (Section 1.1). To date, various models have been proposed to explain the mode of adult NSC division, and the two main schools of thought argue in favour of the existence of either a self-renewing NSC pool, or a disposable/single-use NSC population. Past studies have generated a number of models that align with one of the two schools of thought to describe the maintenance and lineage specification of adult neural stem cells (reviewed in Lazutkin *et al.* 2019).

The Zeb1 loss-of-function-triggered depletion of both quiescent and activated Type 1 cells, followed by an initial surge in proliferation of Type 2 cells, with their subsequent loss as well, indicates aberrant stem cell division. In the current study, I propose that the loss of transcriptional regulation carried out by ZEB1 leads to rapid (and most likely) symmetric division of stem cells favouring cell differentiation, at the expense of self-renewal, thus resulting in the gradual depletion of the Type 1 cell population over the investigated period of six months ensuing Zeb1

deletion. According to the self-renewing stem cell division model, once activated, NSCs can undergo either asymmetric division to give rise to one lineage-committed progenitor, and another NSC, following which the NSC can return to quiescence, or symmetric division to give rise to two self-renewing NSCs (Bonaguidi *et al.* 2011); this model emphasises the maintenance of self-renewal throughout the lifespan of an animal, although some reduction in the self-renewal capacity can occur with age. Whilst the current dataset at hand aligns with the features presented in the sustained self-renewal model, the existence of a disposable stem cell population is also feasible (Encinas *et al.* 2011); in this scenario, the deletion of Zeb1 would once again tip the balance in favour of symmetric divisions of Type 1 cells that give rise to neuronal-lineage committed progeny (Sections 5.3.1 and 5.3.2). In 2018, a novel study utilised live imaging *in vivo* and reported that Type 2 cells possess the ability to divide asymmetrically, by which this cell population can provide an additional fount for clonal expansion in the SGZ (Pilz *et al.* 2018); this model may also fit the current data set as it would allow for the observed expansion of the Type 2 cell population with a resultant amplification in the neuronal population (discussed in the next chapter). These models and their relevance to the current study will be further discussed in Section 6.2.

4.4.1.2 ZEB1 does not regulate SOX2 expression in the adult hippocampus

I investigated the expression of SOX2, which is expressed in Type 1, Type 2a, and astrocytes in the dentate gyrus, in both the control and $Zeb1^{-/-}$ mice; I found a significant decrease in the number of SOX2-expressing cells at 12 weeks following loss of Zeb1, but the size of this cell population remained comparable between the two mouse lines before this timepoint.

The regulation of SOX2 expression by ZEB1 has been evidenced in the context of tumours (Wellner *et al.* 2009); recently, an important study highlighted the existence of an interdependent transcription factor regulatory loop formed by SOX2, ZEB1, and OLIG2 (oligodendrocyte transcription factor 2) that drives the progression of GBM tumours (Singh *et al.* 2017); the authors reported that Zeb1 is a target gene of SOX2, which corroborates the previously reported function of ZEB1 in the maintenance of SOX2 expression in GBM (Siebzehnrubl *et al.* 2013).

Unexpectedly, I observed no significant change in the SOX2-expressing cell population in the SGZ of the ZEB1$^{-/-}$ mice compared to the control group for the first 8 weeks following Zeb1 deletion; based on the GFAP+ Type 1 cell population observations, it was expected that the SOX2+ cells would follow a similar trend as SOX2 is expressed in Type 1 cells (Steiner *et al.* 2006; Favaro *et al.* 2009; Nicola *et al.* 2015). The only explanation at hand for the discrepancy observed in the current study is that ZEB1 does not regulate the expression of SOX2 in the adult healthy hippocampus; however, further studies will need to be carried out to confirm this.

4.4.2 Zeb1 deletion-mediated self-renewal loss of Type 1 cells increased the IPC pool size

Following the observation of the depletion of Type 1 cells, I queried whether this was due to an increase in their lineage specification, and thus carried out IF staining for a variety of markers that distinguish the Type 2 population as well as proliferating cells. I observed an increase in the GFAP-MCM2+ Type 2 cell population at 1 week post-Zeb1 deletion, which reversed at 4 weeks when the size of this population was reduced in the Zeb1$^{-/-}$ mice. Importantly, the latter not only coincided with the suggestive decline in quiescent Type 1 cells, but also with the initial increase and subsequent reduction in TBR2-expressing Type 2 IPC numbers in the Zeb1-deficient mice. Over the period of 3 months following the loss of ZEB1 expression there was a decline in proliferating Ki67+ cells in the SGZ. These multiple observations highlight the initial surge in Type 2 cells followed by their depletion and, coupled with the gradual exhaustion of the Type 1 cell population, point towards an exclusive pro-differentiation switch in the Type 1 cell population division mode with Zeb1 deficiency.

Taken together, the findings from this chapter reveal that loss of Zeb1 results in the gradual disappearance of Type 1 cells in the SGZ, with an initial surge in proliferating Type 2 IPC numbers, followed by their steep decline, over the period of three months post-deletion in the Zeb1$^{-/-}$ mice. A published mathematical model that was developed based on experimental data suggested that an increase in division rates of stem cells would result in the depletion of the stem cell pool, alongside an increase in astrocytic transformation of the proliferating stem cells (Ziebell *et al.*

2014); this model partly fits with the present experimental findings, although instead of astrocytic transformation, I observed division cycles that favour neurogenesis (as discussed further in Sections 5.3.1 and 5.3.2). Furthermore, the mathematical model also supports my observation of the initial increase in the proliferation rates amongst the IPCs, followed by a steady decline over time, as an initial amplification of differentiation will results in greater numbers of proliferating IPCs, which will then be lost over time as the stem cell pool becomes steadily depleted.

Thus, based on the findings in this chapter, consistent with other reports in the literature and the aforementioned mathematical model (Ziebell *et al.* 2018), I propose that ZEB1 may function to provide homeostatic dynamic control of asymmetric and symmetric division within the SGZ, to sustain the stem cell population as well as to generate new neurons and astrocytes needed to maintain the plasticity of the brain throughout adulthood for environmental adaptation. This is investigated further in the next chapter, where I assess downstream effects of Zeb1 deletion on the resulting numbers of new adult-born granule cells and astrocytes, as well as on hippocampal-based memory function.

Chapter 5 - Loss of Zeb1 alters adult hippocampal NSC lineage commitment

5.1 Introduction

The function of adult hippocampal neurogenesis is the sustained generation of new granule neurons that contribute to synaptic plasticity in hippocampal-dependent memory processing and consolidation. Young granule neurons show greater excitability than mature granule neurons, which functions to mediate long-term potentiation through synaptic strengthening (Snyder *et al.* 2001). Moreover, they have also been associated with improved pattern separation which allows for the distinction between similar memories (Nakashiba *et al.* 2012).

During the process of stem cell division to generate neuronal progenitors, that subsequently differentiate and mature into granule neurons, there are various critical stages that govern the successful generation of the latter cell population. One of these is the apoptosis of neuronal-committed progenitors and young granule neurons, which occurs within the first few post-mitotic weeks as a mechanism to ensure correct functionality of the adult-born neurons, as well as regulating the proliferating progenitor cell pool size. Subsequently, surviving cells in the GL mature over four to eight weeks, which includes the extension of dendrites into the ML and axonal projections into the hilar mossy fibre network. Adult-born granule neurons eventually begin to transmit perforant pathway inputs from the entorhinal cortex to the CA3 region via the mossy fibres (reviewed in Toda *et al.* 2019). Studies have reported an additive phenotype of hippocampal neurogenesis to the total number of granule neurons in mice with age (Bayer 1985; Kempermann *et al.* 2003; Ninkovic *et al.* 2007), and it has been suggested that approximately 10-15% of adult-born neurons are stably incorporated into the DG that last for the lifetime of an animal (Ninkovic *et al.* 2007).

Alongside the creation of new neurons, astrogliogenesis during adulthood also occurs in the SGZ; astrocytes are crucial for the proliferation of Type 1 cells as well as aiding the function of granule neurons (Song *et al.* 2002). The identity of the NSC subpopulation that is responsible for adult neurogenesis and astrogliogenesis is still debated, as although these two processes are independent, it is speculated that they originate from the same precursor cell in the dentate gyrus (Bonaguidi *et al.* 2011). This will be further discussed in Section 5.4.2.

In the previous chapter, I found that the loss of Zeb1 in hippocampal Type 1 cells resulted in their gradual depletion, with a simultaneous upregulation in the number of neuroblasts. In this chapter, the main aim was to evaluate the functionality of the newborn adult neuroblasts in the hippocampus. To investigate the fate of cells generated following the deletion of Zeb1, I employed the GLAST-driven induction of the tdTomato fluorescent reporter combined with the assessment of the mature granule cell marker, NeuN. I also evaluated the incorporation of the thymidine analogue, 5-ethynyl-2'-deoxyuridine (EdU), for the assessment of Type 1 cell and progenitor cell proliferation, as well as label retention of the ensuing progeny. Subsequently, I carried out a set of behavioural tasks to assess potential differences in hippocampal-dependent memory function in the control and Zeb1$^{-/-}$ mice. This was carried out with the objective to identify potential functions of ZEB1 in the neuronal-lineage divisions of Type 1 cells that would give rise to mature and functional adult-born neurons in the mouse hippocampus.

5.2 Aims and objectives

1) To determine whether the amplified neuroblast population in the Zeb1$^{-/-}$ mice survived and matured into functional granule neurons.
2) To investigate the downstream effects of Type 1 cell depletion on astrogliogenesis in the dentate gyrus of Zeb1$^{-/-}$ mice.
3) To assess hippocampal-dependent memory function in control and Zeb1$^{-/-}$ mice.

5.3 Results

5.3.1 Loss of Zeb1 results in preferential neuronal lineage specification

Doublecortin (DCX) is a microtubule-binding protein that is transiently expressed in neuronal-committed cells. It is detected primarily in migrating post-mitotic neuroblasts, but can also be identified in late proliferating progenitor cells and early immature neurons; subsequently it becomes downregulated once cells begin expressing mature neuronal markers such as NeuN (Brown *et al.* 2003). This designates it as an ideal marker for the identification of the transient early post-mitotic cell population following neuronal commitment in the neurogenic niche.

At 2, 4, and 8 weeks following the deletion of Zeb1, the numbers of DCX and tdTomato-expressing late Type 2b and 3 cells were probed with IF staining; cells with colocalisation of DCX and tdTomato represented the number of neuronal-committed cells born post-transgene recombination with tamoxifen, in the control and $Zeb1^{-/-}$ mouse lines.

Zeb1 deletion resulted in a significant increase in DCX-expressing Type 2b and Type 3 cells 2 weeks after induction in the dentate gyrus of the $Zeb1^{-/-}$ group in which I quantified 34,996 ± 2,284 cells/mm^3, while 20,534 ± 274 cells/mm^3 were present in the control group (p=0.0033; **Figure 5.1A**). This amplification of the DCX+ cell population continued at 4 weeks at which timepoint I report 24,265 ± 1,454 cells/mm^3 in the $Zeb1^{-/-}$ group, compared to 15,351 ± 2,371 cells/mm^3 in the control group (p=0.0327; **Figure 5.1B**). Conversely, at 8 weeks post-Zeb1 deletion, the number of DCX+ Type 2b and Type 3 cells in the dentate gyrus of the $Zeb1^{-/-}$ mice was decreased by about 60%, with a yield of 6,882 ± 257 cells/mm^3; this was significantly lower than the number of cells in the control group at this timepoint, which was 11,562 ± 576 cells/mm^3 (p=0.0008; **Figure 5.1C**).

In summary, the neuroblast population slowly declines in the control group over the 8 weeks, whilst the deletion of Zeb1 results in initially a remarkable increase in the number of neuroblasts at 2 weeks, which is sustained at 4 weeks. The neuroblast population in the $Zeb1^{-/-}$ group subsequently significantly declines, and at 8 weeks there are significantly fewer neuroblasts in comparison to the control mice.

Representative IF staining images in **Figure 5.1D-I** demonstrate the relatively steady (although slowly declining) numbers of DCX+ neuroblasts in the control mice at 2, 4, and 8 weeks post-induction of tdTomato expression (**Figure 5.1D, F,** and **H**, respectively; yellow arrows), in comparison to the transient amplification of the neuroblast population in the Zeb1$^{-/-}$ mice at 2 and 4 weeks (**Figure 5.1E,** and **G**), followed by the significant decrease in these cells by 8 weeks (**Figure 5.1I**). **Figure 5.1J** exhibits a side-by side comparison of the neuroblast numbers over the 8 week period following transgene recombination in the control and Zeb1$^{-/-}$ mice.

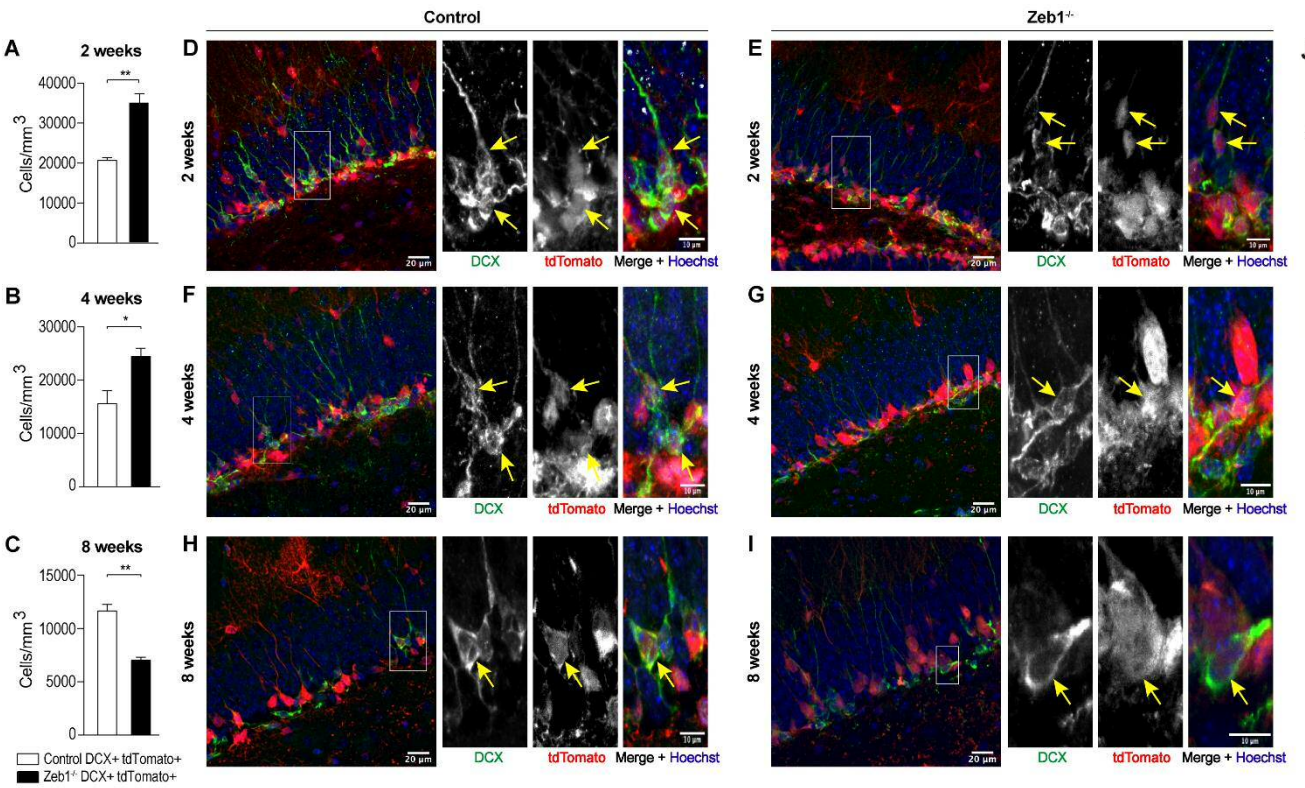

Figure 5.1. Loss of ZEB1 protein induces a transient increase in hippocampal neuronal lineage commitment – (A-B) initial significant increase was observed in the number of neuroblasts at 2 and 4 weeks post-recombination in the Zeb bars represent control and Zeb1$^{-/-}$ groups, respectively). (C) The neuroblast population declined between 4 and 8 weeks in the Zeb1$^{-/-}$ mice by 8 weeks, in comparison to the control group. Numerical values shown as mean ± SEM and are re animals per genotype, with a minimum of two sections analysed per animal, two-tailed t-test, * p<0.05, ** p<0.0 demonstrating the DCX-expressing neuroblasts (yellow arrows) in the dentate gyrus of the control and Zeb1$^{-/-}$ mice at 2 (H, I) weeks post-recombination of transgenes. Nuclei were counterstained with Hoechst (blue). Scale bar represents 2 (J) Comparison of the trajectory of neuroblast generation over the 8 weeks post-tamoxifen administration in the contr

Section 1.5.3), a marker of mature neurons, I quantified the number of neurons within the dentate gyrus that co-expressed tdTomato, indicating that they were generated following the tamoxifen-driven induction of the endogenous tdTomato reporter.

At 4 weeks, there was no difference in the number of NeuN+ neurons between the control and Zeb1$^{-/-}$ groups (16,358 ± 2,544, and 18,704 ± 2,144 cells/mm^3, respectively; p=0.2597; **Figure 5.2A**). However, by 8 weeks, the neuronal population in the dentate gyrus was significantly increased in the Zeb1$^{-/-}$ mice (median of 53,190 cells/mm^3, IQR = 7,293) compared to the control group (median of 28,168 cells/mm^3, IQR = 10,424; p=0.05; **Figure 5.2B**). By 12 weeks, neuron numbers had further increased in the Zeb1$^{-/-}$ group relative to the control group (62,449 ± 12,447 vs. 32,155 ± 3,417, respectively; p=0.0394; **Figure 5.2C**). Unexpectedly, at 26 weeks the neuronal numbers in the control and Zeb1$^{-/-}$ mice annealed: in the former group I quantified 89,255 ± 9,431 cells/mm^3 whilst in the latter there were 91,948 ± 5,052 neurons/mm^3 (p=0.4068; **Figure 5.2D**). **Figure 5.2E-L** exhibit representative IF staining images and **Figure 5.2M** shows the trajectory of neuron generation in the control and Zeb1$^{-/-}$ mice over the 26 weeks following the induction of transgene recombination.

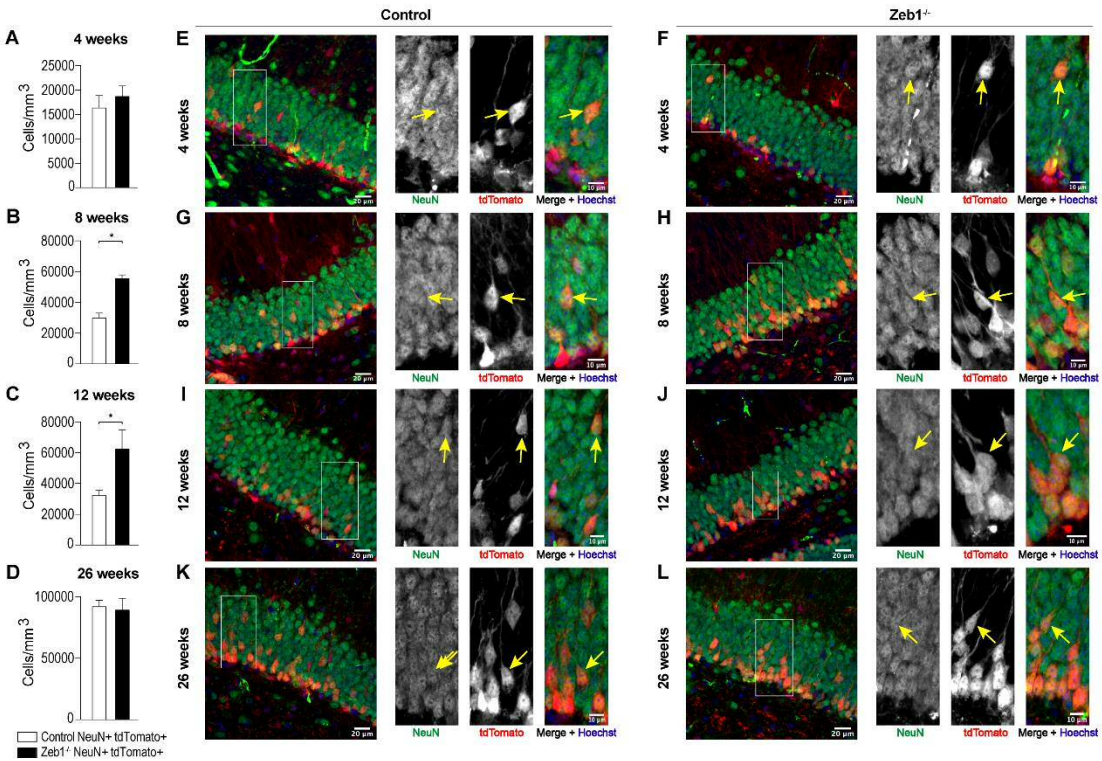

Figure 5.2. Granule cell generation occurs at a faster rate with loss of Zeb1 – (A) At 4 week following the deletion of Zeb1, the n
the control and Zeb1$^{-/-}$ mice (white and black bar, respectively). (B-C) By 8 and 12 weeks, however, there was a great increase ir
mice in comparison to the control mice. (D) This difference levelled out by 26 weeks, when both groups of mice exhibited simi
Numerical values shown as mean ± SEM and are representative of three independent animals per genotype, with a minimum of
t-test, * p<0.05. (E-L) Representative IF images demonstrate that both groups exhibited a similar number of NeuN-expressing gr
by 4 weeks post-tamoxifen administration (control: E, and Zeb1$^{-/-}$: F), after which there was a slow increase in the granule neur
(G, I at 8 and 12 weeks post-tdTomato induction, respectively), in comparison to the greater numbers in the Zeb1$^{-/-}$ mice at 8 a
the numbers of neurons were once again comparable by 26 weeks (panels K and L for the control and Zeb1$^{-/-}$ mice, respective
(blue). Scale bar represents 20 μm, and for inset images 10 μm. (M) A side-by-side comparison of the trajectory of granule neuron
administration.

5.3.3 Loss of astroglial lineage specification following deletion of Zeb1 in the adult mouse SGZ Type 1 cells

The putative multipotency of hippocampal Type 1 cells allows them to generate both neurons and astrocytes (Bonaguidi *et al.* 2011), the latter of which reside within the neurogenic niche and are speculated to promote the proliferation and differentiation of Type 1 cells, as well as aid the functionality of newborn neurons (reviewed in Cassé *et al.* 2018). As I observed a significant increase in neurogenesis following Zeb1 deletion, I queried whether Zeb1-deficient mice would also demonstrate altered astrogliogenesis.

A cell population that lies parallel to the SGZ, with short branches projecting into the SGZ and hilus (characteristic of astrocytic morphology), has been identified as GFAP+ astrocytes that lack nestin expression (Encinas *et al.* 2011). Whilst Encinas and colleagues reported that adult hippocampal Type 1 cells undergo a limited number of neurogenic divisions following which they transform into this astroglial population, it is possible that a subset of these astrocytes is derived through *de novo* hippocampal astrogliogenesis (Bonaguidi *et al.* 2011; Bonzano *et al.* 2018). The latter study utilised a fluorescent Cre reporter mouse that was driven by the promoter of Ascl1 (Achaete-Scute homolog 1), a transcription factor that is expressed in activated Type 1 cells (Andersen *et al.* 2014) and demonstrated that Ascl1-Cre cells originate either labelled neurons or astrocytes based on the expression of a nuclear hormone receptor (Bonzano *et al.* 2018). This provides some evidence of the localisation of hippocampal adult-born astrocytes in the SGZ, although it must be noted that the proximity of niche astrocytes to the Type 1 cells and the SGZ is not definitive proof of their derivation from these cells. With this caveat in mind, I used immunoreactivity to GFAP and lack of nestin expression to identify Type 1 cell-derived astrocytes. I first sought to assess whether the deletion of Zeb1 would result in a decrease in the number of GFAP+/nestin- horizontally-orientated astrocytes in the SGZ, starting at 4 weeks, and subsequently investigated further at 8 and 12 weeks.

I found that at 4 weeks, the number of SGZ-associated astrocytes was comparable between the control and $Zeb1^{-/-}$ groups (2,050 ± 182 cells/mm^3, and 2,572 ± 263 cells/mm^3, respectively; p=0.1779; **Figure 5.3A**). However, by 8 weeks

there was an approximately four-fold reduction in the astrocyte population in the SGZ of the Zeb1$^{-/-}$ mice (515 ± 37 cells/mm^3), in comparison to the control group (2,218 ± 143 cells/mm^3; p=0.0003; **Figure 5.3B**). This was sustained at 12 weeks, at which timepoint there were 2,230 ± 546 cells/mm^3 in the control mice, which was significantly greater than the number of niche astrocytes in the Zeb1-deficient mice (406 ± 113 cells/mm^3; p=0.0307; **Figure 5.3C**). Thus, there was a gradual reduction in the astrocytes that were putatively derived from Type 1 cells in the SGZ of Zeb1$^{-/-}$ mice, whilst this cell population pool was stable in the control mice over the timepoints investigated.

Representative images in **Figure 5.3D-I** demonstrate the morphology of the GFAP-expressing but nestin-deficient astrocytes in the SGZ of the control and Zeb1$^{-/-}$ mice.

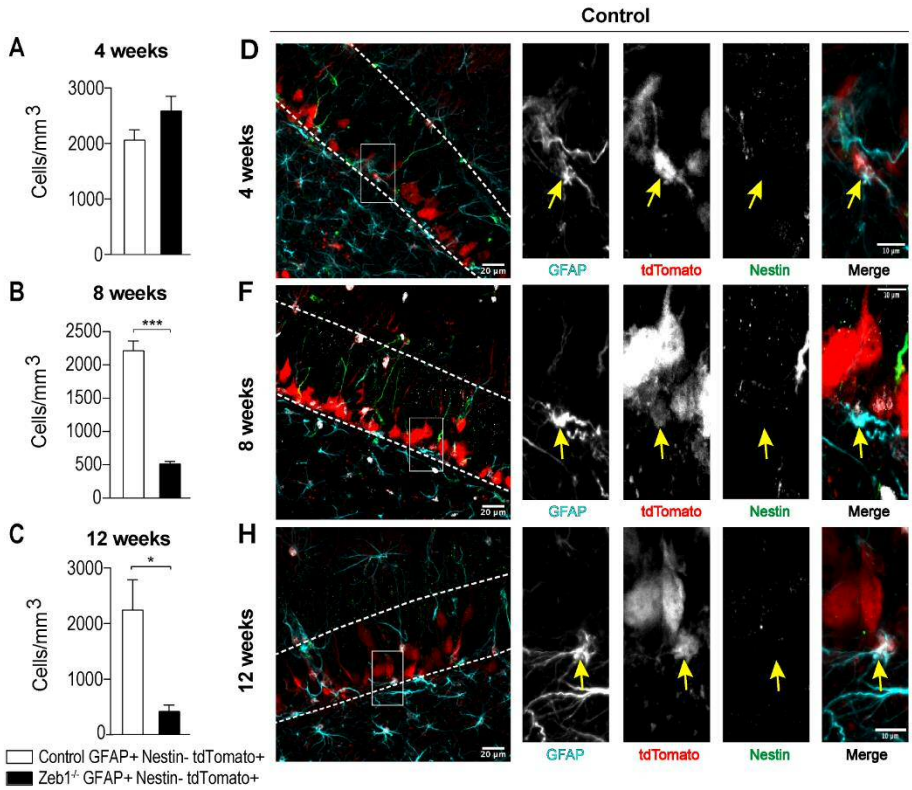

Figure 5.3. Reduction in SGZ-associated astroglia in Zeb1-deficient mice – (A-C) The number of astrocytes in the SGZ of stable over 12 weeks post-tamoxifen administration, but whilst the astroglia cell population size was also comparab (black bars), there was a significant decline at 8 weeks which was sustained at 12 weeks post-Zeb1 deletion. Numeri representative of three independent animals per genotype, with a minimum of two sections analysed per animal, tw (D-I) Representative IF images demonstrate the morphology of the GFAP+/nestin- astrocytes that are putatively origin (yellow arrows). Dashed lines delineate the boundaries of the DG. Scale bar represents 20 µm, and for inset images 1

133 cells/mm^3, respectively; p=0.0026; **Figure 5.4A**). Similarly, I observed reduced numbers of S100β+ astrocytes in the GL (Zeb1$^{-/-}$: 3,154 ± 285 cells/mm^3; control: 4.917 ± 362 cells/mm^3; p=0.0187; **Figure 5.4B**), and in the ML of Zeb1$^{-/-}$ mice (16,155 ± 693 cells/mm^3), compared to control mice (28,646 ± 1,664 cells/mm^3; p=0.0023; **Figure 5.4C**).

This trend was sustained at 12 weeks post-deletion, although the number of astrocytes in the control mice was almost six-fold greater than in the Zeb1$^{-/-}$ mice at this time point (3,194 ± 102, and 542 ± 10 cells/mm^3, respectively; p<0.0001; **Figure 5.4D**). At this timepoint, the number of astrocytes in the GL was once again decreased in the Zeb1$^{-/-}$ mice relative to the control group, but this difference was not statistically significant (2,430 ± 436, and 4,029 ± 643 cells/mm^3, respectively; p=0.1088; **Figure 5.4E**). Likewise, the tdTomato-expressing astrocyte population in the ML of the Zeb1$^{-/-}$ mice was reduced in comparison to the control group (11,591 ± 1,130, and 18,568 ± 2,959 cells/mm^3, respectively), but this was not statistically significant (p=0.0923; **Figure 5.4F**).

Representative IF staining images in **Figure 5.4G-J** exhibit the abundant presence of S100β-expressing astrocytes in the SGZ, GL, and ML of control mice at 8 and 12 weeks (**Figure 5.4G** and **I**, respectively), in comparison to the sparsely located astrocytes in the dentate gyrus of the Zeb1$^{-/-}$ mice at the same timepoints (**Figure 5.4H** and **J**).

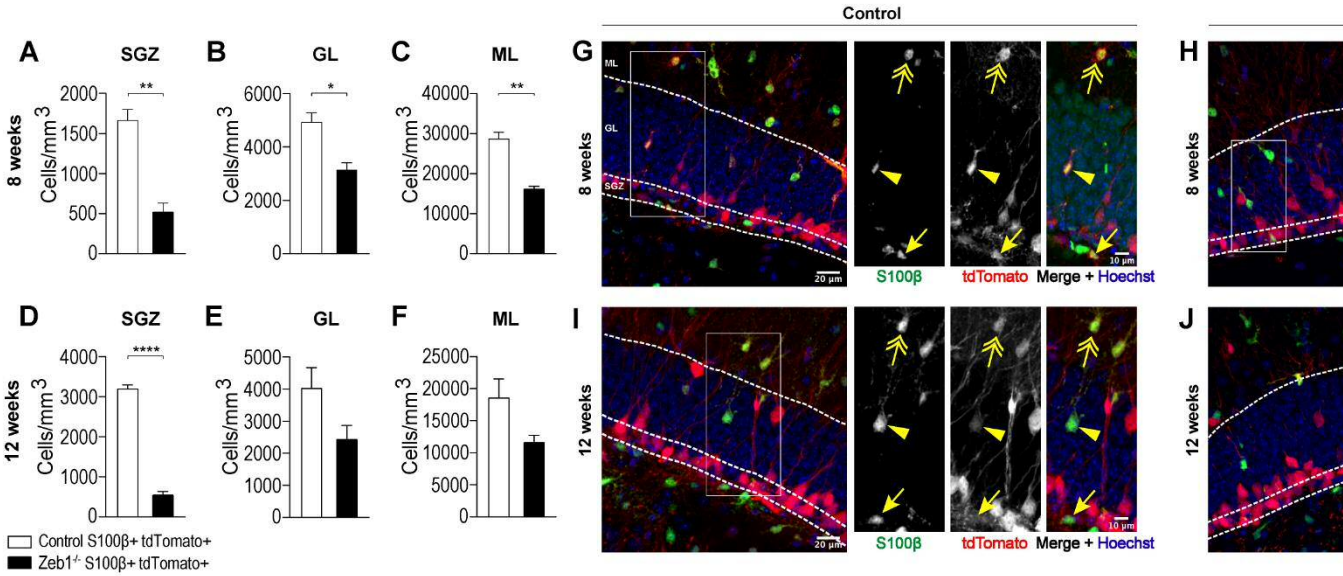

Figure 5.4. Zeb1 ablation results in a gradual decrease in the number of S100β+ astrocytes in the SGZ, as well as
Quantification of the dual expression of tdTomato and S100β+ astrocytes demonstrated that at 8 weeks post-Ze
significantly decreased in all three layers of the dentate gyrus, the SGZ, GL, and ML, of the Zeb1$^{-/-}$ mice (black bars) in
bars). (D-F) Similar observations were made at 12 weeks post-Zeb1 deletion, with a significant reduction in the astrogli
of the dentate gyri of the Zeb1$^{-/-}$ mice. Numerical data shown as mean ± SEM and are representative of three inde
minimum of two sections analysed per animal, two-tailed t-test/Mann-Whitney U-test, * p<0.05, ** p<0.01,**** p<0
(G-J) Representative images generated with IF staining for quantification of tdTomato and S100β co-expressio
administration in the control and Zeb1-/- mice (G and I, and H and J, respectively). Dashed lines demarcate the three d
arrows, arrowheads, and double-headed arrows distinguish SGZ, GL, and ML-associated astrocytes. Nuclei were cou
bar represents 20 μm, and for inset images 10 μm.

5.3.4 Cell death but not cell proliferation is altered in Zeb1$^{-/-}$ mice

In Sections 5.3.1 and 5.3.2, I described increased numbers of neuroblasts and in turn, granule cells in the dentate gyri of Zeb1$^{-/-}$ mice in comparison to the control group, over a period of 26 weeks post-Zeb1 deletion. However, the granule cell numbers annealed in both groups by 26 weeks, which indicates that adult-born neurons develop and become integrated in the hippocampal functional circuits to a similar extent in both groups; this suggests that the regulation of neurogenesis by ZEB1 occurs at an earlier stage in the process of neurogenesis, which could be either during the phase of precursor cell proliferation, or at the stage of programmed cell death during maturation and integration.

To evaluate how cell proliferation and cell death contribute to the surge of newborn granule neurons in the Zeb1$^{-/-}$ mice, I first investigated cell proliferation rates using EdU incorporation. The practise of using a nucleotide analogue for a cell proliferation read-out as well as subsequent lineage tracing relies on the incorporation of these modified nucleotides during the DNA synthesis phase of the cell cycle into proliferating cells at the time of administration. Subsequent quantification of these "tagged" cells allows the enumeration of cells that have undergone DNA synthesis in the experimental window frame, providing information on the rate of cell proliferation. Longer chase times following nucleotide analogue administration also enable lineage tracing as these analogues get passed onto their successive progeny. Therefore, the cell lineage specification of these progenies can be traced back to cycling precursor cells at the time of administration (Hsu 2015). I chose to start EdU labelling at 4 weeks after tamoxifen administration, with a 50 mg/kg daily EdU dose for five consecutive days. Then subsequent to either a 24-hour (for cell proliferation investigation) or 4-week (for lineage tracing) chase period, I harvested and processed the tissue for cell quantification (Section 2.1.6). In conjunction with EdU labelling, I carried out IF co-staining for a neuronal (NeuN) lineage marker at the 4 week time point to investigate whether neuronal lineage-specifying cell division and survival was altered. Cell proliferation was assessed at 4 weeks post-Zeb1 deletion as after this timepoint, there was a steady decline in the numbers of Type 1 cells, and so this investigation would elucidate the proliferation

of these cells during this critical period; meanwhile, cell fate specification and survival were evaluated at 8 weeks post-transgene recombination due to the surge in the neuronal population seen at this timepoint.

In the evaluation of total EdU-labelled tdTomato+ cells in the dentate gyri of the control and Zeb1$^{-/-}$ mice, I did not observe a significant difference at either 24 hours (control: 508 ± 61 cells/mm^3, and Zeb1$^{-/-}$: 583 ± 96 cells/mm^3; p=0.5863; **Figure 5.5A**), or 4 weeks (control: 698 ± 80 cells/mm^3, and Zeb1$^{-/-}$: 603 ± 62 cells/mm^3; p=0.2157; **Figure 5.5B**), following EdU administration. Importantly, the ratio of EdU+tdTomato+ cells at 24 hours to 4 weeks was 0.73 for the control, and 0.97 for the Zeb1$^{-/-}$ mice; this suggests that after 4 weeks post-tamoxifen administration, there may have been a greater amount of cell division taking place in the control mice, in comparison to the Zeb1$^{-/-}$ mice that had a comparable number of EdU-labelled cells immediately after administration and at 4 weeks later. This provides evidence that compliments the observations made in the previous chapter (Section 4.3.2.2) of reduced Type 1 cell proliferation (indicated by decreased Ki67 immunopositivity in comparison to the control) in the Zeb1$^{-/-}$ mice (probably due to their depletion), by 4 weeks following the ablation of Zeb1.

At 4 weeks post-EdU administration, and thus 8 weeks post-tamoxifen-induced Zeb1 deletion, I observed no significant difference in the percentage of NeuN+EdU+ cells of the total EdU-labelled cells, that had been derived from proliferating stem cells at the time of EdU administration in the Zeb1$^{-/-}$ mice (87.8% ± 3.9%) in comparison to the control group (90.1% ± 1.1% cells, p=0.6465, **Figure 5.5C**). **Figure 5.5D** and **E** show representative images of the dentate gyrus of the control (panel C) and Zeb1$^{-/-}$ mice, with a very similar number of cells that were immunoreactive for EdU, tdTomato, and NeuN.

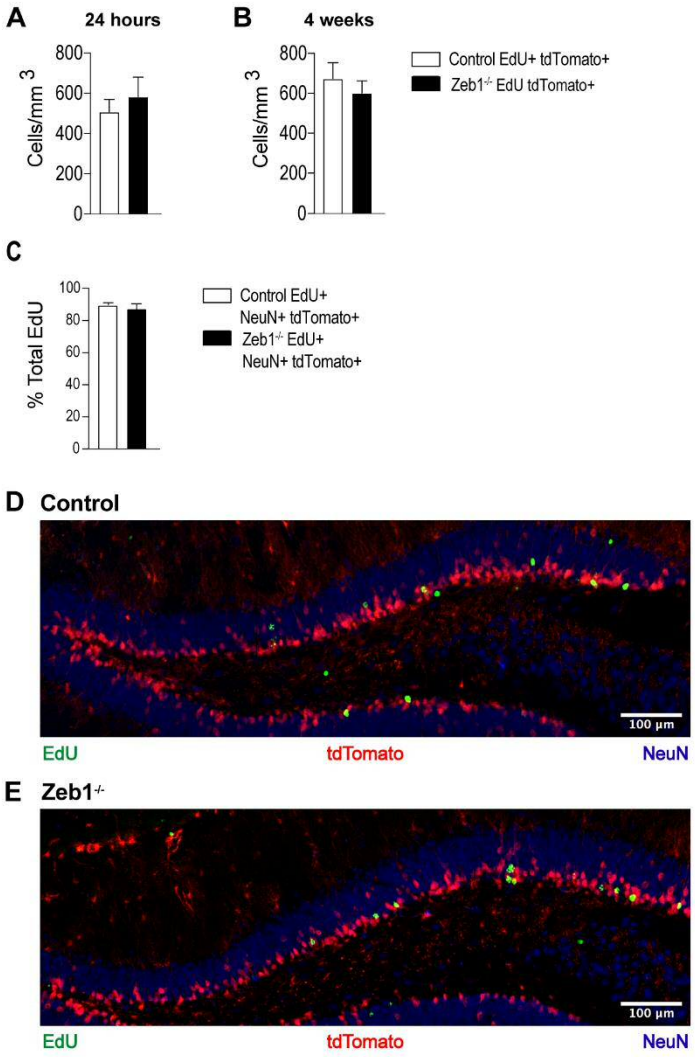

Figure 5.5. Cell proliferation and subsequent neuronal lineage specification of progenitor cells occurs at similar levels in control and Zeb$^{-/-}$ mice from 4 weeks post-Zeb1 deletion – (A) At 24 hours post-EdU administration, the number of tdTomato+ cells that had undergone division, indicated by EdU incorporation, were similar between the control and Zeb1$^{-/-}$ mice (white and black bar, respectively). (B) Similarly, by 4 weeks after EdU administration, the total number of tdTomato+ EdU-labelled cells in the dentate gyri of the control and Zeb1$^{-/-}$ mice was once again not significantly different. (C) Also at 4 weeks post-EdU treatment, neuronal lineage tracing of the progeny of the precursor cells that had been proliferating at the time of EdU administration revealed a comparable percentage of NeuN-expressing neurons generated in the control and Zeb1$^{-/-}$ mice. Numerical data shown as mean ± SEM and are representative of three independent animals per genotype, with 7-10 sections analysed per animal, two-tailed t-test.
(D-E) Representative images of the entire dentate gyrus of control and Zeb1$^{-/-}$ mice with comparable numbers of EdU-labelled cells co-expressing tdTomato. Nuclei were counterstained with Hoechst (blue). Scale bar represents 100 µm.

In this chapter, I set out to understand whether the great amplification in the neuronal population in the Zeb1$^{-/-}$ mice was due to increased cell proliferation at the progenitor level, or reduced neuronal programmed cell death whilst undergoing maturation. I observed no significant difference in the overall cell proliferation occurring at 24 hours post-EdU administration in the control and Zeb1$^{-/-}$ mice, and the percentage of neurons that were generated in both mouse lines following EdU administration was also comparable; this suggested that there was no significant difference in the cell proliferation rates at least 4 weeks post-Zeb1 deletion. Consequently, I next investigated the effects of Zeb1 deletion on the survival of neurons undergoing maturation and incorporation into the functional hippocampal networks. I carried out IF staining for cleaved caspase 3, a mediator of programmed cell death, in the neuroblast and neuronal populations at 2 and 4 weeks following Zeb1 deletion. Cleaved caspase 3, the activated form of the executioner protein, is involved in multiple steps of the apoptotic cascade, ranging from the activation of other apoptotic caspases, to the carrying out of DNA fragmentation as well as cleavage of other cellular proteins (McIlwain *et al.* 2013).

At 2 weeks ensuing ablation of Zeb1, the percentage of cells expressing both DCX and cleaved caspase 3 (indicative of activated caspase 3) did not differ significantly between the control and Zeb1$^{-/-}$ groups (52.6% ± 15.8% and 22.3% ± 14.7% neuroblasts, respectively; p=0.2312; **Figure 5.6A**). However, by 4 weeks, the percentage of apoptotic NeuN-expressing granule cells was remarkably reduced in the Zeb1-deficient mice in comparison to the control group (38.7% ± 3.4%, and 62.4% ± 3.1% apoptotic neurons, respectively; p=0.0161; **Figure 5.6B**). Taken together, this suggests that the deletion of Zeb1 results in increased neuronal survival during the maturation phase in the dentate gyrus. Representative images are provided in **Figure 5.6C-F**, demonstrating the IF staining images that were used for cell quantification for the DCX+ apoptotic cells in the control and Zeb1$^{-/-}$ groups (panels C and D, respectively), as well as NeuN-expressing apoptotic neurons (panel E for control, and panel F for Zeb1$^{-/-}$ mice).

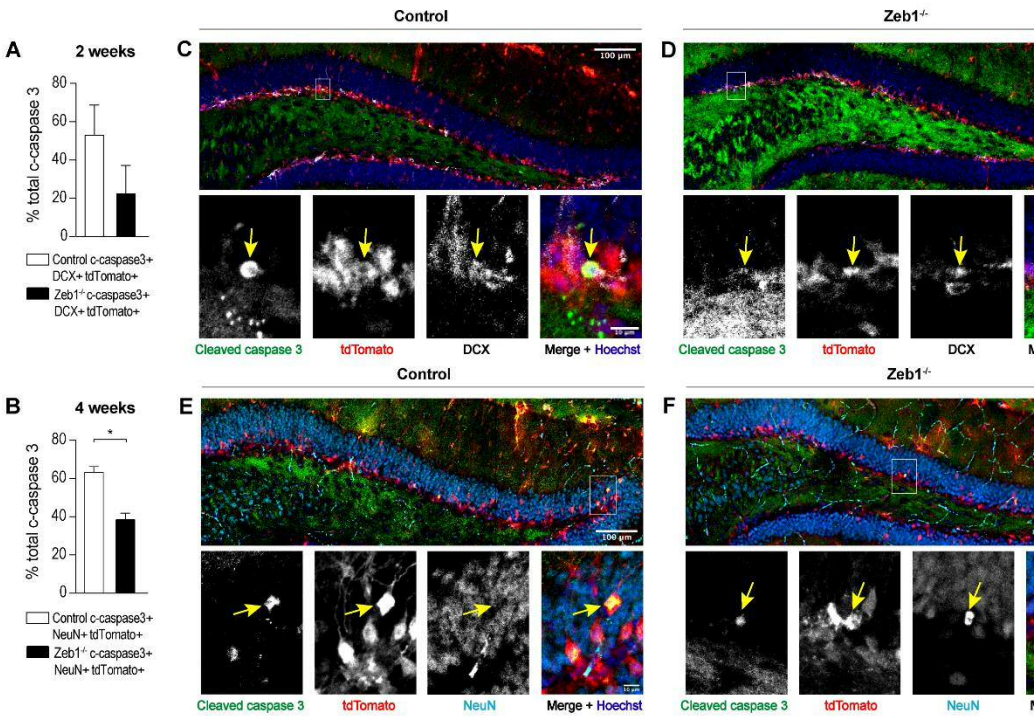

Figure 5.6. Neuronal survival is increased at 4 weeks post-birth in the absence of ZEB1 expression – Co-expressio
DCX or NeuN was investigated in the hippocampus of control and Zeb1$^{-/-}$ mice to assess alterations in immature
undergoing programmed cell death. (A) At 2 weeks post-transgene recombination, no significant difference w
expressing neuroblasts that were immunoreactive for cleaved-caspase 3 in the control and Zeb1-deficient mice (wh
(B) However, by 4 weeks, there was a significant reduction in the percentage of NeuN+ neurons expressing cleav
mice (black bar), in comparison to the former group (white bar). Numerical data shown as mean ± SEM and are re
animals per genotype, with 3-6 sections analysed per animal, two-tailed t-test, * $p<0.05$.
(C-F) Representative IF staining images of the entire dentate gyrus of control and Zeb1$^{-/-}$ mice with cleaved cas
yellow arrows), and NeuN (E, F; indicated by yellow arrows) expression at 2 and 4 weeks post-tamoxifen admin
counterstained with Hoechst (blue). Scale bar represents 100 µm in entire dentate gyrus images, and 10 µm in the

5.3.5 Zeb1$^{-/-}$ mice display normal learning and anxiety-related behaviour

Recognition memory is defined as the ability to recall and identify previously encountered objects and events, and the hippocampal formation has been shown to play a large part in memory consolidation. Although the specific function of the hippocampus in declarative memory is still debated, several studies agree upon its involvement in the merging of object recognition with temporal and spatial information, thus contextualising memories (Snyder *et al.* 2001; Aimone *et al.* 2006). It has been further suggested that the hippocampus functions as a gateway for long-term memory storage in the cortex. Thus, it is speculated that the addition of new neurons in the hippocampus serves the purpose of enhancing the ability to process environmental information in a more efficient way (Kempermann 2002; Deng *et al.* 2010).

With the aim of investigating whether the amplified granule cell population in the Zeb1$^{-/-}$ mice resulted in altered hippocampal-based cognitive function, I decided to carry out the novel object recognition (NOR) as well as novel object location (NOL) tasks; these behavioural tests were initially developed as a means to test memory in rats (Ennaceur and Delacour 1988), and later modified for use in mice (Ennaceur *et al.* 1997; Murai *et al.* 2007). They employ the innately exploratory behaviour of rodents towards novel objects. The experimental design of the NOR and NOL tasks encompasses several variable factors that can affect the results; these include factors such as length and number of habituation and familiarisation sessions, as well as the delay period between the sample and test phases on the test day (Antunes and Biala 2012). Furthermore, the gender of the mice can also result in variabilities in the data due to the estrous cycle of the females (Ter Horst *et al.* 2012); consequently, I chose to only test male mice in this study.

5.3.5.1 Levels of locomotor activity during the habituation and familiarisation sessions

The mice were acclimatised to the open field-style test arena in an initial 10-minute habituation session to reduce their anxiety and to help their performance in the subsequent sessions of the task. I investigated locomotor activity by quantifying the distance moved over the course of the habituation session, as well as during the

habituation session and the last familiarisation session (F6). The cumulative distances moved over the course of the habituation session are exhibited in **Figure 5.7A** and show that both groups displayed high levels of locomotor activity. The main effects of genotype, as well as elapsed minutes of the task, had a significant effect on the distance moved across both groups ($F_{1,160}$=51.1, p<0.0001, and $F_{9,160}$=158.3, p<0.0001; two-way ANOVA modelling as described in Section 2.4.2), but there was no significant interaction between these two factors, indicating that there was no significant difference in the distance moved by the Zeb1$^{-/-}$ mice at each elapsed minutes in comparison to the control mice.

I then investigated the difference in distance moved, as well as maximum number of zone alterations in the habituation session (here, mins 0-5 and 5-10 of the task were grouped to reflect categorised time-dependent changes in habituation) as well as the final familiarisation session, in which the mice were presented with two identical objects for exploration for 5 minutes. Both the genotype and task session factors had an individual significant effect on the distance moved ($F_{1,48}$=7.14, p=0.0103, and $F_{2,48}$=3.78, p=0.0299, respectively), but there was no significant interaction between the two factors (**Figure 5.7B**). In the same vein, the interaction between the two factors did not affect the maximum number of zone alterations, although both genotype and task session once again demonstrated significant main effects ($F_{1,48}$=11.16, p=0.0016, and $F_{2,48}$=3.49, p=0.0383, respectively; **Figure 5.7C**). The lack of interactions between the two main effects indicates that the total distance moved and maximum zone alterations carried out by the Zeb1$^{-/-}$ mice over the task sessions was comparable to the control group.

Notably, using the Sidak's multiple comparisons test in the two-way ANOVA revealed that the maximum number of zone alterations was significantly higher for the Zeb1$^{-/-}$ group during the final familiarisation session, in comparison to the control (p=0.0073), further evidencing the greater locomotor activity of the former group, even after several sessions of exploration in the same test arena. However, another plausible explanation for this could be that the Zeb1$^{-/-}$ mice display forgetfulness of the surroundings; this is further substantiated by the comparison of the movement and zone alterations of the Zeb1$^{-/-}$ mice for the F6 and H0-5 sessions, which are very

similar, in comparison to the control group that display a downward trend throughout the task.

Representative heat maps as well as corresponding movement track images are provided in **Figure 5.7D** and **E**, and further evidence the greater locomotor activity of the $Zeb1^{-/-}$ group, especially during the habituation session.

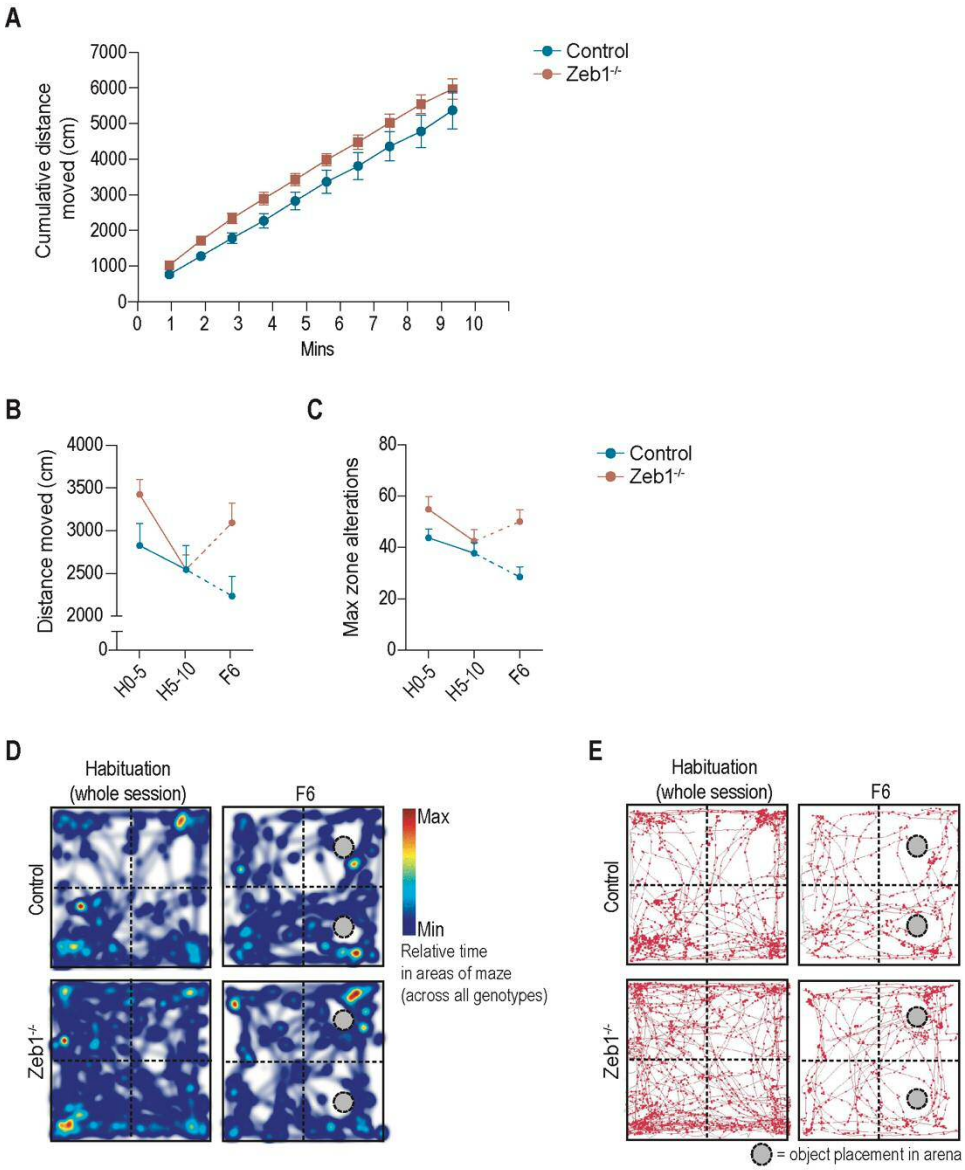

Figure 5.7. Locomotor activity in the habituation and final familiarisation sessions of the control and Zeb1$^{-/-}$ mice - (A) Comparison of cumulative distance moved by control (blue) and Zeb1$^{-/-}$ (red) mice during initial 10-minute habituation session in the arena, tracked per elapsed minute of the task. Further locomotor activity of the two groups of mice was assessed through distance moved (B) and maximum number of zone alterations (C) in the habituation session (represented per initial, H0-H5, and final, H5-H10, 5 minutes of the task), as well as last familiarisation session (F6) prior to the test day. Representative heatmaps and animal tracks (D and E, respectively) demonstrate the greater ambulation of the Zeb1$^{-/-}$ mice (bottom panels) in comparison to the control mice (top panels). Control group n=8 mice, Zeb1$^{-/-}$ group n=10; videos analysed and heatmaps and mouse track images generated with Noldus EthoVision XT software.

5.3.5.2 Novel object recognition task

Following the habituation (Day 1) and familiarisation sessions (Days 2 and 3) of the NOR task, I conducted the sample and test sessions on Day 4. The 10-minute sample phase (with two identical objects) was repeated three times, followed by a 5-minute delay period between the last sample phase and the 10-minute test phase (**Table 2.8**).

I first evaluated the total number of contacts that the mice made with the objects in the three sample phases. As discussed previously in Section 2.3.1.6, I defined object exploration by a mouse with an orientation of its snout towards the object within a distance of approximately 1-2 cm, or active sniffing/touching of the object with the snout or paws (Antunes and Biala 2012). I found that the total number of contacts was significantly affected by the genotype of the mice ($F_{1,48}$=4.26, p=0.0444; **Figure 5.8A** line graph). However, sample session number did not have a significant effect on the total number of contacts, and the interaction between genotype and sample phase number was also non-significant, indicating that the Zeb1$^{-/-}$ mice and control group made a comparable number of contacts over the sample sessions. Interestingly, when I evaluated the overall object exploration across the sample phases by summing the total number of contacts for all three sessions per genotype, the Zeb1$^{-/-}$ mice made significantly greater contact with the objects than the control group (p=0.05; **Figure 5.8A** bar graph). This indicates that the Zeb1$^{-/-}$ mice displayed greater exploratory behaviour due to which they may have engaged more with the objects.

I also assessed the total duration of the contacts made between the three sample sessions and found that once again, genotype significantly altered the total contact duration ($F_{1,48}$=4.38, p=0.0416; **Figure 5.8B** line graph), whilst the sample phase session number, and the overall interaction between these two main effects did not have a significant effect, implying that the Zeb1$^{-/-}$ mice did not make significantly longer lasting contacts with the objects at each sample session in comparison to the control mice. I further assessed the effect of genotype on the total contact duration, and the results demonstrated that the Zeb1$^{-/-}$ mice made longer-lasting contacts with the objects compared to the control group (p=0.0394; **Figure**

5.8B bar graph), which further corroborates the increased total number of contacts made by the Zeb1$^{-/-}$ mice due to possibly enhanced exploratory behaviour. Lastly, I investigated the duration of each individual contact made by the control and Zeb1$^{-/-}$ mice and although this was not affected by the genotype across all three sessions (**Figure 5.8C**), the data displayed trends; the control group but not the Zeb1$^{-/-}$ mice demonstrated a downward trend in the duration per contact. This indicates an increasing familiarity with the objects in the control mice, which results in decreased interaction times. By contrast, the Zeb1$^{-/-}$ mice displayed the opposite trend and made more contacts that lasted longer in comparison to the control group, which suggests that the Zeb1$^{-/-}$ mice remained equally interested and exploratory over time.

Next, I evaluated the ability of the mice to distinguish between familiar and novel objects in the test phase, with the same parameters used in the sample phase exploration assessment (total number of contacts, total duration of contacts, and the duration per contact). Here, I found that the object identity (whether it was familiar or novel) significantly affected the total number of interactions both groups of mice made with the objects and accounted for 26.5% of the total observed variance ($F_{1,31}$=12.23, p=0.0014; **Figure 5.8D**); the percentage of total variance denotes the importance of a factor in determining the observed trend. Although the genotype was not a significant main effect and neither was the interaction between the genotype and object identity, multiple comparisons evaluation demonstrated that the Zeb1$^{-/-}$ mice made significantly more contacts with the novel object in comparison to the familiar object (p=0.0444). Assessment of the total duration of the contacts revealed that this was also affected by the object identity ($F_{1,31}$=12.96, p=0.0011; **Figure 5.8E**), although the genotype and the interaction between the two main effects did not have a significant effect on the exploration of the objects. Nevertheless, multiple comparisons revealed that the control group made significantly longer contacts with the novel objects in comparison to the familiar ones (p=0.0089), which was suggestive but not significant in the Zeb1$^{-/-}$ mice. The duration of each contact was affected by neither genotype nor the object identity, and I found no interactions between these two factors (**Figure 5.8F**).

In summary, when exposed to a set of familiar and novel objects, the Zeb1$^{-/-}$ mice made a greater number of contacts whilst the control mice made longer contacts with the novel objects; this suggests that both groups of mice could distinguish between familiar and novelty. The lack of significance of the number of contacts made by the control group and the duration of contacts made by the Zeb1$^{-/-}$ mice could be due to the small cohort size, which is further discussed in Section 5.4.3.3.

Subsequently, I calculated the discrimination index (DI) for evaluating possible exploration differences, assessed through the total number of contacts as well as total duration of contacts, between the control and Zeb1$^{-/-}$ mice. The DI is a measure used to gauge preference for novelty, based on the exploration time of the novel object divided by the total exploration time of objects over the duration of the session. This index approaches 0.5 (representing the chance level of recognition of novelty) if the rodent interacts equally with the familiar and novel objects, whilst the value approximates 1 if the rodent recognises and interacts more with the novel object. I carried out t-tests to evaluate differences between the DI values of the control and Zeb1$^{-/-}$ mice, as well as one-sample t-tests for comparing the DI values of each genotype to the chance level 0.5. There were no significant differences in the recognition of novelty between the control and Zeb1$^{-/-}$ mice through a comparison of the total number of contacts as well as total duration of contacts (**Figure 5.8G**), which indicates that both control and Zeb1$^{-/-}$ mice had a similar ability to recognise novel objects. However, the preference for the novel object demonstrated by the Zeb1$^{-/-}$ mice through the total number of contacts was significantly greater than the chance level ($t=3.668$, $p=0.0052$), indicating that this group of mice was able to recognise the novel object, which was not observed for the control group; however, this discrepancy may be due to a low sample size (further discussed in Section 5.4.3.3). Thus, these findings indicate the following; 1) the NOR test worked successfully as both groups of mice were able to distinguish between familiar and novel objects (to varying capacities dependent on the parameter evaluated), and 2) the deletion of Zeb1 did not lead to an impairment in the novel object recognition.

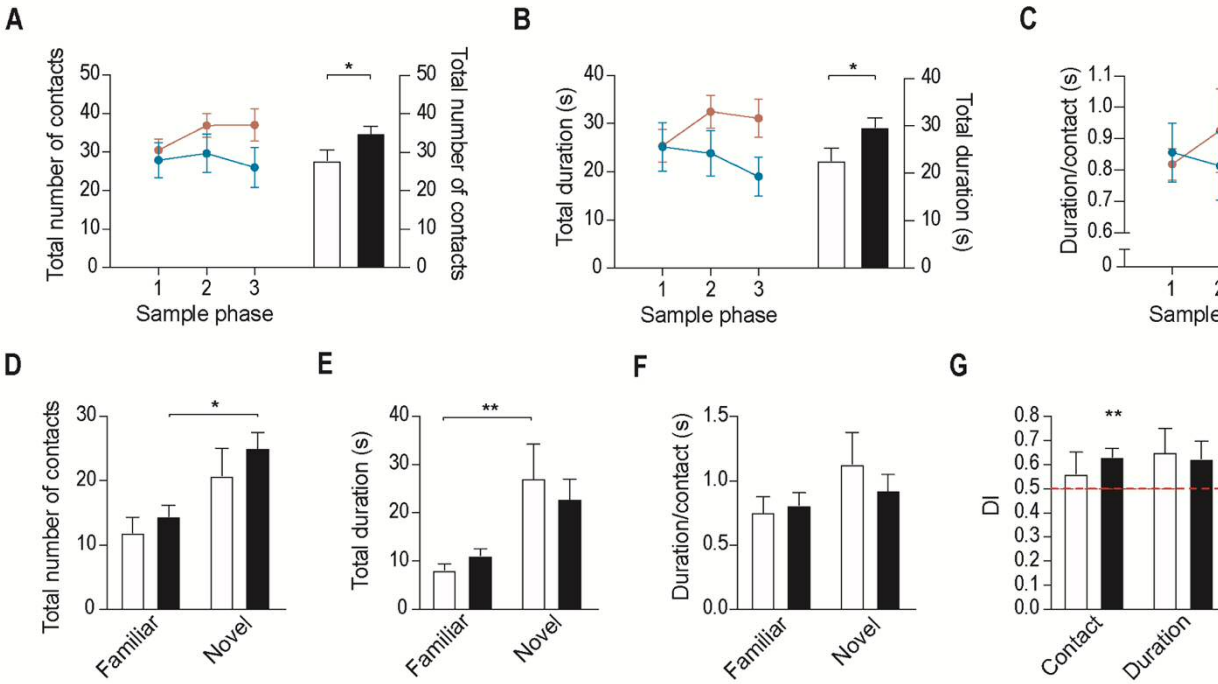

Figure 5.8. Object attendance of control and Zeb1$^{-/-}$ mice in the sample and test phases of the NOR task - (A
of contacts, total duration of contacts, and duration/contact of the two groups of mice over the three sam
panels A and B, the data from individual sample phases are provided (line graphs, left), alongside the s
parameter across the three sample phases (bar graphs, right). (D-F) Total number of contacts, tot
duration/contacts made by control and Zeb1$^{-/-}$ group (white and black bars, respectively) in the 10-minute te
a 5-minute delay period after the last sample phase. (G) The discrimination index (DI), calculated as the e
divided by the total object exploration during the test phase, for the control and Zeb1$^{-/-}$ groups (white an
assessed for the total number of contacts and the total duration of object attendance over the test phase; r
the familiar and novel object interaction occurring by chance. Control group n=8 mice, Zeb1$^{-/-}$ group n=1
EthoVision XT software, two-tailed t-test used for statistical analysis of bar graphs in panels A and B, * p<0.05

5.3.5.3 Novel object location task

I subsequently carried out a similar set of analyses to evaluate the exploratory behaviour of the control and Zeb1$^{-/-}$ mice in the NOL task. Whilst the habituation and familiarisation sessions were not repeated prior to the NOL task (a single rest day was provided for the mice between the NOR and NOL test days), the test day comprised of the three 10-minute sample phases with a successive 5-minute delay period between the last sample phase and the 10-minute test phase, identical to the test day of the NOR task. I found no significant differences between the control and Zeb1$^{-/-}$ mice in the total number of contacts made (**Figure 5.9A**) and the total duration of the contacts between the three separate sample phases or over the sum of the three sessions (**Figure 5.9B**; line and bar graphs, respectively, for each parameter). Similarly, the duration of each contact was also non-significant between the two groups, over the three sample phase sessions (**Figure 5.9C**). Taken together, this suggests that both groups of mice displayed similar exploration of the two identical objects over the three sample sessions. Previously, following the habituation session as well as final familiarisation session, the Zeb1$^{-/-}$ mice demonstrated a greater exploration of the arena (assessed by the total distance moved and maximum zone alterations carried out; Section 5.3.5.1), which seemingly contradicts this set of results; here, it is important to bear in mind that the NOL task was performed after four days of time spent in the arena for the previous set of tasks, which could possibly imply that the Zeb1$^{-/-}$ mice eventually habituate to the arena and objects, but they need more time in comparison to the control mice.

Subsequently, I assessed the discrimination behaviour of the two groups of mice in response to the location change of one of the familiar objects to a novel location. Using a two-way ANOVA, the object placement (defined as familiar or displaced), was found to significantly impact the total number of times both groups of mice made contact with said objects ($F_{1,32}$=9.27, p=0.0046; **Figure 5.9D**). However, the genotype of the mice, as well as the interaction between genotype and object placement did not affect the total number of mouse-object interactions. Similarly, the total duration of the interactions made by both groups was also significantly higher for the displaced objects, in comparison to the familiar objects, indicated by a

significant main effect of object placement ($F_{1,23}$=13.35, p=0.0009, **Figure 5.9E**). On the other hand, neither genotype nor the interaction between the two main effects in the two-way ANOVA model demonstrated significant effects on the duration of the contacts made by the two groups of mice. Furthermore, I found no significant main effect of genotype and object placement, as well as their interactions on the duration per contact between the familiar and displaced objects (**Figure 5.9F**). These results indicate that whilst the NOL task worked as both groups of mice were able to recognise and thus devoted more time in exploring the displaced objects, this recognition capacity did not differ between the two groups.

I next assessed the DIs of the control and Zeb1$^{-/-}$ mice with regards to the number of contacts, as well as duration of contacts. There was no significant difference in the discrimination of the familiar and displaced objects between the control and Zeb1-deficient mice assessed in terms of both total contacts and total duration of contacts. Moreover, neither group of mice displayed a significantly higher number of contacts when compared to the chance level, indicating that their contacts with the displaced object could have occurred by chance. However, the control group of mice displayed a significantly greater DI for interaction duration with the displaced objects in comparison to chance (t-test; t=2.466, p=0.0431, **Figure 5.9G**), which was not seen in the Zeb1$^{-/-}$ mice. This could be interpreted to suggest that the Zeb1$^{-/-}$ group cannot discriminate between the familiar and displaced objects, whilst the control group did have this ability. However, the graphical data suggests that a low sample size more likely accounts for this divergence, and thus a greater number of biological replicates is required before concluding that Zeb1 deficiency results in impaired memory.

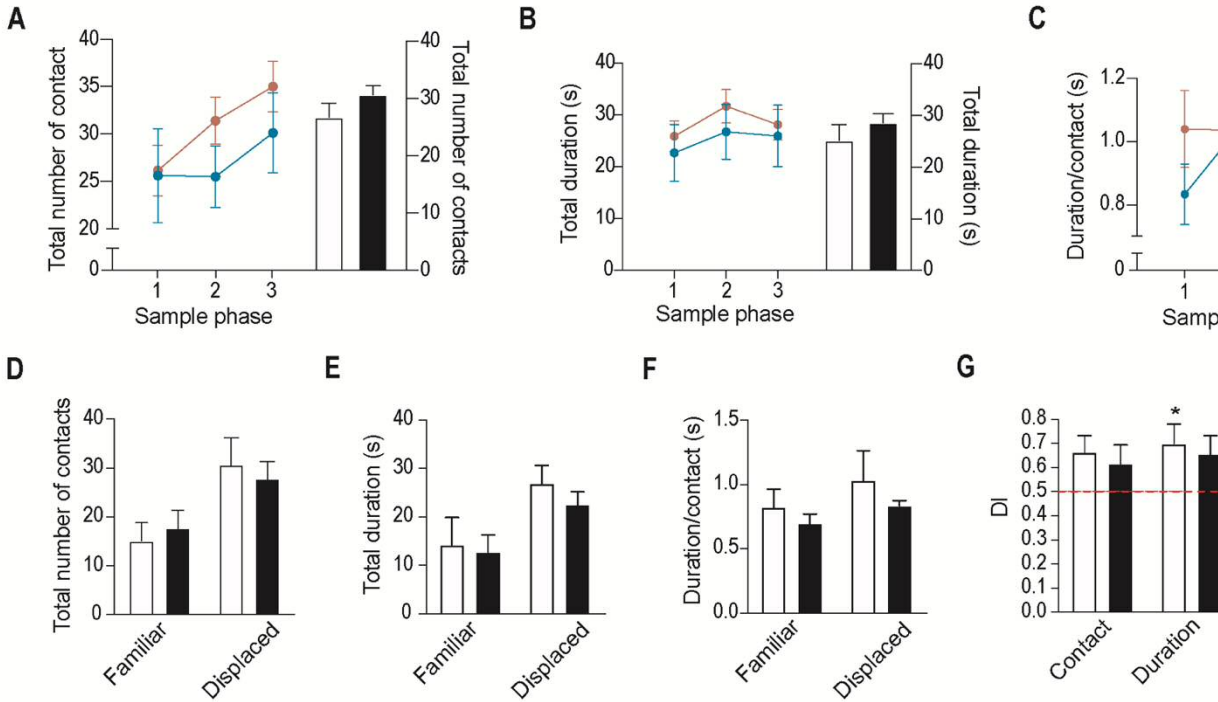

Figure 5.9. Interaction of control and Zeb1$^{-/-}$ mice with objects presented in the sample and test phases of the NO number of contacts, total duration of contacts, and duration/contact of the two groups of mice over the three s panels A and B, the data from individual sample phases are provided (line graphs, left), alongside the summation of the three sample phases (bar graphs, right). (D-F) Total number of contacts, total duration of contacts, and durati Zeb1$^{-/-}$ group (white and black bars, respectively) in the 10-minute test phase of the NOR task, following a 5- discrimination index (DI), calculated as the exploration of the displaced objects divided by the total object explora control and Zeb1$^{-/-}$ groups (white and black bars, respectively), was assessed for the total number of contacts attendance over the test phase; red line at 0.5 represents the level of familiar and displaced object attendance o group n=8 mice, Zeb1$^{-/-}$ group n=10, videos analysed with Noldus EthoVision XT software, one-sample Wilcoxon test to 0.5 in panel G, * $p<0.05$.

5.3.5.4 Levels of locomotor activity during sample and test phases of the NOR and NOL tasks

I chose to further investigate the locomotion of the control and Zeb1$^{-/-}$ mice in the sample and test phases of the NOR and NOL tasks, to determine if the increased locomotor activity of the latter group of mice was sustainably increased, as previously seen in the habituation and familiarisation sessions (Section 5.3.5.1). Using two-way ANOVA testing, I evaluated the effects of 1) genotype and 2) sample vs. test phase, as individual factors, on the distance moved and maximum number of zone alterations.

For the NOR task, the genotype of the mice had a remarkably significant main effect on the total distance moved, regardless of the type of session ($F_{1,64}$=20.48, p<0.0001; **Figure 5.10A**). Moreover, the genotype factor accounted for 40.12% of the observed total variance in the maximum number of zone alterations, with the Zeb1$^{-/-}$ mice displaying significantly higher numbers of zone alterations, in comparison to the control group ($F_{1,64}$=49.91, p<0.0001, **Figure 5.10B**), although there was no significant interaction between genotype and session type. At the simple effects level of individual sample and test phases, there was a significant difference between the maximum number of zone alterations between the control and Zeb1$^{-/-}$ mice at sample phases 2 and 3, as well as the test phase (p=0.0213, 0.0068, and 0.0031, respectively), indicating that the Zeb1$^{-/-}$ mice moved a significantly greater distance during these sessions, in comparison to the control mice.

Similar results were observed for the locomotor activity of the mice during the NOL task. The total distance moved was found to be affected by the type of session, with both groups of mice travelling a greater distance with each sample phase and subsequent test session ($F_{3,64}$=4.18, p=0.0091; **Figure 5.10C**). However, the genotype of the mice, as well as the interaction between genotype and type of session did not affect the total distance moved. When investigating the maximum number of zone alterations in the NOL task sessions, I found that both genotype and the type of session demonstrated main effects on this parameter ($F_{1,64}$=14.29, p=0.0003, and $F_{3,64}$=8.15, p=0.0001, respectively; **Figure 5.10D**), with the Zeb1$^{-/-}$ mice displaying a greater number of zone alterations in comparison to the control mice

across all three sample sessions as well as the test phase. Notably, the Zeb1$^{-/-}$ mice demonstrated a significantly greater number of maximum zone alterations between the first sample session and final test session through multiple comparisons in the two-way ANOVA model (p=0.0093).

Taken together, these results indicate that the deletion of Zeb1 increases the locomotion in mice, in part through the total distance moved, but greatly seen in the number of zone alterations; this will be further discussed in Section 5.4.3.1.

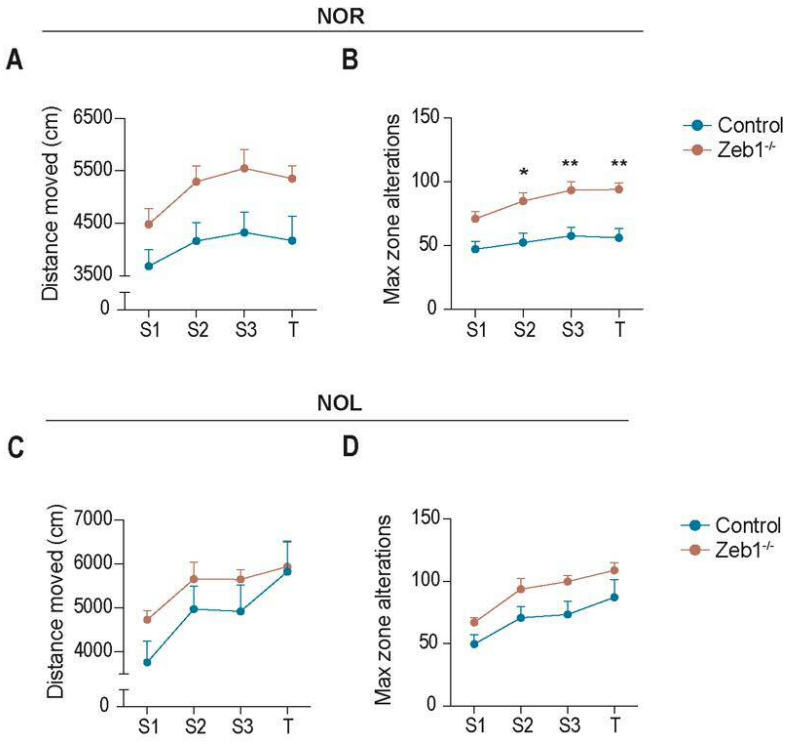

Figure 5.10 Locomotion of control and Zeb1$^{-/-}$ mice during the NOR and NOL task sample and test phases - The locomotion activity of the two groups of mice was assessed by total distance moved, as well as number of maximum zone alterations during the NOR (A and B, respectively) and NOL (C and D, respectively) tasks. Control group n=8 mice, Zeb1$^{-/-}$ group n=10, videos analysed with Noldus EthoVision XT software, two-way ANOVA with Sidak's multiple comparisons test, * p<0.05, ** p<0.001.

5.4 Discussion

Although adult neurogenesis in the hippocampus is responsible for the generation of only one type of excitatory granule neuron (in comparison to the SVZ where multiple types of interneurons are generated), it has gathered great research interest as this process impacts the structural and functional plasticity that contributes to hippocampal-dependent cognitive function in rodents (Kempermann *et al.* 2015).

In this chapter, I investigated the consequences of the initial boost in the population of proliferating progenitors after the ablation of Zeb1 in hippocampal NSCs described in the previous chapter. Specifically, I queried whether the increase in progenitors would translate into a greater number of newborn neurons that would become incorporated in the established hippocampal network. Here, I discuss the key observations.

5.4.1 Zeb1 deletion results in an increased granule neuron pool due to their increased survival

The increased progenitor cell proliferation rate and ensuing neuroblast population resulted in an expanded pool of newborn neurons that was greater in the $Zeb1^{-/-}$ mice by 8 weeks post-deletion, in comparison to the control group. To investigate whether this increase in the population of newborn neurons was due to either a potential increase in Type 1 cell division and Type 2 cell proliferation, or increased survival of newly generated granule neurons, I assessed EdU incorporation and carried out immunostaining for apoptosis markers. By 24 hours post-EdU administration there was no significant difference in the number of EdU-labelled cells between the control and $Zeb1^{-/-}$ mice; this indicated that the proliferation levels were similar in both mouse lines at the time of EdU administration. Interestingly, I observed no differences in the total number of EdU-labelled cells at 4 weeks post-EdU treatment either; this suggests that the number of EdU-labelled cells in the control and $Zeb1^{-/-}$ groups may have aligned at both timepoints due to either a similar amount of proliferation occurring, or less proliferation occurring in the $Zeb1^{-/-}$ mice but a greater amount of newly generated progeny surviving. However, it must be noted that the EdU administration was performed at 4 weeks post-tamoxifen

administration; it is possible that the majority of the proliferation may have occurred prior to this timepoint, which would result in the EdU administration at 4 weeks post-tamoxifen not targeting the bulk of the proliferative cells. This is a limitation of the study that does not allow definitive conclusions regarding the role of ZEB1 in lineage specification, and so an earlier timepoint should be investigated in future studies to confirm the present findings.

As there were similar numbers of proliferating progenitors at 24 hours, and consequent progeny at 4 weeks post-EdU in the control and Zeb1$^{-/-}$ mice, this did not account for the great amplification in granule neuron population in the latter mouse line. Thus, I next investigated the survival of newborn neurons through activated caspase 3 staining and observed a remarkably greater survival of neurons generated in the dentate gyrus of the Zeb1$^{-/-}$ mice, compared to the mice with wild-type ZEB1 expression. These observations suggest that ZEB1 expression is correlated with a decreased survival of adult-born neurons, but no conclusions can be drawn regarding the role of ZEB1 in neuronal lineage specification. Importantly, the proposed limitation of the timepoint chosen for the investigation of cell proliferation through EdU administration (as discussed in the previous paragraph) corroborates with the increased survival; neuronal maturation takes between 4 to 8 weeks post-cell birth, and a greater cell proliferation between 0 and 4 weeks post-tamoxifen administration would result in a greater number of neurons maturing around 4 weeks, which is subsequently reflected in their greater survival at this timepoint in the Zeb1-deficient mice.

As previously discussed in Section 1.5.3, programmed cell death is an integral aspect of neurogenesis with the function of maintaining homeostatic intraneuronal circuit connections, as well as regulating the size of the proliferating precursor cell pool. Functional integration has been shown to be key for the survival of neurons, and immature neurons unsuccessful in making connections with the pre-existing circuits undergo apoptosis. Caspase-mediated apoptosis has been suggested to account for a large portion of programmed cell death in adult neurogenesis, and Biebl and colleagues demonstrated that the administration of pan-caspase inhibitors could reduce cell death in the neurogenic niches of adult rats (Biebl *et al.* 2005). However,

there are several other mechanisms through which programmed cell death is induced, including extracellular signalling factors, hormones, and neurotransmitters (extensively reviewed in Kuhn 2015). The observation of a reduced population of immature and mature neurons that expressed activated caspase 3 demonstrates that ZEB1 is involved in the regulation of neuronal survival in the adult dentate gyrus. It is likely that this occurs through a non-cell autonomous mechanism as ZEB1 deletion was targeted to the hippocampal Type 1 cells and astrocytes, and the survival effects were seen in granule neurons that do not normally express ZEB1.

Microglia have been implicated in correct circuit formation in the developing and postnatal brain through synaptic pruning of immature synapses, as well as programmed cell death in the hippocampus. A study reported that in the adult brain, apoptotic newborn neurons are phagocytosed by unchallenged microglia, in the first few days of their life during the transition from the progenitor to neuroblast stage (Sierra *et al.* 2010); the hippocampal microglia were reported to carry out phagocytosis through the modification of their ramified processes. Thus, in the present study it is plausible that there is decreased phagocytosis by microglia in the dentate gyrus, which leads to a deficiency in the removal of immature neurons during their development. In the future, microglial-specific IF staining will be carried out to elucidate possible changes in their population in the dentate gyrus following the deletion of Zeb1.

In the developing and postnatal CNS, astrocytic processes are closely associated with live synapses where they are known to regulate synaptic transmission (Volterra and Steinhäuser 2004), and this has prompted great research to understand the function of this glial subpopulation in the correct formation of synapses. Astrocytes have been shown to directly contribute to this process by the expression of phagocytic receptors such as MEGF10 and MERTK that allow them to actively eliminate synapses (Chung *et al.* 2013). An indirect mechanism for synaptic modulation by astrocytes has also been identified in a series of studies led by Beth Stevens, in which the authors identified a pathway associating astrocytes and microglia in the correct maturation of synapses during development. They reported that retinal ganglion cells respond to astrocyte-secreted TGFβ signalling by secreting

complement cascade initiating protein q (C1q) that localises to weak synapses, and triggers the complement cascade, which recruits phagocytic microglia, subsequently resulting in the elimination of the unrefined synapse (Stevens *et al.* 2007; Bialas and Stevens 2013). In the current study, I observed a reduction in the population of DG-associated astrocytes; it is possible that a similar interaction of astrocytes with other cell populations, such as the microglia, could be contributing to the reduced apoptosis of immature neurons seen following the ablation of Zeb1.

Interestingly, a study showed the neuroprotective role of ZEB1 in an ischemic stroke model; Bui and colleagues demonstrated that ZEB1 expression is induced by p63 in an experimental model of stroke as well as in the human cortex following ischemic episodes, and functions to potentially inhibit neuronal apoptosis by reducing the pro-apoptotic gene Tap73 (Bui *et al.* 2009). However, this does not directly contradict the findings in the current study, as I propose that Zeb1 deletion results in the enhanced survival of neurons through a non-cell autonomous mechanism, as discussed in the above paragraphs.

In the developing CNS, ZEB1 inhibits the expression of NeuroD1 (Wang *et al.* 2019), which is a transcription factor that controls developmental neurogenesis as well as promotes adult neurogenesis in both the hippocampus and the SVZ (Gao *et al.* 2009; D'Amico *et al.* 2013). Furthermore, NeuroD1 expression is correlated with the survival of hippocampal neurons; Gao *et al*. reported that a conditional deletion of NeuroD1 driven by the Nestin promoter in the hippocampus resulted in a greater number of activated caspase 3-expressing cells that did not co-express DCX, suggesting that neuronal death occurs at the stages of neuronal development either before or after DCX expression is switched off. The group also found that the loss of NeuroD1 resulted in reduced dendritic length of granule neurons; taken together, these findings indicate that NeuroD1 is involved in the correct development and survival of granule neurons (Gao *et al.* 2009). Similar findings were reported by a separate study that employed retroviral delivery of the NeuroD1 gene into adult progenitor cells that subsequently demonstrated increased neuronal differentiation (Richetin *et al.* 2015). In the current study, I observed 1) increased hippocampal neurogenesis, and 2) reduced neuronal cell death. If ZEB1 acts as a repressor of

NeuroD1, this would be consistent with the loss of ZEB1 expression resulting in increased NeuroD1 levels, which would elicit increased neuronal differentiation, reduced apoptosis, and increased neuronal maturation and hippocampal integration. Thus, in light of these findings, it is conceivable that ZEB1 may be a transcriptional repressor of NeuroD1 in the adult brain, in line with its reported function in the embryonal CNS (Wang *et al.* 2019). Whether ZEB1 directly represses NeuroD1 in the present model will be further explored in future work.

5.4.1.1 Consequences of Zeb1 loss for pro-neurogenic cell division of Type 1 cells

As previously discussed in Section 4.4.1.1, multipotent self-renewing stem cells are capable of giving rise to multiple cell lineages whilst maintaining their own cell population within a tissue. In a short-term lineage trace, Obernier and colleagues demonstrated that the majority of Type B cells in the SVZ (approximately 70%) undergo symmetric divisions towards differentiation, whilst a smaller percentage is capable of symmetrically diving for self-renewal, following which they can either enter quiescence or undergo further rounds of division (Obernier *et al.* 2018); a study further reported limited Type B cell self-renewal *in vivo*, with the majority of the NSCs producing neurons destined for integration in the olfactory circuits (Calzolari *et al.* 2015). Similar multipotency and self-renewal characteristics of hippocampal Type 1 cells have also been described through which they can undergo either neurogenesis or astrogliogenesis, or self-renew (Bonaguidi *et al.* 2011).

In the present study, Zeb1 deficiency resulted in the gradual depletion of both the quiescent and activated Type 1 cell pools, as well as in decrement in the number of hippocampal niche astrocytes, with a simultaneous *increase* in the granule neuron population over a period of 26 weeks following the induction of Zeb1 deletion. As previously mentioned in Section 4.4.1.1 and fully discussed later in Section 6.2, there are various models that strive to explain the cell fate choices that govern the division mode of adult NSCs, and the data presented in this thesis aligns with the majority of models presented in Section 6.2.

Importantly, I propose that ZEB1 functions to maintain self-renewal of Type 1 cells, which has been observed during embryonic development; a study has previously reported the role of ZEB1 in mediating correct cleavage plane orientation

to set a balance between neuron generation and Type 1 cell self-renewal in the developing cortex (Liu *et al.* 2019). The change in cell numbers (decreased Type 1 cells/astrocytes, and simultaneously increased neurons) following Zeb1 deletion could indicate a shift from asymmetric to symmetric divisions; the former is required for the maintenance of the balance between neurogenesis and Type 1 cell self-renewal, whilst the latter induces precocious neuronal differentiation and subsequent Type 1 cell pool depletion. However, there is no definitive evidence of this at present with the current dataset.

It was previously briefly discussed (Section 4.4.1) that the depletion of Type 1 cells with the ablation of Zeb1 targeted to these cells indicates a loss-of-function phenotype associated with this genetic alteration. However, the deletion of Zeb1 also resulted in an enhanced production of neurons at the expense of the NSC pool. ZEB1 acts as both a transcriptional activator and repressor (Section 1.8.1), and importantly, its ablation will inevitably result in the transcriptional induction of previously repressed genes, with the simultaneous downregulation of previously actively transcribed genes. Thus, whilst in the current study there is a gain in neurogenesis following Zeb1 deletion, which is also phenotypically observed in a heterozygous Zeb1 deletion model (see Appendix B), there is also a simultaneous loss of stem cells, and this dual effect mirrors the twofold function of ZEB1 as a transcription factor; it is plausible that the increase in adult-born granule neurons may be a by-product of the NSC division mode shift from self-renewal to differentiation, which will be further discussed in Section 6.2.

5.4.2 Decline in astroglial numbers in the dentate gyrus of Zeb1-deficient mice

Several decades of research have elucidated the important roles of astrocytes that range from the correct function of neurons and maintenance of homeostasis, to causatives in disease development and progression; this has shifted the view of the brain from a neurocentric one to the acceptance of astroglia as equally important brain cells. They also form a part of the adult hippocampal neurogenic niche, as evidenced by Song and colleagues in a formative study that demonstrated the ability of hippocampal astrocytes to induce proliferation and neuronal fate-specification of NSCs *in vitro* (Song *et al.* 2002). As described earlier in Section 1.3.1, one of the

seminal discoveries in the field was the identification of the radial astroglial characteristics of the adult NSC population (Seri *et al.* 2001; Merkle *et al.* 2004).

A still much debated matter concerns the identity of the NSC pool that generates adult-born hippocampal neurons and astrocytes. Neurogenesis and gliogenesis are relatively independent processes that do not share a late precursor cell, as evidenced by the lack of overlap between astrocytic and neuronal markers in hippocampal fate-specified post-mitotic cells (Steiner *et al.* 2004). However, it is posited that the two processes have a common early progenitor cell, identified as the adult hippocampal Type 1 cell; lineage tracing has been widely used to assess fate specification to support this hypothesis (Bonaguidi *et al.* 2011; Encinas *et al.* 2011; Bonzano *et al.* 2018). However, based on the great heterogeneity of the adult NSC population (reviewed in Gonçalves *et al.* 2016), it is also plausible that entirely separate stem cell pools exist, with very similar cell marker expression such as GFAP (Steiner *et al.* 2004), that generate the two neural populations. In the same vein, it can be speculated that there is an occurrence of a stochastic lineage decision in adult hippocampal Type 1 cells to either generate neurons or astrocytes, but never both during the postnatal mammalian lifetime. Finally, another possibility is that rather than the *de novo* generation of astrocytes, after a certain number of divisions activated Type 1 cells transform into astrocytes, mimicking the perinatal transformation of radial glia into parenchymal astrocytes (Encinas *et al.* 2011).

In the current study, I observed a decrease in the number of astroglial cells in the SGZ (as well as throughout the GL and ML) simultaneous to an amplification of the granule cell population in the $Zeb1^{-/-}$ mouse hippocampus. This suggests that following the deletion of Zeb1, there is a loss of astrocytes associated to the hippocampal niche. As the data do not allow the drawing of conclusions at present, I propose three scenarios that may explain the reduction of the astroglial population: 1) ZEB1 represses pro-neuronal transcriptional regulators, whilst activating pro-astrocyte regulators, 2) ZEB1 is an astrocyte survival factor, and 3) ZEB1 mediates the transformation of Type 1 cells into astrocytes. These will be discussed in the subsequent sections.

5.4.2.1 ZEB1 represses pro-neuronal transcriptional regulation whilst activating pro-astrocytic factors

With the increase in granule neurons, and the decrease in dentate gyrus astrocytes following the deletion of Zeb1, it may be speculated that ZEB1 represses the expression of pro-neuronal transcriptional regulators, such as NeuroD1 (as discussed in Section 5.4.1), whilst inducing pro-astrocyte regulating factors, such as nuclear factor IA (NFIA) under homeostatic conditions. A study demonstrated that ZEB1 is expressed in early spinal astrocyte precursors that originate in the SVZ (Ohayon *et al.* 2016); astrocyte precursors also express pro-gliogenesis factors such as NFIA (Tchieu *et al.* 2019). Thus, it is possible that ZEB1 induces transcription factors that promote gliogenesis. Moreover, this proposed dual role of ZEB1 fits with its recognised function in the context-dependent activation and repression of downstream targets.

Importantly, here it is crucial to take into consideration the possibility that there may be two separate populations of Type 1 cells that are responsible for neurogenesis and astrogliogenesis in the adult brain (Decarolis *et al.* 2013; Gebara *et al.* 2016). This would account for the incongruous effects of Zeb1 deletion in the two main cell populations in the adult hippocampus, with the increment in adult-born neurons and the reduction in niche astrocytes. However, this would require both subpopulations of Type 1 cells to have highly divergent expression of co-regulatory factors. Thus, in the current study, it is more plausible to speculate that there is a single Type 1 cell population that generates both neurons and astrocytes, depending on transcriptional regulatory signals.

5.4.2.2 ZEB1 functions as a survival factor in GLAST-expressing astroglial cells

Another plausible explanation for the loss of a subpopulation of S100β-expressing astrocytes in the mouse dentate gyrus following Zeb1 deletion is the necessity of ZEB1 expression for the survival of astrocytes. However, no previously published study has provided evidence for the occurrence of this.

It is known that the astrocyte population is highly heterogeneous (reviewed in Matias *et al.* 2019), and mature astrocytes express ZEB1 in the spinal cord and

dentate gyrus (Ohayon *et al.* 2016; Hochgerner *et al.* 2018). However, mining of the dataset extracted from single-cell RNA-Seq analysis of the juvenile and adult rodent dentate gyrus indicated that the expression of ZEB1 is heterogeneous in the resident astrocyte population (Hochgerner *et al.* 2018); in the present study, I observed that the staggering majority of dentate gyrus astrocytes expressed ZEB1, and thus the random distribution of ZEB1 over the majority of astrocytes in the RNA-Seq dataset may suggest a temporal fluctuation of gene expression in the dentate gyrus. Thus, it can be speculated that ZEB1 is expressed in astrocytes where it may be regulating some processes that could be implicated in their survival.

A previously published study highlighted S100β as a target of ZEB1 in glioblastoma cells (Rosmaninho *et al.* 2018); whilst there is limited evidence to support that S100β is crucial for the survival of astrocyte, apart from a study that demonstrated the mitotic function of S100β in the astroglial population (Selinfreund *et al.* 1991), it is plausible the deletion of Zeb1 may result in the downregulation of S100β, which may either inhibit the proliferation of niche astrocytes or cause astroglial apoptosis in the adult hippocampus in the current model.

5.4.2.3 Conversion of radial glial cells into astrocytes

A final possibility is that ZEB1 is a cell fate determination factor in the context of Type 1 cell conversion to astrocytes following a number of division cycles. This transformation has previously been reported by Encinas and colleagues who observed an increase in the niche astrocytes simultaneous to a depletion of Type 1 cells in the adult dentate gyrus (Encinas *et al.* 2011). ZEB1 may contribute to this process by promoting the conversion, which in the current model was potentially seen be inhibited by the absence of ZEB1.

A similar phenomenon is seen in development; following the bulk of neurogenesis in the developing CNS, the majority of radial glial cells have been shown to transform into parenchymal astrocytes (Section 1.3.1; reviewed in Kriegstein and Alvarez-Buylla 2009). Mechanistically, neuregulin1 signalling via ErbB2 inhibits this transformation, and it has also been shown that this signalling axis can also result in the dedifferentiation of astrocytes into precursor radial glia, with the capacity to generate neurons (Patten *et al.* 2003; Schmid *et al.* 2003; Ghashghaei *et al.* 2007).

Although there is no direct evidence of the involvement of ZEB1 in the neuregulin1-ErbB2 signalling pathway, a study reported the inhibition of EMT (and in particular EMT-inducing genes such as Zeb1) through the downregulation of neuregulin1-ErbB2 signalling via miR-296 in hepatocellular carcinoma (Shi *et al.* 2018). It can be speculated that there may exist a feedback loop between ZEB1 and miR-296, based on the known regulatory functions of ZEB1 of microRNA subclasses in EMT, but this will need further research.

Whether astrogliogenesis is affected in Zeb1-deficient mice, or SGZ-associated astroglia undergo apoptosis following Zeb1 deletion will be further explored in future experiments with the assessment of co-expression of astrocytic markers with apoptotic cell markers, as well as possible EdU incorporation in the astroglia over the weeks following ablation of Zeb1.

As a final thought on this matter, astrocytes within the neurogenic niche are known to secrete several factors that aid the proliferation of Type 1 cells in the hippocampus; these include adenosine 5'-triphosphate (Cao *et al.* 2013) and fibroblast growth factor 2 (Kirby *et al.* 2013). It can be proposed that the loss of astrocytes, whether or not that is due to the ablation of Zeb1 in mature astrocytes in $Zeb1^{-/-}$ mice (section 5.4.2.2), further mediates the depletion of the Type 1 cell pool due to the loss of proliferative aid provided by the astroglia. This poses a chicken and egg dilemma; astrocytes mediate hippocampal Type 1 cell proliferation, and Type 1 cell division gives rise to astrocytes, but which is affected first with loss of Zeb1?

5.4.3 Deletion of Zeb1 does not alter hippocampal-based novel object recognition and spatial memory

Adult neurogenesis produces hippocampal neurons that become integrated into the functional hippocampal circuitry (Jessberger and Kempermann 2003; Vivar and van Praag 2013). The young and more excitable granule neurons have been shown to mediate long-term potentiation, strengthening the synapse and in turn accelerating the rate of information processing at the afferent branch of the trisynaptic circuit (Snyder *et al.* 2001). It has also been proposed that the continuous production of groups of transiently juvenile neurons serves the purpose of generating temporal memories, through the separation of these memories by the

distinct groups of young neurons encoding them in a temporally categorised manner (Aimone *et al.* 2006).

As adult hippocampal neurogenesis is important for memory consolidation, I was interested in investigating whether resulting aberrant neurogenesis following the ablation of Zeb1 in hippocampal Type 1 cells would affect the performance of $Zeb1^{-/-}$ mice in hippocampus-dependent behavioural tasks. I carried out the novel object recognition (NOR) as well as the novel object location (NOL) tasks with control and $Zeb1^{-/-}$ male mice 12 weeks post-transgene recombination with tamoxifen. Unlike tasks that employ fear or reward-driven learning in rodents to test long-term memory which can induce confounding responses involving emotions and stress, such as the Morris water maze test, the NOR and NOL tasks rely on the inherent exploratory nature of these animals in response to novelty. These two tasks differ in that the former gauges the response of mice to a novel object juxtaposed with a familiar object, whilst the latter assesses spatial awareness by presenting two objects in specific locations, after which one gets moved to a novel location and the interactions are re-assessed. Both tasks assess the ability of the rodents to recognise and interact with the novel object/object placement, thereby testing normal hippocampal function. However, there are various confounding factors such as variances in inter-strain visual abilities (Brown and Wong 2007) and object biases, but these can be accounted for with specific task design considerations (reviewed in Blaser and Heyser 2015). Whilst the NOL task requires solely the hippocampus for the consolidation of previously encountered spatial and contextual information (Mumby *et al.* 2002), the NOR test employs several brain regions including the hippocampus and perirhinal cortex (Hammond *et al.* 2004).

5.4.3.1 $Zeb1^{-/-}$ mice display increased locomotion

Across the habituation and familiarisation sessions, as well as sample and test phases of the NOR and NOL tasks, one of the most remarkable observations was the increased locomotor activity of Zeb1-deficient mice. Enhanced locomotion can be suggestive of either reduced anxiety, or generalised motor dysfunction; I will briefly discuss these in the context of the current study, as it is largely outside the remit of this thesis.

Reduced anxiety has been observed in a number of cognitive and neurodegenerative disorders. In the present study, mice with Zeb1 deficiency displayed increased locomotion, which in a strict sense cannot be extrapolated to mean increased exploration, as the current data set is somewhat inconclusive due to a small sample size. However, in the locomotion activity analysis during the NOL task, the Zeb1$^{-/-}$ mice displayed a significantly higher number of maximum zone alterations in the test phase in comparison to the first sample session; this could be indicative of increased locomotion due to increased exploration of the displaced object setting, although this is purely speculative. Increased exploration in response to a novel environment is seen in "high-responder" rodents; this group of rodents was first described in a model investigating the effects of D-amphetamine on psychomotor activity (Piazza *et al.* 1989), and since then, this model has been used to relate high responsiveness in a novel environment to decreased stress levels (Kabbaj 2008). Taken together, this suggests that Zeb1 deletion in mice may display a phenotype akin to the increased locomotion/decreased anxiety phenotype observed in high-responder rodents. The action of glucocorticoids mediates the response to stress, and a study has previously highlighted nervous system development as a glucocorticoid receptor (GR)-responsive process in developing zebrafish, with simultaneous identification of ZEB1 as a potential interactor within this network (Nesan and Vijayan 2013); as the GR, and mineralocorticoid receptor (the closest analogue to the GR) are highly expressed in the hippocampus (Zhe *et al.* 2008), it is possible that Zeb1 deletion impacts glucocorticoid-mediated signalling in the hippocampus, which has a downstream anti-anxiolytic effect in Zeb1-deficient mice.

Astrocytes are widely recognised as primary mediators of correct synaptic activity (Chung *et al.* 2015). Moreover, astrocytes are present in abundance in areas of the brain that regulate motor function, such as the basal ganglia, cerebral cortex, and cerebellum (Kettenmann and Verkhratsky 2011). Thus, it is plausible to speculate that the loss of astrocytes seen in the hippocampi of the Zeb1$^{-/-}$ mice may also occur in these motor function-implicated brain regions, which could disrupt neurotransmission and consequently alter motor function. This will however need to

be confirmed in future studies with further astrocyte-specific immunostaining in the aforementioned regions.

To further explore a possible anti-anxiolytic phenotype following the loss of Zeb1 in GLAST-expressing Type 1 cells as well as astrocytes, future studies should assess the behaviour of Zeb1$^{-/-}$ mice in tasks that aim to evaluate rodent anxiety levels such as the elevated plus maze assay (Walf and Frye 2007).

5.4.3.2 Zeb1$^{-/-}$ mice show normal object attendance in NOR task

In the test phase of the NOR task, the total number of contacts that the Zeb1$^{-/-}$ mice made with the novel objects in comparison to the familiar objects was significantly greater than the chance level. This indicated that this group of mice had the ability to discriminate between familiar and novel and thus showed greater object attendance towards the latter. It must be noted that although the number of contacts between familiar and novel object in the control mice was not significantly different, this may be confounded by a small sample size. This is substantiated by the fact that the total duration of the contacts with the novel objects made by the control mice in the NOL task was significantly higher than one would expect to occur by chance. The total number of contacts was not found to be significant, which further evidences the necessity for a greater sample size (section 5.4.3.3). Taken together, these findings suggest that Zeb1 deficiency does not affect the ability of these mice to recognise and interact with novelty, indicating that accelerated neurogenesis following deletion of Zeb1 does not lead to memory improvement. This is somewhat confounded by the lack of significant object attendance by the Zeb1$^{-/-}$ mice in the NOL task, which relies solely on hippocampal function, but this may be an artefact of a low cohort size which is crucial for the generation of an accurate mean, as well as to better identify outliers.

Thus, the results from the present dataset indicate that Zeb1 deletion does not affect hippocampal memory. To further validate this, other tests that rely on hippocampal function should be carried out, such as the pattern separation task. Pattern separation is the process by which similar inputs are separated into less similar outputs, to establish distinctions between similar memories, which is dependent on hippocampal function (reviewed in Yassa and Stark 2011). Testing of

the ability of a rodent to discriminate between small spatial shifts in objects can be used to assess hippocampal integrity and function. Whilst this task is very similar to the NOL test, it takes the evaluation one step further by using an increasing distance in the spatial movement of the objects to tease out small variations in the memory of the rodents.

5.4.3.3 Assessment of the test methodology

With the current set of observations reported in Section 5.3.5, I can conclude that the task was carried out to effect, with a few changes that can be implemented in future studies to refine the protocol.

The control group showed a suggestive trend of declining locomotion over the course of the habituation and familiarisation sessions. Decreasing locomotion in an experimental arena occurs as an effect of the increasing familiarisation of the rodents to a similar environment over the course of time (Oliveira *et al.* 2010). This indicates that the control mice exhibit "normal" behaviour as expected, and that subsequent object attending behaviour results, of which the majority showed a trend but did not reach significance, could be assigned to a low number of biological replicates.

Furthermore, the main effect of object identity (familiar vs. novel) and object placement (familiar vs. displaced) in the total number of contacts and total duration of these interactions yielded successful results; this observation indicated that all tested mice (regardless of genotype as the interaction between genotype and the object identity/placement was not found to be significant in a two-way ANOVA) had the ability to show greater object attendance in favour of the novel objects, in comparison to the familiar. As this is an innate behavioural feature of rodents, this finding is suggestive of a successful recognition of novelty by the mice, indicating success in object choice and displacement, with a 5-minute delay period between the sample and test phases.

To improve the methodology used in this study, I suggest using a larger sample size to increase the biological replicates. A large number of results showed suggestive trends, although they did not reach significance levels; I predict that this is due to a cohort size of 8 control mice, and 10 $Zeb1^{-/-}$ mice. In animal behavioural

tasks it is crucial to have a sample size large enough to reach power levels for confidence in the results, as well as reproducibility due to the innate heterogeneity in animal behaviour (reviewed in Gulinello *et al.* 2018). In addition to a bigger intra-strain sample size, published studies have employed a minimum exploration criterion, in which the rodents were required to attend objects for a certain amount of time (usually 20-30 seconds), and the study subsequently assessed the length of time required for reaching the exploration criterion (reviewed in Cohen and Stackman 2015). This eliminates the ambiguity of differential interaction times when set session lengths are utilised instead, which could result in different levels of learning if a strain shows signs of anxiety. Thus, I suggest utilising a minimum interaction criterion for future studies. Lastly, in this study I focused on the effects on memory of a short delay period of 5 minutes. Previous studies have assessed a series of delay periods, ranging from 10 seconds to 48 hours (reviewed in Antunes and Biala 2012); the length of the rest time between training and testing sessions can be altered to test either short or long-term retention of object identity/placement. In future studies, I will consider using a longer delay period to test the effects of Zeb1 deletion in the hippocampus on the long-term memory of the mice.

In summary, Zeb1 deletion resulted in an overamplification of the neuroblast pool, and subsequent adult-born granule neuron population in the mouse hippocampus. This is proposed to be in part due to a greater neuronal survival in Zeb1$^{-/-}$ mice as the data suggest. Moreover, a decrease in hippocampal astroglia, including the SGZ-associated niche astrocytes was observed. Whilst the cause for this remains undetermined, it is possible that reduced astrocytes could be a consequence of either a loss of astrogliogenesis or reduced astrocyte survival with the deletion of Zeb1. Lastly, preliminary data from novel object recognition and object displacement tasks indicate that the increased granule neuron population in the Zeb1$^{-/-}$ mice does not improve their hippocampal-dependent memory function, although they exhibit increased locomotion activity; it will be interesting to assess the cognitive function of aged Zeb1$^{-/-}$ mice to evaluate whether the depletion of hippocampal Type 1 cells will have long-term effects on hippocampal function due

to a greatly reduced generation of neurons over time. Taken together, the results from this chapter suggest that ZEB1 maintains a fine balance between the number of neurons and astrocytes in the hippocampus.

Chapter 6 - Conclusions

In this study, I sought to elucidate the function of ZEB1 in adult hippocampal neurogenesis. In particular, I queried whether 1) ZEB1 is involved in the self-renewal of Type 1 cells, 2) deletion of Zeb1 would have a downstream effect on the proliferation and lineage-commitment of Type 2 cells, and 3) ZEB1 is necessary for the correct development and survival of adult-born granule neurons. This was investigated in a novel transgenic mouse model with Zeb1 loss-of-function specific to adult Type 1 cells and astrocytes; this allowed the labelling and subsequent study of the Type 1 cell lineage (summary of resultant cell counts is summarised in **Figure 6.1**). I report that ZEB1 regulates the self-renewal of Type 1 cells and consequently lineage specification of Type 2 cells, through which it contributes to the maintenance of a steady addition of neuronal-committed progeny to the adult DG, whilst maintaining the population of niche astrocytes (summarised in **Figure 6.7**). This study highlights a novel role for ZEB1 in the *adult* mammalian brain and lays the foundation for future work that can identify downstream targets of this transcription factor in the maintenance of the self-renewal of adult NSCs.

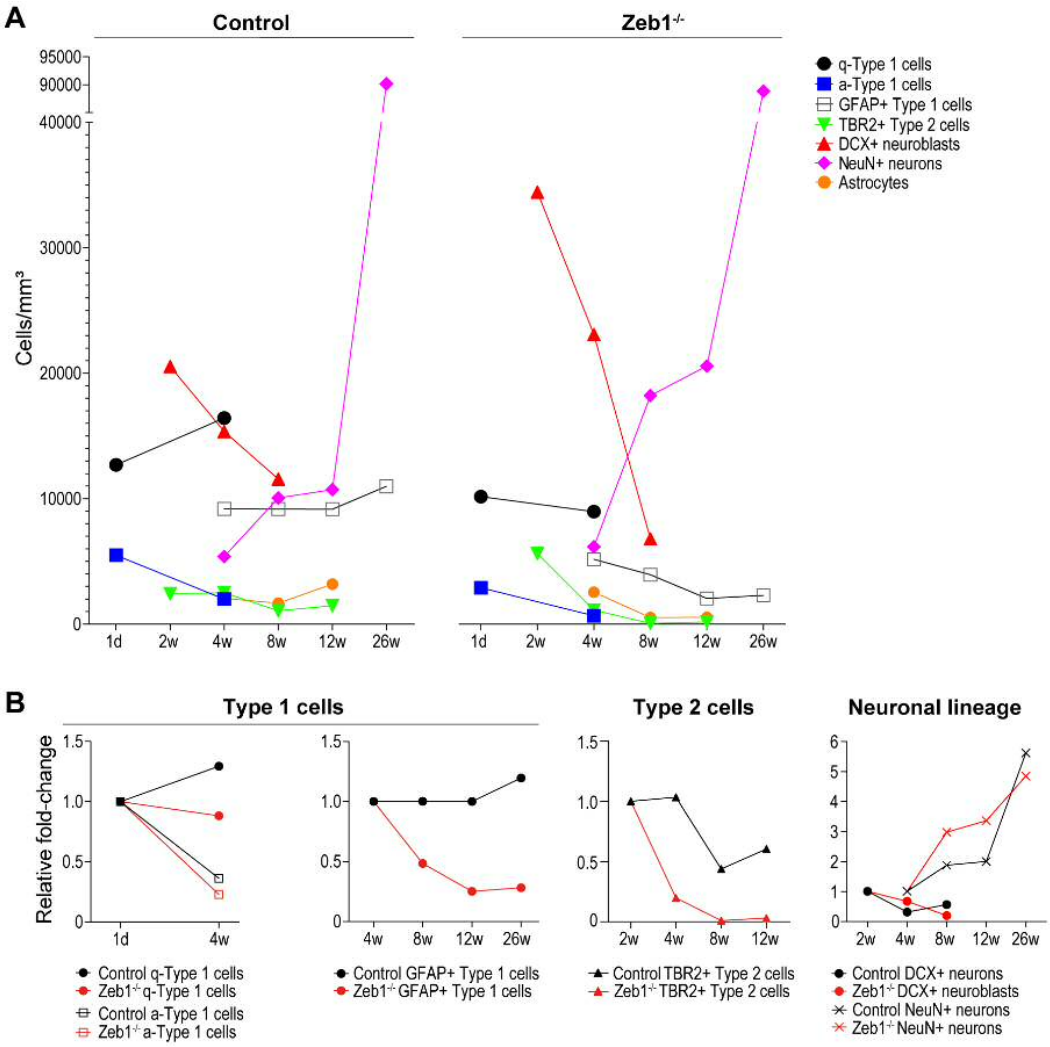

Figure 6.1. Summary of cell population changes (as seen in the previous results chapters) in the hippocampal neurogenic compartments of control and Zeb1$^{-/-}$ mice – (A) Absolute cell counts of the Type 1, Type 2, Type 3, neuronal, and astrocytic populations in the DG at 1 day, as well as 2, 4, 8, 12, and 26 weeks post-tamoxifen administration. (B) Relative fold-changes in the Type 1, Type 2, and neuronal lineage-specified cell populations in the control and Zeb1$^{-/-}$ mice, at various time-points post-tamoxifen induction in both groups.

6.1 ZEB1 maintains the self-renewal of Type 1 cells

In the present study, I found that ZEB1 expression is predominantly restricted to NSCs (in both the SVZ and hippocampus), and astrocytes, and there was little to no ZEB1 protein detected once precursors became neuronal-lineage committed. Previous studies have focused on the function of ZEB1 in neurodevelopment; one study reported that ZEB1 expression was high in unpolarized cerebellar granule neuron progenitors, which subsequently decreased as these cells became lineage-

committed and underwent migration (Singh *et al.* 2016); ZEB1 has also been implicated in the correct rate of differentiation of cortical progenitors in the development of the neocortex, with the ablation of Zeb1 resulting in precocious neuronal differentiation and consequential progenitor pool depletion (Wang *et al.* 2019). These previous studies support my observations in the context of adult neurogenesis, which suggests that the pro-stemness role of ZEB1 in development is maintained in the adult stem cell niche. The molecular mechanism and downstream targets of ZEB1 remain to be elucidated. As ZEB1 appears to be important for the maintenance of the Type 1 cell population, this has possible implications in the contribution of the steady supply of new adult-born neurons throughout the lifetime of an animal.

The gradual decrease in Type 1 cells, with a suggestive plateau in their numbers between 12 and 26 weeks suggests that Zeb1 deficiency contributes to a loss of NSCs in an age-accelerated manner. In the ageing mammalian brain, it has been shown that neurogenesis gradually declines, with either 1) a loss of precursor cells, 2) a lower propensity for neurogenesis, or 3) a lengthening of the cell cycle (reviewed in Drapeau and Abrous 2008). A number of studies have also assessed BrdU incorporation in the DG at various timepoints throughout the rodent lifetime, ranging from 2 to 28 months, and have demonstrated that BrdU incorporation steadily decreases, with either a significantly lower number of BrdU-labelled cells towards the latter months in comparison to all earlier timepoints, or a gradual decrease through the earlier timepoints, with a stabilising of low cell numbers towards the later timepoints in ageing (reviewed in Drapeau and Abrous 2008). In the current study, I observed that the number of Type 1 cells in the $Zeb1^{-/-}$ mice steadily declined with time, seemingly reaching a plateau between 12 and 26 weeks, albeit much lower than the cell pool size at 1 day post-tamoxifen administration. This depletion of hippocampal NSCs in Zeb1-deficient mice could be comparable to a premature ageing process, and future studies should assess the effects of Zeb1 deletion on the numbers of new adult-born neurons in the brains of aged rodents, as well as any resulting effects on cognitive function later in life.

6.2 Neural stem cell division mode models

Because the depletion of Type 1 cells is accompanied by the precocious production of neurons and continuous loss of astroglia in the DG, the data from this study indicate aberrant stem cell division following Zeb1 deletion. Various models have been proposed to date to describe the mode of NSC division, through which they propagate their own population as well as maintain neuron production through the lifetime of an animal (with some age-related reduction in the rate of neurogenesis; see Lazutkin et al., 2019). Lineage tracing and live imaging have been predominantly used to analyse NSC division modes in transgenic lines. The main limitation of these studies lies in the labelling of different subpopulations of NSCs due to the heterogeneous expression of cell markers (Decarolis *et al.* 2013); this may account for observed discrepancies between the different models. Here I discuss the major models that propose different modes of NSC division, and the implications of my observations for each model.

1) The first paradigm makes a case for the existence of a population of NSCs that can shuttle between a state of quiescence and activation for self-maintenance. Once activated, proliferating NSCs can undergo either: i) self-renewing symmetric division (producing two NSCs; **Figure 6.2A**), or (ii) asymmetric multipotent division producing one NSC and either a neuronal progenitor (**Figure 6.2B**) or an astrocyte (**Figure 6.2C**) (Bonaguidi *et al.* 2011); in all division modes, the daughter NSCs return to a state of quiescence to preserve the stem cell pool. Thus, with age there is an inconsequential reduction in the NSC pool, although the number of symmetric divisions decreases with time.

   One of the key findings of the current study is the depletion of first the activated followed by the quiescent stem cell pools, simultaneous to an amplification in the population of adult-born granule neurons. The exhaustion of the former cell populations suggests that the ablation of Zeb1 leads to a loss in the return of activated NSCs to their quiescent state. Moreover, it is also possible that the decrease in quiescent and activated NSCs occurs as a result of little to no self-renewal of Type 1 cells in the Zeb1$^{-/-}$ SGZ; here I suggest an additional mode of

NSC division in the absence of ZEB1-mediated transcriptional regulation, whereby the Type 1 cells divide symmetrically towards a pro-neuronal fate (**Figure 6.2D**). To ascertain whether division mode D occurs as a consequence of Zeb1 deletion, which would account for the increment in granule neurons, it will be imperative to carry out clonal analysis *in vivo* (as carried out in Bonaguidi et al., 2011; Pilz et al., 2018; and reviewed in Xu et al., 2018) as this will reveal whether a switch from asymmetric to symmetric division occurs in the current model at a single cell level.

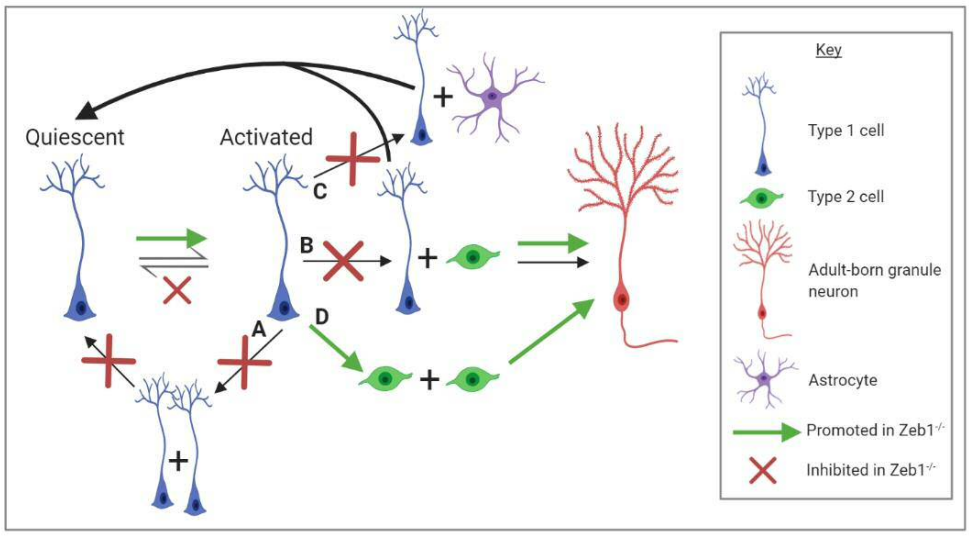

Figure 6.2. Model 1 proposes the maintenance of the NSC pool throughout the lifetime of an animal, sustained by self-renewing symmetric and asymmetric divisions. Image created in Biorender.

2) The second paradigm is termed the "disposable stem cell model" and posits that quiescent NSCs become activated and undergo an average of three asymmetric pro-neuronal divisions (**Figure 6.3A and B),** following which they terminally transform into astrocytes (**Figure 6.3**, Encinas *et al.* 2011). Within this paradigm, it is also proposed that Type 2 cells themselves undergo approximately 2.3 rounds of division before differentiating into neurons. This models supports the age-related depletion of the NSC pool as well as the previously observed increment in the number of niche astrocytes (Pilegaard and Ladefoged 1996; Mouton *et al.* 2002; Ziebell *et al.* 2018).

The depletion of the NSC population with age due to the pro-differentiation divisions described in this model aligns with the observation in the current study of the Type 1 cell pool depletion with the concurrent increase in adult-born granule neurons. Should ZEB1 truly function in correct cleavage plane orientation (Section 5.4.1.1), a distinct mode of division is conceivable through which Zeb1 ablation forces a pro-neuronal symmetrical division switch in the activated Type 1 cells (akin to the division mode D described in the previous paradigm), which would lead to an acceleration of both Type 1 cell population depletion as well as granule neuron production (**Figure 6.3D**). Furthermore, in the current study, I observed a decrease in the number of astrocytes following the deletion of Zeb1. As discussed previously (cite section), this could be due to either a decreased propensity for *de novo* hippocampal astrogliogenesis, increased astrocyte apoptosis, or a loss of terminal astrocyte transformation of NSCs following their activation. This latter postulation indicates that under healthy conditions, Zeb1 may play a role in promoting the transformation of NSCs into astrocytes, which in the Zeb1$^{-/-}$ model is possibly lost due to a shift to an exclusively pro-neuronal NSC division strategy which depletes the NSC pool through a different mechanism.

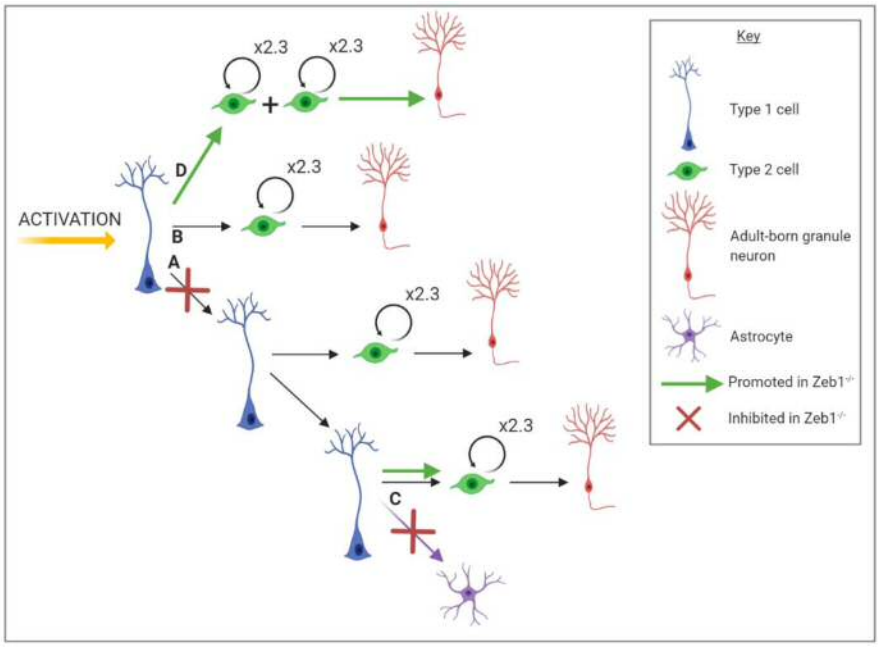

Figure 6.3. Model 2 supports the existence of single-use adult NSCs, resulting in an age-related exhaustion of the stem cell pool. Image created in Biorender.

3) A third paradigm was recently proposed in a study that utilised *in vivo* live tracing of adult NSCs (Pilz *et al.* 2018); based on their findings, the authors suggested that once activated, adult NSCs undergo a developmental-like program in which initial symmetric self-renewing divisions (**Figure 6.4A**) are followed by asymmetric divisions with the production of both neuronal and glial progeny (**Figure 6.4B** and **C**, respectively). Importantly, regarding the differentiated progeny of the NSCs, this model proposes the following: i) that NSCs can give rise to neurons directly, without the necessity of an intermediate cell (**Figure 6.4B**), and ii) that the production of astrocytes is very limited, with no occurrence of terminal transformation of Type 1 cells into astrocytes (at least within the investigated 2-month period). Moreover, this paradigm also suggests that Type 2 cells possess "stemness" characteristics, displaying the ability to stochastically divide symmetrically or asymmetrically, approximately 3-6 times, to self-renew as well as generate neuronal progeny (**Figure 6.4D**). In a similar vein to the second paradigm described above, activated NSCs do not revert to a quiescent state, implying an age-related depletion of the NSC pool; however, in this scenario the self-renewal capacity of Type 2 cells may maintain long-term neurogenesis rates.

   The findings of the current study can be fitted to this model, whereby Zeb1 deletion results in the inhibition of NSC divisions that promote self-renewal as well as glial production, with the promotion of an alternative division mode that only supports symmetric pro-neuronal divisions (**Figure 6.4E**). Furthermore, it is also possible that the NSCs continue to give rise to neuronal daughter cells directly, bypassing the need for a transitionary cell type to increase the rate of neuronal production (**Figure 6.4F**); however, in the current study I observed a significant amplification of the neuroblast population as early as 2 weeks and up to 4 weeks post-Zeb1 deletion, suggesting that the majority of neurogenic NSC divisions involve an intermediary cell population in the $Zeb1^{-/-}$ model. It can also be speculated that the deficiency of Zeb1 limits the self-renewal of both Type 1 and Type 2 cells, which was observed through the constant progressive loss of

the former cell population, and the initial transient increase in Type 2 cells, followed by a remarkable decrement in their population.

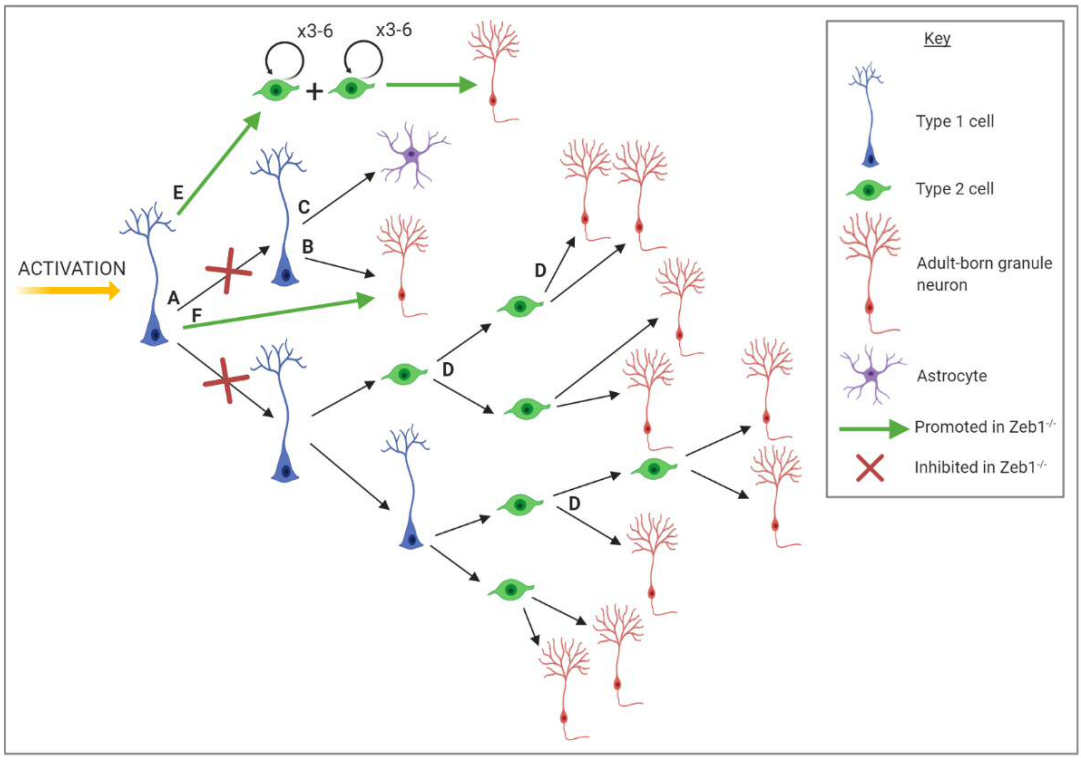

Figure 6.4. Model 3 proposes life-long maintenance of neurogenesis through the self-renewal potential of Type 2 cells. Image created in Biorender.

4) A fourth model was developed that combined data from the various models discussed above with a mathematical model to test the viability of crucial parameters, including Type 1 cell activation, proliferation, and depletion rates (Ziebell *et al.* 2018). Subsequently, the authors suggested the existence of a separate pool of neural precursors, termed "resilient NSCs" that account for 10% of the global NSC population in mice aged 10 weeks, are indefinitely quiescent, and can become activated in old age under stimulation (**Figure 6.5**); taken together, these characteristics of the resilient NCS can explain the slow rate of depletion of quiescent NSCs seen in the clonal data provided by Bonaguidi and colleagues (Bonaguidi *et al.* 2011). Importantly, the existence of a resilient NSC pool could account for the slow rate of exhaustion of the quiescent Type 1 cell pool that I observed in the current study; hypothetically speaking, whilst the activated Type 1 cell pool becomes depleted through differentiation-coupled

divisions, the quiescent Type 1 cell pool could become activated to support this downstream depletion, which is in turn supported by the resilient NSC pool. This latter subpopulation eventually also becomes depleted, which aligns with the reduction in the global Type 1 cell population by 26 weeks post-Zeb1 deletion. However, it must be noted that a very small subset of GFAP-expressing Type 1 cells that lacked ZEB1 expression was also still detectable at 26 weeks, and it is possible that this represents a subpopulation of resilient NSCs that are resistant to the effects of Zeb1 deletion on the NSC population, as they do not undergo differentiation-coupled divisions, resulting in their maintenance over time. Lastly, analogous to the previously mentioned disposable NSC model, this model proposes that the Type 1 cells eventually transform into astrocytes, and thus an increase in the astroglial population should occur with time; with Zeb1 deletion in the current study, I observed a decrease in astrocytes over time, suggesting that in this mode of NSC division and terminal transformation, under homeostatic conditions ZEB1 would function to promote this transformation process.

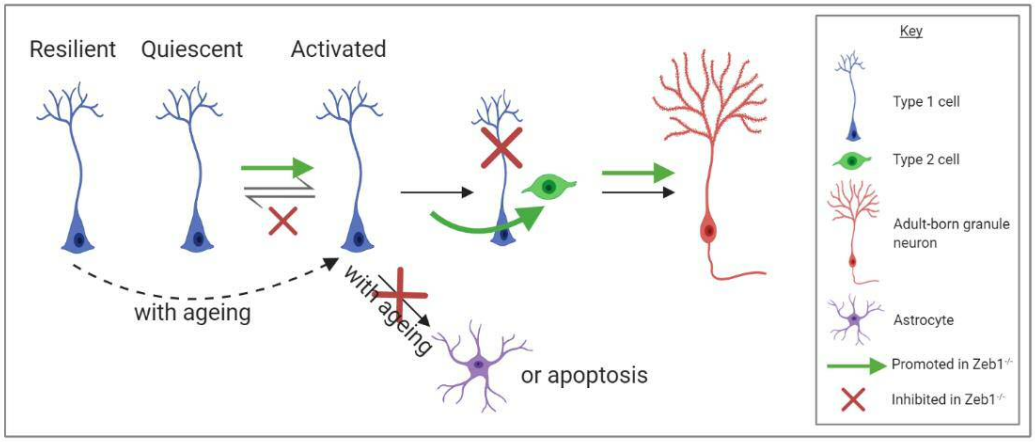

Figure 6.5. Model 4 suggests the existence of a "resilient" NSC pool that resides in a state of indefinite quiescence, and upholds the NSC pool in the ageing brain to prevent its depletion. Image created in Biorender.

5) A fifth paradigm has been suggested that proposes the existence of two types of NSCs that differ in their astroglial and neuronal lineage-commitment potential (Gebara *et al.* 2016; **Figure 6.6)**; this model is not wholly mutually-exclusive to the other described models.

This model is mostly compatible with all other models, as in each of the above described scenarios, it is possible that there are two separate neuronal and glial stem cells. The occurrence of this scenario in the adult hippocampus is plausible, as evidenced by the great heterogeneity of adult Type 1 cells (reviewed in Song et al. 2018), and studies have evidenced the existence of multiple Type 1 cells, distinguishable through different marker-dependent lineage tracing (Decarolis *et al.* 2013; Gebara *et al.* 2016). However, in the current study, it was found that whilst ZEB1 is present in GLAST-expressing Type 1 cells, its depletion exerts effect on downstream neuronal and glial production; this renders the reconciliation of the model and the current data somewhat difficult as for there to be two separate NSC pools, both would have to express ZEB1, and whilst Zeb1 deficiency would promote neurogenesis in one, it would repress astrogliogenesis in the other. However, there is a paucity of evidence to completely refute this model.

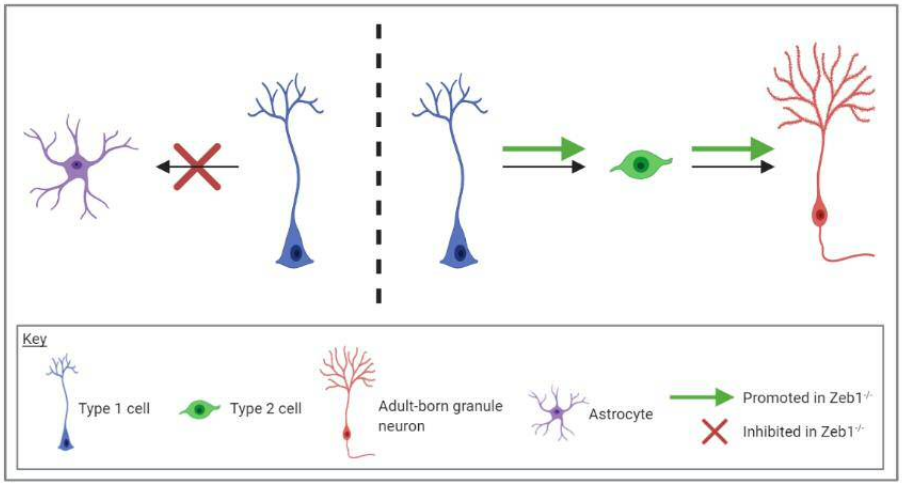

Figure 6.6. Model 5 advocates the co-existence of two populations of NSCs, responsible for the separate neuronal and astroglial lineages. Image created in Biorender.

6.3 Zeb1 deficiency results in a loss of hippocampal astrocytes

The detection of ZEB1 in astrocytes in the cortex and hippocampus in the current study largely corroborates findings from an earlier study that identified ZEB1 expression in mature astrocyte subpopulations in the adult spinal cord (Ohayon *et al.* 2016). Following the deletion of Zeb1, I observed a reduction of a horizontally-placed astrocyte population within the SGZ, that was identified as SGZ-associated

astroglia that may arise during astrogliogenesis stemming from Type 1 cells (Encinas *et al.* 2011). This was further supported by a significant decline in S100β–expressing astrocytes in all subcompartments of the DG.

This can be attributed to two possible scenarios: 1) ZEB1 functions to promote pro-astrocyte transcriptional regulators, and 2) ZEB1 expression is required for the survival of astrocytes in the dentate gyrus. Published studies support the former scenario, as factors such as NFIA and S100β have been shown to promote gliogenesis (Villarreal *et al.* 2014; Tchieu *et al.* 2019), and are also either expressed in astrocyte precursors alongside ZEB1 (NFIA; Ohayon *et al.* 2016), or have been identified as a target of ZEB1 in GBM (S100β; Rosmaninho *et al.* 2018). However, no definitive conclusions can be drawn regarding the mechanism by which Zeb1 deletion results in a decline in astrocytes in the dentate gyrus. Future work will aim to further investigate underlying mechanisms through IF staining for the expression of the aforementioned gliogenic factors, as well as investigation into the survival of the astrocytes following Zeb1 deletion.

6.4 ZEB1 does not regulate SOX2 expression in the adult SGZ

Recently, an important study highlighted the existence of an interdependent transcription factor regulatory loop formed by SOX2, ZEB1, and OLIG2 (oligodendrocyte transcription factor 2) that drive the progression of GBM tumours (Singh *et al.* 2017); the authors reported that Zeb1 is a target gene of SOX2, and coupled with the previously reported function of ZEB1 in the maintenance of SOX2 expression in GBM (Siebzehnrubl *et al.* 2013; Jimenez-Pascual *et al.* 2019), the findings proposed a positive feedback loop between the factors.

In the current study, I observed that the expression of SOX2 in the adult hippocampal neurogenic niche was unaltered up to 12 weeks post-Zeb1 deletion, following which there was a remarkable decrement in SOX2+ cells. As SOX2 is expressed in Type 1 cells, early Type 2a cells, and astrocytes, it is possible that this reflects the sudden reduction observed at 12 weeks with the loss of all aforementioned cell populations; however, this does not explain the comparable numbers of SOX2+ cells in the control and $Zeb1^{-/-}$ mice prior to this timepoint. The dichotomy between the lack of immediate changes in SOX2 following ZEB1 deletion

in the healthy brain, and the transcriptional feedback loop present in cancer suggests that ZEB1 does not regulate SOX2 expression in the adult hippocampus. It is possible that that this regulation is context-dependent and is triggered in a tumour setting. However, more experimental data are needed to fully substantiate whether there is an interaction between ZEB1 and SOX2 in the adult hippocampus.

6.5 ZEB1 is correlated with programmed cell death in adult-born neurons

In this study, I detected an aberrant surge in the number of newly generated hippocampal neuroblasts following Zeb1 deletion, which is partly due to a greater number of divisions of Type 1 cells, and is further augmented by the increased survival of neuronal progenies, which was also observed in this study. Whilst more research is needed to understand the mechanism of how ZEB1 affects programmed cell death in adult neurogenesis, NeuroD1 is an attractive candidate as it a downstream target of ZEB1 in the developing brain (Wang *et al.* 2019), and capable of upregulating neuronal differentiation and survival (Gao *et al.* 2009). Thus, NeuroD1 expression and function in the model presented in this study will be evaluated in the future.

A number of non-cell autonomous factors may also contribute to the increased survival of immature neurons following the loss of Zeb1. The surrounding microenvironment of immature neuroblasts in the hippocampus is highly complex, with a plethora of intrinsic and extrinsic cues governing the survival and maturation of these cells. A possible contribution to this process by niche astrocytes and microglia, as well as their crosstalk, may also be proposed as a mechanism through programmed cell death. Niche astrocytes directly mediate neuronal cell death through the expression of phagocytic receptors (Chung *et al.* 2013), and furthermore, the activation of TGFβ signalling by astrocytes has been demonstrated to recruit microglia for the phagocytosis of weak synapses (Bialas and Stevens 2013). As ZEB1 deletion resulted in the elimination of hippocampal astrocytes, the model used in this study sets a foundation for future studies involving the investigation of the role of glial cells in the regulation of programmed cell death by ZEB1.

6.6 Zeb1 deletion may not affect cognitive function of young adult mice

The precocious differentiation of Type 1 cells into adult-born neurons in the Zeb1-deficient mice prompted my investigation into any possible effects on hippocampal-based cognitive function. I probed this by carrying out memory-dependent behavioural tasks at 3 months post-ablation of Zeb1 (at which time mice were 4 months old). The performance of the $Zeb1^{-/-}$ mice was comparable to the control group with wild-type ZEB1 expression, which suggests that at a young age, the adult-born neurons become successfully incorporated into the pre-existing hippocampal synaptic circuits, or at least do not affect the function of memory in these mice. Moreover, at 26 weeks following the deletion of Zeb1, the number of granule cells was comparable to controls, which further indicates a normal development and survival of adult-born neurons in the $Zeb1^{-/-}$ mice. Based on this as well as the time-dependent depletion of Type 1 cells in the $Zeb1^{-/-}$ mice, further research should be carried out to determine whether the deletion of Zeb1 and the consequent loss of neurogenesis over time results in hippocampal-based cognitive impairments at later stages in the lifespan of the mice.

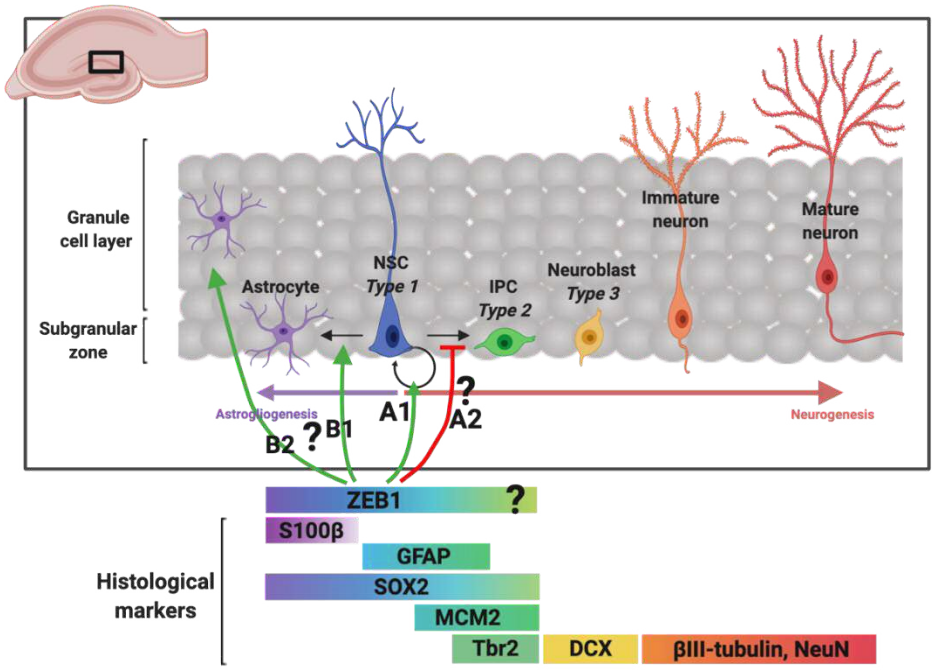

Figure 6.7. Model for proposed functions of ZEB1 in the adult hippocampal neurogenic niche – (A1) Adult hippocampal Type 1 cells express ZEB1 that mediates their self-renewal, and the deletion of Zeb1 results in the loss of self-renewal capacity, resulting in their depletion. (A2) ZEB1 inhibits the neuronal-lineage commitment division of Type 1 cells, although it is unclear whether this occurs due to an active inhibition of pro-neuronal transcriptional regulators, or as a by-product of the promotion of self-renewing divisions of Type 1 cells. (B1) During astrogliogenesis, ZEB1 may either promote *de novo* Type 1 cell-astrogliogenesis, or it may enhance the age-related transformation of Type 1 cells into astrocytes (Encinas et al., 2011). (B2) ZEB1 may also promote the survival of astrocytes residing in the dentate gyrus. Image created in Biorender.

6.7 Final comments

Hippocampal adult neurogenesis is reminiscent of events that occur in embryonic neurodevelopment, based on the sequence of events that result in the generation as well as in the establishment of functional connectivity of the granule neurons (Espósito *et al.* 2005).

The data generated in this study indicate a pro-stemness function of ZEB1 in the postnatal hippocampus. ZEB1 plays a similar function in the embryonic development of the cerebral cortex and the cerebellum, where it maintains precursor cells in an undifferentiated state and is subsequently downregulated during the migration of lineage-committed progenies (Singh *et al.* 2016; Liu *et al.* 2019; Wang *et al.* 2019). Loss of Zeb1 in the embryonic CNS results in the precocious differentiation of RG cells into neurons, both in the cortex and the cerebellum (Singh

et al. 2016; Wang *et al.* 2019). In the present study, the ablation of Zeb1 in hippocampal NSCs resulted in their premature differentiation, which in turn led to the depletion of the NSC pool; thus, these observations mirror the findings from neurogenesis in the developing CNS. This suggests that the function of distinct EMT-TFs in neurodevelopment is potentially recapitulated in the adult brain.

This study has laid the foundations for future research in elucidating the pro-stemness function of ZEB1-mediated transcriptional regulation that determines whether an adult NSC will self-renew or become lineage-committed. Moreover, the correlation of ZEB1 deficiency to impaired programmed cell death, through which early neuronal progenitors and immature neurons are eliminated during neurogenesis, indicates that this transcription factor has an important role in the correct development of neurons, as well as the regulation of the progenitor pool size in the dentate gyrus. Taken together, these findings hold important implications in the ageing process of the mammalian brain, in which the maintenance of a stem cell pool is essential for ongoing neurogenesis and its contribution to cognitive function.

References

Ables, J.L., DeCarolis, N.A., Johnson, M.A., Rivera, P.D., Gao, Z., Cooper, D.C., … Eisch, A.J. (2010). Notch1 is required for maintenance of the reservoir of adult hippocampal stem cells. *Journal of Neuroscience* **30**(31):10484–92.

Adlard, P.A., Perreau, V.M., Engesser-Cesar, C. and Cotman, C.W. (2004). The timecourse of induction of brain-derived neurotrophic factor mRNA and protein in the rat hippocampus following voluntary exercise. *Neuroscience Letters* **363**(1):43–8.

Aimone, J.B., Wiles, J. and Gage, F.H. (2006). Potential role for adult neurogenesis in the encoding of time in new memories. *Nature Neuroscience* **9**(6):723–7.

Akkerman, S., Prickaerts, J., Steinbusch, H.W.M. and Blokland, A. (2012). Object recognition testing: Statistical considerations. *Behavioural Brain Research* **232**(2):317–33.

Altman, J. and Das, G.D. (1965). Autoradiographic and histological evidence of postnatal hippocampal neurogenesis in rats. *Journal of Comparative Neurology* **124**(3):319–35.

Andersen, J., Urbán, N., Achimastou, A., Ito, A., Simic, M., Ullom, K., … Guillemot, F. (2014). A Transcriptional Mechanism Integrating Inputs from Extracellular Signals to Activate Hippocampal Stem Cells. *Neuron* **83**(5):1085–1097.

Antunes, M. and Biala, G. (2012). The novel object recognition memory: Neurobiology, test procedure, and its modifications. *Cognitive Processing* **13**(2):93–110.

Bai, F., Bergeron, M. and Nelson, D.L. (2003). Chronic AMPA receptor potentiator (LY451646) treatment increases cell proliferation in adult rat hippocampus. *Neuropharmacology* **44**(8):1013–21.

Barres, B.A. (2008). The Mystery and Magic of Glia: A Perspective on Their Roles in Health and Disease. *Neuron* **60**(3):430–440.

Basu, J. and Siegelbaum, S.A. (2015). The corticohippocampal circuit, synaptic plasticity, and memory. *Cold Spring Harbor Perspectives in Biology* **7**(11).

Bayer, S.A. (1985). Neuron Production in the Hippocampus and Olfactory Bulb of the Adult Rat Brain: Addition or Replacement? *Annals of the New York Academy of Sciences* **457**(1):163–172.

Beclin, C., Follert, P., Stappers, E., Barral, S., Nathalie, C., De Chevigny, A., … Cremer, H. (2016). MiR-200 family controls late steps of postnatal forebrain neurogenesis via Zeb2 inhibition. *Scientific Reports*.

Bédard, A. and Parent, A. (2004). Evidence of newly generated neurons in the human olfactory bulb. *Developmental Brain Research* **151**(1–2):159–68.

Bekiari, Chryssa, Giannakopoulou, A., Siskos, N., Grivas, I., Tsingotjidou, A., Michaloudi, H. and Papadopoulos, G.C. (2015). Neurogenesis in the septal and temporal part of the adult rat dentate gyrus. *Hippocampus* **25**(4):511–23.

Bekiari, C, Grivas, I., Giannakopoulou, A., Michaloudi-Pavlou, H., Kostopoulos, G. and Papadopoulos, G.C. (2015). *Dentate Gyrus Variation along Its Septo-Temporal*

Axis: Structure and Function in Health and Disease. Lowes, Z. (ed.). USA: Nova Science Publishers, Inc.

Berg, D.A., Su, Y., Jimenez-Cyrus, D., Patel, A., Huang, N., Morizet, D., … Bond, A.M. (2019). A Common Embryonic Origin of Stem Cells Drives Developmental and Adult Neurogenesis. *Cell* **177**(3):654–668.

Berg, D.A., Yoon, K.J., Will, B., Xiao, A.Y., Kim, N.S., Christian, K.M., … Ming, G. li (2015). Tbr2-expressing intermediate progenitor cells in the adult mouse hippocampus are unipotent neuronal precursors with limited amplification capacity under homeostasis. *Frontiers in Biology* **10**(3):262–271.

Bertollini, L., Ciotti, M.T., Cherubini, E. and Cattaneo, A. (1997). Neurotrophin-3 promotes the survival of oligodendrocyte precursors in embryonic hippocampal cultures under chemically defined conditions. *Brain Research* **746**(1–2):19–24.

Bialas, A.R. and Stevens, B. (2013). TGF-β signaling regulates neuronal C1q expression and developmental synaptic refinement. *Nature Neuroscience* **16**(12):1773–82.

Biebl, M., Winner, B. and Winkler, J. (2005). Caspase inhibition decreases cell death in regions of adult neurogenesis. *NeuroReport* **16**(11):1147–50.

Blaser, R. and Heyser, C. (2015). Spontaneous object recognition: A promising approach to the comparative study of memory. *Frontiers in Behavioral Neuroscience* **9**.

Boldrini, M., Fulmore, C.A., Tartt, A.N., Simeon, L.R., Pavlova, I., Poposka, V., … Mann, J.J. (2018). Human Hippocampal Neurogenesis Persists throughout Aging. *Cell Stem Cell* **22**(4):589–99.

Bonaguidi, M.A., Wheeler, M.A., Shapiro, J.S., Stadel, R.P., Sun, G.J., Ming, G.L. and Song, H. (2011). In vivo clonal analysis reveals self-renewing and multipotent adult neural stem cell characteristics. *Cell* **145**(7):1142–1155.

Bonzano, S., Crisci, I., Podlesny-Drabiniok, A., Rolando, C., Krezel, W., Studer, M. and De Marchis, S. (2018). Neuron-Astroglia Cell Fate Decision in the Adult Mouse Hippocampal Neurogenic Niche Is Cell-Intrinsically Controlled by COUP-TFI In Vivo. *Cell Reports* **24**(2):329–41.

Brabletz, S., Bajdak, K., Meidhof, S., Burk, U., Niedermann, G., Firat, E., … Brabletz, T. (2011). The ZEB1/miR-200 feedback loop controls Notch signalling in cancer cells. *EMBO Journal* **30**(4):770–82.

Brabletz, S., Lasierra Losada, M., Schmalhofer, O., Mitschke, J., Krebs, A., Brabletz, T. and Stemmler, M.P. (2017). Generation and characterization of mice for conditional inactivation of Zeb1. *Genesis* **55**(4).

Bracken, C.P., Gregory, P.A., Kolesnikoff, N., Bert, A.G., Wang, J., Shannon, M.F. and Goodall, G.J. (2008). A double-negative feedback loop between ZEB1-SIP1 and the microRNA-200 family regulates epithelial-mesenchymal transition. *Cancer Research* **68**(19):7846–54.

Broadbent, N.J., Gaskin, S., Squire, L.R. and Clark, R.E. (2010). Object recognition memory and the rodent hippocampus. *Learning and Memory* **17**(1):5–11.

Brown, J.P., Couillard-Després, S., Cooper-Kuhn, C.M., Winkler, J., Aigner, L. and Kuhn, H.G. (2003). Transient Expression of Doublecortin during Adult Neurogenesis. *Journal of Comparative Neurology* **467**(1):1–10.

Brown, R.E. and Wong, A.A. (2007). The influence of visual ability on learning and memory performance in 13 strains of mice. *Learning and Memory* **14**(3):134–44.

Buffo, A., Rite, I., Tripathi, P., Lepier, A., Colak, D., Horn, A.-P., … Gotz, M. (2008). Origin and progeny of reactive gliosis: A source of multipotent cells in the injured brain. *Proceedings of the National Academy of Sciences* **105**(9):3581–3586.

Bui, T., Sequeira, J., Chun Wen, T., Sola, A., Higashi, Y., Kondoh, H. and Genetta, T. (2009). ZEB1 links p63 and p73 in a novel neuronal survival pathway rapidly induced in response to cortical ischemia. *PLoS ONE* **4**(2).

Calzolari, F., Michel, J., Baumgart, E.V., Theis, F., Götz, M. and Ninkovic, J. (2015). Fast clonal expansion and limited neural stem cell self-renewal in the adult subependymal zone. *Nature Neuroscience* **18**(4):490–2.

Cao, X., Li, L.P., Qin, X.H., Li, S.J., Zhang, M., Wang, Q., … Zhu, X.H. (2013). Astrocytic adenosine 5'-triphosphate release regulates the proliferation of neural stem cells in the adult hippocampus. *Stem Cells* **31**(8):1633–43.

Caramel, J., Ligier, M. and Puisieux, A. (2018). Pleiotropic roles for ZEB1 in cancer. *Cancer Research* **78**(1):30–35.

Cassandri, M., Smirnov, A., Novelli, F., Pitolli, C., Agostini, M., Malewicz, M., … Raschellà, G. (2017). Zinc-finger proteins in health and disease. *Cell Death Discovery* **3**.

Cassé, F., Richetin, K. and Toni, N. (2018). Astrocytes' contribution to adult neurogenesis in physiology and Alzheimer's disease. *Frontiers in Cellular Neuroscience* **12**.

Chen, C., Lee, G.A., Pourmorady, A., Sock, E. and Donoghue, M.J. (2015). Orchestration of neuronal differentiation and progenitor pool expansion in the developing cortex by SoxC genes. *Journal of Neuroscience* **35**(29):10629–42.

Chen, Y., Ai, Y., Slevin, J.R., Maley, B.E. and Gash, D.M. (2005). Progenitor proliferation in the adult hippocampus and substantia nigra induced by glial cell line-derived neurotrophic factor. *Experimental Neurology* **196**(1):87–95.

Cheng, M.F. (2013). Hypothalamic neurogenesis in the adult brain. *Frontiers in Neuroendocrinology* **34**(3):167–178.

Chung, W.S., Allen, N.J. and Eroglu, C. (2015). Astrocytes control synapse formation, function, and elimination. *Cold Spring Harbor Perspectives in Biology* **7**(9).

Chung, W.S., Clarke, L.E., Wang, G.X., Stafford, B.K., Sher, A., Chakraborty, C., … Barres, B.A. (2013). Astrocytes mediate synapse elimination through MEGF10 and MERTK pathways. *Nature* **504**(7480):394–400.

Clark, P.J., Kohman, R.A., Miller, D.S., Bhattacharya, T.K., Brzezinska, W.J. and Rhodes, J.S. (2011). Genetic influences on exercise-induced adult hippocampal neurogenesis across 12 divergent mouse strains. *Genes, Brain and Behavior* **10**(3):345–53.

Codega, P., Silva-Vargas, V., Paul, A., Maldonado-Soto, A.R., DeLeo, A.M., Pastrana, E. and Doetsch, F. (2014). Prospective Identification and Purification of Quiescent Adult Neural Stem Cells from Their In Vivo Niche. *Neuron* **82**(3):545–59.

Cohen, S.J. and Stackman, R.W. (2015). Assessing rodent hippocampal involvement in the novel object recognition task. A review. *Behavioural Brain Research* **285**:105–17.

Cooper-Kuhn, C.M., Winkler, J. and Kuhn, H.G. (2004). Decreased neurogenesis after cholinergic forebrain lesion in the adult rat. *Journal of Neuroscience Research* **77**(2):155–65.

Costa, M.R., Ortega, F., Brill, M.S., Beckervordersandforth, R., Petrone, C., Schroeder, T., … Berninger, B. (2011). Continuous live imaging of adult neural stem cell division and lineage progression in vitro. *Development* **1051**:1–11.

Curtis, M.A., Kam, M., Nannmark, U., Anderson, M.F., Axell, M.Z., Wikkelso, C., … Eriksson, P.S. (2007). Human neuroblasts migrate to the olfactory bulb via a lateral ventricular extension. *Science* **315**(5816):1243–9.

D'Amico, L.A., Boujard, D. and Coumailleau, P. (2013). The Neurogenic Factor NeuroD1 Is Expressed in Post-Mitotic Cells during Juvenile and Adult Xenopus Neurogenesis and Not in Progenitor or Radial Glial Cells. *PLoS ONE* **8**(6).

Dayer, A.G., Ford, A.A., Cleaver, K.M., Yassaee, M. and Cameron, H.A. (2003). Short-term and long-term survival of new neurons in the rat dentate gyrus. *Journal of Comparative Neurology* **460**(4):563–72.

Decarolis, N.A., Mechanic, M., Petrik, D., Carlton, A., Ables, J.L., Malhotra, S., … Eisch, A.J. (2013). In vivo contribution of nestin- and GLAST-lineage cells to adult hippocampal neurogenesis. *Hippocampus* **23**(8):708–719.

Deleyrolle, L.P. and Reynolds, B.A. (2009). Isolation, expansion, and differentiation of adult Mammalian neural stem and progenitor cells using the neurosphere assay. *Methods Mol Biol* **549**:91–101.

Denecker, G., Vandamme, N., Akay, Ö., Koludrovic, D., Taminau, J., Lemeire, K., … Berx, G. (2014). Identification of a ZEB2-MITF-ZEB1 transcriptional network that controls melanogenesis and melanoma progression. *Cell Death and Differentiation* **21**(8):1250–61.

Deng, W., Aimone, J.B. and Gage, F.H. (2010). New neurons and new memories: How does adult hippocampal neurogenesis affect learning and memory? *Nature Reviews Neuroscience* **11**(5):339–50.

Deng, Y., Zhu, G., Luo, H. and Zhao, S. (2016). MicroRNA-203 as a stemness inhibitor of glioblastoma stem cells. *Molecules and Cells* **39**(8):619–24.

Doetsch, F., Caillé, I., Lim, D.A., García-Verdugo, J.M. and Alvarez-Buylla, A. (1999). Subventricular Zone Astrocytes Are Neural Stem Cells in the Adult Mammalian Brain. *Cell* **97**(6):703–716.

Doetsch, F., García-Verdugo, J.M. and Alvarez-Buylla, A. (1997). Cellular composition and three-dimensional organization of the subventricular germinal zone in the adult mammalian brain. *Journal of Neuroscience* **17**(13):5046–61.

Dohadwala, M., Yang, S.C., Luo, J., Sharma, S., Batra, R.K., Huang, M., … Dubinett, S.M. (2006). Cyclooxygenase-2-dependent regulation of E-cadherin: Prostaglandin E2induces transcriptional repressors ZEB1 and snail in non-small cell lung cancer. *Cancer Research* **66**(10):5338–5345.

Drapeau, E. and Abrous, D.N. (2008). Stem Cell Review Series: Role of neurogenesis in age-related memory disorders. *Aging Cell* **7**(4):569–89.

Duband, J.L. (2010). Diversity in the molecular and cellular strategies of epithelium-to- mesenchyme transitions: Insights from the neural crest. *Cell Adhesion and Migration* **4**(3):458–82.

Duman, R.S. and Monteggia, L.M. (2006). A Neurotrophic Model for Stress-Related Mood Disorders. *Biological Psychiatry* **59**(12):1116–27.

Ehm, O., Göritz, C., Covic, M., Schäffner, I., Schwarz, T.J., Karaca, E., … Lie, D.C. (2010). RBPJκ-dependent signaling is essential for long-term maintenance of neural stem cells in the adult hippocampus. *Journal of Neuroscience* **30**(41):13794–807.

Eisinger, B.E. and Zhao, X. (2018). Identifying molecular mediators of environmentally enhanced neurogenesis. *Cell and Tissue Research* **371**(1):7–21.

Encinas, J.M., Michurina, T. V., Peunova, N., Park, J.H., Tordo, J., Peterson, D.A., … Enikolopov, G. (2011). Division-coupled astrocytic differentiation and age-related depletion of neural stem cells in the adult hippocampus. *Cell Stem Cell* **8**(5):566–79.

Encinas, J.M., Vaahtokari, A. and Enikolopov, G. (2006). Fluoxetine targets early progenitor cells in the adult brain. *Proceedings of the National Academy of Sciences of the United States of America* **103**(21):8233–8.

Ennaceur, A. and Delacour, J. (1988). A new one-trial test for neurobiological studies of memory in rats. 1: Behavioral data. *Behavioural Brain Research* **31**(1):47–59.

Ennaceur, A., Neave, N. and Aggleton, J.P. (1997). Spontaneous object recognition and object location memory in rats: The effects of lesions in the cingulate cortices, the medial prefrontal cortex, the cingulum bundle and the fornix. *Experimental Brain Research* **113**(3):509–19.

Eriksson, P.S., Perfilieva, E., Björk-Eriksson, T., Alborn, A.M., Nordborg, C., Peterson, D.A. and Gage, F.H. (1998). Neurogenesis in the adult human hippocampus. *Nature Medicine* **4**(11):1313–7.

Espósito, M.S., Piatti, V.C., Laplagne, D.A., Morgenstern, N.A., Ferrari, C.C., Pitossi, F.J. and Schinder, A.F. (2005). Neuronal differentiation in the adult hippocampus recapitulates embryonic development. *Journal of Neuroscience* **25**(44):10074–86.

Euskirchen, P., Radke, J., Schmidt, M.S., Heuling, E.S., Kadikowski, E., Maricos, M., … Harms, C. (2017). Cellular heterogeneity contributes to subtype-specific expression of ZEB1 in human glioblastoma. *PLoS ONE* **12**(9).

Fabel, K., Wolf, S.A., Ehninger, D., Babu, H., Leal-Galicia, P. and Kempermann, G. (2009). Additive effects of physical exercise and environmental enrichment on adult hippocampal neurogenesis in mice. *Frontiers in Neuroscience* **3**.

Fardi, M., Alivand, M., Baradaran, B., Farshdousti Hagh, M. and Solali, S. (2019). The crucial role of ZEB2: From development to epithelial-to-mesenchymal transition and cancer complexity. *Journal of Cellular Physiology* **234**(9).

Favaro, R., Valotta, M., Ferri, A.L.M., Latorre, E., Mariani, J., Giachino, C., … Nicolis, S.K. (2009). Hippocampal development and neural stem cell maintenance require Sox2-dependent regulation of Shh. *Nature Neuroscience* **12**(10):1248–56.

Feliciano, D.M., Bordey, A. and Bonfanti, L. (2015). Noncanonical sites of adult neurogenesis in the mammalian brain. *Cold Spring Harbor Perspectives in Biology* **7**(10).

Filippov, V., Kronenberg, G., Pivneva, T., Reuter, K., Steiner, B., Wang, L.P., … Kempermann, G. (2003). Subpopulation of nestin-expressing progenitor cells in the adult murine hippocampus shows electrophysiological and morphological characteristics of astrocytes. *Molecular and Cellular Neuroscience* **23**(3):373–82.

Foltran, R.B. and Diaz, S.L. (2016). BDNF isoforms: a round trip ticket between neurogenesis and serotonin? *Journal of Neurochemistry* **138**(2):204–21.

Fortini, M.E., Lai, Z. and Rubin, G.M. (1991). The Drosophila zfh-1 and zfh-2 genes encode novel proteins containing both zinc-finger and homeodomain motifs. *Mechanisms of Development* **34**(2–3):113–122.

Freund, J., Brandmaier, A.M., Lewejohann, L., Kirste, I., Kritzler, M., Krüger, A., … Kempermann, G. (2013). Emergence of individuality in genetically identical mice. *Science* **340**(6133):756–9.

Fuentealba, L.C., Rompani, S.B., Parraguez, J.I., Obernier, K., Romero, R., Cepko, C.L. and Alvarez-Buylla, A. (2015). Embryonic Origin of Postnatal Neural Stem Cells. *Cell* **161**(7):1644–55.

Gage, F.H.H., Coates, P.W.W., Palmer, T.D.D., Kuhn, H.G.G., Fisher, L.J.J., Suhonen, J.O.O., … Ray, J. (1995). Survival and differentiation of adult neuronal progenitor cells transplanted to the adult brain. *Proceedings of the National Academy of Sciences of the United States of America* **92**(25):11879–83.

Gao, Z., Ure, K., Ables, J.L., Lagace, D.C., Nave, K.A., Goebbels, S., … Hsieh, J. (2009). Neurod1 is essential for the survival and maturation of adult-born neurons. *Nature Neuroscience* **12**(9):1090–2.

Gao, Z., Ure, K., Ding, P., Nashaat, M., Yuan, L., Ma, J., … Hsieh, J. (2011). The master negative regulator REST/NRSF controls adult neurogenesis by restraining the neurogenic program in quiescent stem cells. *Journal of Neuroscience* **31**(26):9772–86.

Garcia, A.D.R., Doan, N.B., Imura, T., Bush, T.G. and Sofroniew, M. V. (2004). GFAP-expressing progenitors are the principal source of constitutive neurogenesis in adult mouse forebrain. *Nature Neuroscience* **7**(11):1233–41.

Garthe, A., Roeder, I. and Kempermann, G. (2016). Mice in an enriched environment learn more flexibly because of adult hippocampal neurogenesis. *Hippocampus* **26**(2):261–71.

Gebara, E., Bonaguidi, M.A., Beckervordersandforth, R., Sultan, S., Udry, F., Gijs, P.J., … Toni, N. (2016). Heterogeneity of Radial Glia-Like Cells in the Adult

Hippocampus. *Stem Cells* **34**(4):997–1010.

Geschwind, D.H., Yu, T.W., Leibowitz, R.T., Parent, J.M., Sloviter, R.S. and Lowenstein, D.H. (2018). Dentate Granule Cell Neurogenesis Is Increased by Seizures and Contributes to Aberrant Network Reorganization in the Adult Rat Hippocampus. *The Journal of Neuroscience* **17**(10):3727–38.

Ghashghaei, H.T., Weimer, J.M., Schmid, R.S., Yokota, Y., McCarthy, K.D., Popko, B. and Anton, E.S. (2007). Reinduction of ErbB2 in astrocytes promotes radial glial progenitor identity in adult cerebral cortex. *Genes and Development* **21**(24):3258–71.

Gierut, J.J., Jacks, T.E. and Haigis, K.M. (2014). Strategies to achieve conditional gene mutation in mice. *Cold Spring Harbor Protocols* **2014**(4):339–349.

Gloushankova, N.A., Rubtsova, S.N. and Zhitnyak, I.Y. (2017). Cadherin-mediated cell-cell interactions in normal and cancer cells. *Tissue Barriers* **5**(3).

Goldman, S.A. and Nottebohm, F. (1983). Neuronal production, migration, and differentiation in a vocal control nucleus of the adult female canary brain. *Proceedings of the National Academy of Sciences of the United States of America* **80**(8):2390–4.

Gómez-López, S., Lerner, R.G. and Petritsch, C. (2014). Asymmetric cell division of stem and progenitor cells during homeostasis and cancer. *Cellular and Molecular Life Sciences* **71**(4):575–97.

Gómez-Pinilla, F., Dao, L. and So, V. (1997). Physical exercise induces FGF-2 and its mRNA in the hippocampus. *Brain Research* **764**(1–2):1–8.

Gonçalves, J.T., Schafer, S.T. and Gage, F.H. (2016). Adult Neurogenesis in the Hippocampus: From Stem Cells to Behavior. *Cell* **167**(4):897–914.

Gonzalez-Perez, O. (2012). Neural stem cells in the adult human brain. *Biological and biomedical reports* **2**(1):59–69.

Goossens, S., Vandamme, N., Van Vlierberghe, P. and Berx, G. (2017). EMT transcription factors in cancer development re-evaluated: Beyond EMT and MET. *Biochimica et Biophysica Acta - Reviews on Cancer* **1868**(2):584–91.

Gotts, J.E. and Chesselet, M.F. (2005). Vascular changes in the subventricular zone after distal cortical lesions. *Experimental Neurology* **194**(1):139–50.

Götz, M., Stoykova, A. and Gruss, P. (1998). Pax6 controls radial glia differentiation in the cerebral cortex. *Neuron* **21**(5):1031–44.

Gould, E., Cameron, H.A. and McEwen, B.S. (1994). Blockade of NMDA receptors increases cell death and birth in the developing rat dentate gyrus. *Journal of Comparative Neurology* **340**(4):551–65.

Gould, E. and Tanapat, P. (1997). Lesion-induced proliferation of neuronal progenitors in the dentate gyrus of the adult rat. *Neuroscience* **80**(2):427–36.

Gregory, P.A., Bert, A.G., Paterson, E.L., Barry, S.C., Tsykin, A., Farshid, G., … Goodall, G.J. (2008). The miR-200 family and miR-205 regulate epithelial to mesenchymal transition by targeting ZEB1 and SIP1. *Nature Cell Biology* **10**(5):593–601.

Gu, Y., Arruda-Carvalho, M., Wang, J., Janoschka, S.R., Josselyn, S.A., Frankland, P.W. and Ge, S. (2012). Optical controlling reveals time-dependent roles for adult-born dentate granule cells. *Nature Neuroscience* **15**(12):1700–6.

Gualtieri, F., Brégère, C., Laws, G.C., Armstrong, E.A., Wylie, N.J., Moxham, T.T., … Smulders, T. V. (2017). Effects of environmental enrichment on doublecortin and BDNF expression along the dorso-ventral axis of the dentate gyrus. *Frontiers in Neuroscience* **11**.

Gulinello, M., Mitchell, H.A., Chang, Q., Timothy O'Brien, W., Zhou, Z., Abel, T., … Crawley, J.N. (2018). Rigor and reproducibility in rodent behavioral research. *Neurobiology of Learning and Memory* **165**.

Haam, J. and Yakel, J.L. (2017). Cholinergic modulation of the hippocampal region and memory function. *Journal of Neurochemistry* **142**(2):111–21.

Hammond, R.S., Tull, L.E. and Stackman, R.W. (2004). On the delay-dependent involvement of the hippocampus in object recognition memory. *Neurobiology of Learning and Memory* **82**(1):26–34.

Haslinger, A., Schwarz, T.J., Covic, M. and Chichung Lie, D. (2009). Expression of Sox11 in adult neurogenic niches suggests a stage-specific role in adult neurogenesis. *European Journal of Neuroscience* **29**(11):2103–14.

Higashi, Y., Moribe, H., Takagi, T., Sekido, R., Kawakami, K., Kikutani, H. and Kondoh, H. (1997). Impairment of T cell development in δEF1 mutant mice. *Journal of Experimental Medicine* **185**(8):1467–79.

Hochgerner, H., Zeisel, A., Lönnerberg, P. and Linnarsson, S. (2018). Conserved properties of dentate gyrus neurogenesis across postnatal development revealed by single-cell RNA sequencing. *Nature Neuroscience* **21**(2):290–99.

Hodge, R.D., Nelson, B.R., Kahoud, R.J., Yang, R., Mussar, K.E., Reiner, S.L. and Hevner, R.F. (2012). Tbr2 Is Essential for Hippocampal Lineage Progression from Neural Stem Cells to Intermediate Progenitors and Neurons. *Journal of Neuroscience* **32**(18):6275–87.

Ter Horst, J.P., De Kloet, E.R., Schächinger, H. and Oitzl, M.S. (2012). Relevance of stress and female sex hormones for emotion and cognition. *Cellular and Molecular Neurobiology* **32**(5):725–35.

Hsu, Y.C. (2015). Theory and practice of lineage tracing. *Stem Cells* **33**(11):3197–204.

Huang, Y.Q., Wu, C., He, X.F., Wu, D., He, X., Liang, F.Y., … Lan, Y. (2018). Effects of voluntary wheel-running types on hippocampal neurogenesis and spatial cognition in middle-aged mice. *Frontiers in Cellular Neuroscience* **12**.

Ickes, B.R., Pham, T.M., Sanders, L.A., Albeck, D.S., Mohammed, A.H. and Granholm, A.C. (2000). Long-term environmental enrichment leads to regional increases in neurotrophin levels in rat brain. *Experimental Neurology* **164**(2):45–52.

Imayoshi, I., Isomura, A., Harima, Y., Kawaguchi, K., Kori, H., Miyachi, H., … Kageyama, R. (2013). Oscillatory control of factors determining multipotency and fate in mouse neural progenitors. *Science* **342**(6163):1203–8.

Imayoshi, I., Sakamoto, M., Yamaguchi, M., Mori, K. and Kageyama, R. (2010). Essential roles of Notch signaling in maintenance of neural stem cells in developing and adult brains. *Journal of Neuroscience* **30**(9):3489–98.

Islam, M.M., Smith, D.K., Niu, W., Fang, S., Iqbal, N., Sun, G., … Zhang, C.L. (2015). Enhancer analysis unveils genetic interactions between TLX and SOX2 in neural stem cells and in vivo reprogramming. *Stem Cell Reports* **5**(5):805–815.

Iwano, T., Masuda, A., Kiyonari, H., Enomoto, H. and Matsuzaki, F. (2012). Prox1 postmitotically defines dentate gyrus cells by specifying granule cell identity over CA3 pyramidal cell fate in the hippocampus. *Development (Cambridge)* **139**(16):3051–62.

Jahn, H.M., Kasakow, C. V., Helfer, A., Michely, J., Verkhratsky, A., Maurer, H.H., … Kirchhoff, F. (2018). Refined protocols of tamoxifen injection for inducible DNA recombination in mouse astroglia. *Scientific Reports* **8**(1).

Jessberger, S. and Kempermann, G. (2003). Adult-born hippocampal neurons mature into activity-dependent responsiveness. *European Journal of Neuroscience* **18**(10):2707–12.

Jessberger, S., Nakashima, K., Clemenson, G.D., Mejia, E., Mathews, E., Ure, K., … Hsieh, J. (2007). Epigenetic modulation of seizure-induced neurogenesis and cognitive decline. *Journal of Neuroscience* **27**(22):5967–75.

Jiang, Y., Yan, L., Xia, L., Lu, X., Zhu, W., Ding, D., … Hu, B. (2018). Zinc finger E-box– binding homeobox 1 (ZEB1) is required for neural differentiation of human embryonic stem cells. *Journal of Biological Chemistry* **293**(50):19317–10329.

Jimenez-Pascual, A., Hale, J.S., Kordowski, A., Pugh, J., Silver, D.J., Bayik, D., … Siebzehnrubl, F.A. (2019). ADAMDEC1 maintains a growth factor signaling loop in cancer stem cells. *Cancer Discovery* **9**(11):1574–1589.

Jin, K., Sun, Y., Xie, L., Batteur, S., Mao, X.O., Smelick, C., … Greenberg, D.A. (2003). Neurogenesis and aging: FGF-2 and HB-EGF restore neurogenesis in hippocampus and subventricular zone of aged mice. *Aging cell* **2**(3):175–83.

Jin, K., Zhu, Y., Sun, Y., Mao, X.O., Xie, L. and Greenberg, D.A. (2002). Vascular endothelial growth factor (VEGF) stimulates neurogenesis in vitro and in vivo. *Proceedings of the National Academy of Sciences of the United States of America* **99**(18):11946–50.

Jungblut, M., Tiveron, M.C., Barral, S., Abrahamsen, B., Knöbel, S., Pennartz, S., … Bosio, A. (2012). Isolation and characterization of living primary astroglial cells using the new GLAST-specific monoclonal antibody ACSA-1. *GLIA* **60**(6):894–907.

Kabbaj, M. (2008). Individual Differences in Vulnerability to Drug Abuse: The High Responders/Low Responders Model. *CNS & Neurological Disorders - Drug Targets* **5**(5):513–20.

Kang, W. and Hébert, J.M. (2015). FGF signaling is necessary for neurogenesis in young mice and sufficient to reverse its decline in old mice. *Journal of Neuroscience* **35**(28):10217–23.

Kee, N., Teixeira, C.M., Wang, A.H. and Frankland, P.W. (2007). Preferential incorporation of adult-generated granule cells into spatial memory networks in the

dentate gyrus. *Nature Neuroscience* **10**(3):355–62.

Kempermann, G. (2002). Why new neurons? Possible functions for adult hippocampal neurogenesis. *Journal of Neuroscience* **22**(3):635–8.

Kempermann, G., Gast, D., Kronenberg, G., Yamaguchi, M. and Gage, F.H. (2003). Early determination and long-term persistence of adult-generated new neurons in the hippocampus of mice. *Development* **130**(2):391–9.

Kempermann, G., Jessberger, S., Steiner, B. and Kronenberg, G. (2004). Milestones of neuronal development in the adult hippocampus. *Trends in Neurosciences* **27**(8):447–52.

Kempermann, G., Kuhn, G. and Gage, F.H. (1997). Genetic influence on neurogenesis in the dentate gyrus of. *Proceedings of the National Academy of Sciences of the United States of America* **94**(19):10409–14.

Kempermann, G., Kuhn, H.G. and Gage, F.H. (1997). More hippocampal neurons in adult mice living in an enriched environment. *Nature*.

Kempermann, G., Song, H. and Gage, F.H. (2015). Neurogenesis in the adult hippocampus. *Cold Spring Harbor Perspectives in Biology* **7**(9).

Kettenmann, H. and Verkhratsky, A. (2011). Neuroglia-living nerve glue. *Fortschritte der Neurologie Psychiatrie* **79**(10):588–97.

Kim, H.J., Denli, A.M., Wright, R., Baul, T.D., Clemenson, G.D., Morcos, A.S., … Kagalwala, M.N. (2015). Rest regulates non-cell-autonomous neuronal differentiation and maturation of neural progenitor cells via secretogranin II. *Journal of Neuroscience* **35**(44):14872–84.

Kim, J.W., Nam, S.M., Yoo, D.Y., Jung, H.Y., Kim, I.Y., Hwang, I.K., … Yoon, Y.S. (2017). Comparison of Adult Hippocampal Neurogenesis and Susceptibility to Treadmill Exercise in Nine Mouse Strains. *Neural Plasticity* **2017**.

Kim, J.Y., Choi, K., Shaker, M.R., Lee, J.H., Lee, B., Lee, E., … Sun, W. (2016). Promotion of Cortical Neurogenesis from the Neural Stem Cells in the Adult Mouse Subcallosal Zone. *Stem Cells* **34**(4):888–901.

Kim, K.K., Adelstein, R.S. and Kawamoto, S. (2009). Identification of neuronal nuclei (NeuN) as Fox-3, a new member of the Fox-1 gene family of splicing factors. *Journal of Biological Chemistry* **284**(45):31052–61.

Kirby, E.D., Kuwahara, A.A., Messer, R.L. and Wyss-Coray, T. (2015). Adult hippocampal neural stem and progenitor cells regulate the neurogenic niche by secreting VEGF. *Proceedings of the National Academy of Sciences of the United States of America* **112**(13):4128–33.

Kirby, E.D., Muroy, S.E., Sun, W.G., Covarrubias, D., Leong, M.J., Barchas, L.A. and Kaufer, D. (2013). Acute stress enhances adult rat hippocampal neurogenesis and activation of newborn neurons via secreted astrocytic FGF2. *eLife* **2**.

Knoth, R., Singec, I., Ditter, M., Pantazis, G., Capetian, P., Meyer, R.P., … Kempermann, G. (2010). Murine features of neurogenesis in the human hippocampus across the lifespan from 0 to 100 years. *PLoS ONE* **5**(1).

Korpal, M., Lee, E.S., Hu, G. and Kang, Y. (2008). The miR-200 family inhibits

epithelial-mesenchymal transition and cancer cell migration by direct targeting of E-cadherin transcriptional repressors ZEB1 and ZEB2. *Journal of Biological Chemistry* **283**(22):14910–4.

Kotani, S., Yamauchi, T., Teramoto, T. and Ogura, H. (2006). Pharmacological evidence of cholinergic involvement in adult hippocampal neurogenesis in rats. *Neuroscience* **142**(2):505–14.

Kriegstein, A. and Alvarez-Buylla, A. (2009). The Glial Nature of Embryonic and Adult Neural Stem Cells. *Annual Review of Neuroscience* **17**(9):537–49.

Kronenberg, G., Bick-Sander, A., Bunk, E., Wolf, C., Ehninger, D. and Kempermann, G. (2006). Physical exercise prevents age-related decline in precursor cell activity in the mouse dentate gyrus. *Neurobiology of Aging* **27**(10):1505–13.

Kronenberg, G., Reuter, K., Steiner, B., Brandt, M.D., Jessberger, S., Yamaguchi, M. and Kempermann, G. (2003). Subpopulations of Proliferating Cells of the Adult Hippocampus Respond Differently to Physiologic Neurogenic Stimuli. *Journal of Comparative Neurology* **467**(4):455–63.

Kuhn, H.G. (2015). Control of cell survival in adult mammalian neurogenesis. *Cold Spring Harbor Perspectives in Biology* **7**(12).

Kuhn, H.G., Dickinson-Anson, H. and Gage, F.H. (1996). Neurogenesis in the dentate gyrus of the adult rat: age-related decrease of neuronal progenitor proliferation. *The Journal of neuroscience : the official journal of the Society for Neuroscience* **16**(6):2027–33.

Lagace, D.C., Donovan, M.H., Decarolis, N.A., Farnbauch, L.A., Malhotra, S., Berton, O., … Eisch, A.J. (2010). Adult hippocampal neurogenesis is functionally important for stress-induced social avoidance. *Proceedings of the National Academy of Sciences of the United States of America* **107**(9):4436–41.

Lavado, A., Lagutin, O. V., Chow, L.M.L., Baker, S.J. and Oliver, G. (2010). Prox1 Is required for granule cell maturation and intermediate progenitor maintenance during brain neurogenesis. *PLoS Biology* **8**(8).

Lazutkin, A., Podgorny, O. and Enikolopov, G. (2019). Modes of division and differentiation of neural stem cells. *Behavioural Brain Research* **374**.

Lee, J., Duan, W. and Mattson, M.P. (2002). Evidence that brain-derived neurotrophic factor is required for basal neurogenesis and mediates, in part, the enhancement of neurogenesis by dietary restriction in the hippocampus of adult mice. *Journal of Neurochemistry* **82**(6):1367–75.

Lei, W., Li, W., Ge, L. and Chen, G. (2019). Non-engineered and engineered adult neurogenesis in mammalian brains. *Frontiers in Neuroscience* **13**.

Li, Y., Luikart, B.W., Birnbaum, S., Chen, J., Kwon, C.H., Kernie, S.G., … Parada, L.F. (2008). TrkB Regulates Hippocampal Neurogenesis and Governs Sensitivity to Antidepressive Treatment. *Neuron* **59**(3):399–412.

Lin, H. (2008). Cell biology of stem cells: An enigma of asymmetry and self-renewal. *Journal of Cell Biology* **180**(2):257–60.

Liu, J., Liu, Y., Shao, J., Li, Y., Qin, L., Shen, H., … Gao, W.Q. (2019). Zeb1 is

important for proper cleavage plane orientation of dividing progenitors and neuronal migration in the mouse neocortex. *Cell Death and Differentiation* **26**(11):2479–92.

Liu, P.P., Tang, G. Bin, Xu, Y.J., Zeng, Y.Q., Zhang, S.F., Du, H.Z., … Liu, C.M. (2017). MiR-203 Interplays with Polycomb Repressive Complexes to Regulate the Proliferation of Neural Stem/Progenitor Cells. *Stem Cell Reports* **9**(1):190–202.

Liu, Y., El-Naggar, S., Darling, D.S., Higashi, Y. and Dean, D.C. (2008). Zeb1 links epithelial-mesenchymal transition and cellular senescence. *Development* **135**(3):579–588.

Llorens, M.C., Lorenzatti, G., Cavallo, N.L., Vaglienti, M. V., Perrone, A.P., Carenbauer, A.L., … Cabanillas, A.M. (2016). Phosphorylation Regulates Functions of ZEB1 Transcription Factor. *Journal of Cellular Physiology* **231**(10):2205–17.

Lugert, S., Basak, O., Knuckles, P., Haussler, U., Fabel, K., Götz, M., … Giachino, C. (2010). Quiescent and active hippocampal neural stem cells with distinct morphologies respond selectively to physiological and pathological stimuli and aging. *Cell Stem Cell* **6**(5):445–56.

Lukaszewicz, A., Savatier, P., Cortay, V., Kennedy, H. and Dehay, C. (2002). Contrasting effects of basic fibroblast growth factor and neurotrophin 3 on cell cycle kinetics of mouse cortical stem cells. *Journal of Neuroscience* **22**(15):6610–22.

Madisen, L., Zwingman, T.A., Sunkin, S.M., Oh, S.W., Zariwala, H.A., Gu, H., … Zeng, H. (2010). A robust and high-throughput Cre reporting and characterization system for the whole mouse brain. *Nature Neuroscience* **13**(1):133–40.

Maekawa, M., Takashima, N., Arai, Y., Nomura, T., Inokuchi, K., Yuasi, S. and Osumi, N. (2005). Pax6 is required for production and maintenance of progenitor cells in postnatal hippocampal neurogenesis. *Genes to Cells* **10**(10):1001–14.

Magavi, S.S., Leavitt, B.R. and Macklis, J.D. (2000). Induction of neurogenesis in the neocortex of adult mice. *Nature* **405**(6789):951–5.

Malatesta, P. and Gotz, M. (2013). Radial glia - from boring cables to stem cell stars. *Development*.

Malberg, J.E., Eisch, A.J., Nestler, E.J. and Duman, R.S. (2000). Chronic antidepressant treatment increases neurogenesis in adult rat hippocampus. *Journal of Neuroscience* **28**(6):1374–84.

Mao, X.O., Greenberg, D.A., Simon, R.P., Jin, K., Minami, M., Batteur, S. and Lan, J.Q. (2002). Neurogenesis in dentate subgranular zone and rostral subventricular zone after focal cerebral ischemia in the rat. *Proceedings of the National Academy of Sciences* **98**(8):4710–5.

Maric, D., Pla, A.F., Yoong, H.C. and Barker, J.L. (2007). Self-renewing and differentiating properties of cortical neural stem cells are selectively regulated by basic fibroblast growth factor (FGF) signaling via specific FGF receptors. *Journal of Neuroscience* **27**(8):1836–52.

Mark Redmond, J., Zehr, K.J., Blue, M.E., Lange, M.S., Marc Gillinov, A., Troncoso, J.C., … Baumgartner, W.A. (1995). AMPA glutamate receptor antagonism reduces neurologic injury after hypothermic circulatory arrest. *The Annals of Thoracic Surgery* **59**(3):579–84.

Matias, I., Morgado, J. and Gomes, F.C.A. (2019). Astrocyte Heterogeneity: Impact to Brain Aging and Disease. *Frontiers in Aging Neuroscience* **11**.

McIlwain, D.R., Berger, T. and Mak, T.W. (2013). Caspase functions in cell death and disease. *Cold Spring Harbor Perspectives in Biology* **5**(4).

Merkle, F.T., Tramontin, A.D., Garcia-Verdugo, J.M. and Alvarez-Buylla, A. (2004). Radial glia give rise to adult neural stem cells in the subventricular zone. *Proceedings of the National Academy of Sciences* **101**(50):17528–32.

Metzger, D. and Chambon, P. (2001). Site- and time-specific gene targeting in the mouse. *Methods* **24**(1):71–80.

Mignone, J.L., Kukekov, V., Chiang, A.S., Steindler, D. and Enikolopov, G. (2004). Neural Stem and Progenitor Cells in Nestin-GFP Transgenic Mice. *Journal of Comparative Neurology* **469**(3):311–24.

Mills, J.C., Stanger, B.Z. and Sander, M. (2019). Nomenclature for cellular plasticity: are the terms as plastic as the cells themselves? *The EMBO Journal* **38**(19).

Miquelajauregui, A., Van De Putte, T. De, Polyakov, A., Nityanandam, A., Boppana, S., Seuntjens, E., … Tarabykin, V. (2007). Smad-interacting protein-1 (Zfhx1b) acts upstream of Wnt signaling in the mouse hippocampus and controls its formation. *Proceedings of the National Academy of Sciences of the United States of America* **104**(31):12919–24.

Misson, J.P., Edwards, M.A., Yamamoto, M. and Caviness, V.S. (1988). Identification of radial glial cells within the developing murine central nervous system: studies based upon a new immunohistochemical marker. *Developmental Brain Research* **44**(1):95–108.

Miyoshi, T., Maruhashi, M., Van De Putte, T., Kondoh, H., Huylebroeck, D. and Higashi, Y. (2006). Complementary expression pattern of Zfhx1 genes Sip1 and δEF1 in the mouse embryo and their genetic interaction revealed by compound mutants. *Developmental Dynamics* **235**(7):1941–52.

Morfini, G., Ditella, M.C., Feiguin, F., Carri, N. and Cáceres, A. (1994). Neurotrophin-3 enhances neurite outgrowth in cultured hippocampal pyramidal neurons. *Journal of Neuroscience Research* **39**(2):219–32.

Mori, T., Tanaka, K., Buffo, A., Wurst, W., Kühn, R. and Götz, M. (2006). Inducible gene deletion in astroglia and radial glia--a valuable tool for functional and lineage analysis. *Glia* **54**(1):21–34.

Mouton, P.R., Long, J.M., Lei, D.L., Howard, V., Jucker, M., Calhoun, M.E. and Ingram, D.K. (2002). Age and gender effects on microglia and astrocyte numbers in brains of mice. *Brain Research* **956**(1):30–5.

Mu, L., Berti, L., Masserdotti, G., Covic, M., Michaelidis, T.M., Doberauer, K., … Chichung Lie, D. (2012). SoxC transcription factors are required for neuronal differentiation in adult hippocampal neurogenesis. *Journal of Neuroscience* **32**(9):3067–80.

Mumby, D.G., Gaskin, S., Glenn, M.J., Schramek, T.E. and Lehmann, H. (2002). Hippocampal damage and exploratory preferences in rats: Memory for objects, places, and contexts. *Learning and Memory* **9**(2):49–57.

Murai, T., Okuda, S., Tanaka, T. and Ohta, H. (2007). Characteristics of object location memory in mice: Behavioral and pharmacological studies. *Physiology and Behavior* **90**(1):116–24.

Nacher, J., Crespo, C. and McEwen, B.S. (2002). Doublecortin expression in the adult rat telencephalon. *European Journal of Neuroscience* **14**(4):629–44.

Nácher, J., Varea, E., Miguel Blasco-Ibáñez, J., Gómez-Climent, M.Á., Castillo-Gómez, E., Crespo, C., … McEwen, B.S. (2007). N-methyl-d-aspartate receptor expression during adult neurogenesis in the rat dentate gyrus. *Neuroscience* **144**(3):855–64.

Nakashiba, T., Cushman, J.D., Pelkey, K.A., Renaudineau, S., Buhl, D.L., McHugh, T.J., … Tonegawa, S. (2012). Young dentate granule cells mediate pattern separation, whereas old granule cells facilitate pattern completion. *Cell* **149**(1):188–201.

Namba, T., Mochizuki, H., Onodera, M., Mizuno, Y., Namiki, H. and Seki, T. (2005). The fate of neural progenitor cells expressing astrocytic and radial glial markers in the postnatal rat dentate gyrus. *European Journal of Neuroscience* **22**(8):1928–41.

Nesan, D. and Vijayan, M.M. (2013). The transcriptomics of glucocorticoid receptor signaling in developing zebrafish. *PLoS ONE* **8**(11).

Nicola, Z., Fabel, K. and Kempermann, G. (2015). Development of the adult neurogenic niche in the hippocampus of mice. *Frontiers in Neuroanatomy* **9**.

Nilsson, M., Perfilieva, E., Johansson, U., Orwar, O. and Eriksson, P.S. (1999). Enriched environment increases neurogenesis in the adult rat dentate gyrus and improves spatial memory. *Journal of Neurobiology* **39**(4):569–78.

Ninkovic, J., Mori, T. and Gotz, M. (2007). Distinct Modes of Neuron Addition in Adult Mouse Neurogenesis. *Journal of Neuroscience* **27**(40):10906–10911.

Niu, W., Zou, Y., Shen, C. and Zhang, C.L. (2011). Activation of postnatal neural stem cells requires nuclear receptor TLX. *Journal of Neuroscience* **31**(39):13816–28.

Obernier, K., Cebrian-Silla, A., Thomson, M., Parraguez, J.I., Anderson, R., Guinto, C., … Alvarez-Buylla, A. (2018). Adult Neurogenesis Is Sustained by Symmetric Self-Renewal and Differentiation. *Cell Stem Cell* **22**(2):221–34.

Ohayon, D., Garcès, A., Joly, W., Soukkarieh, C., Takagi, T., Sabourin, J.C., … Pattyn, A. (2016). Onset of Spinal Cord Astrocyte Precursor Emigration from the Ventricular Zone Involves the Zeb1 Transcription Factor. *Cell Reports* **17**(6):1473–81.

Okuyama, N., Takagi, N., Kawai, T., Miyake-Takagi, K. and Takeo, S. (2004). Phosphorylation of extracellular-regulating kinase in NMDA receptor antagonist-induced newly generated neurons in the adult rat dentate gyrus. *Journal of Neurochemistry* **88**(3):717–25.

Oliveira, A.M.M., Hawk, J.D., Abel, T. and Havekes, R. (2010). Post-training reversible inactivation of the hippocampus enhances novel object recognition memory. *Learning and Memory* **17**(3):155–60.

Olson, A.K., Eadie, B.D., Ernst, C. and Christie, B.R. (2006). Environmental

enrichment and voluntary exercise massively increase neurogenesis in the adult hippocampus via dissociable pathways. *Hippocampus* **16**(3):250–60.

Orban, P.C., Chui, D. and Marth, J.D. (1992). Tissue- and site-specific DNA recombination in transgenic mice. *Proceedings of the National Academy of Sciences of the United States of America* **89**(15):6861–5.

Paik, J. hye, Ding, Z., Narurkar, R., Ramkissoon, S., Muller, F., Kamoun, W.S., … DePinho, R.A. (2009). FoxOs Cooperatively Regulate Diverse Pathways Governing Neural Stem Cell Homeostasis. *Cell Stem Cell* **5**(5):540–53.

Palmer, T.D., Markakis, E.A., Willhoite, A.R., Safar, F. and Gage, F.H. (1999). Fibroblast growth factor-2 activates a latent neurogenic program in neural stem cells from diverse regions of the adult CNS. *The Journal of neuroscience : the official journal of the Society for Neuroscience* **19**(19):8487–97.

Parihar, V.K., Hattiangady, B., Kuruba, R., Shuai, B. and Shetty, A.K. (2011). Predictable chronic mild stress improves mood, hippocampal neurogenesis and memory. *Molecular Psychiatry* **16**(2):171–83.

Pastrana, E., Cheng, L.-C. and Doetsch, F. (2009). Simultaneous prospective purification of adult subventricular zone neural stem cells and their progeny. *Proceedings of the National Academy of Sciences* **106**(15):6387–92.

Pataskar, A., Jung, J., Smialowski, P., Noack, F., Calegari, F., Straub, T. and Tiwari, V.K. (2016). NeuroD1 reprograms chromatin and transcription factor landscapes to induce the neuronal program. *The EMBO Journal* **35**(1):24–45.

Patten, B.A., Peyrin, J.M., Weinmaster, G. and Corfas, G. (2003). Sequential signaling through Notch1 and erbB receptors mediates radial glia differentiation. *Journal of Neuroscience* **23**(14):6132–40.

Paxinos, G. and Franklin, K.B.J. (2001). *Paxinos and Franklin's the Mouse Brain in Stereotaxic Coordinates*. 5th ed. Academic Press.

Perdigão-Henriques, R., Petrocca, F., Altschuler, G., Thomas, M.P., Le, M.T.N., Tan, S.M., … Lieberman, J. (2016). MiR-200 promotes the mesenchymal to epithelial transition by suppressing multiple members of the Zeb2 and Snail1 transcriptional repressor complexes. *Oncogene* **35**(2):158–72.

Petrik, D. and Encinas, J.M. (2019). Perspective: Of mice and Men – How widespread is adult neurogenesis? *Frontiers in Neuroscience* **13**.

Piazza, P.V., Deminière, J.M., Le Moal, M. and Simon, H. (1989). Factors that predict individual vulnerability to amphetamine self-administration. *Science* **245**(4925):1511–3.

Pilegaard, K. and Ladefoged, O. (1996). Total number of astrocytes in the molecular layer of the dentate gyrus of rats at different ages. *Analytical and Quantitative Cytology and Histology* **18**(4):279–85.

Pilz, G.A., Bottes, S., Betizeau, M., Jörg, D.J., Carta, S., Simons, B.D., … Jessberger, S. (2018). Live imaging of neurogenesis in the adult mouse hippocampus. *Science*.

Ponti, G., Obernier, K., Guinto, C., Jose, L., Bonfanti, L. and Alvarez-Buylla, A.

(2013). Cell cycle and lineage progression of neural progenitors in the ventricular-subventricular zones of adult mice. *Proceedings of the National Academy of Sciences of the United States of America* **110**(11):1045–54.

Postigo, A.A. and Dean, D.C. (2000). Differential expression and function of members of the zfh-1 family of zinc finger/homeodomain repressors. *Proceedings of the National Academy of Sciences of the United States of America* **97**(12):6391–6.

Potten, C.S. and Loeffler, M. (1990). Stem cells: attributes, cycles, spirals, pitfalls and uncertainties. Lessons for and from the crypt. *Development (Cambridge, England)* **110**(4):1001–20.

Van Praag, H., Kempermann, G. and Gage, F.H. (1999). Running increases cell proliferation and neurogenesis in the adult mouse dentate gyrus. *Nature Neuroscience* **2**(3):266–70.

Pratt, A.J. and MacRae, I.J. (2009). The RNA-induced silencing complex: A versatile gene-silencing machine. *Journal of Biological Chemistry* **284**(27):17897–901.

De Putte, T. Van, Maruhashi, M., Francis, A., Nelles, L., Kondoh, H., Huylebroeck, D. and Higashi, Y. (2003). Mice lacking Zfhx1b, the gene that codes for Smad-interacting protein-1, reveal a role for multiple neural crest cell defects in the etiology of hirschsprung disease-mental retardation syndrome. *American Journal of Human Genetics* **72**(2):465–70.

Qu, Q., Sun, G., Li, W., Yang, S., Ye, P., Zhao, C., … Shi, Y. (2010). Orphan nuclear receptor TLX activates Wnt/B-catenin signalling to stimulate neural stem cell proliferation and self-renewal. *Nature Cell Biology* **12**(1):31–40.

Quesseveur, G., David, D.J., Gaillard, M.C., Pla, P., Wu, M. V., Nguyen, H.T., … Guiard, B.P. (2013). BDNF overexpression in mouse hippocampal astrocytes promotes local neurogenesis and elicits anxiolytic-like activities. *Translational Psychiatry* **3**.

Rai, K.S., Hattiangady, B. and Shetty, A.K. (2007). Enhanced production and dendritic growth of new dentate granule cells in the middle-aged hippocampus following intracerebroventricular FGF-2 infusions. *European Journal of Neuroscience* **26**(7):1765–79.

Ray, J., Peterson, D.A., Schinstine, M. and Gage, F.H. (1993). Proliferation, differentiation, and long-term culture of primary hippocampal neurons. *Proceedings of the National Academy of Sciences of the United States of America* **90**(8):3602–6.

Renault, V.M., Rafalski, V.A., Morgan, A.A., Salih, D.A.M., Brett, J.O., Webb, A.E., … Brunet, A. (2009). FoxO3 Regulates Neural Stem Cell Homeostasis. *Cell Stem Cell* **5**(5):527–39.

Reynolds, B.A. and Weiss, S. (1992). Generation of neurons and astrocytes from isolated cells of the adult mammalian central nervous system. *Science* **255**(5052):1707–10.

Richetin, K., Leclerc, C., Toni, N., Gallopin, T., Pech, S., Roybon, L. and Rampon, C. (2015). Genetic manipulation of adult-born hippocampal neurons rescues memory in a mouse model of Alzheimer's disease. *Brain* **138**(2):440–55.

Rosmaninho, P., Mükusch, S., Piscopo, V., Teixeira, V., Raposo, A.A., Warta, R., … Castro, D.S. (2018). Zeb1 potentiates genome-wide gene transcription with Lef1 to promote glioblastoma cell invasion. *The EMBO Journal* **37**(15).

Saaltink, D.J. and Vreugdenhil, E. (2014). Stress, glucocorticoid receptors, and adult neurogenesis: A balance between excitation and inhibition? *Cellular and Molecular Life Sciences* **71**(13):2499–515.

Sabourin, J.C., Ackema, K.B., Ohayon, D., Guichet, P.O., Perrin, F.E., Garces, A., … Hugnot, J.P. (2009). A mesenchymal-like ZEB1+ niche harbors dorsal radial glial fibrillary acidic protein-positive stem cells in the spinal cord. *Stem Cells* **27**(11):2722–33.

Salic, A. and Mitchison, T.J. (2008). A chemical method for fast and sensitive detection of DNA synthesis in vivo. *Proceedings of the National Academy of Sciences of the United States of America* **105**(7):2415–20.

Sampedro-Piquero, P. and Begega, A. (2016). Environmental Enrichment as a Positive Behavioral Intervention Across the Lifespan. *Current Neuropharmacology* **15**(4):459–70.

Sanai, N., Nguyen, T., Ihrie, R.A., Mirzadeh, Z., Tsai, H.H., Wong, M., … Alvarez-Buylla, A. (2011). Corridors of migrating neurons in the human brain and their decline during infancy. *Nature* **478**(7369):382–6.

Sanai, N., Tramontin, A.D., Quiñones-Hinojosa, A., Barbaro, N.M., Gupta, N., Kunwar, S., … Sana N. and Alvarez-Buylla A. (2004). Unique astrocyte ribbon in adult human brain contains neural stem cells but lacks chain migration. *Nature* **427**(6976):740–4.

Sandlesh, P., Juang, T., Safina, A., Higgins, M.J. and Gurova, K. V. (2018). Uncovering the fine print of the CreERT2-LoxP system while generating a conditional knockout mouse model of Ssrp1 gene. *PLoS ONE* **13**(6).

Sarkisyan, G. and Hedlund, P.B. (2009). The 5-HT7 receptor is involved in allocentric spatial memory information processing. *Behavioural Brain Research* **202**(1):26–31.

Sauer, B. (1998). Inducible gene targeting in mice using the Cre/lox system. *Methods (San Diego, Calif.)* **14**(4):381–92.

Sauer, B. and Henderson, N. (1988). Site-specific DNA recombination in mammalian cells by the Cre recombinase of bacteriophage P1. *Proceedings of the National Academy of Sciences of the United States of America* **85**(14):5166–70.

Schmid, R.S., McGrath, B., Berechid, B.E., Boyles, B., Marchionni, M., Šestan, N. and Anton, E.S. (2003). Neuregulin 1-erbB2 signaling is required for the establishment of radial glia and their transformation into astrocytes in cerebral cortex. *Proceedings of the National Academy of Sciences of the United States of America* **100**(7):4251–6.

Schmidt, B., Marrone, D.F. and Markus, E.J. (2012). Disambiguating the similar: The dentate gyrus and pattern separation. *Behavioural Brain Research* **226**(1):55–65.

Sekido, R., Takagi, T., Okanami, M., Moribe, H., Yamamura, M., Higashi, Y. and

Kondoh, H. (1996). Organization of the gene encoding transcriptional repressor δEF1 and cross-species conservation of its domains. *Gene* **173**(2):227–32.

Selinfreund, R.H., Barger, S.W., Pledger, W.J. and Van Eldik, L.J. (1991). Neurotrophic protein S100β stimulates glial cell proliferation. *Proceedings of the National Academy of Sciences of the United States of America* **88**(9):3554–8.

Seri, B., Garcia-Verdugo, J.M., McEwen, B.S. and Alvarez-Buylla, A. (2001). Astrocytes give rise to new neurons in the adult mammalian hippocampus. *The Journal of neuroscience : the official journal of the Society for Neuroscience* **21**(18):7153–7160.

Shi, D.M., Li, L.X., Bian, X.Y., Shi, X.J., Lu, L.L., Zhou, H.X., … Wu, W.Z. (2018). MiR-296-5p suppresses EMT of hepatocellular carcinoma via attenuating NRG1/ERBB2/ERBB3 signaling. *Journal of Experimental and Clinical Cancer Research* **37**(1).

Shi, Yujiang, Sawada, J.I., Sui, G., Affar, E.B., Whetstine, J.R., Lan, F., … Shi, Y. (2003). Coordinated histone modifications mediated by a CtBP co-repressor complex. *Nature* **422**(6933):735–8.

Shihabuddin, L.S., Horner, P.J., Ray, J. and Gage, F.H. (2000). Adult spinal cord stem cells generate neurons after transplantation in the adult dentate gyrus. *The Journal of neuroscience : the official journal of the Society for Neuroscience* **20**(23):8727–35.

Siebzehnrubl, F.A., Silver, D.J., Tugertimur, B., Deleyrolle, L.P., Siebzehnrubl, D., Sarkisian, M.R., … Steindler, D.A. (2013). The ZEB1 pathway links glioblastoma initiation, invasion and chemoresistance. *EMBO Molecular Medicine* **5**(8):1196–1212.

Sierra, A., Encinas, J.M., Deudero, J.J.P., Chancey, J.H., Enikolopov, G., Overstreet-Wadiche, L.S., … Maletic-Savatic, M. (2010). Microglia shape adult hippocampal neurogenesis through apoptosis-coupled phagocytosis. *Cell Stem Cell* **7**(4):483–95.

Singh, D.K., Kollipara, R.K., Vemireddy, V., Yang, X.L., Sun, Y., Regmi, N., … Bachoo, R.M. (2017). Oncogenes Activate an Autonomous Transcriptional Regulatory Circuit That Drives Glioblastoma. *Cell Reports* **18**(4):961–976.

Singh, S., Howell, D., Trivedi, N., Kessler, K., Ong, T., Rosmaninho, P., … Solecki, D.J. (2016). Zeb1 controls neuron differentiation and germinal zone exit by a mesenchymal-epithelial-like transition. *eLife* **5**.

Slezak, M., Göritz, C., Niemiec, A., Frisén, J., Chambon, P., Metzger, D. and Pfrieger, F.W. (2007). Transgenic mice for conditional gene manipulation in astroglial cells. *GLIA* **55**(15):1565–76.

Smith, G.E. and Darling, D.S. (2003). Combination of a Zinc Finger and Homeodomain Required for Protein-Interaction. *Molecular Biology Reports* **30**(4):199–206.

Snyder, J.S., Ferrante, S.C. and Cameron, H.A. (2012). Late Maturation of Adult-Born Neurons in the Temporal Dentate Gyrus. *PLoS ONE* **7**(11).

Snyder, J.S., Kee, N. and Wojtowicz, J.M. (2001). Effects of adult neurogenesis

on synaptic plasticity in the rat dentate gyrus. *Journal of Neurophysiology* **85**(6):2423–31.

Song, H., Berg, D.A., Bond, A.M. and Ming, G. li (2018). Radial glial cells in the adult dentate gyrus: What are they and where do they come from? *F1000Research* **7**.

Song, H., Stevens, C.F. and Gage, F.H. (2002). Astroglia induce neurogenesis from adult neural stem cells. *Nature* **417**(6884):39–44.

Song, J., Zhong, C., Bonaguidi, M.A., Sun, G.J., Hsu, D., Gu, Y., … Song, H. (2012). Neuronal circuitry mechanism regulating adult quiescent neural stem-cell fate decision. *Nature* **489**(7414):150–4.

Sorrells, S.F., Paredes, M.F., Cebrian-Silla, A., Sandoval, K., Qi, D., Kelley, K.W., … Alvarez-Buylla, A. (2018). Human hippocampal neurogenesis drops sharply in children to undetectable levels in adults. *Nature* **555**(7696):377–81.

Spaderna, S., Schmalhofer, O., Hlubek, F., Berx, G., Eger, A., Merkel, S., … Brabletz, T. (2006). A Transient, EMT-Linked Loss of Basement Membranes Indicates Metastasis and Poor Survival in Colorectal Cancer. *Gastroenterology* **131**(3):830–840.

Spalding, K.L., Bergmann, O., Alkass, K., Bernard, S., Salehpour, M., Huttner, H.B., … Frisén, J. (2013). Dynamics of hippocampal neurogenesis in adult humans. *Cell* **153**(6):1219–1227.

Speisman, R.B., Kumar, A., Rani, A., Pastoriza, J.M., Severance, J.E., Foster, T.C. and Ormerod, B.K. (2013). Environmental enrichment restores neurogenesis and rapid acquisition in aged rats. *Neurobiology of Aging* **34**(1):263–74.

Squire, L.R., Wixted, J.T. and Clark, R.E. (2007). Recognition memory and the medial temporal lobe: A new perspective. *Nature Reviews Neuroscience* **8**(11):872–83.

Steiner, B., Klempin, F., Wang, L., Kott, M., Kettenmann, H. and Kempermann, G. (2006). Type-2 cells as link between glial and neuronal lineage in adult hippocampal neurogenesis. *GLIA* **54**(8):805–14.

Steiner, B., Kronenberg, G., Jessberger, S., Brandt, M.D., Reuter, K. and Kempermann, G. (2004). Differential Regulation of Gliogenesis in the Context of Adult Hippocampal Neurogenesis in Mice. *GLIA* **46**(1):41–52.

Steiner, B., Zurborg, S., Hörster, H., Fabel, K. and Kempermann, G. (2008). Differential 24 h responsiveness of Prox1-expressing precursor cells in adult hippocampal neurogenesis to physical activity, environmental enrichment, and kainic acid-induced seizures. *Neuroscience* **154**(2):521–9.

Stevens, B., Allen, N.J., Vazquez, L.E., Howell, G.R., Christopherson, K.S., Nouri, N., … Barres, B.A. (2007). The Classical Complement Cascade Mediates CNS Synapse Elimination. *Cell* **131**(6):1164–78.

Suh, H., Consiglio, A., Ray, J., Sawai, T., D'Amour, K.A. and Gage, F.H.H. (2007). In Vivo Fate Analysis Reveals the Multipotent and Self-Renewal Capacities of Sox2+ Neural Stem Cells in the Adult Hippocampus. *Cell Stem Cell* **1**(5):515–28.

Suhonen, J.O., Peterson, D.A., Ray, J. and Gage, F.H. (1996). Differentiation of

adult hippocampus-derived progenitors into olfactory neurons in vivo. *Nature* **383**(6601):624–7.

Sun, G.J., Zhou, Y., Stadel, R.P., Moss, J., Yong, J.H.A., Ito, S., … Ming, G.L. (2015). Tangential migration of neuronal precursors of glutamatergic neurons in the adult mammalian brain. *Proceedings of the National Academy of Sciences of the United States of America* **112**(30):9484–9.

Sun, G.Q., Yu, R.T., Evans, R.M. and Shi, Y. (2007). Orphan nuclear receptor TLX recruits histone deacetylases to repress transcription and regulate neural stem cell proliferation. *Proceedings of the National Academy of Sciences of the United States of America* **104**(39):15282–7.

Sun, M.Y., Yetman, M.J., Lee, T.C., Chen, Y. and Jankowsky, J.L. (2014). Specificity and efficiency of reporter expression in adult neural progenitors vary substantially among nestin-CreERT2 lines. *Journal of Comparative Neurology* **522**(5):1191–208.

Sun, Y., Jin, K., Childs, J.T., Xie, L., Mao, X.O. and Greenberg, D.A. (2006). Vascular endothelial growth factor-B (VEGFB) stimulates neurogenesis: Evidence from knockout mice and growth factor administration. *Developmental Biology* **289**(2):329–35.

Suzuki, K., Kawataki, T., Endo, K., Miyazawa, K., Kinouchi, H. and Saitoh, M. (2018). Expression of Zebs in gliomas is associated with invasive properties and histopathological grade. *Oncology Letters* **16**(2):1758–64.

Takagi, T., Moribe, H., Kondoh, H. and Higashi, Y. (1998). DeltaEF1, a zinc finger and homeodomain transcription factor, is required for skeleton patterning in multiple lineages. *Development (Cambridge, England)* **125**(1):21–31.

Tchieu, J., Calder, E.L., Guttikonda, S.R., Gutzwiller, E.M., Aromolaran, K.A., Steinbeck, J.A., … Studer, L. (2019). NFIA is a gliogenic switch enabling rapid derivation of functional human astrocytes from pluripotent stem cells. *Nature Biotechnology* **37**(3):267–75.

Toda, T., Parylak, S.L., Linker, S.B. and Gage, F.H. (2019). The role of adult hippocampal neurogenesis in brain health and disease. *Molecular Psychiatry* **24**(1):67–87.

Toni, N. and Schinder, A.F. (2016). Maturation and functional integration of new granule cells into the adult hippocampus. *Cold Spring Harbor Perspectives in Biology* **8**(1).

Tozuka, Y., Fukuda, S., Namba, T., Seki, T. and Hisatsune, T. (2005). GABAergic excitation promotes neuronal differentiation in adult hippocampal progenitor cells. *Neuron* **47**(6):803–15.

Tramontin, A.D., García-Verdugo, J.M., Lim, D.A. and Alvarez-Buylla, A. (2003). Postnatal development of radial glia and the ventricular zone (VZ): A continuum of the neural stem cell compartment. *Cerebral Cortex* **13**(6):580–7.

Uda, M., Ishido, M. and Kami, K. (2007). Features and a possible role of Mash1-immunoreactive cells in the dentate gyrus of the hippocampus in the adult rat. *Brain Research* **1171**:9–17.

Urbán, N. and Guillemot, F. (2014). Neurogenesis in the embryonic and adult brain: Same regulators, different roles. *Frontiers in Cellular Neuroscience* **8**.

Vannier, C., Mock, K., Brabletz, T. and Driever, W. (2013). Zeb1 regulates E-cadherin and Epcam (epithelial cell adhesion molecule) expression to control cell behavior in early zebrafish development. *Journal of Biological Chemistry* **288**(26):18643–59.

Villarreal, A., Seoane, R., Torres, A.G., Rosciszewski, G., Angelo, M.F., Rossi, A., … Ramos, A.J. (2014). S100B protein activates a RAGE-dependent autocrine loop in astrocytes: Implications for its role in the propagation of reactive gliosis. *Journal of Neurochemistry* **131**(2):190–205.

Vivar, C. and van Praag, H. (2013). Functional circuits of new neurons in the dentate gyrus. *Frontiers in Neural Circuits* **7**.

Vogel-Ciernia, A. and Wood, M.A. (2014). Examining object location and object recognition memory in mice. *Current Protocols in Neuroscience* **69**(1).

Voigt, T. (1989). Development of glial cells in the cerebral wall of ferrets: Direct tracing of their transformation from radial glia into astrocytes. *Journal of Comparative Neurology* **289**(1):74–88.

Volterra, A. and Steinhäuser, C. (2004). Glial modulation of synaptic transmission in the hippocampus. *GLIA* **47**(3):249–57.

Walf, A.A. and Frye, C.A. (2007). The use of the elevated plus maze as an assay of anxiety-related behavior in rodents. *Nature Protocols* **2**(2):322–8.

Wang, H., Xiao, Z., Zheng, J., Wu, J., Hu, X.L., Yang, X. and Shen, Q. (2019). ZEB1 Represses Neural Differentiation and Cooperates with CTBP2 to Dynamically Regulate Cell Migration during Neocortex Development. *Cell Reports* **27**(8):2335–53.

Wang, J.W., David, D.J., Monckton, J.E., Battaglia, F. and Hen, R. (2008). Chronic fluoxetine stimulates maturation and synaptic plasticity of adult-born hippocampal granule cells. *Journal of Neuroscience* **28**(6):1374–84.

Waterhouse, E.G., An, J.J., Orefice, L.L., Baydyuk, M., Liao, G.Y., Zheng, K., … Xu, B. (2012). BDNF promotes differentiation and maturation of adult-born neurons through GABArgic transmission. *Journal of Neuroscience* **32**(41):14318–30.

Wegner, M. (2010). All purpose Sox: The many roles of Sox proteins in gene expression. *International Journal of Biochemistry and Cell Biology* **42**(3):381–90.

Wellner, U., Schubert, J., Burk, U.C., Schmalhofer, O., Zhu, F., Sonntag, A., … Brabletz, T. (2009). The EMT-activator ZEB1 promotes tumorigenicity by repressing stemness-inhibiting microRNAs. *Nature Cell Biology* **11**(12):1487–1495.

Werner, S., Unsicker, K. and von Bohlen und Halbach, O. (2011). Fibroblast growth factor-2 deficiency causes defects in adult hippocampal neurogenesis, which are not rescued by exogenous fibroblast growth factor-2. *Journal of Neuroscience Research* **89**(10):1605–17.

Wharton, S.B., Chan, K.K., Anderson, J.R., Stoeber, K. and Williams, G.H. (2001). Replicative Mcm2 protein as a novel proliferation marker in oligodendrogliomas and its relationship to Ki67 labelling index, histological grade and

prognosis. *Neuropathology and Applied Neurobiology* **27**(4):305–13.

Winner, B., Kohl, Z. and Gage, F.H. (2011). Neurodegenerative disease and adult neurogenesis. *European Journal of Neuroscience* **33**(6):1139–51.

Xu, M., Wang, J., Guo, X., Li, T., Kuang, X. and Wu, Q.F. (2018). Illumination of neural development by in vivo clonal analysis. *Cell Regeneration* **7**(2):33–9.

Yamaguchi, M., Saito, H., Suzuki, M. and Mori, K. (2000). Visualization of neurogenesis in the central nervous system using nestin promoter-GFP transgenic mice. *NeuroReport* **11**(9):1991–6.

Yang, S.M., Alvarez, D.D. and Schinder, A.F. (2015). Reliable genetic labeling of adult-born dentate granule cells using ascl1CreERT2 and glastCreERT2 murine lines. *Journal of Neuroscience* **35**(46):15379–90.

Yassa, M.A. and Stark, C.E.L. (2011). Pattern separation in the hippocampus. *Trends in Neurosciences* **71**(6).

Zakrzewski, W., Dobrzyński, M., Szymonowicz, M. and Rybak, Z. (2019). Stem cells: Past, present, and future. *Stem Cell Research and Therapy* **10**(1).

Zhang, J. and Jiao, J. (2015). Molecular Biomarkers for Embryonic and Adult Neural Stem Cell and Neurogenesis. *BioMed Research International* **2015**.

Zhe, D., Fang, H. and Yuxiu, S. (2008). Expressions of hippocampal mineralocorticoid receptor (MR) and glucocorticoid receptor (GR) in the single-prolonged stress-rats. *Acta Histochemica et Cytochemica* **41**(4):89–95.

Zhou, Z.D., Kumari, U., Xiao, Z.C. and Tan, E.K. (2010). Notch as a molecular switch in neural stem cells. *IUBMB Life* **62**(8):618–23.

Ziebell, F., Dehler, S., Martin-Villalba, A. and Marciniak-Czochra, A. (2018). Revealing age-related changes of adult hippocampal neurogenesis using mathematical models. *Development (Cambridge)* **145**(1).

Ziebell, F., Martin-Villalba, A. and Marciniak-Czochra, A. (2014). Mathematical modelling of adult hippocampal neurogenesis: Effects of altered stem cell dynamics on cell counts and bromodeoxyuridine-labelled cells. *Journal of the Royal Society Interface* **11**(94).

Appendix A

Expression of ZEB1 and ZEB2 across juvenile and adult DG cell populations

Through data mining of single-cell RNA-Seq data of the dentate gyrus that was generated and made available by the Linnarsson lab, it was possible to observe the expression of different gene sets, including ZEB1 and ZEB2, across the various hippocampal cell populations that they investigated in their main study (Hochgerner *et al.* 2018). I found that the two ZEB transcription factors are differentially expressed in the neuron development timeline, from the neural precursor cell stage to fully differentiated mature neurons (Appendix A). Whilst ZEB1 appears to be expressed predominantly in the neural stem and early intermediate progenitor cell clusters (including RG, RGL, neuronal IPC, and immature astrocytes; Appendix A-**A**), ZEB2 was expressed further along the differentiation continuum, in the immature and differentiated neuronal clusters (including granule and pyramidal neurons; Appendix A-**B**). ZEB1 was also observed to be expressed in mature astrocytes (Appendix A-**C**), whilst ZEB2 was expressed primarily in oligodendrocytes in this region (Appendix A-**D**). The differential expression of ZEB1 and ZEB2 in adult hippocampal cells in this dataset points towards possible divergent functions of the two transcription factors in the adult CNS.

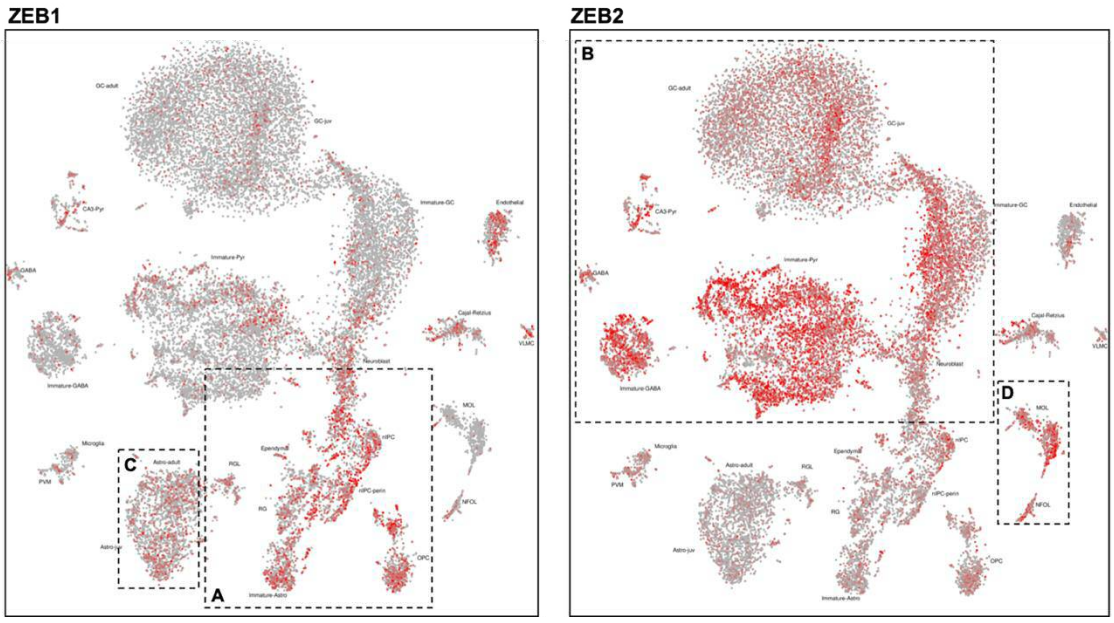

Appendix A. Differential expression of ZEB1 and ZEB2 in the juvenile and adult hippocampus – (A) ZEB1 expression is detected largely in the neural precursors as well as early neuronal intermediate progenitor cells. (B) Meanwhile, ZEB2 is expressed primarily in more differentiated neuronal cells, including both immature and mature stages during their development. (C) Lastly, whilst ZEB1 is expressed in a considerable number of mature astrocytes in the hippocampus, but importantly not in all of them, (D) ZEB2 is expressed in a large number of oligodendrocytes. Image modified from single-cell RNA Seq DataSet C made publicly available by the Linnarsson group (Hochgerner *et al.* 2018).

Appendix B

Quantification of tdTomato+/NeuN+ granule cells in the dentate gyrus of control, Zeb1$^{+/-}$, and Zeb1$^{-/-}$ mice

In previously published research reporting the use of the inducible Zeb1 knockout mouse model, it has been observed that heterozygous loss-of-function of Zeb1 exhibits a wild-type phenotype and no defects were detected (Brabletz *et al.* 2017). As this strain would possibly be a more accurate control for the complete loss-of-function model that I utilised in the current project due to the presence of a floxed Zeb1 allele, in comparison to the wild-type Zeb1 gene in the other control at hand (GLAST:CreER^{T2}-Rosa26$^{lsl\text{-}tdTomato}$), I sought to determine whether the heterozygous expression of Zeb1 would exhibit a wild-type phenotype, or whether partial Zeb1 deficiency would have effects in the hippocampal neurogenic niche. I investigated the number of tdTomato+/NeuN+ granule neurons generated in the dentate gyrus of three mouse strains at 8 weeks post-tamoxifen induced transgene recombination, as this was the timepoint at which I observed a striking difference in the number of granule neurons between the control and Zeb1$^{-/-}$ mice. I observed a significant increase in granule neuron population in the Zeb1$^{+/-}$ mice (15,832 ± 1,859 cells/mm^3) in comparison to the control mice (10,052 ± 951 cells/mm^3; p=0.0171; Appendix B); there was also a significant increase in neuronal numbers in the Zeb1$^{-/-}$ mice (18,452 ± 1,487) in comparison to the control (p<0.0001).

As the number of granule neurons generated in the dentate gyrus of the control and Zeb1$^{+/-}$ mice was significantly different by 8 weeks following transgene recombination, I decided that this the latter would not be a suitable control for the inducible Zeb1 knockout mouse model due to the phenotypic effects of the genotype in the neurogenic niche in the hippocampus.

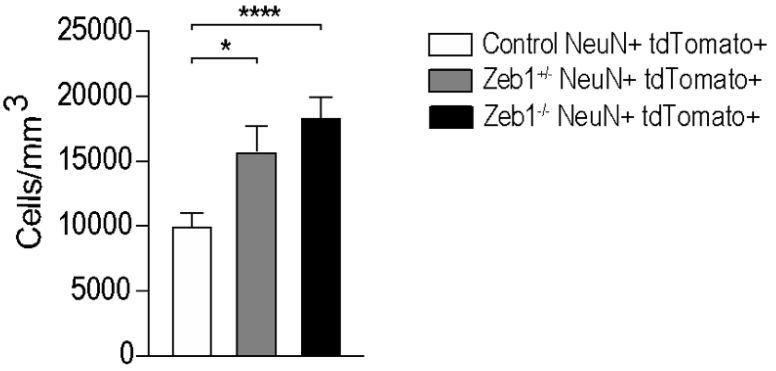

Appendix B. Heterozygous loss of Zeb1 results in aberrant neurogenesis – At 8 weeks post-Zeb1 deletion, $Zeb1^{+/-}$ mice (grey bar) displayed increased numbers of granule neurons in comparison to the control (white bar), which was further amplified in the complete loss-of-function strain (black bar). Numerical data shown as mean ± SEM and are representative of three independent animals per genotype, with a minimum of two sections analysed per animal, two-tailed t-test/Mann-Whitney U-test, * $p<0.05$, **** $p<0.0001$.

Appendix C

Leakiness of GLAST:CreER^{T2}-dependent recombination

To assess the leakiness of the transgene recombination driven by the GLAST:CreER^{T2} construct, I quantified the number of tdTomato-labelled radial cells in the SGZ (that were likely Type 1 cells) in control mice treated with oil (vehicle control), and compared the number of cells to the number of tdTomato-labelled Type 1 cells in control mice treated with tamoxifen, at 4 weeks post-oil/tamoxifen administration. The dentate gyrus of the control group treated with oil hosted 230 ± 67 tdTomato+ cells/mm^3, whilst the control mice treated with tamoxifen exhibited 16,423 ± 1,213 tdTomato+ cells/mm^3 which was significantly higher than the former group ($p<0.0001$; Appendix C). Thus, whilst the GLAST:CreER^{T2}-mediated recombination was slightly leaky, it occurred in significantly fewer cells in comparison to the tamoxifen-treated group. This corroborates observations from previous studies that have also reported a slight leakiness with the GLAST:CreER^{T2} construct (Mori *et al.* 2006; Yang *et al.* 2015).

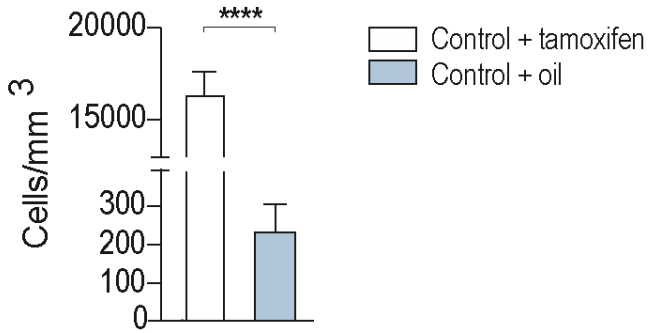

Appendix C. Quantification of GLAST-CreER^{T2}-dependent leakiness in Type 1 cells – At 4 weeks post-oil/tamoxifen treatment, the number of Type 1 cells labelled with tdTomato was significantly higher in the tamoxifen-treated group (white bar), in comparison to the mice that received oil (blue bar). Numerical data shown as mean ± SEM and are representative of 2-3 independent animals per genotype, with at least three whole DG analysed per animal, two-tailed t-test, **** $p<0.0001$.